OCS Study
BOEM 2019-017

Tracking Offshore Occurrence of Common Terns, Endangered Roseate Terns, and Threatened Piping Plovers with VHF Arrays

Appendices A-K

US Department of the Interior
Bureau of Ocean Energy Management
Office of Renewable Energy Programs

OCS Study
BOEM 2019-017

Tracking Offshore Occurrence of Common Terns, Endangered Roseate Terns, and Threatened Piping Plovers with VHF Arrays

April 2019

Authors:

Pamela H. Loring, US Fish and Wildlife Service (USFWS), Division of Migratory Birds
Peter W.C. Paton, Department of Natural Resources Science, University of Rhode Island
James D. McLaren, Environment and Climate Change Canada, Science and Technology Branch
Hua Bai, University of Massachusetts Amherst, Department of Electrical and Computer Engineering
Ramakrishna Janaswamy, University of Massachusetts Amherst, Department of Electrical and Computer Engineering
Holly F. Goyert, University of Massachusetts Amherst, Department of Environmental Conservation
Curtice R. Griffin, University of Massachusetts Amherst, Department of Environmental Conservation
Paul R. Sievert, University of Massachusetts Amherst, Department of Environmental Conservation

Prepared under BOEM Intra-Agency Agreement No. M13PG00012

By
US Department of Interior
US Fish and Wildlife Service
Division of Migratory Birds
300 Westgate Center Dr.
Hadley, MA 01035

US Department of the Interior
Bureau of Ocean Energy Management
Office of Renewable Energy Programs

Appendix A

Comparing Satellite and Digital Radio Telemetry to Estimate Space and Habitat Use of American Oystercatchers (*Haematopus palliatus*) in Massachusetts

Pamela H. Loring[1], Curtice R. Griffin[2], Paul R. Sievert[2], and Caleb S. Spiegel[1]

[1]U.S. Fish and Wildlife Service, Division of Migratory Birds, Northeast Region, 300 Westgate Center Drive, Hadley, Massachusetts, 01035, USA

[2]Department of Environmental Conservation, University of Massachusetts Amherst, 160 Holdsworth Way, Amherst, Massachusetts, 01003, USA

Citation: Loring PH, Griffin CR, Sievert PR, Spiegel CS. 2017. Comparing satellite and digital radio telemetry to estimate space and habitat use of American Oystercatchers (*Haematopus palliatus*) in Massachusetts, USA. Waterbirds, 40(1):19-31.

Abstract. — The use of digital VHF telemetry is expanding as a relatively light weight and cost-effective alternative to satellite-based technologies for tracking bird movements, though few studies have compared how they perform. During 2013, satellite telemetry and digital VHF telemetry were compared for estimating the length of stay, home ranges, and habitat characteristics of American Oystercatchers (*Haematopus palliatus*) on their breeding grounds in coastal Massachusetts, USA. American Oystercatchers ($n = 5$) were captured at their nest sites and tagged with both a 9.5 g solar-powered satellite transmitter, and a 2.6 g digitally coded VHF transmitter, and tracked using the Argos satellite system, an array of eight automated radio telemetry stations, and periodic land-based and aerial telemetry surveys. Estimates of mean minimum length of stay in the study area were slightly longer for satellite telemetry at 118 ± 12 days vs, digital VHF telemetry which was 108 ± 11 days. Size estimates of mean (± SE) fixed kernel 95% utilization distributions were similar for satellite telemetry (22.53 ± 16.87 km^2) and VHF telemetry (27.27 ± 21.58 km^2), as were size estimates of 50% core-use areas (4.14 ± 2.99 km^2 for satellite telemetry and 4.80 ± 4.05 km^2 for VHF telemetry). Both satellite and VHF telemetry found tagged individuals most frequently occurring on coarse-grained sand beaches (mean proportion: 0.58 - 0.77), and salt to brackish marshes (mean proportion: 0.06 - 0.29). Despite a small sample size, digital VHF telemetry, when combined with automated radio telemetry stations and recurrent telemetry surveys, performed similarly to satellite telemetry for estimating timing and home range size of shorebirds on their breeding grounds, although spatial distributions of home ranges varied between the two techniques.

Key words. — American Oystercatcher, automated radio telemetry, breeding, digital VHF telemetry, *Haematopus palliatus*, home range, PTT, satellite telemetry

INTRODUCTION

Advances in tracking technologies are expanding opportunities to collect new information on the movements and space use of shorebirds with important applications to conservation and management efforts (Brown *et al.* 2001; O'Connell *et al.* 2011). Various types of tracking technologies are used to monitor the movements of shorebirds (Warnock and Takekawa 2003; Schwemmer and Garthe 2011; Burger *et al*. 2012), each offering a unique set of tradeoffs in spatial and temporal resolution of location estimates, data storage and acquisition, cost per unit, and weight. Satellite-based Global Positioning System (GPS) technologies offer high spatial accuracy (< 30 m) and sampling rates (one location per sec.; Tomkiewicz *et al*. 2010). However, the lightest available GPS units (currently 1 g) acquire limited numbers of locations (< 100) stored in the unit, requiring recovery of the device (M. van den Tillaart, pers. commun.). Other satellite-based technologies include Platform Transmitter Terminals (PTTs), which estimate locations using the Doppler effect, can obtain multiple locations per day with an optimal accuracy of ≥250 m, and relay data in near-real time to an online server (Argos 2015). However, the smallest available PTTs are still relatively heavy (2 - 5 g) for use on small-bodied shorebird species since tags should be restricted to < 3 - 5% of body mass (Fair *et al*. 2010) and are available on a limited production run basis only (C. Bykowsky, pers. comm.). Further, at thousands of dollars per unit, the high cost of satellite-based tags may preclude robust sample sizes (Hebblewhite and Haydon 2010). Other types of tracking technologies used on shorebirds include light-level geolocators that are light-weight (< 1 g), but are limited to estimating two locations per day and routinely subject to errors of > 200 km, so are of limited use for studies requiring locations with high spatial and temporal resolution (Bridge *et al*. 2011). As with GPS units, geolocators also require that individuals are re-trapped to retrieve the data.

For small-bodied species (< 100 g), radio telemetry remains one of the sole options for collecting frequent, high-accuracy (optimally < 10 m) location data over extended durations (Ponchon *et al*. 2013). Radio transmitters are light-weight (≥ 0.25 g) devices with high pulse-rates (tens to hundreds of signals per minute) and relatively long operating life (> 4 months for 1-g units), that are tracked using specialized antennas and receiving systems (Kenward 1987). Automated radio telemetry stations, consisting of one or more antennas elevated on a mast and connected to a data-logging radio receiver, allow researchers to track animals continuously within target geographic areas (Cochran *et al*. 1965; Larkin *et al*. 1996). Automated radio telemetry has been used to examine shorebird foraging ecology and movements during the nesting period (Sherfy *et al*. 2012.), duration and movements during staging (Verkuil *et al*. 2010), home ranges and local movements on wintering grounds (Leyrer *et al*. 2006), and long-distance movements along migratory corridors (Green *et al*. 2002).

With traditional radio telemetry, each transmitter operates on a unique frequency and receiving systems monitor a single transmitter at a time, resulting in a trade-off between sample size and sampling frequency (Kenward 1987). Recent advances in the development of light-weight, digitally-coded VHF transmitters now make it possible to continuously track the movements of hundreds of individuals on a single frequency (Mills *et al*. 2011; Taylor *et al*. 2011; Woodworth *et al*. 2014). With some limitations, digital VHF telemetry can thus offer a lightweight alternative to satellite-based tracking technologies for monitoring movements of small-bodied species at regional scales.

In this study, we compared digital VHF telemetry and satellite telemetry for estimating length of stay, home range size and distribution, and habitat characteristics of a coastal-nesting shorebird, the American Oystercatcher (*Haematopus palliatus*), on breeding grounds within coastal Massachusetts, USA.

METHODS

Study Area

We conducted fieldwork in eastern Nantucket Sound, Massachusetts, USA (Fig. A-1). We captured and tagged American Oystercatchers on Monomoy National Wildlife Refuge (NWR; 41° 36’ 31.53” N, 69° 59’ 12.86” W), a 30 km^2 barrier beach and island complex, and on Coskata-Coatue Wildlife Refuge on Nantucket Island, Massachusetts (41°19′26.23” N 70°03′49.22” W), a 10 km^2 barrier beach system. Monomoy NWR and adjacent South Beach in Chatham, Massachusetts, support 30 to 35 breeding pairs of American Oystercatchers annually and over 200 individuals during the fall staging period (Schulte *et al*. 2007). Coaskata-Coatue Wildlife Refuge on Nantucket has a high density of nesting sites for American Oystercatchers in the Northeast, supporting up to 40 nesting pairs annually and flocks of 15 to 20 individuals during the fall staging period (Schulte *et al*. 2007).

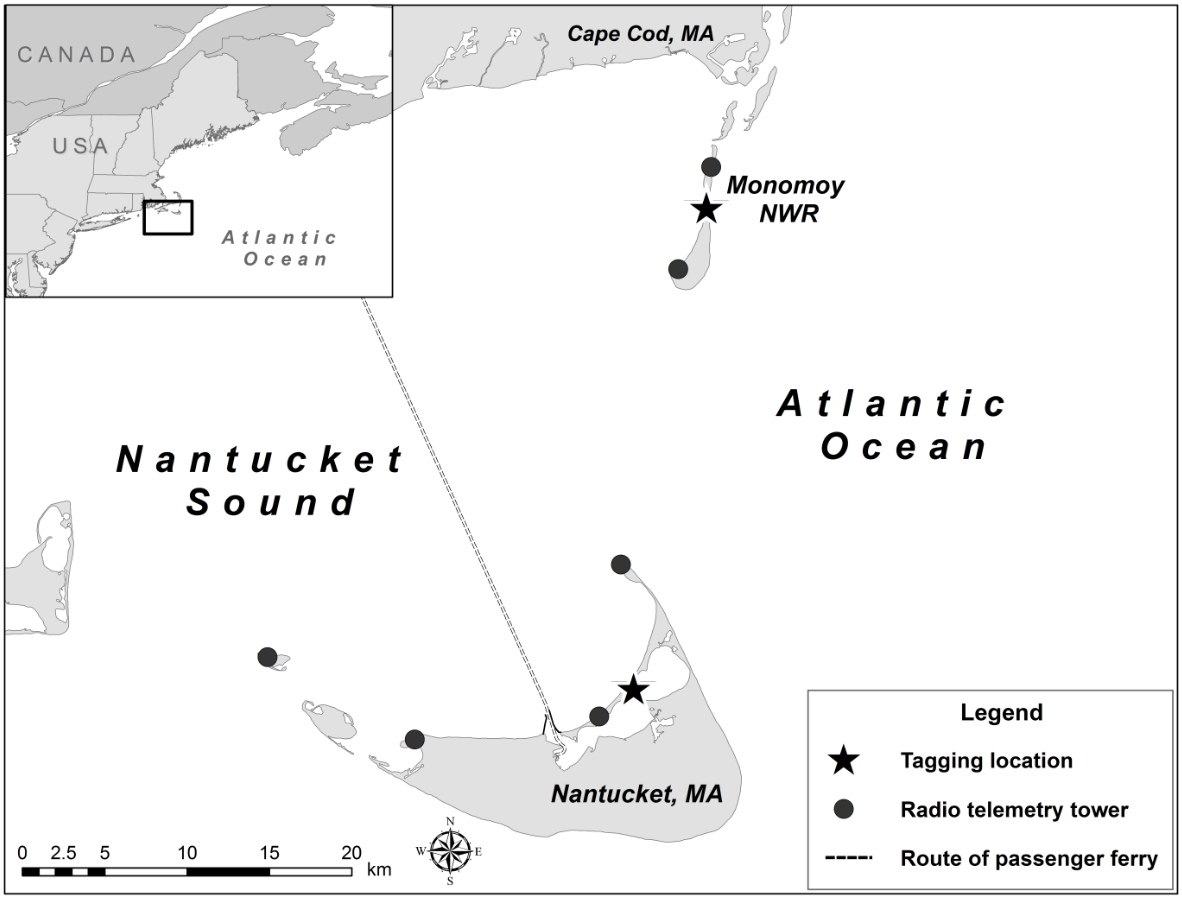

Figure A-1. Map of 2013 study area in coastal Massachusetts, USA, showing tagging locations (black stars) of American Oystercatchers (*n*=5) at breeding sites on Monomoy National Wildlife Refuge (NWR) and Coskata-Coatue Wildlife Refuge (Nantucket), locations of six land-based automated radio telemetry towers (black circles), and the route (dashed line) of an automated radio telemetry receiver on a passenger ferry in Nantucket Sound.

Capture and Transmitter Attachment

From 16 May to 5 June 2013, we used decoys, playback calls, and whoosh nets to capture nesting adult American Oystercatchers during the incubation period. We banded each American Oystercatcher with an incoloy U.S. Geological Survey band below the tarso-metatarsal joint and duplicate engraved color Darvic bands with a unique alpha-numeric combination above each tarso-metatarsal joint. We used a modified version of the figure-8 leg loop harness (Sanzenbacher *et al*. 2000) to attach a combination of a 9.5 g (38 x 17 x 12 mm) solar-powered PTT (Microwave Telemetry, Inc.) and a 1.0 g (11 x 8 x 7 mm) digital VHF transmitter ('Avian NanoTag'; Lotek Wireless, Inc.) to a total of five American Oystercatchers, two from Monomoy NWR and three from Nantucket. We modified the Sanzanbacher design by using Teflon ribbon (4 mm width) as harness ligature, and by gluing a 40 x 20 x 2 mm square of Neoprene fabric to the base of the satellite transmitter to provide padding at the attachment site. The combined weight of the PTT, VHF transmitter, and attachment materials did not exceed 3% of the body mass of each tagged individual. Since there was no overlap in the operating frequencies or harmonics of the PTT (401.650 MHz) and NanoTags (166.380 MHz), we assumed that electrical interference between the two devices was not a factor.

Satellite Telemetry

PTTs were programmed to transmit locations to Argos satellites on a 10 hr on, 24 hr off, duty cycle for an expected operating life of approximately two years. Locations had an optimal accuracy of < 250 m (Argos Accuracy Classification "L3"; Argos 2015) and were relayed to an online server. We used the Douglas-Argos program (Douglas *et al*. 2012) in SAS (SAS Institute 2008) to download and process Argos data transmitted by the PTTs, and retained all locations with estimated accuracy classifications < 500 m (Argos Accuracy Classification "L2") for subsequent analysis.

Digital VHF Telemetry

VHF transmitters were programmed to transmit signals on 166.380 MHz every 5 - 6 seconds, for a total expected operational life of 163 days. Signals from VHF transmitters were received by a network of six automated radio telemetry towers erected at coastal and island sites in eastern Nantucket Sound, Massachusetts (Fig. 1). Each tower consisted of an array of six Yagi antennas end-mounted in a radial configuration atop a 9.2 m mast. Each antenna was separated by 60° with a horizontal plane beam-width of 35°. The antennas were connected to a solar-powered, automated receiving unit (SRX 600; Lotek Wireless, Inc.) that scanned for signals with each antenna for 6.5 seconds in succession, around the clock.

We also operated a receiving station consisting of a SRX-600 receiver equipped with a single omnidirectional (200 W) antenna on a passenger ferry that followed a north-south route across Nantucket Sound two to six times per day. All receiving units were programmed to automatically log several types of data from each antenna, including: transmitter ID number, time stamp (synchronized among all receivers in network using GPS clocks), antenna (defined by receiving station and bearing), and signal strength (non-linear scale: 0 to 255). We tested detection ranges of the radio telemetry stations to ground-level targets by placing a test transmitter at known distances and orientations from the receiving antennas**.** From these tests, we determined that the maximum range of the automated radio telemetry towers with Yagi antennas was approximately 1 km to targets at ground level. The range of the omni-directional antenna on the ferry was < 0.5 km to targets at ground level.

In addition to tracking American Oystercatchers using automated radio telemetry techniques, we also conducted land-based and aerial telemetry surveys to relocate individuals that may have moved outside of the range of our automated radio telemetry array. From June through September 2013, we used land-based VHF telemetry techniques to relocate tagged individuals at nesting, feeding, and roosting sites up to five days per week. During these surveys, we used a hand-held, 3-element Yagi antenna and a SRX-600 receiver to scan for VHF transmitters. We followed individuals on foot and used a hand-held compass to record the bearing of maximum signal strength of the VHF transmitter. When individuals were in view, we estimated their locations using bearings of maximum signal strength and distance. When possible we determined their position using bi-angulation or triangulation techniques from multiple bearing and distance estimates.

From July through September, 19 aerial VHF telemetry surveys were conducted to search for tagged American Oystercatchers along 1,540 km of transects throughout Nantucket Sound and adjacent coastal waters. Transects were flown in a fixed-wing aircraft at an altitude of 229 m (750 ft) and an air speed of approximately 100 knots. The aircraft was equipped with a pair of 4-element, Yagi antennas, mounted at a 45° angle to each strut. Each antenna connected to a SRX-600 receiver via a switchbox that was used to toggle between antennas so that signals could be isolated on one side of the airplane to localize individuals.

We used a filtering algorithm in the statistical program R (R Development Core Team 2015) to remove false detections from the raw VHF telemetry data collected by the automated radio telemetry stations, and during land and boat-based telemetry surveys, based on the following parameters: minimum of three consecutive bursts required to comprise a run, a maximum of 20 consecutive missed bursts allowed within each run, and a maximum deviation of four milliseconds from a tag's unique burst interval between its consecutive bursts (J. Brzustowski, pers. commun.). For aerial telemetry data, we used the same criteria as above but allowed a minimum of two consecutive bursts to comprise a run because the relatively high speed (100 knots) of the aircraft resulted in missed detections of test beacons using the three consecutive burst criteria (P. Loring, unpubl. data).

Data Analyses

We conducted all statistical analyses using the program R (R Development Core Team 2015). We tested for differences between PTTs and VHF transmitters in total number of detections, number of unique days detected, and estimated length of stay in study area using non-parametric Wilcoxon signed-rank tests, since the data were non-normally distributed. To examine home ranges, we randomly selected datasets consisting of 25 locations per individual and transmitter to generate kernel density estimates (Worton 1989). For each dataset, we determined the sample size by visually delineating asymptotes of area-observation curves (Kernohan *et al*. 2001), and randomly sampled locations that were separated in time by a minimum of 12-hrs to reduce serial autocorrelation (Swihart and Slade 1997). We generated home ranges as kernel density estimates (0.95 utilization distributions and 0.50 core use areas) with the software Geospatial Modeling Environment (Beyer 2011), using a Gaussian kernel and cross-validation bandwidth estimator, which has been shown to outperform other estimators when estimating kernel density estimates from sample sizes < 50 (Horne and Garton 2006), and selected a grid size of 250-m to correspond with optimal locational accuracy of the PTTs. We used Wilcoxon signed-rank tests to examine differences between VHF and PTT data in the total area of both 0.95 utilization distributions and 0.50 core-use areas estimated for each bird. We examined static interaction of kernel density estimates (0.95 and 0.50, respectively) by quantifying the proportion of overlap among kernel density estimates generated from VHF and PTT data for each double-tagged bird (Kernohan *et al*. 2001).

We used Environmental Sensitivity Index (ESI) data (National Oceanic and Atmospheric Administration 2004) to compare the proportion of shoreline habitat types within 0.95 utilization distributions and 0.50 core-use areas generated by PTT versus VHF transmitters. ESI habitat types were categorized as coarse-grained sand beaches, fine-grained sand beaches, exposed rocky shores, riprap structures, sheltered human-made structures, salt to brackish marshes, and exposed tidal flats.

RESULTS

Location data were collected from two of the American Oystercatchers until 15 to 19 August, 2013, when the tags were lost as confirmed by band resighting. Locations were collected from two additional individuals later into the season (9 September and 25 October 2013), though PTTs never transmitted locations outside of the study area, indicating transmitter loss or malfunction prior to fall migration. The remaining bird retained its PTT through migration, departing from the study area on 29 October 2013 to wintering areas in the southeastern United States, where it transmitted location data through 4 January 2014.

The mean (± SE) number of locations with estimated accuracy ≤ 500 m recorded per tagged individual was 317 (± 42) for PTTs and 375 (± 169) for VHF transmitters, with no significant difference among transmitter type (Wilcoxon Signed Rank Test $V = 8$, $P = 1$; Table A-1). A higher mean (± SE) proportion of PTT locations per individual were obtained within the < 250 m accuracy class (0.61 ± 0.01) than the 250 to 500 m accuracy class (0.39 ± 0.01; Table A-1). For VHF transmitters, the mean (± SE) proportion of locations recorded per bird was similar between those detected by automated radio telemetry stations (0.50 ± 0.20) and by manual telemetry surveys (0.50 ± 0.20; Table 1). However, the mean (± SE) number of days that each bird was detected was higher (Wilcoxon Signed Rank Test $V = 0$, $P = 0.062$) for PTTs (61 ± 5 days) than VHF transmitters (30 ± 10 days), indicating that PTT locations were more evenly sampled in time than VHF locations (Table A-2). The PTT data also indicated a slightly longer (Wilcoxon Signed Rank Test V = 0, $P = 0.063$) mean length of stay in the study area (118 ± 12 days) than did the VHF data (108 days ± 11; Table A-2).

Three American Oystercatchers provided enough data for comparisons of utilization distributions between their PTT and VHF locations (Figs. A-2 to A-4). For these three individuals, estimates of mean (± SE) fixed kernel 95% utilization distribution and 50% core-use areas estimated from PTT locations did not significantly differ (Wilcoxon Signed-Rank Test $V = 5$, $P = 0.5$ for 95% UD and V = 3, $P = 1$ for 50% CU) from estimates of mean fixed kernel 95% home range and 50% core use areas estimated from VHF locations (Table A-3). Mean (± SE) percent spatial overlap of kernel density estimates from satellite telemetry and digital VHF telemetry was 67% (± 6%) for 95% utilization distributions and 32% (± 11%) for 50% core use areas.

The mean (± SE) proportion of shoreline habitat types in the 95% utilization distributions was similar between satellite telemetry estimates and VHF telemetry estimates, and was predominantly coarse-grained sand beaches (0.58 ± 0.22 and 0.58 ± 0.21) and salt to brackish marshes (0.29 ± 0.20 and 0.19 ± 0.12), with lesser mean proportions (≤ 0.15) of riprap structures, exposed rocky shorelines, sheltered human-made structures, fine-grained sand beaches, and exposed tidal flats (Fig. A-5A). Similar to the 95% utilization distributions, mean (± SE) proportion of habitat types within 50% core use areas for both satellite and VHF telemetry estimates was predominantly coarse-grained sand beaches (0.63 ± 0.20 and 0.77 ± 0.18, respectively), and salt to brackish marshes (0.24 ± 0.13 and 0.06 ± 0.03, respectively), with lesser proportions (≤ 0.05) of the other shoreline habitat types (Fig. A-5B).

Table A-1. Identification number (ID) and frequency count (*n*) of locations of American Oystercatchers estimated by satellite Platform Transmitter Terminals (PTT) and VHF radio transmitters on breeding grounds in coastal Massachusetts in 2013. Proportions are shown for PTT locations by estimated accuracy intervals (LC 3: < 250 m and LC 2: 250 to < 500 m), and for VHF locations by tracking method: automated radio telemetry tower (Tower), receiving station on passenger ferry (Ferry), land-based radio telemetry survey (Land), and aerial radio telemetry survey (Aerial).

			Proportion of locations by type					
	Locations (n)		PTT		VHF			
ID	PTT	VHF	LC3	LC2	Tower	Ferry	Land	Aerial
68	240	48	0.65	0.35	0.00	0.00	0.85	0.15
69	326	950	0.59	0.41	0.13	0.70	0.14	0.03
70	208	297	0.58	0.42	0.45	0.46	0.08	0.01
71	386	53	0.63	0.37	0.00	0.00	0.00	1.00
72	427	529	0.62	0.38	0.75	0.00	0.00	0.25

Table A-2. Identification number (ID), capture site (Coskata-Coatue Wildlife Refuge, Nantucket [Nantucket] and Monomoy National Wildlife Refuge [Monomoy]), capture date, number of unique days tracked (unique days), estimated length of stay in study area, and last date in study area for American Oystercatchers (*n*=5) fitted with satellite Platform Transmitter Terminals (PTTs) and VHF transmitters on breeding grounds in coastal Massachusetts in 2013.

			Unique days		Length of stay		Last date in study area	
ID	Capture site	Capture date	PTT	VHF	PTT	VHF	PTT	VHF
68	Nantucket	05/16/13	52	9	90	83	08/07/13	08/14/13
69	Nantucket	05/17/13	62	47	115	111	09/05/13	09/09/13
70	Nantucket	05/16/13	46	28	95	90	08/14/13	08/19/13
71	Monomoy	6/5/2013	71	10	142	112	09/25/13	10/25/13
72	Monomoy	6/5/2013	73	57	146	145	10/28/13	10/29/13

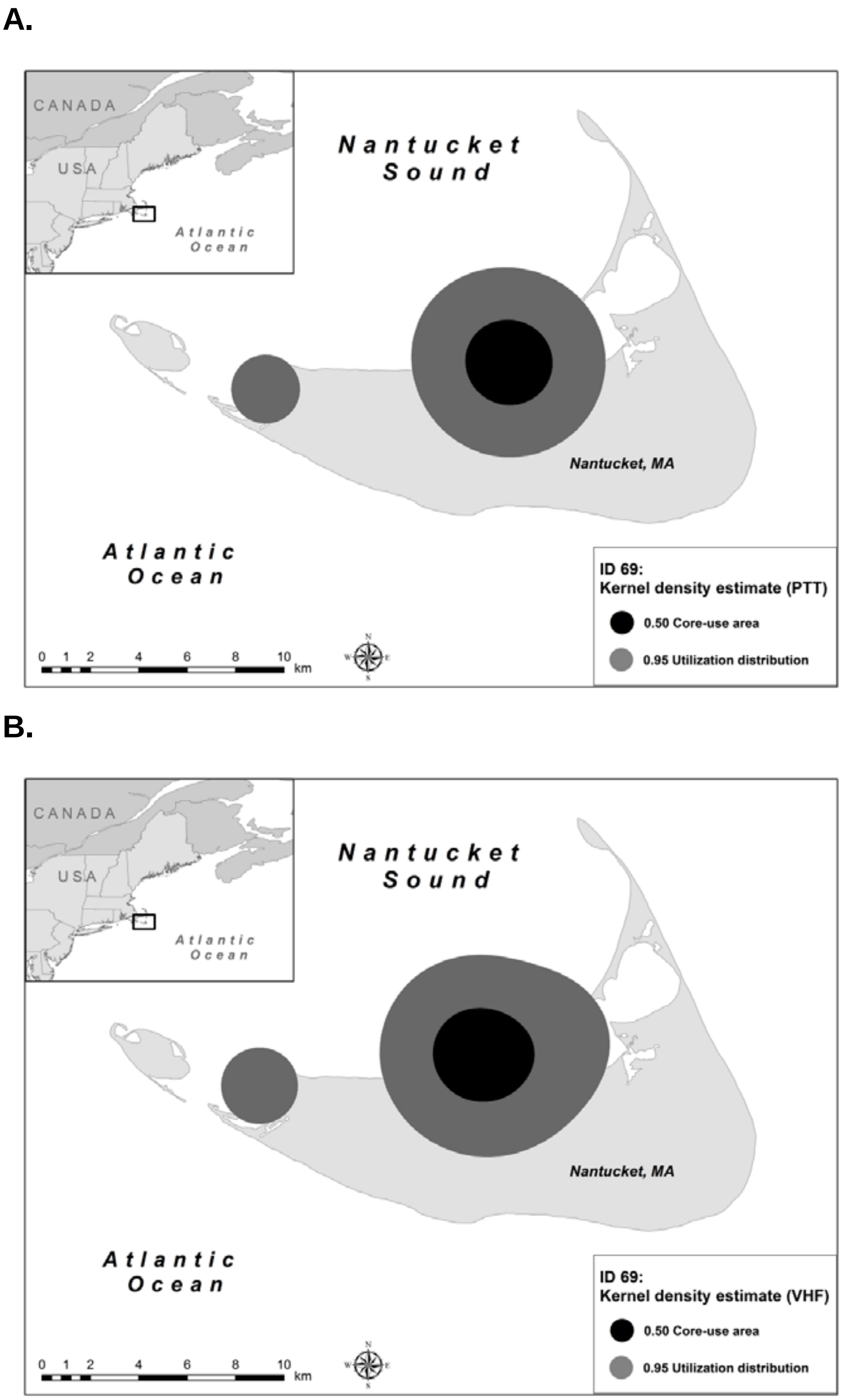

Figure A-2. Kernel density estimate (KDE) of the core-use areas (dark grey, 50% isopleth) and utilization distribution (light grey, 95% isopleth) of a double-tagged American Oystercatcher (ID number 69), estimated by locations from a satellite Platform Transmitter Terminal (PTT; A-2-A, top) and a VHF radio transmitter (A-2-B, bottom) on breeding grounds in coastal Massachusetts during 2013.

A.

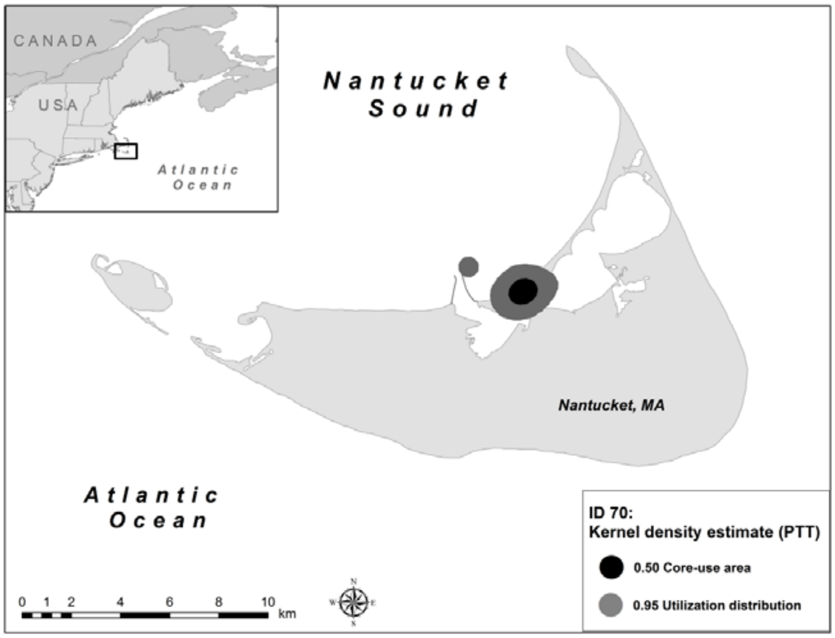

B.

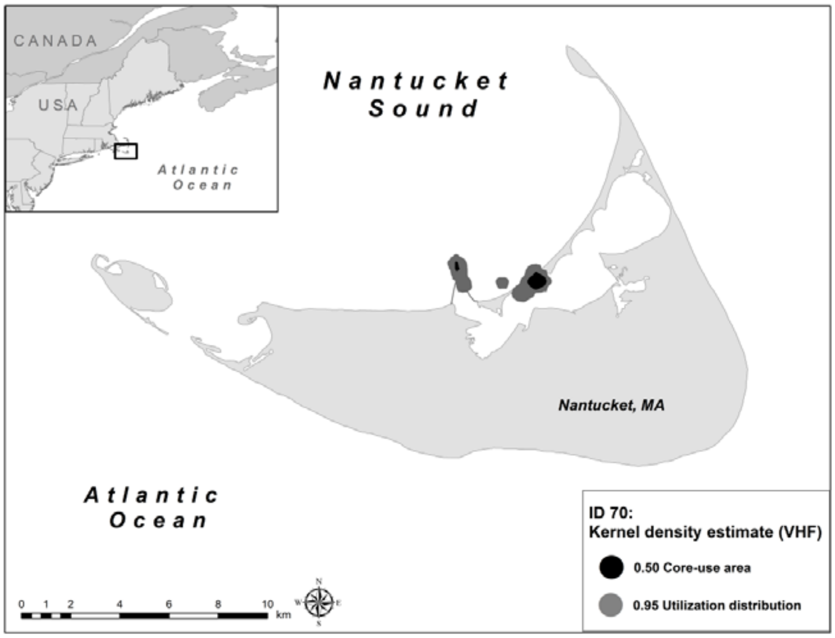

Figure A-3. Kernel density estimate (KDE) of the core-use areas (dark grey, 50% isopleth) and utilization distribution (light grey, 95% isopleth) of a double-tagged American Oystercatcher (ID number 70), estimated by locations from a satellite Platform Transmitter Terminal (PTT; A-3-A) and a VHF radio transmitter (A-3-B) on breeding grounds in coastal Massachusetts during 2013.

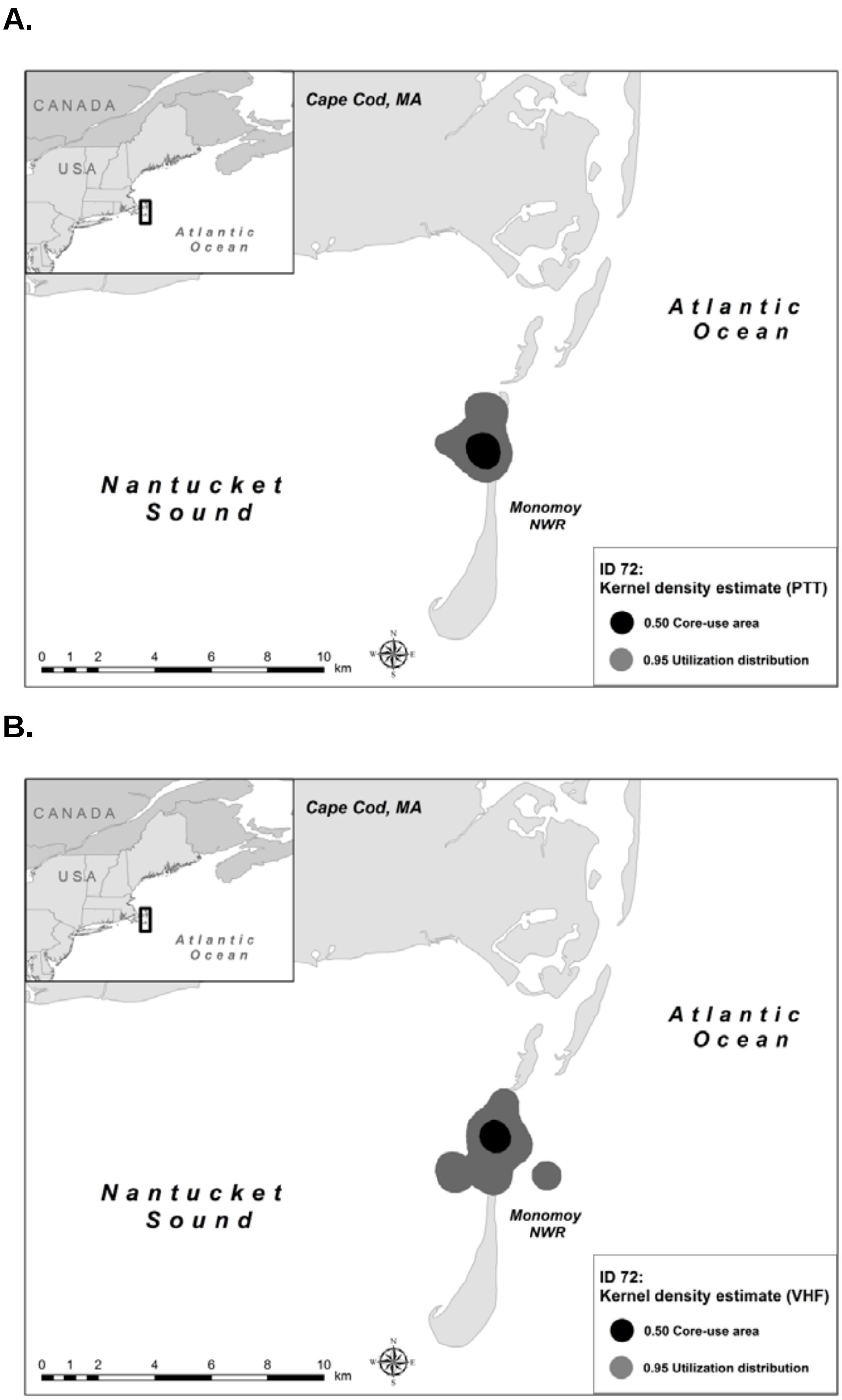

Figure A-4. Kernel density estimate (KDE) of the core-use areas (dark grey, 50% isopleth) and utilization distribution (light grey, 95% isopleth) of a double-tagged American Oystercatcher (ID number 72), estimated by locations from a satellite Platform Transmitter Terminal (PTT; A-4-A) and a VHF radio transmitter (A-4-B) on breeding grounds in coastal Massachusetts during 2013.

Table A-3. Total area (km^2) by transmitter type and percent (%) overlap between transmitter type of individual core-use areas (50% isopleth) and utilization distributions (95% isopleth) for American Oystercatchers (*n*=3) fitted with satellite Platform Transmitter Terminals (PTTs) and VHF transmitters on breeding grounds in coastal Massachusetts in 2013.

	Area (km^2)							
	50%		95%		Overlap (km^2)		Overlap (%)	
ID	PTT	VHF	PTT	VHF	50%	95%	50%	95%
69	10.11	12.89	56.27	70.29	6.85	52.01	53	74
70	1.02	0.46	5.46	2.79	0.12	1.99	25	71
72	1.30	1.05	5.87	8.71	0.18	4.85	17	56

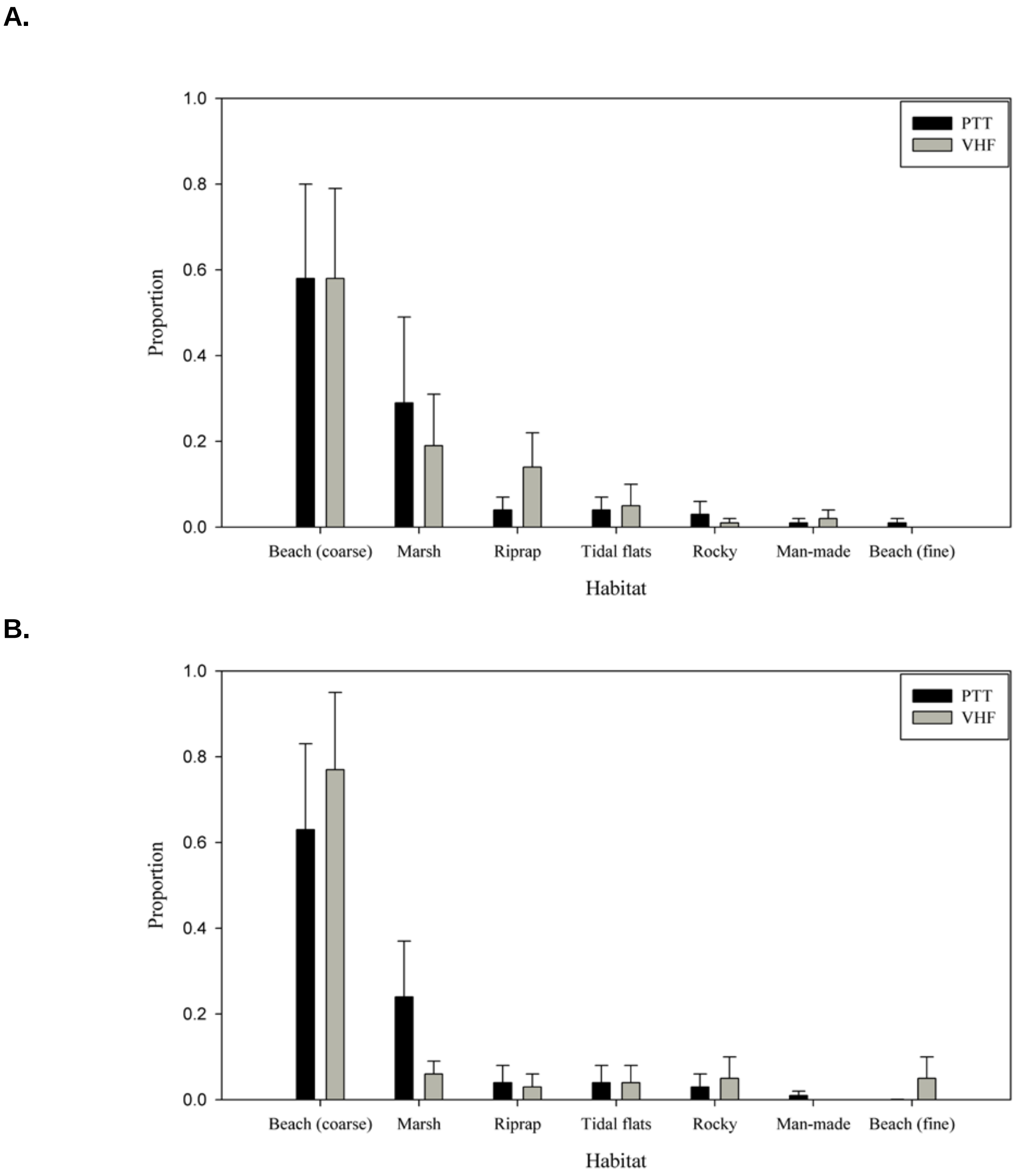

Figure A-5. Mean (± SE) proportion of shoreline habitat type comprising the core-use areas (50% isopleth; A-5-A) and utilization distributions (95% isopleth; A-5-B) estimated by locations from satellite Platform Transmitter Terminals (PTT, black) and VHF radio transmitters (grey) fitted to American Oystercatchers (*n* = 3) on breeding grounds in coastal Massachusetts in 2013.

DISCUSSION

Our study found that digital VHF telemetry generally performed similarly to satellite telemetry for quantifying timing and space-use of American Oystercatchers on their breeding grounds, although the scope of inference from our results is limited due to small sample sizes and tag loss. Estimates of length of stay and home range size should be considered a minimum since the majority of tagged individuals in our study lost their back-pack units prior to departing from the study area. However, metrics obtained from PTTs could still be directly compared to those obtained from VHF transmitters because individual American Oystercatchers dropped their PTT and VHF transmitters simultaneously.

Studies on Black Oystercatcher (*Haematopus bachmani*) have also reported poor retention of dorsal-mounted transmitters attached with similar leg-loop harnesses (e.g., Johnson *et al*. 2010). Double-layered teflon ribbon harnesses may help improve retention, however to our knowledge this has not been widely field tested. Other methods of attaching transmitters to shorebirds including coelemic implants and epoxy to the leg band (Warnock and Takekawa 2003), may also increase retention time. However, injuries (Nisbet *et al*. 2011) and high mortality rates (Johnson *et al*. 2010) have been associated with these techniques.

In our study, three of five VHF tags and all five PTTs provided enough data to estimate home ranges. Due to the small sample size and high variability, our results should be interpreted cautiously (Kernohan *et al*. 2001). However, the home range sizes of American Oystercatchers in our study are consistent with other studies reporting individual-based movements of *Haematopus* oystercatchers on breeding grounds, and documented movements between nesting and foraging areas that ranged from < 1 km (Ens *et al*. 1992; Virzi and Lockwood 2010; Schwemmer and Garthe 2011) to over 5 km (Schwemmer and Garthe 2011). Within home ranges, American Oystercatchers in our study primarily used coarse-grained sand and marsh habitats, a finding similar to several other studies (Nol and Humphrey 2012). Due to sample size limitations, we did not have enough data ($n = 6$ individuals) to statistically compare habitat use between VHF and PTT location estimates (Aebischer *et al*. 1993).

Estimates of timing, home range size, and habitat proportion were generally similar between VHF and PTT data. However, because the VHF locations were more clumped in time and space than PTTs, the PTTs were detected on twice as many unique days relative to VHF transmitters. The extent of spatial overlap among home range estimates from PTTs and VHF locations was also variable. These differences in the spatial and temporal resolution between VHF and PTT data likely resulted from the way locations were acquired using each tracking technology. The VHF transmitters were programmed to emit signals every five to six seconds, but needed to be within range of an automated radio telemetry station, or detected during manual telemetry surveys, to be relocated. The PTTs, in contrast, transmitted signals every 90 to 200 sec. during a 10-hr transmission period, which occurred every 24 hrs, and needed only to be within range of visibility of polar-orbiting satellites to acquire a location. The clear advantage of satellite-based tracking technology over VHF technology is that it permits systematic sampling anywhere on the globe, so it is an especially suitable tool for studying the movements of wide-ranging species (Hebblewhite and Haydon 2010). However, the spatial and temporal resolution of PTT data is relatively coarse, and PTTs require prolonged off periods necessary for conserving battery power. In contrast, VHF locations can achieve optimal accuracy of < 10 m, and can be monitored nearly continuously through targeted geographic areas using automated radio telemetry stations as long as tagged individuals are within range of a receiver (Bridge *et al*. 2011).

To maximize the quality of location estimates from automated radio telemetry stations, it is important to consider the height, spacing, and positioning of antennas, and the life histories of target species. Accuracy of position estimates is improved when antenna beams from multiple stations detect animals simultaneously (White and Garrott 1990), so the home range size of target species and detection range of the telemetry system should be considered when siting automated radio telemetry stations on the landscape. Maximizing detection range also depends largely on maximizing antenna height (Cochran 1980), and since VHF waves emitted by transmitters travel within line-of-sight, factors such as topography, vegetation, and electronic noise can block, reflect, or attenuate the signal (Kenward 1987).

Conducting regular telemetry surveys, by foot, boat, or plane is an effective way to supplement locations collected by the automated radio telemetry towers, and relocate individuals that may have moved outside the range of automated radio telemetry towers. Land-based telemetry surveys can be used to search for tags within targeted areas, and facilitate direct observations of marked individuals that can be combined with behavioral or *in situ* habitat sampling. By comparison, boat-based and aerial telemetry surveys permit systematic searches over larger geographic areas While conventional telemetry surveys are useful for searching for individuals that may have moved outside of the detection range of automated radio telemetry stations, these surveys can incur considerable effort, personnel, and travel costs. The cost of the tracking VHF transmitters is scaled according to the number of VHF transmitters deployed on the shared frequency, and may be partially offset by coordinating efforts with complimentary studies, cost comparisons of tracking VHF transmitters and PTTs are not straightforward. Ground work is useful for supplementing VHF stations but may not be necessary depending on the objectives and design of the telemetry study. Conventional telemetry surveys are most effective for studies where tagged individuals do not range widely, such as tracking American Oystercatchers on their breeding grounds. Remote tracking of satellite-tagged individuals is thus more suitable for studies covering a wider geographic extent, such as migration.

Despite the considerable resources required to track VHF transmitters over long-distances, efforts are underway in the western Hemisphere to coordinate digital VHF tracking projects and receiving stations on a shared frequency (e.g., the Motus Wildlife Tracking System.), allowing for thousands of tagged animals to be detected on an expanding network of receiving stations throughout North and South America. Thus, with strategic deployment and coordination of receiving equipment, digital VHF telemetry can now be used to track land-scape scale movements of birds with relatively high spatial and temporal resolution, something that was recently only possible with satellite-based technologies. However, satellite-based technologies remain the sole option for global, high-resolution wildlife tracking throughout the annual cycle.

ACKNOWLEDGMENTS

This study was funded in part by the U.S. Department of the Interior, Bureau of Ocean Energy Management through Interagency Agreement M13PG00012 with the U.S. Department of the Interior, Fish and Wildlife Service. This work was also funded in part by the U.S. Fish and Wildlife Service Division of Migratory Birds, Northeast Region; and the National Science Foundation IGERT Offshore Wind Energy Program at the University of Massachusetts Amherst. We also thank the staff at Monomoy National Wildlife Refuge, Nantucket Conservation Foundation, Nantucket National Wildlife Refuge, Manomet Center for Conservation Sciences, Nantucket Islands Land Bank, and UMass Boston Nantucket Field Station for providing field and logistical support. Cape Wind Avian Pre-Construction Monitoring Program provided supplemental aerial survey data. Shearwater Excursions and HyLine Cruises provided boat support. P. Taylor and J. Brzustowski of Acadia University and Stuart Mackenzie of Bird Studies Canada provided technical support and coordination with digital radio telemetry data. American Oystercatchers were tagged under Federal Bird Banding Permit 23140 and Massachusetts State Scientific Collecting Permit 022.13BB. This research was conducted under the approval of the University of Massachusetts Amherst Institutional Animal Care and Use Committee (protocol 2013-0024).

LITERATURE CITED

Aebischer, N. J., P. A. Robertson and R. E. Kenward. 1993. Compositional analysis of habitat use from animal radio-tracking data. Ecology 74: 1313-1325.

American Oystercatcher Working Group, E. Nol and R. C. Humphrey. 2012. No. 082 in The Birds of North America Online (A. Poole, Ed.). Cornell Lab of Ornithology, Ithaca, New York. http://bna.birds.cornell.edu/bna/species/082, accessed 3 June 2015.

Argos. 2015. Argos user's manual. Collecte Localisation Satellites/Argos, Toulouse, France. http://www.argos-system.org, accessed 30 June 2015.

Beyer. 2011. Geospatial modelling environment software v. 0.7.2.1. Spatial Ecology, LLC, Toronto, Canada. http://www.spatialecology.com/gme, accessed 10 June 2015.

Bridge, E. S., K. Thorup, M. S. Bowlin, P. B. Chilson, R. H. Diehl, R. W. Fléron, P. Hartl, R. Kays, J. F. Kelly and W. D. Robinson. 2011. Technology on the move: recent and forthcoming innovations for tracking migratory birds. BioScience 61: 689-698.

Brown, S., C. Hickey, B. Harrington and R. Gill, Eds. 2001. The U. S. Shorebird conservation plan, 2nd ed. Manomet Center for Conservation Sciences, Manomet, Massachusetts.

Burger, J., L. J. Niles, R. R. Porter, A. D. Dey, S. Koch and C. Gordon. 2012. Migration and over-wintering of Red Knots (*Calidris canutus rufa*) along the Atlantic Coast of the United States. Condor 114: 302-313.

Cochran, W. W. 1980. Wildlife telemetry. Pages 507-520 *in* Wildlife Management Techniques (S. P. Schemnitz, Ed.), 4th ed. The Wildlife Society, Inc., Washington, D.C.

Cochran, W. W., D. W. Warner, J. R. Tester and V. B. Kuechle. 1965. Automatic radio-tracking system for monitoring animal movements. BioScience 15: 98-100.

Douglas, D. C., R. Weinzierl, S. C. Davidson, R. Kays, M. Wikelski and G. Bohrer. 2012. Moderating Argos location errors in animal tracking data. Methods in Ecology and Evolution 3: 999-1007.

Ens, B. J., M. Kersten, A. Brenninkmeijer and J. B. Hulscher. 1992. Territory quality, parental effort and reproductive success of oystercatchers (*Haematopus ostralegus*). Journal of Animal Ecology 61: 703-715.

Fair, J. M., E. Paul, J. Jones, A. B. Clark, C. Davie and G. Kaiser. 2010. Guidelines to the Use of Wild Birds in Research. Third edition. Ornithological Council, Washington, DC. www.nmnh.si.edu/BIRDNET/guide, accessed 21 July 2015.

Green, M., T. Piersma, J. Jukema, P. De Goeij, B. Spaans and J. Van Gils. 2002. Radio-telemetry observations of the first 650 km of the migration of Bar-tailed Godwits (*Limosa lapponica)* from the Wadden Sea to the Russian Arctic. Ardea 90: 71-80.

Hebblewhite, M. and D. T. Haydon. 2010. Distinguishing technology from biology: a critical review of the use of GPS telemetry data in ecology. Philosophical Transactions of the Royal Society of London B: Biological Sciences 365: 2303-2312.

Horne, J. S. and E. O. Garton. 2006. Likelihood cross-validation versus least squares cross-validation for choosing the smoothing parameter in kernel home-range analysis. Journal of Wildlife Management 70: 641-648.

Johnson, M., P. Clarkson, M. I. Goldstein, S. M. Haig, R. B. Lanctot, D. F. Tessler and D. Zwiefelhofer. 2010. Seasonal movements, winter range use, and migratory connectivity of the Black Oystercatcher. Condor 112: 731-743.

Kenward, R. 1987. Wildlife radio tagging. Academic Press, San Diego, California.

Kernohan, B. J., R. A. Gitzen and J. J. Millspaugh. 2001. Analysis of animal space use and movements. Pages 125-166 *in* Radio tracking and animal populations (J.J. Millspaugh and J.M. Marzluff, eds). Academic Press, San Diego, California.

Larkin, R. P., A. Raim and R. H. Diehl. 1996. Performance of a non-rotating direction-finder for automatic radio tracking. Journal of Field Ornithology 67: 59-71.

Leyrer, J., B. Spaans, M. Camara and T. Piersma. 2006. Small home ranges and high site fidelity in Red Knots (*Calidris c. canutus*) wintering on the Banc d'Arguin, Mauritania. Journal of Ornithology 147: 376-384.

Mills, A. M., B. G. Thurber, S. A. Mackenzie and P. D. Taylor. 2011. Passerines use nocturnal flights for landscape-scale movements during migration stopover. Condor 113: 597-607.

National Oceanic and Atmospheric Administration. 2004. Sensitivity of Coastal Environments and Wildlife to Spilled Oil: Massachusetts. Unpublished report, National Ocean Service, Office of Response and Restoration, Hazardous Materials Response Division, Seattle, Washington and the Coastal Services Center, Charleston, South Carolina. http://response.restoration.noaa.gov/maps-and-spatial-data/download-esi-maps-and-gis-data.html, accessed 15 June, 2015.

Nisbet, I. C. T., C. S. Mostello, R. R. Veit, J. W. Fox and V. Afanasyev. 2011. Migrations and winter quarters of five Common Terns tracked using geolocators. Waterbirds 34: 32-39.

O'Connell, A., C. S. Spiegel and S. M. Johnston. 2011. Compendium of Avian Occurrence Information for the Continental Shelf Waters along the Atlantic Coast of the United States, Final Report (Database Section - Shorebirds). Unpublished report, U.S. Department of the Interior, Fish and Wildlife Service, Hadley, Massachusetts.

Ponchon, A., D. Gremillet, B. Doligez, T. Chambert, T. Tveraa, J. González-Solís and T. Boulinier. 2013. Tracking prospecting movements involved in breeding habitat selection: insights, pitfalls and perspectives. Methods in Ecology and Evolution 4: 143-150.

R Development Core Team. 2015. R: a language and environment for statistical computing v. 3.0.2. R Foundation for Statistical Computing, Vienna, Austria. http://www.R-project.org/, accessed 17 May 2015.

Sanzenbacher, P., S. M. Haig and L. W. Oring. 2000. Application of a modified harness design for attachment of radio transmitters to shorebirds. Wader Study Group Bulletin 91: 16-20.

SAS Institute, Inc. 2008. SAS statistical software v. 9.2. SAS Institute, Inc., Cary, North Carolina.

Schwemmer, P. and S. Garthe. 2011. Spatial and temporal patterns of habitat use by Eurasian Oystercatchers (*Haematopus ostralegus*) in the eastern Wadden Sea revealed using GPS data loggers. Marine Biology 158: 541-550.

Sherfy, M. H., M. J. Anteau, T. L. Shaffer, M. A. Sovada and J. H. Stucker. 2012. Foraging ecology of least terns and piping plovers nesting on central Platte River sandpits and sandbars. Open-File Report 2012-1059, U.S. Department of the Interior, U.S. Geological Survey, Reston, Virginia.

Swihart, R. K. and N. A. Slade. 1997. On testing for independence of animal movements. Journal of Agricultural, Biological, and Environmental Statistics 2: 48-63.

Taylor, P. D., S. A. Mackenzie, B. G. Thurber, A. M. Calvert, A. M. Mills, L. P. McGuire and C. G. Guglielmo. 2011. Landscape movements of migratory birds and bats reveal an expanded scale of stopover. PLOS ONE 6:e27054.

Tomkiewicz, S. M., M. R. Fuller, J. G. Kie and K. K. Bates. 2010. Global positioning system and associated technologies in animal behaviour and ecological research. Philosophical Transactions of the Royal Society of London B: Biological Sciences 365: 2163-2176.

Verkuil, Y. I., J. J. Wijmenga, J. C. E. W. Hooijmeijer and T. Piersma. 2010. Spring migration of Ruffs *Philomachus pugnax* in Fryslân: estimates of staging duration using resighting data. Ardea 98: 21-33.

Virzi, T. and J. L. Lockwood. 2010. Conservation of American Oystercatchers in New Jersey. Unpublished report. Unpublished report, Rutgers, New Brunswick, New Jersey.

Warnock, N. and J. Y. Takekawa. 2003. Use of radio telemetry in studies of shorebirds: past contributions and future directions. Wader Study Group Bulliten. 100: 138-150.

White, G. and R. Garrott. 1990. Analysis of wildlife radio-tracking data. Academic Press, San Diego, California.

Woodworth, B. K., C. M. Francis and P. D. Taylor. 2014. Inland flights of young Red-eyed Vireos *Vireo olivaceus* in relation to survival and habitat in a coastal stopover landscape. Journal of Avian Biology 45: 387-395.

Worton, B. J. 1989. Kernel methods for estimating the utilization distribution in home-range studies. Ecology 70: 164-168.

Appendix B

Post-breeding dispersal and staging of Common and Arctic Terns throughout the western North Atlantic

Pamela H. Loring[1], Robert A. Ronconi[2,3], Linda J. Welch [4], Philip D. Taylor [2] and Mark L. Mallory [2]

[1]U.S. Fish and Wildlife Service, Division of Migratory Birds, Northeast Region, Hadley, MA, USA
[2]Acadia University, Wolfville, NS, Canada
[3]Canadian Wildlife Service, Environment and Climate Change Canada, Dartmouth, NS, Canada
[4]U.S. Fish and Wildlife Service, Maine Coastal Islands NWR, Milbridge, ME, USA

Citation: Loring PH, Ronconi RA, Welch LJ, Taylor PD, Mallory ML. 2017. Post-breeding dispersal and staging of Common and Arctic Terns throughout the western North Atlantic. Avian Conservation and Ecology 12(2):20.

Abstract. — In the western North Atlantic, Common (*Sterna hirundo*) and Arctic (*S. paradisaea*) Terns are sympatric at breeding colonies but show divergent migration strategies to coastal areas of South America and pelagic regions of the Antarctic, respectively. During 2013, we studied postbreeding movements of adult Common (n = 130) and Arctic (n = 52) Terns from four breeding colonies in the eastern USA and Canada using digital very high frequency (VHF) transmitters and an array of 62 automated radio telemetry towers. Relative to hatch dates at respective colonies, Arctic Terns departed breeding sites an average of eight days later than Common Terns. Common Terns were detected during the postbreeding period by coastal towers upward of 850 km south of their original nesting sites. The telemetry array detected postbreeding movements of Arctic Terns from the Petit Manan Island colony in the Gulf of Maine as they traveled eastward past Nova Scotia, Canada, mostly during the night. Nantucket Sound, Massachusetts, USA was identified as an important staging area for Common Terns from all colonies, whereby 26% of 53 tagged Common Terns from colonies in the Gulf of Maine and Canada were detected for up to three weeks. Common Terns typically arrived at Nantucket Sound within 2 h of sunset, 2 to 10 days after their last detection at Gulf of Maine and Canadian colonies, suggesting rapid postbreeding dispersal. Postbreeding dispersal of Arctic Terns was poorly documented with the telemetry array, suggesting that this species is not using coastal sites for staging, and is instead departing directly from colonies to offshore staging areas prior to long-distance migrations. We conclude that digital VHF telemetry is a useful method for monitoring regional movements of Common Terns, but additional offshore receiving stations are needed to effectively monitor movements of Arctic Terns away from their nesting colonies.

Key words. — Arctic Tern; automated radio telemetry; Common Tern; dispersal; seabird; staging; Sterna hirundo; Sterna paradisaea; very high frequency (VHF) tags.

INTRODUCTION

During the post-breeding period, seabirds use various dispersal and staging strategies to build energy reserves for migration (Huettmann and Diamond 2000, Klaassen et al. 2011, Montevecchi et al. 2012). High-quality staging areas provide sufficient space for roosting aggregations, abundant prey, and minimal disturbance by humans and predators (Warnock 2010). Species that disperse along the coast may use persistent staging areas with reliable roosting and foraging habitats (Trull et al. 1999), whereas species that roost and feed offshore may use dynamic staging areas in response to patchy prey distributions (Suryan et al. 2006, Guilford et al. 2009, Hedd et al. 2012). Advances in tracking technologies are increasing our understanding of the connectivity between nesting populations and staging areas of seabirds (Mosbech et al. 2012, Gilg et al. 2013, van der Winden et al. 2014). However, detailed information on post-breeding dispersal and staging movements is lacking for many species of seabirds, such as the small-bodied terns, due to limitations of the spatial and temporal resolution of lightweight tracking devices (Bridge et al. 2011).

In the western North Atlantic, from southern Labrador, Canada (52° N) to Cape Cod, Massachusetts, USA (41° N), the breeding ranges of Common (*Sterna hirundo*) and Arctic (*S. paradisaea*) Terns overlap and the two species nest sympatrically on nearshore and offshore islands (Kress et al. 1983, Gaston et al. 2009). The wintering ranges of these populations are geographically separated, with Common Terns wintering along the coasts of Central and South America (Hays et al. 1997, Nisbet et al. 2011*a*), and Arctic Terns wintering along the Antarctic pack ice (Hatch 2002). The migratory routes of the two species differ substantially. Austin (1928) proposed that Arctic Terns used an oceanic route to get to their (then unknown) wintering areas, based on observations during August between Ireland and Newfoundland from a ship at sea. Salomonsen (1967) assessed the state of the knowledge of the migration and wintering areas of Arctic Tern and provided evidence for an easterly movement of the species from the northeastern North American breeding populations during autumn. The oceanic route is also consistent with the sparse records for the species along the east coast of North America in the autumn (Lee and Cardiff 1993). In recent years, studies using archival light-level loggers (geolocators) have shown that Common Terns migrate south across the western North Atlantic toward Puerto Rico (Nisbet et al. 2011*a*) whereas Arctic Terns breeding in East Greenland stage in oceanic areas of the central North Atlantic (Egevang et al. 2010). Arctic Terns from breeding colonies in eastern North America stage offshore in the North Atlantic and then also follow an oceanic route to their wintering areas (L. Welch, unpublished data).

Prior to migration, mixed flocks of terns (primarily Common and Roseate (*S. dougallii*) Terns) stage at sites along the USA Atlantic coast from Maine through New Jersey (Shealer and Kress 1994, Nisbet 2002), with large flocks of over >10,000 terns reported on Cape Cod, Massachusetts (Trull et al. 1999). Consistent with their trans-Atlantic migratory route, Arctic Terns are rarely seen staging at these coastal sites, but are thought to stage at offshore sites, specifically Sable Island, Canada (Ronconi et al. 2016a), though it is not known if these staging birds are only from local colonies on the island or include breeding birds dispersing from mainland sites.

Although Common and Arctic Terns target similar species of prey fish and invertebrates (Rock et al. 2007) differences in the proportions of prey types consumed by each species, and differences in habitat use, with Common Terns tending to feed inshore and Arctic Terns tending to feed offshore, suggest a degree of resource partitioning (Braune and Gaskin 1982, Hall et al. 2000, Hatch 2002). These differences in habitat and foraging behavior, coupled with the known differences in their migratory routes, suggests that patterns of movement during the post-breeding season (post-breeding staging and dispersal) would likely differ between the species. Here we present the results of a study of the post-breeding movements of Common and Arctic Terns from four nesting colonies in the western North Atlantic extending from Nova Scotia, Canada to Massachusetts, USA.

The objectives of our study were to: 1) quantify the length of stay at four nesting colonies in the region, 2) determine the extent to which individuals from those nesting colonies staged at sites within the telemetry array (specifically: South Monomoy Island off the coast of Cape Cod, Massachusetts, USA and Sable Island off the coast of Nova Scotia, Canada), and 3) determine the timing and length of stay at these staging sites and the ultimate timing of departure from the study area. To accomplish these objectives, we employed digital Very High Frequency (VHF) radio transmitters and an array of coordinated automated radio telemetry stations (Motus telemetry array; Taylor et al. 2017) to track the post-breeding dispersal of these small-bodied seabirds at a regional scale.

METHODS

Study area

During 2013, we tagged individual terns at four breeding colonies ranging from northeastern Nova Scotia, Canada to Massachusetts, USA (Fig. B-1). Petit Manan Island (44°21' N, 67°52' W) is a 6.5-ha island situated approximately 4 km off the coast of Maine, USA and supports a mixed colony of about 1,370 pairs of Common and Arctic Terns (Gulf of Maine Working Seabird Group (GOMSWG) 2013). Country Island (45°06' N, 61°32' W), is a 19-ha island located approximately 5 km off the east coast of Nova Scotia, Canada and contains a mixed colony of about 1,300 pairs of Common and Arctic Terns (GOMSWG 2013). Sable Island (43°55' N, 60°00' W) is a 40 km long, crescent-shaped, 3,400-ha island located approximately 180 km offshore from mainland Nova Scotia, Canada. Approximately 4,200 pairs of Common and Arctic Terns nested in multiple colonies on Sable Island during recent surveys in 2013 (Ronconi et al. 2016b). Monomoy National Wildlife Refuge (NWR; 41°37' N, 69°59' W) is a 2,800-ha barrier beach and island complex located in the eastern Nantucket Sound region of Massachusetts, USA, approximately 400 to 800 km south of the other tern colonies included in this analysis. Situated within Monomoy NWR and < 5 km from the mainland coast of Cape Cod, South Monomoy Island supports one of the largest Common Tern colonies on the Atlantic coast, with over 7,500 nesting pairs in 2013 (GOMSWG 2013). Small numbers (< 18 pairs) of Arctic Terns historically nested on the islands of Monomoy NWR, but have not since 1990 (United States Fish and Wildlife Service, unpublished data).

Among these study sites, two areas are documented or hypothesized as staging areas for terns prior to long-distance migrations. Monomoy NWR is centrally located within the outer Cape Cod and Nantucket Sound region of Massachusetts, a well-documented staging area for multiple species of terns in the western North Atlantic (Trull et al. 1999, Watson and Hatch 1999, Jedrey et al. 2010, Althouse et al. 2016). On Sable Island, the eastern and western ends, situated up to 15 km from the study colonies, are important foraging and roosting sites for both Common and Arctic Terns during the breeding season, and both species are thought to stage there during the post-breeding period (Ronconi et al. 2016a). We hypothesized that Sable Island may also be a staging area for terns departing mainland colonies since large numbers of Arctic and Common Terns use the distal ends of the island in August, and a Roseate Tern was detected here after breeding at a site in Massachusetts (Spendelow and McKnight, unpublished data in Ronconi et al. 2016a).

Automated radio telemetry

In 2013, the Motus telemetry array (Taylor et al. 2017; www.motus-wts.org) was established at the four colony study sites and an additional 62 coastal and island sites, spanning nearly 1,000 km of coastline from northeastern Nova Scotia to Cape Cod (Fig. B-1). Each telemetry station was equipped with automated data-logging VHF receivers (SRX-600, Lotek Wireless Newmarket, ON, or SensorGnome http://www.sensorgnome.org) connected to antennas using RG58 coaxial cable. Antennas included single-pole omni-directional, or an array of two to six directional (Yagi) antennas (five or nine element) mounted on lighthouses, 10-m telescoping tripod poles, or other structures. Receivers were plugged into external AC power sources, or powered by solar panel arrays (one or two 55 or 65 W panels) connected to a battery bank (one to five 12VDC sealed lead acid batteries). Receivers monitored and recorded VHF signals from all tagged birds within detection range (typically < 20 km) continuously from time of tagging at each site through to October (all sites) or December (Sable Island, Country Island, and some coastal sites).

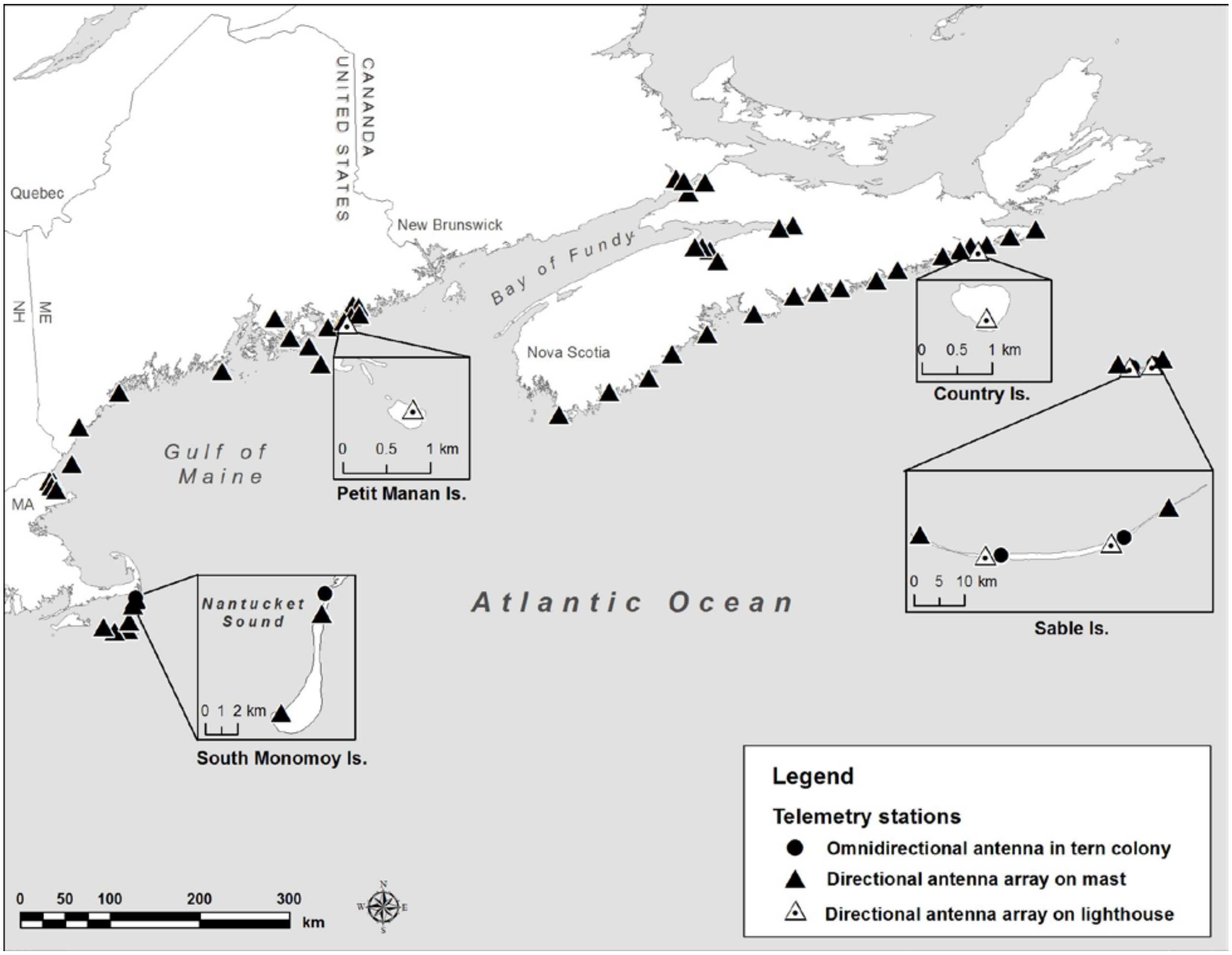

Figure B-1. Map of 2013 study area in the western North Atlantic showing the locations of four tern breeding colonies (insets) and 62 automated radio telemetry stations, each consisting of directional antenna arrays mounted on masts or lighthouses (solid and open triangles, respectively) or omnidirectional antennas positioned in tern colonies (solid points).

Tagging

From early June to mid-July 2013, we used walk-in traps and bow nets to capture terns at their nest sites during the late incubation period through approximately 3 days following hatch. Across the four study sites, we deployed a total of 182 transmitters on 130 adult Common Terns and 52 adult Arctic Terns (Tables B-1 and B-2). All terns were tagged using digitally-coded VHF transmitters (Avian NanoTag series; Lotek Wireless, Newmarket, ON) that allowed over 500 individual identification codes to be monitored simultaneously on a single frequency (166.380 MHz). Depending on the site, transmitters weighed between 1.2 to 1.5 g and were programmed with burst rate intervals that varied between 4.8 to 10.5 seconds, resulting in an expected tag life that ranged from 124 to 240 days. At each site, transmitters were attached to the inter-scapular region using cyanoacrylate adhesive and held in place with subcutaneous sutures that were secured to the transmitter through custom fit end-tubes (inner diameter 1 mm).

We assessed transmitter retention by searching for dropped transmitters within each tern colony, and by examining signals recorded by automated radio telemetry stations, where continuous detections by a single antenna over multiple days indicated a stationary tag. Individuals with dropped transmitters were excluded from subsequent analyses. However, we were unable to account for birds with dropped transmitters that were not recovered by field crews or that were dropped beyond detection range of the automated radio telemetry array.

Table B-1. Sample sizes (n) of Common and Arctic Terns fitted with digital VHF transmitters at four colonies in the western North Atlantic in 2013. Tagged (n) indicates the starting sample size, and Final (n) indicates the sample sized retained for subsequent analyses after removing (and in some instances redeploying) transmitters that were dropped.

	Tagged (*n*)		Final (*n*)	
Colony	Common	Arctic	Common	Arctic
Petit Manan Is.	14	16	14	15
Country Is.	15	15	11	16
Sable Is.	29	21	28	20
Monomoy Is.	72	0	67	0
Total	130	52	120	51

Data processing

All analyses were conducted in R version 3.0.2 (R Development Core Team 2016). We processed raw detection data using a burst rate filter in the R package 'sensorgnome' (version 1.0.16, Brzustowski 2015), that retained data as valid when at least three consecutive detections were separated by the transmitters' burst rate interval.

Length of stay at nesting colonies

Length of stay at the nesting colonies was calculated as the number of days between the estimated hatch date (if possible from individually monitored nests, or from median hatch dates at respective colonies; Table B-2) and the last date an individual was detected by automated telemetry at a colony. We excluded nine nests from Petit Manan Island that failed prior to hatch (three Common Tern nests and six Arctic Tern nests).

For Common and Arctic Terns from colonies within the Gulf of Maine and Canada, we compared the length of stay in the colony by species and across colonies using a general linear model (function ‘lm’ in base R version 3.0.2; R Core Team 2015). Model fit (normality and homoscedasticity of errors) were assessed using residuals plots. We included species (Arctic or Common Tern), and nesting colony (Petit Manan Island, Country Island, or Sable Island) along with the two-way interaction between those terms. The Monomoy colony was excluded from this analysis because Arctic Terns were not present at this site, and Common Tern sample size was considerably larger at Monomoy (n = 72) than at other sites (n = 14-29). We used post-hoc Tukey tests (R package 'multcomp', version 1.4–4, Hothorn 2016) to determine which colonies were significantly different ($p < 0.05$) for all comparisons. For Common Terns only, we used a *t*-test to compare length of stay within the nesting colony between colonies in the Gulf of Maine and Canada (pooled) versus Common Terns from the South Monomoy Island colony in Nantucket Sound.

We conducted this additional comparison to test for differences in length of stay from Common Terns versus northern and southern colonies within our study area.

Dispersal and staging

We assessed differences in post-breeding dispersal and staging between the two species by comparing detections of each at known (Nantucket Sound) or possible (Sable Island) staging areas. We define staging as detection of an individual for greater than 24 h at a site other than its breeding colony, and define post-breeding dispersal as detections at non-colony sites following departure from the nesting colony. Although individuals from South Monomoy Island may also stage in Nantucket Sound, we do not assess "staging" of these individuals as it was not possible to distinguish between dispersal and local post-breeding movements at this scale. On Sable Island, we assessed staging by examining the timing of detections of receiver stations at the eastern and western ends of the island that were situated ~15 km from breeding colonies on the island (Fig. B-1).

We then used logistic regression to estimate the probability of dispersal to the Nantucket Sound staging area by Common Terns among the three other breeding colonies. The binary dependent variable was coded as 1 for individuals that staged in Nantucket Sound and 0 for individuals that did not. The independent variables were nesting colony (Petit Manan Island, Country Island, or Sable Island) and length of stay in the nesting colony during the post-fledging period (in days). Models were fit using function glm with a binomial family and logit link, in base R (version 3.0.2, R Core Development Team 2015). We used a likelihood ratio test (Hosmer and Lemeshow 2001) to determine whether there was any evidence that either independent variable influenced the probability an individual was detected staging in Nantucket Sound.

Finally, we calculated summary statistics of the distance and duration of post-breeding dispersal movements detected by the array. We calculated the distance of dispersal movements as the Euclidian distance traveled between the nesting colony and non-colony sites during the post-breeding dispersal period. We calculated a maximum travel time as the number of days between the last detection at the colony and the first detection at post-breeding dispersal sites. We calculated length of stay at post-breeding dispersal sites as the total amount of time (in days) between the first and last detection recorded by automated radio telemetry station(s) at each site. For all birds, we assumed that the timing of their final observations coincided with departure from the study area. Estimates of length of stay at and departure dates from the nesting colonies and post-breeding dispersal sites are minima because we cannot measure tag failure or loss after the birds have left the nesting colony.

Diel variation in movements

We calculated mean departure times (on a 24-hour clock) and mean resultant length of timing of key movements (ρ, a measure of dispersion of a sample of directional measurements) using R package 'Circular' (v. 0.4–7, Agostinelli and Lund 2013) and used those data to summarize: 1) arrival times of Common Terns at staging sites; 2) timing of detections of post-breeding movements of Arctic Terns; and 3) departure times from the study area for both species.

RESULTS

Tag retention

Of 182 deployed transmitters, 13 transmitters (7%) were dropped before individuals departed their nesting colony (2 of which were redeployed), with Country Island having disproportionately higher rates of confirmed tag loss ($\chi^2 = 41.19$, df = 9, $p < 0.001$). This resulted in a total of 171 tags (120 Common Terns and 51 Arctic Terns) that were included in the final analyses (Table B-1). Mean tracking duration within the study array was approximately 40 d ± 17 (range 7 to 97 d), although total retention duration cannot be quantified once birds departed the study area of the telemetry array.

Length of stay

For terns from colonies in the Gulf of Maine and Canada, length of stay at the colony differed significantly between Arctic and Common Terns ($F_{1,87} = 6.312$, $p = 0.014$) but not among colonies ($F_{2,87} = 1.439$, $p = 0.334$). Overall, mean (± SE) length of stay at the colony was about 8 days longer for Arctic Terns (29 days ± 2 days, range -5 to 48 days) than Common Terns (21 days ± 2 days, range -5 to 71 days). For Common Terns, when comparing length of stay at the nesting colony between colonies in the Gulf of Maine and Canada versus South Monomoy Island, length of stay was significantly longer ($T_{117} = 5.992$, $p < 0.001$) for birds from South Monomoy Island.

For Common and Arctic Terns from colonies in the Gulf of Maine and Canada, mean departure date from the study area was 22 July (range 19 Jun to 7 Sep) and did not differ significantly among colonies ($F_{2,96} = 0.261$, $p = 0.771$) or species ($F_{1,96} = 1.133$, $p = 0.290$; Table B-2). Common Terns from Nantucket Sound departed from the study area significantly later ($t_{117} = 5.91$, $p < 0.001$) relative to Common Terns from colonies in the Gulf of Maine and Canada (Table B-2).

Dispersal of Common Terns

On Sable Island 9 of 28 (32%) Common Terns breeding at this site used the east or west ends of the island during the breeding period, however, during the post-breeding period no tagged individuals used the east end and only two were detected at the west end. Only one individual showed clear evidence of staging behavior at the west end: following the last detection at the colony, this bird was detected almost daily from 17 August to 10 September. No Common Terns from Country Island, Petit Manan Island or Nantucket Sound were detected staging on Sable Island.

Overall, 26% of Common Terns from the three colonies in the Gulf of Maine and Canada were detected in Nantucket Sound during dispersal (Fig. B-2). The colony at South Monomoy Island occurs within the Nantucket Sound staging area, therefore we do not assess the proportion of birds using this site as a post-breeding staging area. The probability of dispersal to Nantucket Sound was positively related to length of stay at the nesting colony (Likelihood Ratio Test: $\chi^2 = 38.341$, $n = 52$, $p < 0.001$) but did not differ among nesting colonies (Likelihood Ratio Test: $\chi^2 = 60.26$, $n = 52$, $p = 0.854$). Individuals that left the nesting colony around 4 days after the fledge date of their chicks had a 25% probability of being detected in Nantucket Sound whereas those that remained for 24 days had a 75% probability of being detected. Travel times and Euclidean travel distances of post-breeding dispersal movements between colonies and Nantucket Sound are presented in Table B-3.

Common Terns from colonies in the Gulf of Maine and Canada arrived in Nantucket Sound between 26 July and 6 Sep, and departed from Nantucket Sound between 7 Aug and 7 Sep. Mean (± SE) length of stay of Common Terns ($n = 14$) in Nantucket Sound was 5.24 days (± 1.58 days; range < 1 to 23.28 days; Table B-3). All of the terns that dispersed to Nantucket Sound area were detected at South Monomoy Island, with some birds remaining for up to three weeks. With the exception of one tern from Country Island, Common Terns that dispersed to Nantucket Sound were not detected again by northern sites within our network of telemetry towers, indicating they likely departed southward from the region to continue migration. The one Country Island tern staged in Nantucket Sound for 2.75 days, and then flew approximately 160 km north to the Isle of Shoals in the Gulf of Maine where it was detected for approximately three hours before departing from the study area.

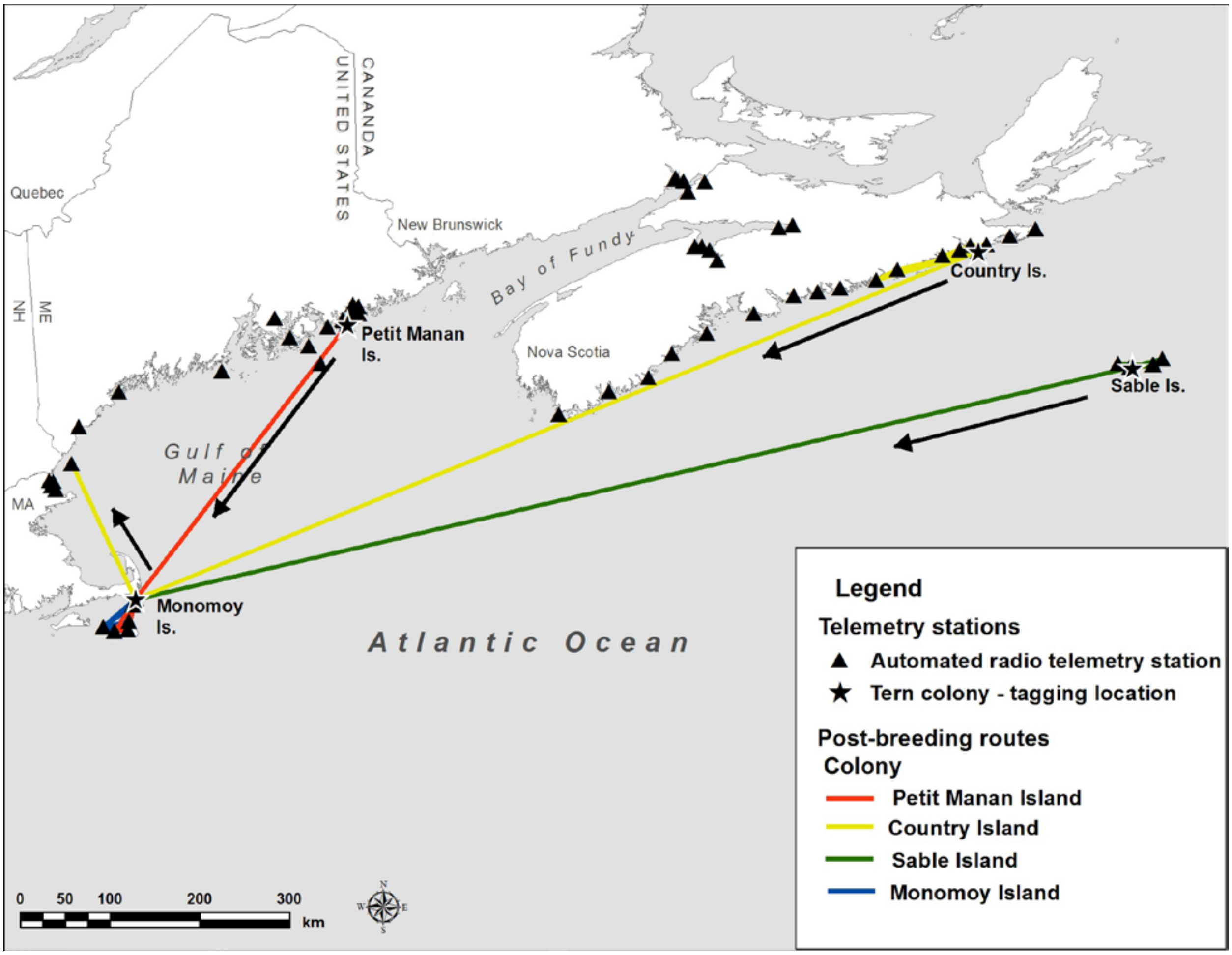

Figure B-2. Euclidian postbreeding movements of tagged Common Terns (n = 120) from four nesting colonies in the northwest Atlantic, Petit Manan Island, Maine, USA (red); Country Island, Nova Scotia, Canada (yellow); Sable Island, Nova Scotia, Canada (green); and South Monomoy Island, Massachusetts, USA (blue), tracked by 62 automated radio telemetry stations during the 2013 postbreeding dispersal period. Black arrows show generalized direction of travel.

Dispersal of Arctic Terns

No Arctic Terns were detected at the Nantucket Sound staging area, and Arctic Terns from Sable Island and Country Island were never detected >100 km from their nesting colonies. On Sable Island, 5 of 22 Arctic Terns (23%) from this site were detected at the east or west ends of the island, but none were detected after July 14, suggesting no evidence of post-breeding staging at these locations on the island. No Arctic Terns from Country Island, Petit Manan Island or Nantucket Sound were detected staging on Sable Island.

Four of 15 Arctic Terns from Petit Manan Island (27%) were detected at sites along the eastern coast of Nova Scotia during post-breeding period, between 25 July and 17 Aug (Fig B-3). The final detections of all four Arctic Terns detected in Nova Scotia were short observations (< 5 minutes) as individuals passed within range of receiving stations. One of these individuals first travelled to the coast of Nova Scotia where it spent ~3 days before travelling back to the breeding colony for one day before again travelling back through coastal Nova Scotia. The mean (± SE) minimum (Euclidian) distance traveled by Arctic

Terns (*n* = 4) from Petit Manan Island to sites in Nova Scotia was 682 km (± 266 km; range 377 to 1,478 km) and the mean (± SE) trip duration was 7.52 days (± 2.85 days; range 1.00 to 17.90 days; Table B-3).

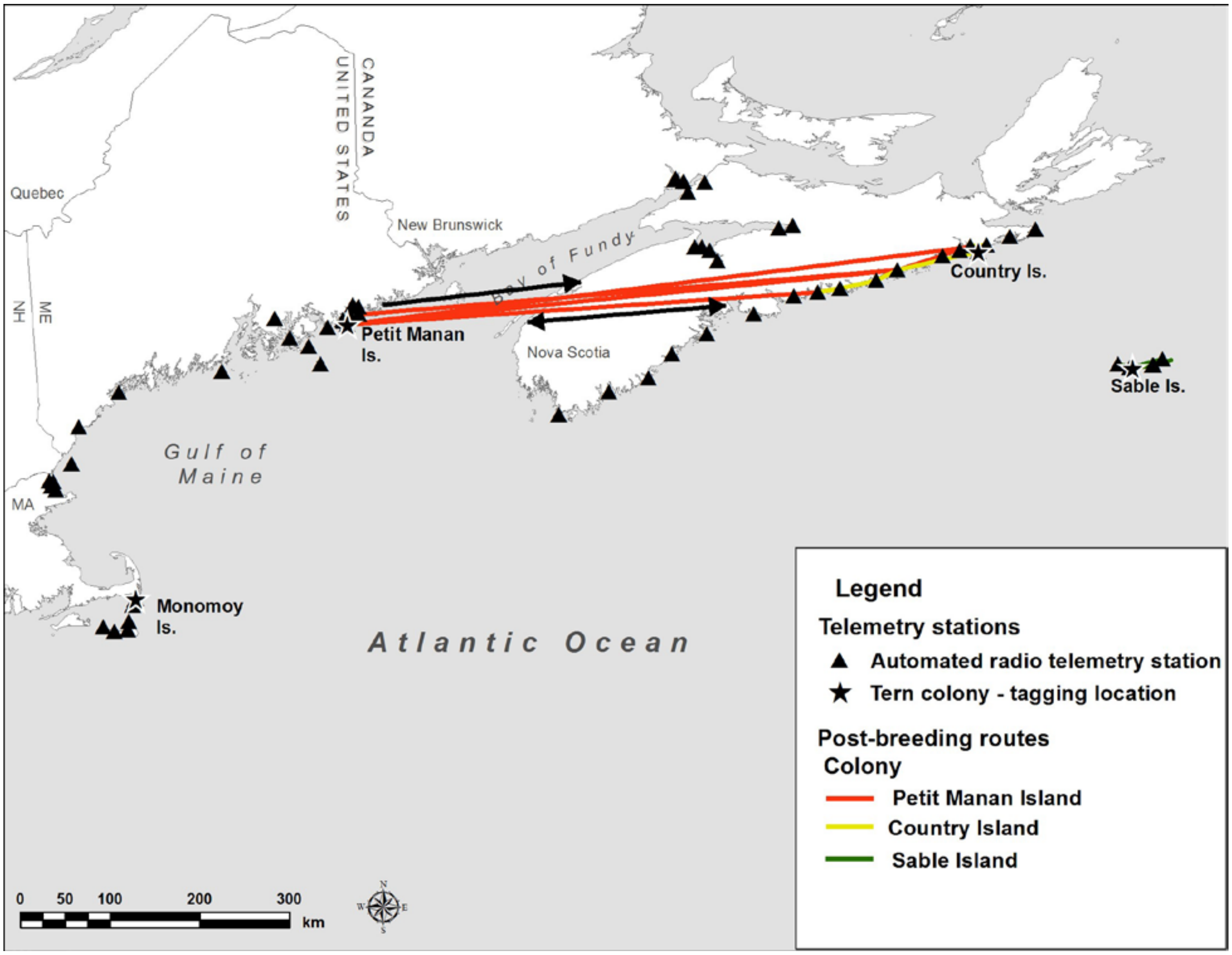

Figure B-3. Euclidian postbreeding movements of tagged Arctic Terns (n = 52) from three nesting colonies in the northwest Atlantic, Petit Manan Island, Maine, USA (red); Country Island, Nova Scotia, Canada (yellow); and Sable Island, Nova Scotia, Canada (green), tracked by 62 automated radio telemetry stations during 2013. Black arrows show generalized direction of travel.

Table B-2. Median and range of dates of transmitter deployment, estimated hatch dates of nests, and final date in study area of nano-tagged Common (*n*=120) and Arctic (*n*=51) terns from four nesting colonies in the northwest Atlantic in 2013.

	Tag dates (median and range)		Hatch dates (median and range)		Final date in study area (median and range)	
Colony	Common	Arctic	Common	Arctic	Common	Arctic
Petit Manan Is.	6/13 (6/13-6/21)	6/13 (6/13-6/20)	6/26 (6/22-6/30)	6/24 (6/20-7/20)	7/23 (6/28-8/19)	7/23 (6/27-8/17)
Country Is.	6/15 (6/14-7/4)	6/15 (6/14-7/14)	6/26 (6/23-7/20)	6/24 (6/20-7/20)	7/9 (6/23-8/18)	7/30 (6/28-8/14)
Sable Is.	6/10 (6/9-6/13)	6/10 (6/9-6/11)	6/24†	6/24†	7/20 (6/20-9/7)	7/30 (6/19-8/10)
Monomoy Is	6/20 (6/4-7/6)	---	6/21 (6/15-7/15)	---	8/5 (7/4-9/15)	---

† On Sable Island, individual nests were not monitored so assumed mean hatch date of 6/24

Table B-3. Mean (± SE and range) distance traveled (km) to post breeding dispersal sites, duration (in days) of post-breeding dispersal movements (assuming Euclidian distances), length of stay (mean ± SE and range, in days), and dates (median and range) of arrival and departure at post-breeding dispersal sites of Common Terns from three nesting colonies throughout the western North Atlantic in 2013of Common (*n*=53) and Arctic (*n*=51) terns from three nesting colonies throughout the western North Atlantic.

Colony	Minimum distance traveled (n=14)	Trip duration (n=14)	Arrival date (median, range; n=53)	Departure date (median, range; n=53)	Length of stay (n=53)
Petit Manan Is.	356 (± 3; 352 - 361)	3.54 (± 0.87; 1.77 - 5.75)	8/4 (7/26 - 8/6)	8/12 (8/7 - 8/19)	10.20 (± 4.41; 4.04 -23.28)
Country Is.	556 (± 199; 160 - 786)	2.35 (± 0.44; 1.48 - 2.83)	8/10 (8/6 - 8/13)	8/16 (8/14 - 8/18)	6.36 (± 1.43; 4.92 - 7.79)
Sable Is.	867 (± 5; 851 - 891)	5.54 (± 0.93, 2.63- 10.00)	8/11 (7/26 - 9/6)	8/12 (7/27 - 9/7)	2.47 (± 0.9; 0.01 - 7.68)

Timing of post-breeding movements

Common Terns from colonies in the Gulf of Maine and Canada arrived at staging areas in Nantucket Sound between 15:00 hrs and 05:00 hrs, peaking within two hours of sunset (Fig. B-4).
Arctic Terns were detected passing by the coast of Nova Scotia at night, between 22:00 hrs and 04:00 hrs (Fig. B-5). Across all terns in the study (*n* = 182), timing of departure from the study area most commonly occurred just before sunrise, with a unimodal distribution that had a mean departure time of 04:49 hrs ($\rho = 0.175$; Figs. B-6 & B-7).

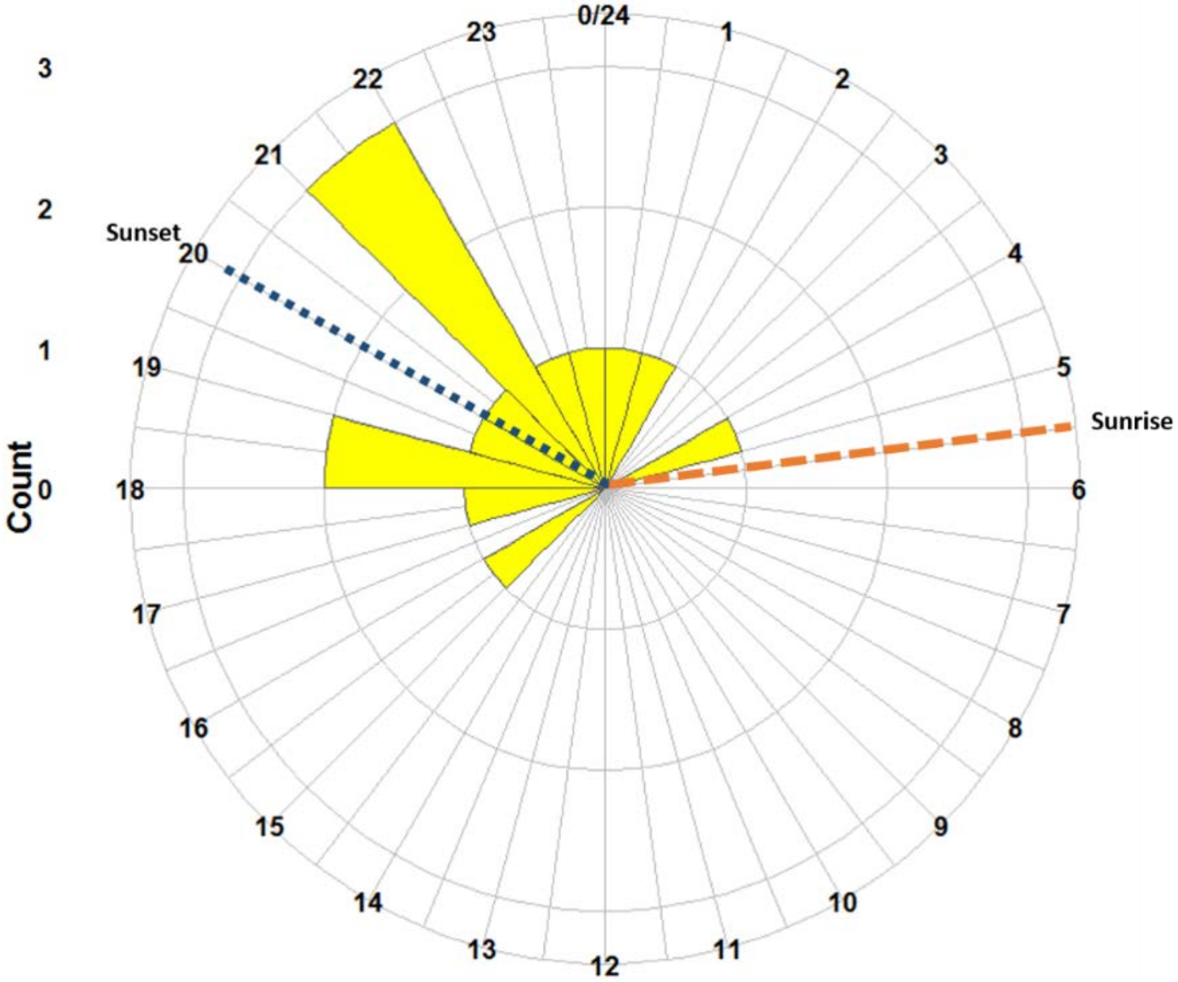

Figure B-4. Diel variation (hrs, in local time) in arrival times of Common Terns (n = 14) from three nesting colonies in the northwest Atlantic (Petit Manan Island, Maine, USA; Country Island, Nova Scotia, Canada; and Sable Island, Nova Scotia, Canada) at staging areas in Nantucket Sound, Massachusetts, USA during 2013. Dashed lines show local times of sunrise (orange) and sunset (blue).

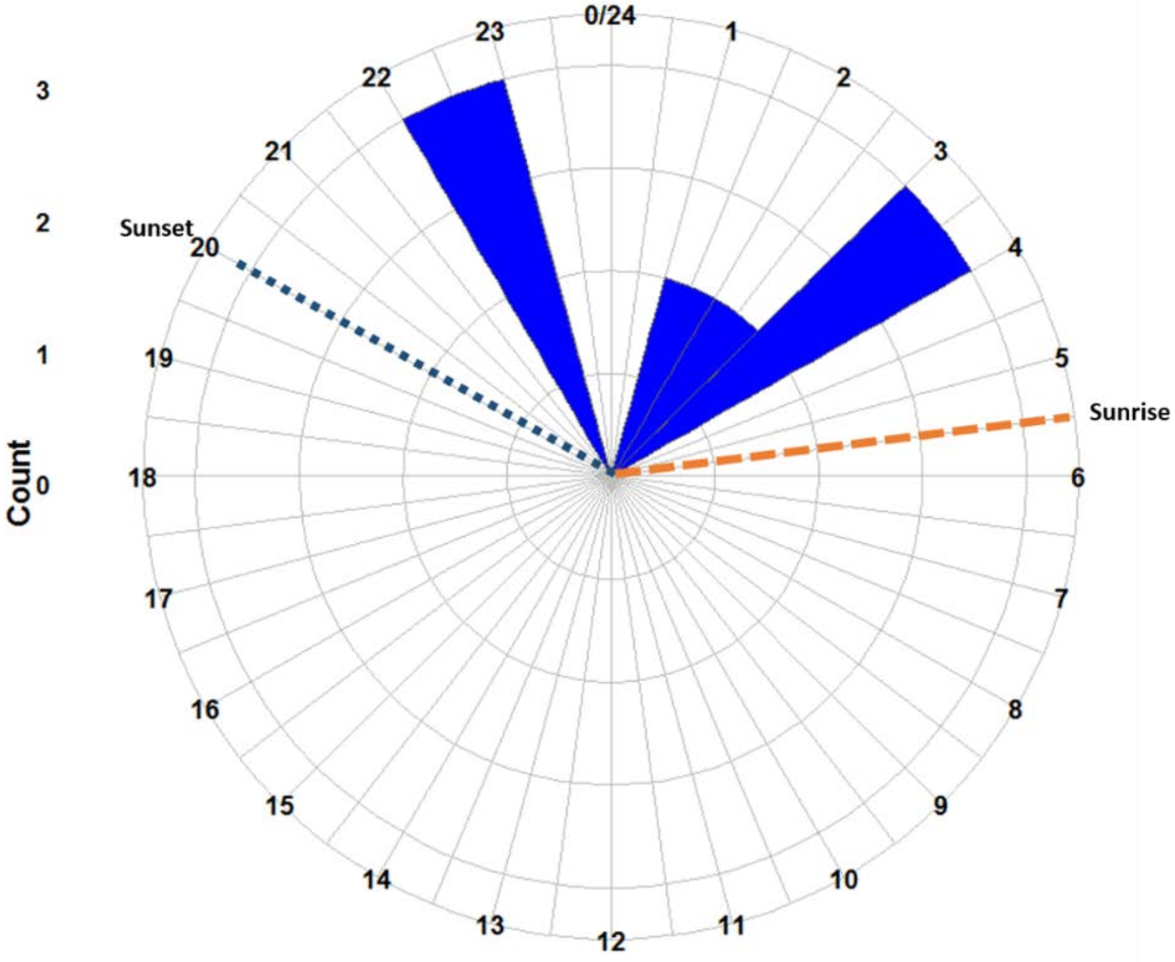

Figure B-5. Diel variation (hrs, in local time) in passage times of Arctic Terns (n = 4) from Petit Manan Island, Maine, USA passing through sites in Nova Scotia, Canada during the postbreeding period in 2013. Dashed lines show local times of sunrise (orange) and sunset (blue).

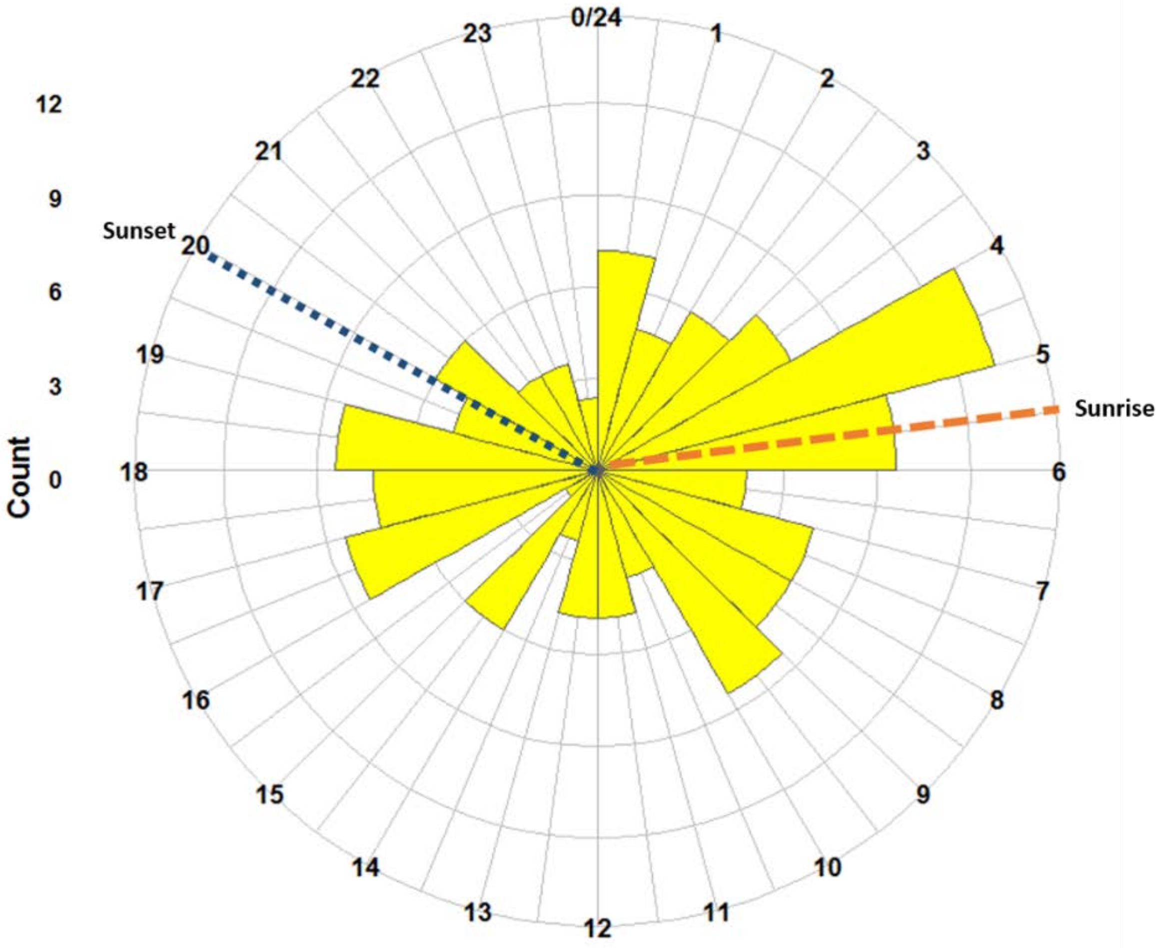

Figure B-6. Diel variation (hrs, local time) of postbreeding departure times of Common Terns (n = 120) from western North Atlantic study area during 2013. Dashed lines show local times of sunrise (orange) and sunset (blue).

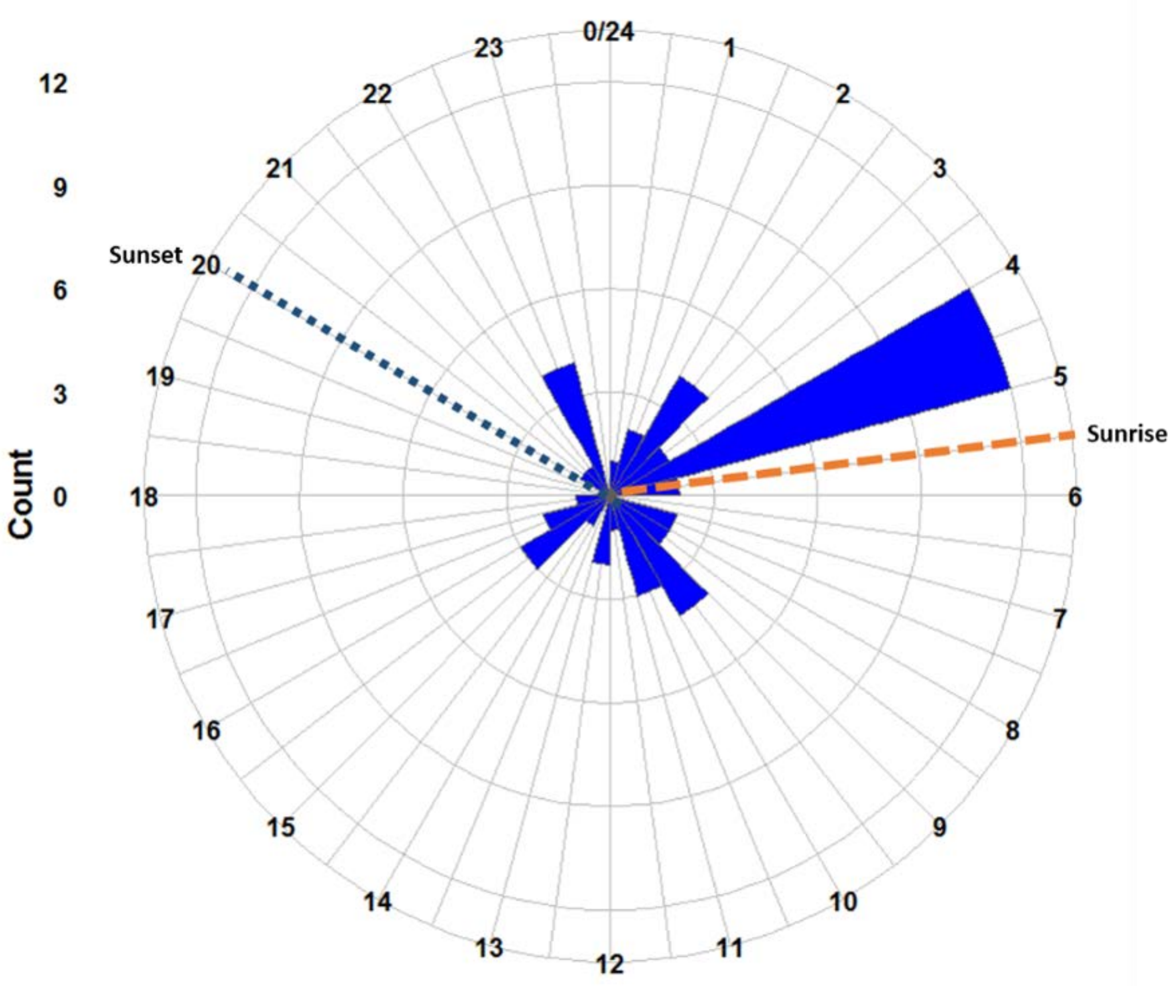

Figure B-7. Diel variation (hrs, local time) of postbreeding departure times of Arctic Terns (n = 52) from western North Atlantic study area during 2013. Dashed lines show local times of sunrise (orange) and sunset (blue).

DISCUSSION

Using an automated international telemetry array and VHF tracking technology, this study offered new insights into the migratory behavior of two seabird species from breeding sites in the western North Atlantic. We documented connectivity among nesting sites in the Gulf of Maine and Canada for Common Terns and a staging site in Massachusetts, USA; a lack of detections during transit suggests direct open-water crossing between breeding colonies and this site. In contrast, the general paucity of detections of Arctic Terns by the array suggests this species is not using coastal staging areas and is possibly transiting directly to offshore staging areas used by Arctic Terns from other regions (e.g. Egevang et al. 2010). From a behavioral perspective, our data show that both tern species initiate post-breeding movements principally at night, typically within two hours prior to sunrise.

Our results showed variation in length of stay of terns by species. Among Common and Arctic Terns, timing of fledging typically varied between 21 to 29 days after eggs hatch and successful breeders disperse away from their colonies between 10 to 20 days after chicks fledge (Nisbet 1976, Hatch 2002). Failed breeders may depart from the colony within days following nest loss (Loring et al. 2016) while others may remain as long as breeders (Nisbet et al. 2011a). However, due to incomplete productivity data across our study sites, we were unable to relate departure date to reproductive success of individual birds in this analysis. Among the three colonies where both species were tagged, we observed that Arctic Terns departed, on average, 8 days later than Common Terns. This difference may reflect the tern's differing migratory strategies. Common Terns depart early for known staging areas in Nantucket Sound, while Arctic Terns, which may need to replenish body reserves locally at colony sites, delay departure for their pelagic staging and migratory routes (this study, Egevang et al. 2010). Among Common Tern study sites, South Monomoy Island birds showed a longer length of stay compared to the three northern colonies, perhaps reflecting latitudinal effects. However, it is more likely that this longer stay was due to the availability of suitable staging habitat at Monomoy, that could therefore prolong their colony attendance. It is also likely that some apparent departures prior to estimated fledge dates was due to tag loss or malfunction, which may have varied among colonies or species. We attempted to control for this by removing known dropped transmitters (7% of deployments) from analyses, but it is possible that additional birds dropped their transmitters beyond the range of the telemetry array prior to colony departure, and thus were not accounted for as dropped. As a consequence, estimates of length of stay at the colony and proportions of terns that staged in the Nantucket Sound region should be considered a minimum.

During the post-breeding period (July and August), Common and Roseate Terns from nesting colonies in the western North Atlantic may disperse hundreds of kilometers to staging areas throughout the region (Austin 1953, Shealer and Kress 1994, Trull et al. 1999). We found that, from late July to early September, our tagged Common Terns from northern colonies dispersed up to 800 km to staging areas in Nantucket Sound, and that their mean travel time (< 1 week) was shorter relative to the dispersal of Roseate Terns across similar distances reported by other studies (mean travel time > 3 weeks; Shealer and Kress 1994). The locations of telemetry receivers in 2013, with limited coastal coverage along the coast of southwestern Nova Scotia and the western Gulf of Maine, did not allow us to distinguish whether individuals used coastal or offshore routes or whether there are additional staging sites in the region.

During the post-breeding period, South Monomoy Island within Nantucket Sound is considered an important staging area for several species of terns in eastern North America, due to its remote location with relatively low levels of human disturbance, large area of sand flats available for roosting, and proximity to foraging areas that include extensive shoals (Trull et al. 1999). The prolonged use of this location by nesting Common Terns tagged in this study align with the findings of Trull et al. (1999), where the majority of staging terns in the Cape Cod and Nantucket Sound region used South Monomoy Island and an adjacent barrier beach as nocturnal roosting areas. We found that a minimum of 25% of our tagged Common Terns from Gulf of Maine and Canadian tern colonies dispersed to South Monomoy Island during the post-breeding period, including some individuals that remained here for up to three weeks, further highlighting the importance of South Monomoy Island for post-breeding terns within the western North Atlantic Ocean.

Common Terns that staged in Nantucket Sound departed from the region between mid-August and early September, which is consistent with past studies (Veit and Petersen 1993, Trull et al. 1999). Using geolocators, Nisbet et al. (2011*b*) found that the mean autumn migration date of female Common Terns from the southern New England area was in mid-August, while the mean date for males was in early September. Most terns that staged in Nantucket Sound appeared to depart from the study area from that region, with the exception of one individual that was detected flying from Nantucket Sound to the Gulf of Maine prior to departure. Northern movements of terns from the southern New England region to sites in Gulf of Maine during the post-breeding period has been documented previously for Common Terns (Austin 1953) and Roseate Terns (Shealer and Kress 1994). We did not document movements of

Common Terns from other colonies to Sable Island, but we found some evidence (1 of 28 birds) of a local breeding bird staging there until 10 September.

With the exception of eastward movements of Arctic Terns from Petit Manan Island that were detected passing through sites in Nova Scotia, we were unable to assess the post-breeding dispersal of Arctic Terns with the telemetry array. This suggests that Arctic Terns are not using coastal sites for staging (within the array of telemetry sites) and are instead departing for offshore staging or migration routes directly from their colonies. This was not entirely unexpected, as prior research to document Arctic Tern migration using geolocators demonstrated that Arctic Terns from colonies in the Gulf of Maine traveled north-northeast after nesting, then migrated east across the Atlantic Ocean (L. Welch, unpublished data). Geolocator studies of Arctic Terns tagged from colonies in Greenland and Iceland revealed that during post-breeding dispersal, individuals traveled to a pelagic stopover region in the eastern Newfoundland Basin and western slope of mid-North Atlantic Ridge (41 to 53° N and 27 to 41° W) where they spent an average of three weeks prior to migrating southeast towards the coast of Africa (Egevang et al. 2010).

Colony departure movements of both species were initiated primarily at night during this study. There is little empirical evidence of the precise timing of tern movements within the literature, but observational and radar data indicate that terns initiate migratory movement at dusk and fly at migratory altitudes (1,000 to 3,000 m) during night (Alerstam 1985, Veit and Petersen 1993). We found that, for both Common and Arctic Terns, departure times from the study area peaked just before dawn (04:00 to 05:00 hrs). It is possible that these departure times coincided with morning foraging flights, as peak foraging activity largely occurs during morning hours (Burger and Gochfeld 1991, Galbraith et al. 1999). Better coverage of automated radio telemetry stations throughout their post-breeding range is needed to more precisely quantify timing of migratory movements using digital VHF technology.

CONCLUSIONS

Common and Arctic Terns from colonies in the western North Atlantic exhibit divergent strategies for dispersal. Nantucket Sound appears to be an important pre-migratory staging area for Common Terns from breeding colonies in the western North Atlantic. More information is needed on post-breeding movements of Arctic Terns to identify important offshore staging areas, although geolocator technology has provided evidence of offshore staging and stopover areas at relatively coarse temporal and spatial scales (Egevang et al. 2010, Duffy et al. 2013, McKnight et al. 2013). Additional automated radio telemetry stations, in both coastal and offshore areas, would be useful for more accurately tracking the post-breeding movements of Common and Arctic Terns in our study area.

ACKNOWLEDGEMENTS

This study was funded in part by the U.S. Department of the Interior, Bureau of Ocean Energy Management through Interagency Agreement M13PG00012 with the U.S. Department of the Interior, Fish and Wildlife Service. Work in Nantucket Sound was also funded in part by the U.S. Fish and Wildlife Service Division of Migratory Birds, Northeast Region; and the National Science Foundation IGERT Offshore Wind Energy Program with logistical support from Eastern Massachusetts National Wildlife Refuge Complex, the Nantucket Conservation Foundation, the Nantucket Island Land Bank, and the University of Rhode Island. Work on Country Island and Sable Island was funded by Encana Corporation Research and Development Fund, Natural Sciences and Engineering Research Council (NSERC) Collaborative Research and Development grant, Canadian Wildlife Federation, and Environment Canada, with in-kind support from Department of Fisheries and Oceans and the Meteorological Service of Canada. The manuscript benefited from the extensive comments of several anonymous referees. For advice, assistance, and support from all projects we thank the following individuals: Karen Beattie, Matt Boarman, John Brzustowski, Zoe Crysler, Danielle Fife, Curt Griffin, Sarah Gutowski, Kate Iaquinto, Scott Johnston, Brian Lang, Stephanie Koch, Peter Paton, Blair Perkins, Ingrid Pollet, Caleb Spiegel, Eric Savetsky, Paul Sievert, Jessica Stephens, Brett Still, and the field crew at Country Island. The findings and conclusions in this article are those of the author(s) and do not necessarily represent the views of the U.S. Fish and Wildlife Service

LITERATURE CITED

Agostinelli, C., and U. Lund. 2013. *Circular: circular statistics*. R package version 0.4–7 edition. R Foundation for Statistical Computing, Vienna, Austria.

Alerstam, T. 1985. Strategies of migratory flight, illustrated by Arctic and Common Terns, *Sterna paradisaea* and *Sterna hirundo*. *Contributions in Marine Science Supplement* 27: 580-603.

Althouse, M. A., J. B. Cohen, J. A. Spendelow, S. M. Karpanty, K. L. Davis, K. C. Parsons, and C. F. Luttazi. 2016. Quantifying the effects of research band resighting activities on staging terns in comparison to other disturbances. *Waterbirds 39*:417-421.

Austin, O. L. 1928. Migration-routes of the Arctic Tern. *Bulletin of the Northeast Bird Banding Association* 4:121-125.

Austin, O. L. 1953. The migration of the Common Tern (*Sterna hirundo*) in the Western Hemisphere. *Bird-Banding* 24:39-55.

Braune, B. M., and D. E. Gaskin. 1982. Feeding ecology of nonbreeding populations of larids off Deer Island, New Brunswick. *Auk* 99:67-76.

Bridge, E. S., K. Thorup, M. S. Bowlin, P. B. Chilson, R. H. Diehl, R. W. Fléron, P. Hartl, R. Kays, J. F. Kelly, and W. D. Robinson. 2011. Technology on the move: recent and forthcoming innovations for tracking migratory birds. *BioScience* 61:689-698. http://dx.doi.org/10.1525/bio.2011.61.9.7

Brzustowski, J. 2015. *SensorGnome*. R package version 1.0.16. R Foundation for Statistical Computing, Vienna, Austria.

Burger, J., and M. Gochfeld. 1991. The Common Tern: Its Breeding Biology and Social Behavior. Columbia University Press, New York, New York, USA, 413 pp.

Duffy, D. C., A. McKnight, and D. B. Irons. 2013. Trans-Andean passage of migrating Arctic Terns over Patagonia. *Marine Ornithology* 41:155-159.

Egevang, C., I. J. Stenhouse, R. A. Phillips, A. Petersen, J. W. Fox, and J. R. D. Silk. 2010. Tracking of Arctic Terns (*Sterna paradisaea)* reveals longest animal migration. *Proceedings of the National Academy of Sciences* 107:2078-2081. http://dx.doi.org/10.1073/pnas.0909493107

Galbraith, H., J. J. Hatch, I. C. T. Nisbet, and T. H. Kunz. 1999. Age-specific reproductive efficiency among breeding Common Terns *Sterna hirundo*: measurement of energy expenditure using doubly-labelled water. *Journal of Avian Biology* 30:85-96. http://dx.doi.org/10.1007/s11357-005-4554-x

Gaston, A. J., D. F. Bertram, A. W. Boyne, J. W. Chardine, G. Davoren, A. W. Diamond, A. Hedd, W. A. Montevecchi, J. M. Hipfner, M. J. F. Lemon, M. L. Mallory, J. F. Rail, and G. J. Robertson. 2009. Changes in Canadian seabird populations and ecology since 1970 in relation to changes in oceanography and food webs. *Environmental Reviews* 17:267-286. http://dx.doi.org/10.1139/A09-013

Gilg, O., B. Moe, S. A. Hanssen, N. M. Schmidt, B. Sittler, J. Hansen, J. Reneerkens, B. Sabard, O. Chastel, J. Moreau, R. A. Phillips, T. Oudman, E. M. Biersma, A. A. Fenstad, J. Lang, and L. Bollache. 2013. Trans-equatorial migration routes, staging sites and wintering areas of a high-arctic avian predator: the Long-tailed Skua (*Stercorarius longicaudus*). *Public Library of Science ONE* 8:e64614. http://dx.doi.org/10.1371/journal.pone.0064614

Guilford, T., J. Meade, J. Willis, R. A. Phillips, D. Boyle, S. Roberts, M. Collett, R. Freeman, and C. M. Perrins. 2009. Migration and stopover in a small pelagic seabird, the Manx shearwater (*Puffinus puffinus)*: insights from machine learning. *Proceedings of the Royal Society of London B: Biological Sciences*:rspb-2008. http://dx.doi.org/10.1098/rspb.2008.1577

Gulf of Maine Seabird Working Group (GOMSWG). 2013. 2013 Gulf of Maine Seabird Working Group Census Results. [online] URL: http://gomswg.org/pdf_files/GOMSWG%20Census%20Data%202013.pdf

Hall, C. S., S. W. Kress, and C. R. Griffin. 2000. Composition, spatial and temporal variation of Common and Arctic Tern chick diets in the Gulf of Maine. *Waterbirds* 23:430-439. http://dx.doi.org/10.2307/1522180

Hatch, J. J. 2002. Arctic Tern (*Sterna paradisaea*), *The Birds of North America Online* (A. Poole, Ed.). Ithaca: Cornell Lab of Ornithology. [online] URL: http://bna.birds.cornell.edu.bnaproxy.birds.cornell.edu/bna/species/707doi:10.2173/bna.707.

Hays, H., J. DiCostanzo, G. Cormons, P. T. Z. Antas, and J. L. X. do Nascimento. 1997. Recoveries of Roseate and Common Terns in South America. *Journal of Field Ornithology* 68:79-90.

Hedd, A., W. A. Montevecchi, H. Otley, R. A. Phillips, and D. A. Fifield. 2012. Trans-equatorial migration and habitat use by Sooty Shearwaters (*Puffinus griseus)* from the South Atlantic during the nonbreeding season. *Marine Ecology Progress Series* 449:277-290.

Hosmer, D. W., and S. Lemeshow. 2000. Applied Logistic Regression. Second edition. John Wiley and Sons, New York, New York, USA.

Hothorn, T., F. Bretz, and P. Westfall. 2015. Multcomp. R package version 1.4–4 edition. R Foundation for Statistical Computing, Vienna, Austria.

Huettmann, F., and A. W. Diamond. 2000. Seabird migration in the Canadian northwest Atlantic Ocean: moulting locations and movement patterns of immature birds. *Canadian Journal of Zoology* 78:624-647.

Jedrey, E.L., R.J. Harris, and E.A. Ray. 2010. Roseate Terns – citizens of the world: the Canada to Cape Cod connection. *Bird Observer* 38:146-150.

Klaassen, R. H. G., B. J. Ens, J. Shamoun-Baranes, K.-M. Exo, and F. Bairlein. 2011. Migration strategy of a flight generalist, the Lesser Black-backed Gull (*Larus fuscus)*. *Behavioral Ecology* 23:58-68.

Kress, S. W., E. H. Weinstein, I. C. T. Nisbet, G. W. Shugart, W. C. Scharf, H. Blokpoel, G. A. Smith, K. Karwowski, G. R. Maxwell, G. Chapdelaine, W. A. Montevecchi, A. R. Lock, C. F. Smith, E. Miller, J. A. Spendelow, M. Gochfeld, J. Burger, and R. M. Erwin. 1983. The status of tern populations in northeastern United States and adjacent Canada. *Colonial Waterbirds* 6:84-106.

Lee, D. S. and S. W. Cardiff. 1993. Status of the Arctic Tern in the Coastal and Offshore Waters of the Southeastern United States (Estatus de Sterna paradisaea en la Costa y el Mar Adentro del Sureste de Los Estados Unidos). *Journal of Field Ornithology* 1993:158-168.

Loring, P. H. 2016. *Evaluating digital VHF technology to monitor shorebird and seabird use of offshore wind energy areas in the western North Atlantic.* Dissertation. University of Massachusetts Amherst, Amherst, Massachusetts, USA.

McKnight, A., A. J. Allyn, and D. B. Irons. 2013. Stepping stone pattern in Pacific Arctic Tern migration reveals the importance of upwelling areas. *Marine Ecology Progress Series* 491:253-264.

Montevecchi, W. A., A. Hedd, L. McFarlane Tranquilla, D. A. Fifield, C. M. Burke, P. M. Regular, G. K. Davoren, S. Garthe, G. J. Robertson, and R. A. Phillips. 2012. Tracking seabirds to identify ecologically important and high risk marine areas in the western North Atlantic. *Biological Conservation* 156:62-71.

Mosbech, A., K. L. Johansen, N. I. Bech, P. Lyngs, A. M. Harding, C. Egevang, R. A. Phillips, and J. Fort. 2012. Inter-breeding movements of little auks (*Alle alle)* reveal a key post-breeding staging area in the Greenland Sea. *Polar Biology* 35:305-311.

Nisbet, I. C. T. 1976. Early stages in postfledging dispersal of Common Terns. *Bird-Banding* 47:163-164.

Nisbet, I. C. T. 2002. Common Tern (*Sterna hirundo*), *The Birds of North America Online* (A. Poole, Ed.). Ithaca: Cornell Lab of Ornithology. [online] URL: http://bna.birds.cornell.edu/bna/species/618doi:10.2173/bna.618.

Nisbet, I. C. T., C. S. Mostello, R. R. Veit, J. W. Fox, and V. Afanasyev. 2011*a*. Migrations and winter quarters of five Common Terns tracked using geolocators. *Waterbirds* 34:32-39.

Nisbet, I. C. T., P. Szczys, C. S. Mostello, and J. W. Fox. 2011*b*. Female Common Terns (*Sterna hirundo)* start autumn migration earlier than males. *Seabird* 24:103-106.

R Core Team. 2015. R: a language and environment for statistical computing. R Foundation for Statistical Computing, Vienna, Austria.

Rock, J. C., M. L. Leonard, and A.W. Boyne. 2007. Do co-nesting Arctic and Common Terns partition foraging habitat and chick diets? *Waterbirds* 30:579-587.

Ronconi, R. A., A. W. Boyne, C. Gjerdrum, and A. G. Horn, 2016a. Population status and ecology of seabirds on Sable Island. Pp. 213-241 in W. Freedman (ed) *Sable Island: Explorations in Ecology and Biodiversity*. Fitzhenry & Whiteside, Markham, ON. *322 pp.*

Ronconi, R. A., J. R. Stephens, Z. J. Crysler, I. L. Pollet, D. T. Fife, A. G. Horn, and P. D. Taylor. 2016b. Distribution, abundance and trends of gulls and terns breeding on Sable Island, Nova Scotia, Canada. *Waterbirds* 39:44-56.

Shealer, D. A., and S. W. Kress. 1994. Post-breeding movements and prey selection of Roseate Terns at Stratton Island, Maine. *Journal of Field Ornithology* 65:349-362.

Salomonsen, F. 1967. Migratory movements of the Arctic Tern (*Sterna paradisaea Pontoppidan*) in the Southern Ocean. *Biol Medd Dan Vid Selsk* 24:1–42.

Suryan, R. M., F. Sato, G. R. Balogh, K. D. Hyrenbach, P. R. Sievert, and K. Ozaki. 2006. Foraging destinations and marine habitat use of short-tailed albatrosses: a multi-scale approach using first-passage time analysis. *Deep Sea Research Part II: Topical Studies in Oceanography* 53:370-386.

Taylor, P. D., T. L. Crewe, S. A. Mackenzie, D. Lepage, Y. Aubry, Z. Crysler, G. Finney, C. M. Francis, C. G. Guglielmo, D. J. Hamilton, R. L. Holberton, P. H. Loring, G. W. Mitchell, D. Norris, J. Paquet, R. A. Ronconi, J. R. Smetzer, P. A. Smith, L. J. Welch and B. K. Woodworth. 2017. The Motus Wildlife Tracking System: a collaborative research network to enhance the understanding of wildlife movement. Avian Conservation and Ecology 12 (1):8. [online] URL: http://www.ace-eco.org/vol12/iss1/art8/.

Trull, P., S. Hecker, M. J. Watson, and I. C. T. Nisbet. 1999. Staging of Roseate Terns (*Sterna dougallii)* in the post-breeding period around Cape Cod, Massachusetts, USA. *Atlantic Seabirds* 1:145-158.

van der Winden, J., R. C. Fijn, P. W. van Horssen, D. Gerritsen-Davidse, and T. Piersma. 2014. Idiosyncratic migrations of Black Terns (*Chlidonias niger*): Diversity in routes and stopovers. *Waterbirds* 37:162-174.

Veit, R. R., and W. R. Petersen. 1993. *Birds of Massachusetts*. Massachusetts Audubon Society, Lincoln, MA, USA.

Watson, M. J., and J. J. Hatch. 1999. Differences in foraging performance between juvenile and adult Roseate Terns at a pre-migratory staging area. *Waterbirds* 22:463-465.

Warnock, N. 2010. Stopping vs. staging: the difference between a hop and a jump. *Journal of Avian Biology* 41:621-626.

Appendix C

Assessing the Effects of Digital VHF Transmitters on Nesting Common Terns

Pamela H. Loring[1], Peter W.C. Paton[2], Curtice R. Griffin[3], and Paul R. Sievert[3]

[1]U.S. Fish and Wildlife Service, Division of Migratory Birds, Northeast Region, 300 Westgate Center Drive, Hadley, Massachusetts, 01035, USA

[2]Department of Natural Resources Science, University of Rhode Island, 1 Greenhouse Rd, Kingston, RI 02881, USA

[3]Department of Environmental Conservation, University of Massachusetts Amherst, 160 Holdsworth Way, Amherst, Massachusetts, 01003, USA

Citation: Loring PH, Paton PWC, Griffin CR, Sievert PR. *In prep.* Assessing the effects of digital VHF transmitters on nesting Common Terns

Abstract. — Recent advances in radio-telemetry techniques now allow biologists to quantify fine-scale movements of seabirds. However, before widespread use of this new technology is permitted, particularly on threatened or endangered species, it is important to monitor transmitter retention times and potential adverse impacts on the behavior of similar species. At Monomoy NWR, MA, USA, we used cyanoacrylate adhesive and subcutaneous sutures to attach 1.5 g (<2% of body mass) digital VHF radio transmitters (hereafter tags) to the interscapular region 50 adult Common Terns (*Sterna hirundo*). We programmed tags to transmit a signal every 5-6 sec for 160 d. We then tracked terns using an array of eight automated radio telemetry stations within 30 km of the colony to quantify tag retention through post-fledging dispersal. We estimated productivity of tagged and non-tagged (control) pairs by following chicks through fledging in 20 productivity plots within the colony. Two tags ceased to function immediately after birds were released. Of the remaining tags, most adult terns (81%, *n* = 48) retained their tags until their chicks had fledged. Mean (± SE) retention time was 48 days (± 2 days, range 22 to 90 days), with females slightly more likely to retain their tag until their chicks fledged than males. Only one tagged pair was unsuccessful in fledging at least one chick, and fledging success did not differ between the tagged and control groups. Using cyanoacrylate adhesive and subcutaneous sutures is a useful technique for attaching lightweight transmitters to Common Terns for studies lasting from one to three months. This technique did not appear to affect nesting productivity, and retention rates were high, therefore we feel this technique could be used successfully on federally-endangered Roseate Terns (*Sterna dougalli*) with no adverse impacts.

Key words. — automated radio telemetry, breeding, digital VHF telemetry, *Sterna hirundo*, tag effects

INTRODUCTION

Recent advances in tracking technologies now allow biologists to gather otherwise unattainable information about avian movement ecology (Bridge et al., 2011, López-López 2016, Taylor et al., 2017). Despite the benefits of information gained by telemetry studies, there are inherent risks associated with attaching transmitters to birds (Barron et al., 2010, Geen et al., 2019). Researchers have legal and ethical responsibilities to assess and minimize adverse effects to tagged individuals, particularly with threatened or endangered populations (Fair et al., 2010). Furthermore, minimizing risks to tagged individuals is critical for studies designed to draw inferences to the broader non-tagged population, as adverse effects on health, behavior, or movements of tagged individuals may bias results (Murray and Fuller 2000, Constantini and Møller 2013).

One approach for reducing adverse effects of transmitters is to minimize their size and mass to under 3 to 5% of the body mass of the tagged individual (White and Garrott 1990, Fair et al., 2010, Vandenabeele et al., 2011; but see Barron et al., 2010, Snijders et al., 2016). Where and how the transmitter is attached can also affect study success, as it can influence tag retention, bird welfare, and study outcomes (Barron et al., 2010, Constantini and Møller 2013, Vandelabeele et al., 2014, Lewis et al., 2017). For short- and moderate-term studies (i.e., lasting a few weeks to a few months), adhesive (Johnson et al., 1991) and tape (Söhle et al., 2000) allow the transmitter to fall off the tagged individual (Hawkins 2004). These temporary attachment methods are generally thought to have less impact than long-term or permanent alternatives (e.g., mounted to leg-bands, surgical implants, backpack harnesses; Barron et al., 2010, Constantini and Møller 2013, Thaxter et al. 2014).

Selecting an appropriate attachment method for seabirds can be challenging because they are wide ranging, occupy marine environments, and some species employ foraging techniques that stress tag attachment (Burger and Shaffer 2008). For terns of the genus *Sterna*, attaching transmitter is particularly difficult due to their small body mass (generally <150 g), and high-impact foraging (i.e., plunge diving from about 3-4 m above the water surface; Duffy 1986). Therefore, depending on study objectives, the transmitter and attachment materials need to be lightweight yet robust. Biologists have used band-mounts, tail-mounts, and back-mounts to attach transmitters to terns (Klaassen et al., 1992, Morris and Burness 1992, Sirdevan and Quinn 1997, Perrow et al., 2006, Mostello et al., 2014). Short-term studies used strong adhesive glue or Tesa tape (Beiersdorf AG, Hamburg, Germany) to allow the transmitter to fall off after a short interval; <10 days for tail mounts (Perrow et al., 2006) and <12 days for transmitters glued to the back (Massey et al., 1988). Long-term studies, tracking terns throughout their entire annual cycle, have glued geolocators to leg bands, although some adverse impacts (i.e., leg injuries, reduced body mass, and reduced inter-annual return rates) were documented (Nisbet et al., 2011, Mostello et al., 2014).

One modification to short-term techniques to increase retention time of transmitters is to use a combination of adhesive and subcutaneous sutures (Warnock and Takekawa 2003, Lewis et al., 2017). Biologists have used this approach a variety of waterbirds including scoters (*Melanitte* spp.; (Lewis et al., 2017), and Forster's Terns (*Sterna forsteri*; (Ackerman et al., 2009)). Thus, adding subcutaneous sutures appears to be a promising attachment method for studies designed to track an individual for one to five months, and may represent a safer alternative than long-term attachment techniques (Wheeler 1991, Thaxter et al., 2014).

To our knowledge, no one has previously assessed the retention time or potential adverse effects of the adhesive and suture technique to attach transmitters on a plunge-diving tern. Using adhesive and subcutaneous sutures, we dorsally-mounted Very High Frequency (VHF) radio-transmitters on adult Common Terns (*Sterna hirundo*), a relatively abundant species that breeds throughout North America (Nisbet et al. 2017). Our specific objectives were to: 1) determine if transmitters attached with cyanoacrylate adhesive and subcutaneous sutures to the inter-scapular region of nesting adult Common Terns affected chick fledging success; 2) quantify retention time of transmitters attached to terns using adhesive and sutures; and 3) compare transmitter retention times between male and female adult Common Terns through the post-fledging period.

METHODS

Study area

We conducted fieldwork on South Monomoy Island (41° 36’ 31.53” N, 69° 59’ 12.86” W), within Monomoy National Wildlife Refuge (NWR), a 30 km^2 barrier beach and island complex located off Cape Cod, Massachusetts, USA (Fig. C-1). South Monomoy Island is approximately 9 km from north to south, and up to 2 km wide. The island supports, one of the largest Common Tern colonies on the Atlantic Coast, with over 7,500 nesting pairs in 2013 (USFWS, unpublished data).

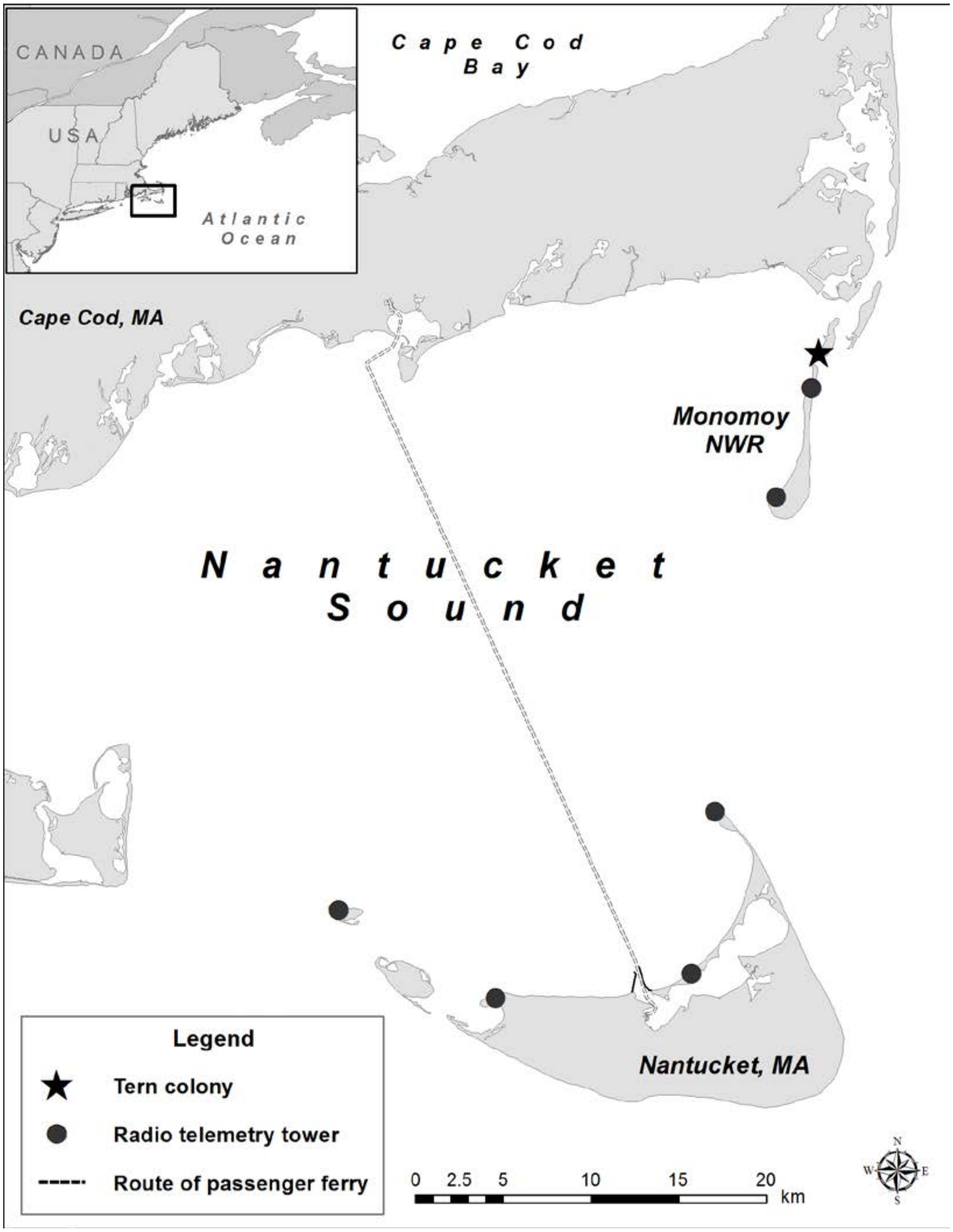

Figure C-1. Study area in Nantucket Sound, Massachusetts, USA where Common Terns were monitored at a colony on Monomoy National Wildlife Refuge in 2013 (NWR; black star), seven land-based Automated Radio Telemetry Stations (ARTS; black circles), and the route of a passenger ferry with an ARTS (dashed line).

Tag deployments

During the mid-incubation through early chick-rearing period, we captured a random sample of 100 adult Common Terns, each from a different nest, in 20 productivity plots that were randomly-located throughout the Monomoy tern colony. Of the 100 terns that we captured, 50 terns were fitted with a digitally-coded VHF transmitter (tagged group) and 50 terns had no VHF transmitter (control group). Productivity plots were designed to estimate fledging rates of Common Tern chicks by retaining chicks near nests until they were nearly capable of sustained flight. Each plot was a hexagon constructed from 15.25 m of 0.3 m tall, 6-mm mesh hardware cloth. We tagged an average of 2.4 (± 0.2 SE, range = 1 to 5) terns per plot from 4 to 25 June 2013 using walk-in treadle traps. We individually marked terns on their tarsometatarsus with an incoloy U.S. Geological Survey band on one leg and a wrap-around black plastic field readable band inscribed in white with a unique 3-digit alphanumeric code on the opposite leg. We also collected three to five contour feathers from each bird to determine gender by molecular analysis (Avian Biotech, Gainesville, FL).

We attached a 1.5 g digital VHF transmitter ('Avian NanoTag'; Lotek Wireless, Inc., Newmarket, Ontario, Canada) to individuals within the tagged group. Digital coding within each transmitter's pulse allowed up to 521 individuals to be uniquely identified on a single VHF frequency by receiving units. We programmed transmitters to transmit signals on 166.380 MHz every five to six seconds, for a total expected operational life of approximately 160 days. Each transmitter body measured 11 mm x 8 mm x 7 mm, and had custom fitted tubes (inner diameter 1 mm) at the anterior and posterior ends for attachment materials, and a 15-cm whip antenna. Total weight of each transmitter and attachment materials was < 2% of the body mass of the birds in our study. We attached transmitters to the dorsal inter-scapular region using cyanoacrylate adhesive and two sutures (Prolene: 45-cm length, 4.0, BB taper point needle, catalog # 8581H) that we inserted subcutaneously and secured to the end-tubes of the transmitter. We captured, processed, banded, and released birds from the control group using the same procedures as tagged birds. Total handling time, from capture to release, ranged between 20 to 40 min per individual for both tagged and control individuals.

Nest monitoring

From nest initiation through fledging, all chicks within productivity plots were monitored every one to three days by U.S. Fish and Wildlife Service biological staff at Monomoy NWR. All chicks were banded within three days of their hatch date with an incoloy U.S. Geological Survey Band. We determined hatch order for each chick within a brood based on size and plumage characteristics, where 'A', 'B', and 'C' was used to identify the first hatched, second hatched, and third hatched chick, respectively. We classified all chicks that survived to 23 days old as successfully fledging (Nisbet 2002). For nests with chicks that did not survive to 23 days, we recorded the nest failure date as the date when the last egg or chick was lost.

Tracking

We tracked the movements of tagged terns using a network of automated radio telemetry stations (hereafter network) established throughout the eastern Nantucket Sound region of Massachusetts (Fig. C-1). The network included six automated radio telemetry towers, each consisting of an array of six 9-element (11.1 dBd) Yagi antennas end-mounted in a radial configuration atop a 9.2

m mast. The antennas were connected to a solar-powered, automated receiving unit (SRX-600, Lotek Wireless, Ontario, Canada) that scanned for signals with each antenna for 6.5 seconds in succession, around the clock.

The network also included a receiving station, consisting of a SRX-600 receiver equipped with a single omnidirectional (200 W) antenna, located on a passenger ferry that followed a north-south route across Nantucket Sound two to six times per day (Fig. C-1). In addition, we operated a receiving station consisting of a SRX-600 receiver equipped with a single omnidirectional (200 W) antenna mounted on a 1.2 m mast that was adjacent to the tern nesting colony and configured to monitor nest attendance. We programmed all receiving units to automatically log the following data from each antenna: transmitter ID number, time stamp (synchronized among all receivers in the array using GPS clocks), antenna (defined by receiving station and bearing), and signal strength (non-linear scale: 0 to 255).

Tag retention

We were unable to calculate the complete duration of tag retention for each bird beyond the post-fledgling period when adults disperse beyond the detection range of our network to staging or wintering grounds (Nisbet et al. 2017). Therefore, we estimated the minimum retention duration as the number of days between the date of tag attachment and date of last detection by our network. We classified transmitters as dropped if we detected a consistent, continuous signal from a single antenna over a period of several days, indicating that the transmitter was stationary. When we did not have direct evidence of a dropped transmitter from our network, we assumed that an individual had dropped their transmitter if they were last detected by our network prior to the estimated fledging date of their chick (for successful nests) or the date of nest failure (for unsuccessful nests). Previous research on Common Terns has determined that both members of the pair remain in the nesting colony until their chicks fledge (Nisbet et al. 2017). Therefore, we assumed that individuals retained their transmitters and successfully dispersed from the nesting colony if their last detection from our network occurred after the estimated fledging date of their chicks.

Data Analyses

We tested for gender-based differences in transmitter retention rates through the fledging period using Pearson's Chi-squared test with Yates' continuity correction. To compare minimum retention time (in days) between genders, we used a Mann-Whitney U test since our data violated the assumption of equal variance (rejected, $P < 0.05$). To examine the effects of transmitters on reproductive success, we used a generalized linear mixed model with a logit link and binomial error distribution (lme4 package; R Development Core Team 2015), with the individual fledge success of each chick as the binary response variable (1 = survived to fledge, 0 = did not survive); hatch order, tag presence, and their interactions as fixed effects, and plot ID as a random effect. We evaluated the significance of fixed effects in the model using Wald z-statistics, to assess whether transmitter presence, hatch order, and their interactions had a significant influence on fledge success of chicks from tagged versus non-tagged nests (Bolker et al. 2009). We present mean ± SE unless stated otherwise.

RESULTS

Tag retention

Two transmitters malfunctioned immediately after deployment (i.e., did not transmit any data after tag date), and were removed from subsequent analyses. We captured most tagged birds during incubation (12.8 d ± 0.9 d before hatching, *n* = 38), whereas others were captured while brooding chicks (2 d ± 0.4 d after hatching, *n* = 10). Of the 48 tagged individuals, we determined gender for 47 individuals: 24 females and 23 males. Nine tagged individuals (7 males and 2 females) were not detected by our automated array up to the estimated fledging date of their chicks, therefore we assumed these tags fell off prematurely. We tracked individuals that dropped their tags for an average of 30.1 d ± 0.6 d before we lost their signals. Apparent detachment of tags occurred an average of 7.7 d ± 0.7 d before estimated fledge date. The remainder of the tagged individuals (81%; *n* = 39) were detected by the network through the fledge date of their chicks.

There was a tendency for females (92% retention, *n* = 24) to be more likely to retain their tags until their chicks' fledged than males (70% retention *n* = 23; χ-squared = 2.4, df = 1, *P* = 0.07, Fig. C-2). For all birds, mean retention time was 48.1 d ± 2.2 d (range 22 d to 90 d, *n* = 48), and for individuals that retained their tags to the post-fledging period the mean retention time was 52.3 d (± 2.2 d, *n* = 39). There was no difference between genders in retention times for individuals that retained their tags until after their chick(s) fledged (Mann-Whitney U-Test 170.5, *P* = 0.65; Fig. 3). For adults tracked during the interval beginning with fledging of their chicks, and ending with their own departure from the study area, there was no difference between males and females in minimum retention times (Mann-Whitney U-Test 181.5, *P* = 0.89; Fig. C-3).

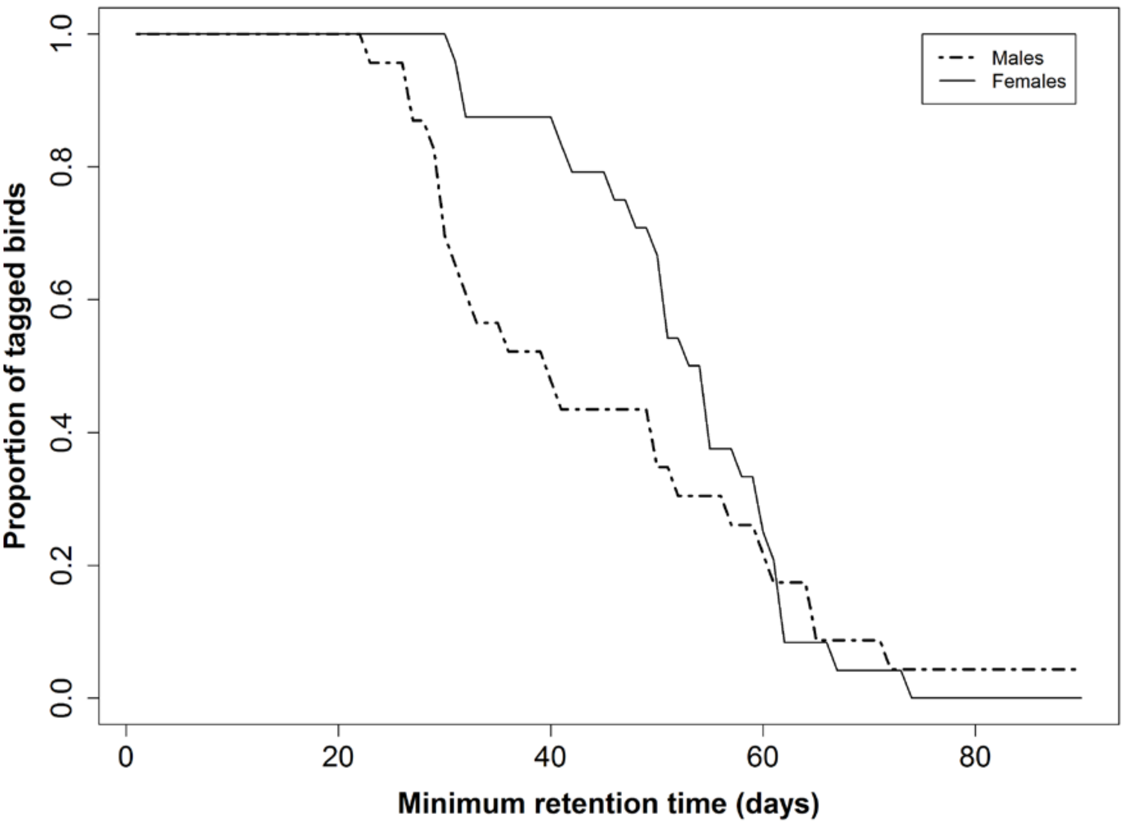

Figure C-2. Cumulative distributions of minimum retention time (days) of VHF transmitters attached to adult male (*n* = 23) and female (*n* = 24) Common Terns tracked at Monomoy NWR in 2013.

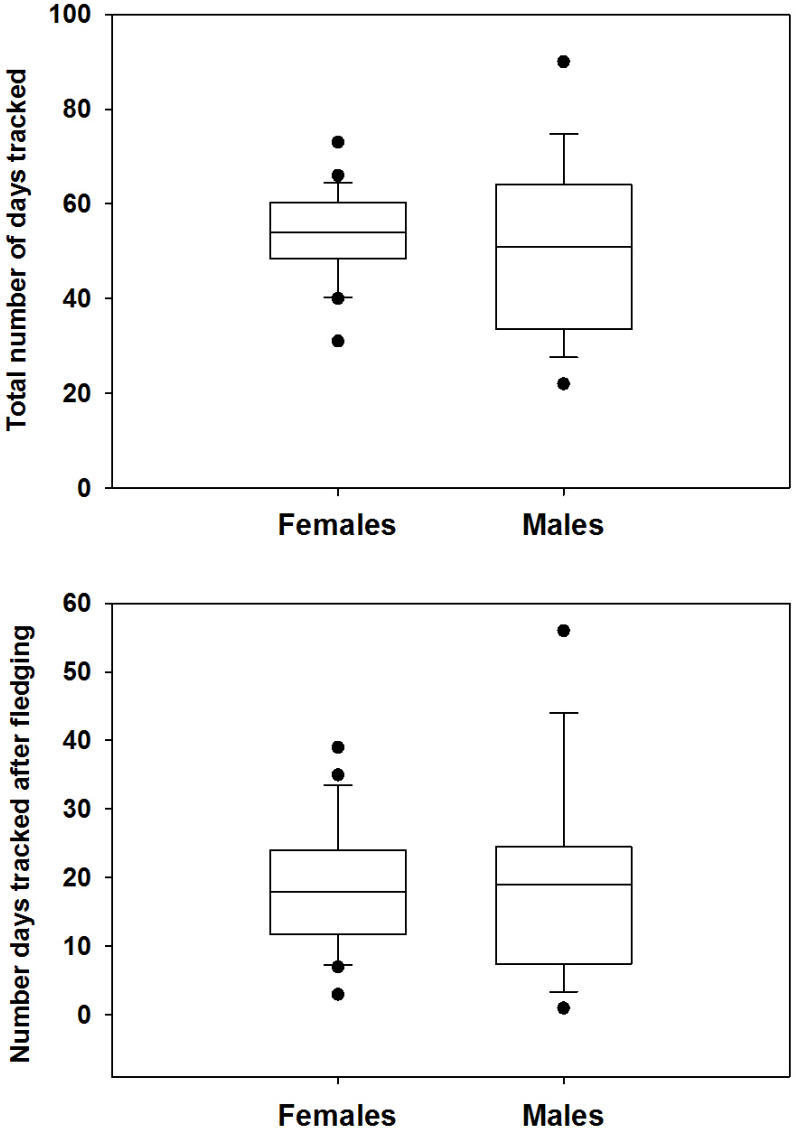

Figure C-3. Gender differences in minimum retention time (in days) of VHF-transmitters back-mounted on adult Common Terns and tracked by a network of automated radio telemetry stations after initial capture (upper panel), and after their chicks had fledged (lower panel). Horizontal lines of the boxes represent 25th, 50th and 75th percentiles, whiskers represent 5th and the 95th percentiles, and points represent outliers.

Tag effects

Of the 48 broods associated with our tagged birds, only one brood did not have at least one chick fledge. There was no evidence of a difference in the fledge success of chicks from nests from tagged nests (1.68 ± 0.09 chicks fledged per brood) versus non-tagged control nests (1.63 ± 0.11 chicks fledged per brood) and no significant interactions between tag presence and hatch order (Table C-1). Across both tagged and non-tagged control nests, probability of fledge was highest for A chicks and decreased with hatch order (Fig. C-4).

Table C-1. Parameter estimates of a Generalized Linear Mixed Model of the effects of VHF transmitters on fledge success of nesting Common Terns, where fledge success is a binomial response variable, and fixed effects are: Group (where 'Tagged' indicates that nesting pair had one VHF tagged adult and 'Control' indicates that both adults in nesting pair were not VHF-tagged); Hatch Order (where A, B, and C indicate the first hatched, second hatched, and third hatched chicks, respectively) and their interactions. The 'Tagged' Group and 'A' chick are the reference classes.

	Estimate	SE	z-value	p-value
(Intercept)	3.31	0.75	4.42	< 0.001
Control Group	-1.02	0.87	-1.18	0.238
B Chick	-2.22	0.81	-2.76	0.006
C Chick	-5.80	1.10	-5.28	< 0.001
Control Group:B Chick	1.27	1.01	1.25	0.210
Control Group:C Chick	2.04	1.34	1.52	0.129

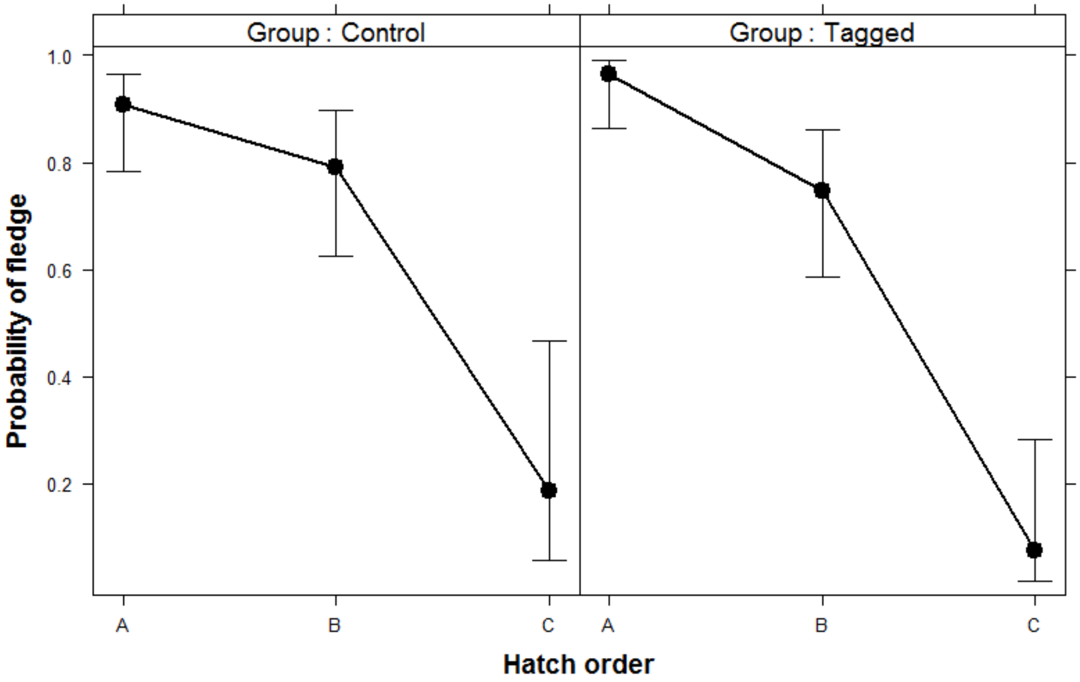

Figure C-4. Probability that a Common Tern chick fledged as a function of hatch order in broods where one adult had a VHF-transmitter (Group: Tagged, *n* = 50) and neither adult had a transmitter (Group: Control, *n* = 50), where 'A', 'B', and 'C' identifies the first hatched, second hatched, and third hatched chick, respectively.

DISCUSSION

Using the glue and subcutaneous suture technique, the majority (81%) of individuals in our study retained their transmitters until they departed from the nesting colony. This estimate is conservative because we assumed that birds that were not detected through the fledge or fail date of their nests dropped their transmitters. However, their tags could have malfunctioned, as occurred with two tags shortly after deployment. We did not recover any dropped tags near our network of land-based telemetry stations, indicating that transmitters may have fallen off while the birds were away from the colony. We found slightly lower tag retention of males relative to females, which may result from male Common Terns spending more time foraging during the breeding period than females (Wiggins and Morris 1987). Thus, transmitters on males may have been subjected to increased levels of stress and impact associated with plunge diving compared to females who spent more time during the chick-rearing period within the nesting colony.

Retention time of transmitters in our study was similar to estimates reported by Ackerman et al., (2009), who used sutures to back-mount VHF transmitters to fledgling Forster's Terns and tracked their movements for up to 44 days. Conversely, studies using different types of temporary attachment methods on terns, such as attaching transmitters to the central rectrices (Black 2006), or back-mounting transmitters with adhesive and/or tape (Perrow et al., 2006), reported considerably lower retention times (i.e., less than two weeks), indicating that these other attachment techniques are more suitable for short-term deployments. Therefore, researchers requiring transmitter retention for one to three months, such as during the breeding period, should consider using glue in combination with sutures as it appears to be a more reliable method of tag attachment.

During the breeding period, radio transmitters can reduce foraging efficiency and chick provisioning rates, leading to reduced chick growth and productivity (Whidden et al., 2007). A reduction in chick provisioning may have had disproportionate influence on younger chicks, as typically the older, larger chicks often outcompete younger and smaller chicks for prey items that adults bring back to the nest (Nisbet et al. 2017). Although we did document an inverse relationship between fledge success and hatch order across all nests in the study, we did not detect any differences among fledge success of chicks between tagged and control nests. Several studies also examined effects of different types of back-mounted transmitters on terns during the breeding period (Massey et al., 1988, Hill and Talent 1990, Becker et al., 1993, Perrow et al., 2006). Although an early study on Least Terns (*Sternula antillarum*) reported abnormal behavior of four birds with radio-tags glued to the inter-scapular region, the behavior was temporary and did not affect nest success or chick provisioning (Massey et al., 1988). In a subsequent study of Least Terns, transmitters weighing 6 to 7% of body weight, and glued over the bird's center of gravity did not affect behavior, nest survival, nest predation, or nest desertion (Hill and Talent 1990). Additionally, transmitters glued to the back of Least Tern chicks did not influence their growth rate or movement, despite being 5 to 8% of a chick's weight (Whittier and Leslie 2005)**.** Perrow et al., (2006) found no apparent adverse effects of back-mounted transmitters on the behavior and nesting success of Little Terns (*Sternula albifrons*) and suggested that the back-mounting attachment technique was "a relatively benign procedure". During the breeding period, Common Terns carrying relatively heavy transmitters (8 g) glued to the skin between their wings, displayed similar behavior, food intake, energy expenditure, and body mass relative to controls (Klaassen et al., 1992, Becker et al., 1993)**.**

The glue and suture technique we used for this study appears to be a suitable technique for attaching transmitters to terns for medium-duration studies, such as during the breeding period, in regards to both transmitter retention and bird welfare. However, because we were not able to track terns after they departed from our study area, the retention times reported herein should be considered minimum estimates. Additional coordinated automated telemetry stations are currently being established throughout the western Hemisphere (Taylor et al., 2017), making it possible to track tagged birds over longer distances and thus will enable improved estimates of transmitter retention on Common Terns and other species after they depart from the breeding grounds.

Although we did not observe adverse effects on the reproductive parameters we examined, we suggest that researchers employing the glue and suture attachment technique in future studies examine additional effects that are specific to their study period (Lewis et al., 2017). For studies during the breeding period, additional metrics could include foraging efficiency, physiological stress, chick growth and survival, and colony attendance (Burger and Shaffer 2008, Barron et al., 2010, Snijders et al. 2017). For studies spanning the annual cycle, additional research on the effects of transmitters on energetics and return rates of tagged individuals may be warranted (Vandenabeele et al., 2011).

ACKNOWLEDGEMENTS

This study was funded in part by the U.S. Department of the Interior, Bureau of Ocean Energy Management through Interagency Agreement M13PG00012 with the U.S. Department of the Interior, Fish and Wildlife Service. Additional funding was provided by the National Science Foundation IGERT Offshore Wind Energy Program. For advice, assistance and logistical support we thank the following entities and individuals: Nantucket Conservation Foundation (Karen Beattie), Nantucket Islands Land Bank (Eric Savetsky), Monomoy National Wildlife Refuge (Kate Iaquinto, Matt Boarman, Stephanie Koch, Carly Congden), U.S. Fish and Wildlife Service Division of Migratory Birds, Northeast Region (Caleb Spiegel, Scott Johnston), U.S. Fish and Wildlife Service, Maine Coastal Islands National Wildlife Refuge (Linda Welch), MassWildlife (Carolyn Mostello), Massachusetts Audubon Society (Norm Smith),University of Massachusetts (Matt Malin, Brett Still, Brian Lang, and Eric LeFlore), Tufts University (Mark Pokras), Acadia University (Rob Ronconi, Phil Taylor, John Brzustowski). This research was conducted under the University of Massachusetts Institutional Animal Care and Use Committee Protocol #2012-0024.

LITERATURE CITED

Ackerman, J. T., J. D. Bluso-Demers and J. Y. Takekawa. 2009. Postfledging Forster's Tern movements, habitat selection, and colony attendance in San Francisco Bay. Condor 111:100-110.

Barron, D. G., J. D. Brawn and P. J. Weatherhead. 2010. Meta-analysis of transmitter effects on avian behaviour and ecology. Methods in Ecology and Evolution 1:180-187.

Becker, P. H., D. Frank and S. R. Sudmann. 1993. Temporal and spatial pattern of Common Tern (*Sterna hirundo*) foraging in the Wadden Sea. Oecologia 93:389-393.

Black, A.L. 2006. Foraging area characteristics of Arctic Terns (*Sterna paradisaea*) and Common Terns (*Sterna hirundo*) breeding on Machias Seal Island. Ph.D. dissertation. University of New Brunswick, Canada.

Bolker, B. M., M. E. Brooks, C. J. Clark, S. W. Geange, J. R. Poulsen, M. H. H. Stevens and J.-S. S. White. 2009. Generalized linear mixed models: a practical guide for ecology and evolution. Trends in Ecology and Evolution 24:127-135.

Burger, A. E. and S. A. Shaffer. 2008. Perspectives in ornithology Application of tracking and data-logging technology in research and conservation of seabirds. Auk 125:253-264

Bridge, E.S., K. Thorup, M.S. Bowlin, P.B. Chilson, R.H. Diehl. R.W. Fléron, P. Hartl, R. Kays, J.F. Kelly, W.D. Robinson, and. M. Wikelski. 2011. Technology on the move: recent and forthcoming innovations for tracking migratory birds. BioScience 61: 689-698.

Constantini, D. and A. P. Møller 2013. A meta-analysis of the effects of geolocation application on birds. Current Zoology 59:697-706.

Duffy, D. C. 1986. Foraging at patches: interactions between Common and Roseate Terns. Ornis Scandinavia 7:47-52.

Fair, J. M., E. Paul, J. Jones, A. B. Clark, C. Davie and G. Kaiser. 2010. Guidelines to the use of wild birds in research. Ornithological Council. <www.nmnh.si.edu/BIRDNET/guide>. Accessed 21 July 2015.

Geen, G. R., R.A. Robinson, and S.R. Baillie. 2019. Effects of tracking devices on individual birds – a review of the evidence. Journal of Avian Biology https://doi.org/10.1111/jav.01823

Hawkins, P. 2004. Bio-logging and animal welfare: practical refinements. Memoirs of National Institute of Polar Research, Special Issue 58:58-68.

Hill, L. A. and L. G. Talent. 1990. Effects of capture, handling, banding, and radio-marking on breeding Least Terns and Snowy Plovers. Journal of Field Ornithology 61:310-319.

Johnson, G. D., J. L. Pebworth and H. O. Krueger. 1991. Retention of transmitters attached to passerines using a glue-on technique. Journal of Field Ornithology 62:486-491.

Lewis, T. L., D. Esler, B. D. Uher-Koch, R. D. Dickson, E. M. Anderson, J. R. Evenson, J.W. Hupp, and P.L. Flint. 2017. Attaching transmitters to waterbirds using one versus two subcutaneous sutures: Retention and survival trade-offs. Wildlife Society Bulletin 41:691-700.

López-López, P. 2016. Individual-based tracking systems in ornithology: Welcome to the era of Big Data. Ardeola 63:103-137.

Klaassen, M., P. H. Becker and M. Wagener. 1992. Transmitter loads do not affect the daily energy expenditure of nesting Common Terns. Journal of Field Ornithology 63:181-185.

Massey, B. W., K. Keane and C. Boardman. 1988. Adverse effects of radio transmitters on the behavior of nesting Least Terns. Condor 90:945-947.

Morris, R. D. and G. P. Burness. 1992. A new procedure for transmitter attachment: effects on brood attendance and chick feeding rates by male Common Terns. Condor 94:239-243.

Mostello, C. S., I. C. Nisbet, S. A. Oswald and J. W. Fox. 2014. Non-breeding season movements of six North American Roseate Terns *Sterna dougallii* tracked with geolocators. Seabirds 27:1-21.

Nisbet I.C.T., J.M Arnold, S. A. Oswald, P. Pyle, and M.A. Patten. 2017. Common Tern (*Sterna hirundo*) version 3.0 In The Birds of North America (P. G. Rodewald, Editor)., Cornell Lab of Ornithology, Ithaca, NY. https://doi.org/10.2173/bna.comter.03

Nisbet, I. C. T., C. S. Mostello, R. R. Veit, J. W. Fox, and V. Afanasyev. 2011. Migrations and winter quarters of five Common Terns tracked using geolocators. Waterbirds 34:32-39.

R Development Core Team. 2015. R: a language and environment for statistical computing v. 3.0.2. R Foundation for Statistical Computing, Vienna, Austria. http://www.R-project.org/, accessed 17 Dec 2015.

Pennycuick, C. J., P. L. F. Fast, N. Ballerstädt, and N. Rattenborg. 2011. The effect of an external transmitter on the drag coefficient of a bird’s body, and hence on migration range, and energy reserves after migration. Journal of Ornithology 153:633-644.

Perrow, M. R., E. R. Skeate, P. Lines, D. Brown, and M. L. Tomlinson. 2006. Radio telemetry as a tool for impact assessment of wind farms: the case of Little Terns *Sterna albifrons* at Scroby Sands, Norfolk, UK. Ibis 148:57-75.

Sirdevan, J. E., and J. S. Quinn. 1997. Foraging patterns of Caspian Terns (*Sterna caspia*) determined using radio-telemetry. Colonial Waterbirds 20:429-435.

Söhle, I. S., H. Moller, D. Fletcher, and C. J. R. Robertson. 2000. Telemetry reduces colony attendance by Sooty Shearwaters (*Puffinus griseus*). New Zealand Journal of Zoology 27:357-365.

Snijders, L., L. E. Nieuwe Weme, P. de Goede, J. L., Savage, K. Van Oers, and M, Naguib. 2017. Context-dependent effects of radio transmitter attachment on a small passerine. Journal of Avian Biology 48:650-659.

Taylor, P. D., T. L. Crewe, S. A. Mackenzie, D. Lepage, Y. Aubry, Z. Crysler, G. Finney, C. M. Francis, C. G. Guglielmo, D. J. Hamilton, R. L. Holberton, P. H. Loring, G. W. Mitchell, D. Norris, J. Paquet, R. A. Ronconi, J. Smetzer, P. A. Smith, L. J. Welch, and B. K. Woodworth. 2017. The Motus Wildlife Tracking System: a collaborative research network to enhance the understanding of wildlife movement. Avian Conservation and Ecology 12:8.

Thaxter, C. B., V. H. Ross-Smith, J. A. Clark, and N. A. Clark, G. J. Conway, and M. Marsh. 2014. A trial of three harness attachment methods and their suitability for long-term use on Lesser Black-backed Gulls and Great Skuas. Ringing and Migration 29:65-76.

Vandenabeele, S. P., E. Grundy, M. I. Friswell, A. Grogan, S. C. Votier, and R. P. Wilson. 2014. Excess baggage for birds: Inappropriate placement of tags on gannets changes flight patterns. PLoS ONE 9:e92657.

Vandenabeele, S. P., E. L. Shepard, A. Grogan, and R. P. Wilson. 2011. When three per cent may not be three per cent; device-equipped seabirds experience variable flight constraints. Marine Biology 159:1-14.

Wanless, S., M. P. Harris, and J. A. Morris. 1988. The effect of radio transmitters on the behavior of Common Murres and Razorbills during chick rearing. Condor 90:816-823.

Warnock, N., and J. Y. Takekawa. 2003. Use of radio telemetry in studies of shorebirds: past contributions and future directions. Wader Study Group Bulletin 100:138-150.

Weimerskirch, H., M. L. Corre, F. Marsac, C. Barbraud, O. Tostain, and O. Chastel. 2006. Postbreeding movements of frigatebirds tracked with satellite telemetry. Condor 108:220-225.

Wheeler, W. E. 1991. Suture and glue attachment of radio transmitters on ducks. Journal of Field Ornithology 62:271-278.

Whidden, S. E., C. T. Williams, A. R. Breton, and C. L. Buck. 2007. Effects of transmitters on the reproductive success of Tufted Puffins. Journal of Field Ornithology 78:206-212.

White, G. and R. Garrott. 1990. Analysis of wildlife radio-tracking data. Academic Press, San Diego, California.

Whittier, J. B., and D. M. Leslie. 2005. Efficacy of using radio transmitters to monitor Least Tern chicks. Wilson Bulletin 117:85-91.

Wiggins, D.A. and R.D. Morris. 1987. Parental care of the Common Tern *Sterna hirundo*. Ibis 129: 533-540.

Appendix D

Metadata for BOEM Tag Deployments

As supplementary material to this report, we have provided tag deployment data and results of exposure analysis for each nano-tagged bird in this study submitted to BOEM, in separate files for each Project Number and tagging site ('Appendix_D-Tag_Metadata_[spp]_[year].csv').

Descriptions of each field appear below:

Fields:

id: nanotag ID number

spp: species (cote = Common Tern, rost = Roseate Tern, pipl = Piping Plover)

depLoc: geographic location of tag deployment

depLat: Latitude of tag deployment (decimal degrees)

depLon: Longitude of tag deployment (decimal degrees)

depDate: Date of tag deployment

age: age of bird. AHY = After Hatch Year

sex: sex of bird. M = male, F = female, U = unknown (not determined)

band: US Geological Survey (USGS) issued band number

aux: code and color of uniquely coded auxiliary marker(s)

tagRet = 1 (tag retention unknown), 0 (known tag drop)

first_date_SA: date of first detection in Study Area (NA if not detected in Study Area)

last_date_SA: date of last detection in Study Area (NA if not detected in Study Area)

days_SA: total number of days detected in Study Area (NA if not detected in Study Area)

fed_waters: 1 = movement model estimated locations in Federal waters of US Atlantic (with standard error in x and y coordiantes <30 km), 0 = movement model did not estimate locations in Federal waters of US Atlantic (NA if tagRet=0).

boem_lease: lists all BOEM wind energy lease areas that movement model estimated exposure to (with standard error in x and y coordinates <30 km)

boem_plan: lists all BOEM wind energy planning areas that movement model estimated exposure to (with standard error in x and y coordinates <30 km)

block_is: 1 = movement model estimated exposure to Block Island Wind Farm (with standard error in x and y coordinates <30 km), 0 = movement model did not estimate exposure to Block Island Wind Farm, (NA if tagRet=0).

Appendix E

Metadata for BOEM Automated Radio Telemetry Stations, 2013-2017

Table E-1. Detailed description of automated receiving stations comprising the BOEM radio telemetry array by site, station code, geographic coordinates (decimal degrees), start year of operation, end year of operation, and installation specifications.

Site	Code	Lat	Long	Start Year	End Year	Installation
Monomoy NWR - N, Chatham, MA	MNYN	41.6088	-69.9870	2014	Still operational	Six, 9-element (11.1 dBd) Yagi antennas oriented radially (60 degree separation) on 12.2-m mast
Monomoy NWR - S, Chatham, MA	MNYS	41.5526	-70.010	2014	Still operational	Six, 9-element (11.1 dBd) Yagi antennas oriented radially (60 degree separation) on 12.2-m mast
Monomoy NWR – Tern Colony, Chatham, MA	TERN	41.6197	-69.9849	2014	2015	One, 5-element (9 dBd) Yagi antenna (oriented S) on 1.4 m post.
Nantucket NWR (Great Point), Nantucket, MA	GTPT	41.3906	-70.0490	2014	Still operational	Six, 9-element (11.1 dBd) Yagi antennas oriented radially (60 degree separation) on 12.2-m mast
Coatue Point, Nantucket, MA	CTPT	41.3073	-70.0640	2014	2017	Six, 9-element (11.1 dBd) Yagi antennas oriented radially (60 degree separation) on 12.2-m mast
Eel Point, Nantucket, MA	CTPT	41.2934	-70.1972	2014	2015	Six, 9-element (11.1 dBd) Yagi antennas oriented radially (60 degree separation) on 12.2-m mast
Muskeget Island, Nantucket, MA	MUSK	41.3373	-70.3050	2014	2017	Six, 9-element (11.1 dBd) Yagi antennas oriented radially (60 degree separation) on 12.2-m mast
Great Point Ferry, Nantucket Sound	GTPF	Mobile	Mobile	2014	2015	One omnidirectional antenna (200 W) on passenger ferry (travels between Hyannis, MA and Nantucket, MA)
R/V Henry Bigelow (NOAA)	NOAA	Mobile	Mobile	2014	2014	One omnidirectional antenna (200 W) on NOAA Research Vessel (travels from Newport, RI to various offshore sites)
Nomans Land Island NWR, MA	NOMA	41.2613	-70.8150	2014	Still operational	Six, 9-element (11.1 dBd) Yagi antennas oriented radially (60 degree separation) on 12.2-m mast
Nomans Land Island NWR, MA - Summit	NOMS	41.2531	-70.8130	2014	Still operational	One, 9-element (11.1 dBd) Yagi antenna oriented SW on a 3 m (10 ft) mast at the summit (110 ft. elevation) of Nomans Land Island
Sachuest Point NWR, Middletown, RI	SACH	41.4787	-71.2440	2014	Still operational	Six, 9-element (11.1 dBd) Yagi antennas oriented radially (60 degree separation) on 12.2-m mast
Southeast Light, Block Island, RI	BISE	41.1532	-71.5530	2014	2017	Six, 9-element (11.1 dBd) Yagi antennas oriented radially (60 degree separation) on 12.2-m mast
Napatree Point, Westerly, RI	NAPA	41.3063	-71.8840	2014	Still operational	Six, 9-element (11.1 dBd) Yagi antennas oriented radially (60 degree separation) on 12.2-m mast
Montauk Point, Montauk, NY	MNTK	41.0723	-71.8560	2014	Still operational	Six, 9-element (11.1 dBd) Yagi antennas oriented radially (60 degree separation) on 12.2-m mast
Great Gull Island, NY	GGIS	41.2018	-72.1190	2014	Still operational	Four 5-element (9 dBd) Yagi antennas oriented radially (90 degree separation) on 11-m observation tower

Site	Code	Lat	Long	Start Year	End Year	Installation
Race Point, Cape Cod National Seashore, Provincetown, MA	RCPT	42.0658	-70.2440	2015	2017	Six, 9-element (11.1 dBd) Yagi antennas oriented radially (60 degree separation) on 12.2-m mast
Marconi, Cape Cod National Seashore, Wellfleet, MA	WELL	41.9147	-69.9720	2015	Still operational	Six, 9-element (11.1 dBd) Yagi antennas oriented radially (60 degree separation) on 12.2-m mast
Waquoit Bay National Estuarine Research Reserve, Mashpee, MA	WAQT	41.5518	-70.5070	2015	Still operational	Six, 9-element (11.1 dBd) Yagi antennas oriented radially (60 degree separation) on 12.2-m mast
Shearwater (Boat), Nantucket, MA	SHEA	Mobile	Mobile	2015	2017	One 200-W omnidirectional antenna on whale watching boat (out of Nantucket, MA)
Trustom Pond NWR, South Kingston, RI	TRUS	41.3734	-71.5760	2015	Still operational	Six, 9-element (11.1 dBd) Yagi antennas oriented radially (60 degree separation) on 12.2-m mast
Fire Island National Seashore, Long Island, NY	FRIS	40.6328	-73.2160	2015	Still operational	Six, 9-element (11.1 dBd) Yagi antennas oriented radially (60 degree separation) on 12.2-m mast
Wings Neck, Bourne, MA	WING	41.6807	-70.6615	2016	Still operational	Two, 9-element antennas on 11-m observation tower
Old Saybrook, CT	OSCT	41.2875	-72.3240	2016	Still operational	Six, 9-element (11.1 dBd) Yagi antennas on 8-m tower
Plum Island Animal Disease Center, Orient, NY	PLIS	41.1894	-72.1630	2016	2017	Six, 9-element (11.1 dBd) Yagi antennas oriented radially (60 degree separation) on 12.2-m mast
New York Aquarium, Coney Is, NY	CONY	40.5738	-73.9770	2016	Still operational	Four, 9-element (11.1 dBd) antennas on 12 m building
Jamaica Bay Unit, Gateway National Recreation Area, NY	JMBY	40.6163	-73.8240	2016	Still operational	Four, 5-element (9 dBd) antennas on 12.2 m utility pole
Sandy Hook Unit, Gateway National Recreation Area, NJ	SHNJ	40.4301	-73.9868	2016	Still operational	Six, 9-element (11.1 dBd) Yagi antennas oriented radially (60 degree separation) on 12.2-m mast
Rutgers Marine Field Station, NJ	RTNJ	39.5090	-74.3240	2016	Still operational	Four, six-element (9 dBd) antennas attached to roof of 12-m building
North Brigantine Natural Area, NJ	NBNJ	39.4218	-74.3477	2016	Still operational	Six, 9-element (11.1 dBd) Yagi antennas oriented radially (60 degree separation) on 12.2-m mast
Avalon Fishing Pier, Avalon, NJ	AVNJ	39.0919	-74.7179	2016	Still operational	Four, 9-element (11.1 dBd) antennas attached to 7-m mast
Cape Henlopen State Park, DE	CHSP	38.7702	-75.0852	2016	Still operational	Six, 9-element (11.1 dBd) Yagi antennas oriented radially (60 degree separation) on 12.2-m mast
Parramore Island, VA Coast Reserve, VA	PARR	37.5737	-75.6174	2016	Still operational	Four, six-element (9 dBd) antennas on existing 21-m tower
Chincoteague NWR, VA	CHIN	37.8627	-75.3703	2016	Still operational	Six, 9-element (11.1 dBd) Yagi antennas oriented radially (60 degree separation) on 12.2-m mast
Eastern Shore NWR, Skidmore Island, VA	SKID	37.1340	-75.9258	2016	Still operational	Six, 9-element (11.1 dBd) Yagi antennas oriented radially (60 degree separation) on 12.2-m mast
Back Bay NWR, VA	BBVA	36.6718	-75.9156	2016	Still operational	Six, 9-element (11.1 dBd) Yagi antennas oriented radially (60 degree separation) on 12.2-m mast

Appendix F

Summary of data from nano-tagged birds that were tagged by partners in the Motus network and detected by BOEM radio telemetry stations

We compiled the total number of nano-tagged birds and bats that were tagged by partners in the Motus network and detected by BOEM-funded radio telemetry stations from 2014 to 2017, and calculated the total number of individuals detected per day at each site. We conservatively removed false detections by retaining only individuals with ≥ 10 detections per tower per day. In 2014, this resulted in 14 detected species of shorebirds, passerines, and raptors (Table F-1). In 2015, detections included 18 detected species of shorebirds, passerines, raptors, and bats (Table F-2). In 2016, detections included 28 species of shorebirds, passerines, raptors, and bats (Table F-3). In 2017, detections included 18 species of shorebirds and passerines (Table F-4). Tags from 52 projects were detected over the four year period (Table F-5).

The entire non-target dataset for BOEM funded towers, consisting of the number of individuals detected per species and tower by date, is provided as supplementary material to this report (Appendix_F_Non-Target_Detection_Data_BOEM_2014.csv', Appendix_F_Non-Target_Detection_Data_BOEM_2015.csv', Appendix_F_Non-Target_Detection_Data_BOEM_2016.csv', Appendix_F_Non-Target_Detection_Data_BOEM_2017.csv'.)

Table F-1. Total number of nano-tagged individuals per species detected by BOEM-funded radio telemetry stations in 2014.

Common name	Scientific name	Num.	Project
Arctic Tern	*Sterna paradisaea*	4	7
Black-bellied Plover	*Pluvialis squatarola*	1	15
Blackpoll Warbler	*Setophaga striata*	11	12, 15, 39, 86
Common Tern	*Sterna hirundo*	12	7, 17
Great Black-backed Gull	*Larus marinus*	2	21
Herring Gull	*Larus argentatus*	1	21
Merlin	*Falco columbarius*	17	45
Red-eyed Vireo	*Vireo olivaceus*	4	12
Red Knot	*Calidris canutus*	34	47, 88
Saltmarsh Sparrow	*Ammospiza caudacuta*	12	29
Semipalmated Sandpiper	*Calidris pusilla*	25	9, 13, 15, 25, 27, 38
Swainson's Thrush	*Catharus ustulatus*	2	49
White-rumped Sandpiper	*Calidris fuscicollis*	5	38
White-throated Sparrow	*Zonotrichia albicollis*	1	24

Table F-2. Total number of nano-tagged individuals per species detected by BOEM-funded radio telemetry stations in 2015.

Common name	Scientific name	Num.	Project
American Woodcock	*Scolopax minor*	2	82
Bank Swallow	*Riparia riparia*	2	26
Common Tern	*Sterna hirundo*	3	7
Dunlin	*Calidris alpina*	1	38
Eastern Red Bat	*Lasiurus borealis*	1	32
Eastern Small-footed Bat	*Myotis leibii*	1	9
Indiana Bat	*Myotis sodalis*	1	54
Merlin	*Falco columbarius*	22	45
Piping Plover	*Charadrius melodus*	1	77
Red-eyed Vireo	*Vireo olivaceus*	1	74
Red Knot	*Calidris canutus*	43	15, 47, 88
Ruddy Turnstone	*Arenaria interpres*	7	27, 47, 66
Saltmarsh Sparrow	*Ammospiza caudacuta*	10	29
Sanderling	*Calidris alba*	8	63, 68, 110
Semipalmated Plover	*Charadrius semipalmatus*	5	27, 67
Semipalmated Sandpiper	*Calidris pusilla*	44	25, 38, 58, 59, 66, 110
White-rumped Sandpiper	*Calidris fuscicollis*	19	38
Yellow-rumped Warbler (Myrtle)	*Setophaga coronata coronata*	18	83

Table F-3. Total number of nano-tagged individuals per species detected by BOEM-funded radio telemetry stations in 2016.

Common name	Scientific name	Num.	Project
American Woodcock	*Scolopax minor*	6	82
Bicknell's Thrush	*Catharus bicknelli*	1	49
Black-bellied Plover	*Pluvialis squatarola*	2	68
Blackpoll Warbler	*Setophaga striata*	6	74, 83
Eastern Red Bat	*Lasiurus borealis*	2	32
Gray-cheeked Thrush	*Catharus minimus*	3	49, 57
Hermit Thrush	*Catharus guttatus*	9	83
Least Sandpiper	*Calidris minutilla*	11	38, 78
Lincoln's Sparrow	*Melospiza lincolnii*	1	74
Little Brown Bat	*Myotis lucifugus*	1	32
Merlin	*Falco columbarius*	11	45
Northern Waterthrush	*Parkesia noveboracensis*	1	74
Pectoral Sandpiper	*Calidris melanotos*	4	38
Prairie Warbler	*Setophaga discolor*	1	95
Red-eyed Vireo	*Vireo olivaceus*	7	83
Red Knot	*Calidris canutus*	53	38, 47, 65, 88
Ruddy Turnstone	*Arenaria interpres*	4	38, 47
Saltmarsh Sparrow	*Ammospiza caudacuta*	8	29
Sanderling	*Calidris alba*	25	47, 63, 68
Semipalmated Plover	*Charadrius semipalmatus*	17	38, 40, 67, 78
Semipalmated Sandpiper	*Calidris pusilla*	39	38, 58, 66, 103, 110
Semipalmated/Western Sandpiper	*Calidris pusilla/mauri*	1	58
Swainson's Thrush	*Catharus ustulatus*	8	74, 104, 109
Swamp Sparrow	*Melospiza georgiana*	1	104
Whimbrel	*Numenius phaeopus*	4	40
White-rumped Sandpiper	*Calidris fuscicollis*	12	38, 68
Wood Thrush	*Hylocichla mustelina*	1	74

Common name	Scientific name	Num.	Project
Yellow-rumped Warbler	*Setophaga coronata*	2	74

Table F-4. Total number of nano-tagged individuals per species detected by BOEM-funded radio telemetry stations in 2017.

Common name	Scientific name	Num.	Project
American Woodcock	*Scolopax minor*	2	82
Barn Swallow	*Hirundo rustica*	1	92
Bicknell's Thrush	*Catharus bicknelli*	9	49
Grasshopper Sparrow	*Ammodramus savannarum*	1	158
Gray-cheeked Thrush	*Catharus minimus*	8	49
Least Sandpiper	*Calidris minutilla*	3	38
Lesser Yellowlegs	*Tringa flavipes*	1	38
Ovenbird	*Seiurus aurocapilla*	4	19, 142
Pectoral Sandpiper	*Calidris melanotos*	3	38
Red Knot	*Calidris canutus*	8	38, 63, 140
Rusty Blackbird	*Euphagus carolinus*	1	161
Saltmarsh Sparrow	*Ammospiza caudacuta*	4	29
Sanderling	*Calidris alba*	17	63
Semipalmated Plover	*Charadrius semipalmatus*	13	38, 67, 78
Semipalmated Sandpiper	*Calidris pusilla*	29	3, 38, 58, 78, 103
Swainson's Thrush	*Catharus ustulatus*	17	74, 90, 109
Tree Swallow	*Tachycineta bicolor*	1	162
White-rumped Sandpiper	*Calidris fuscicollis*	2	38

Table F-5. Projects with nano-tagged birds or bats detected by BOEM radio telemetry array from 2014-2017.

ID	Project Name	Description
3	EC-Quebec-St. Lawrence	Shorebird projects based along the St. Lawrence river. PI: Yves Aubry (Environment Canada)
7	Welch	Maine Coastal Islands National Wildlife Refuge has been tagging common and Arctic terns on a number of breeding colonies in Maine since 2012.
9	Parker River/Great Bay Refuge	bat, shorebird, and saltmarsh sparrows nanotag projects in northeast MA and southern NH. 3 towers at Parker River, 2 at Great Bay
12	Smetzer	Red-eyed vireos and blackpoll warblers stopover and migration at Petit Manan Wildlife Refuge in Steuben Maine.
13	Semipalmated Sandpipers in the Bay of Fundy	Semipalmated Shorebird stopover and migration ecology in the Bay of Fundy.
15	Aubry	Stopover and Migratory behaviour of migratory birds along the St.Lawrence River - Swainson's Thrush, Pine Siskin, as well as some shorebirds.
17	Chapman	Shoals_2014
19	Dossman_Jamaica	Movement and space-use during the non-breeding season and migration.
21	Taylor - Gull	Gull work on Sable Island 2013
22	Taylor - Ipswich Sparrow	Ipswich Sparrow survival and migratory behaviour
24	Norris	White-throated Sparrow orientation and migration studies.
25	obrien	Shorebird work on the Gulf of Maine. Saltmarsh Sparrow migration project.
26	Salda - Atlantic Bank Swallows	Studying foraging and roosting habitat selection in Bank Swallows.
27	Smith	A wide variety of migratory shorebird projects focusing on Semipalmated Sanpipers and Red Knots.
29	R5_SALS	Currently only winter/spring deployments on Saltmarsh Sparrow (SALS) in South Carolina
32	Dowling	Migratory season tracking of eastern red, hoary, and silver-haired bats to inform migration ecology and offshore wind development
38	James Bay Shorebirds	Multi-agency shorebird monitoring on the western coast of James Bay.
39	Nol/Parada- Blackpoll Warbler Migration	Description not available
40	EC - Arctic Shorebirds	Collective of stations throughout the Canadian arctic and subarctic in support of shorebird ecology research.
45	BI_MERL	Digitally-coded tags on southward migrating Merlins captured during fall on Block Island, Rhode Island
47	Red Knot Staging and Migration Ecology	Stopover and migration ecology of Red Knots at Delaware Bay, NJ.

ID	Project Name	Description
49	Thrush post-breeding ecology in Quebec	PIs: Andre Derochers (U Laval), Junior Tremblay & Yves Aubry (Env Canada) Breeding, post-breeding, and migratory ecology of BITH, SWTH, GCTH.
54	Indiana Bats - 2015	Indiana Bats - 2015
55	Norris - MOBU 2015	Monarch butterfly foraging and migration behaviour.
57	Selva Colombia	1) Winter habitat use of Canada Warbler and Swainson's Thrush. 2) Stopover ecology and carry-over effects in migratory landbirds in Colombia.
58	Semipalmated Sandpiper stopover in Plymouth, MA	A joint project between Manomet and MassWildlife will be deploying nanotags on SESAs in Plymouth Bay to learn more about their local stopover ecology.
59	NJ Audubon - Delaware Bay Shorebirds	Track Semipalmated Sandpipers staging in Delaware Bay during spring migration
63	Saskatchewan Migratory Shorebirds	Shorebird stopover timing and habitat use in Saskatchewan
65	Texas Gulf Coast Migratory Shorebirds	Stopover and migration ecology of migratory REKN and SAND on the Texas Coast.
66	New project (#66)- EBM_Coats	Arctic-breeding shorebirds captured on the nest during the breeding season between 2014-2016
67	Nol - Churchill Shorebirds	Assessing Departure and Stopover Ecology of Two Species of Migrating Shorebirds
68	Arctic Shorebirds - CWS Yellowknife	Shorebird study at the Polar Bear Pass National Wildlife Area on Bathurst Island, Nunavut.
73	Mississippi Clapper Rail	Using automated telemetry to estimate seasonal and annual survivorship of Clapper Rails in emergent marshes of the northern Gulf of Mexico
74	CT River Valley Migratory Songbird Study	Migratory passerine use of the Connecticut river valley in Massachusetts, Vermont, and New Hampshire.
77	NJ Chick Survival	This project will examine factors limiting reproductive success in New Jersey.
78	Atlantic Canada Shorebirds	Assessing movement, habitat use and length of stay of migrating shorebirds during stop-over in Atlantic Canada.
82	Maine - American Woodcock	American Woodcock
83	BIMYWA	Digitally-coded tags on southward migrating warblers (Yellow-rumped and Blackpoll) captured during fall on Block Island, Rhode Island
86	Taylor - Blackpoll Warbler	Regional-scale and fine-scale movement decisions of post-breeding and migratory Blackpoll Warblers tagged on Nova Scotia's South Shore
88	Monomoy - Steph Koch	Nanotags are being placed on Red Knots on Cape Cod, MA, with the goal of learning more about important stopover sites and migration pathways.
90	Gerson - Florida Gulf Coast -	We study the body condition and stopover ecology of spring migrants along

ID	Project Name	Description
	Apalachicola	the Florida Gulf coast. Target species are SWTH, NOWA, YBCU.
92	Ontario Barn and Cliff Swallows	Description not available
95	BellVagrantsNS	Studying reorientation of vagrant passerines and near-passerines in Nova Scotia, CA
103	NYC Audubon	NYC Audubon will be using VHF NanoTags in order to track movements of Semipalmated Sandpipers stopping over in Jamaica Bay, NY during their migration.
104	Perlut - Maine Forest Birds	Banding station deploying nanotags on migrant songbirds in a coastal forest in southern Maine (Biddeford).
109	Taylor - SWTH	Post-breeding dispersal of Swainson's Thrush on Bon Portage and Seal Island in Nova Scotia. Research conducted by Lucas Berrigan and Phil Taylor.
110	Holberton 2015-16	Description not available
140	SCDNR Shorebirds	Description not available
142	Effects of mercury on ovenbird migration	Autumn migration speed and success of ovenbirds that are dosed with mercury throughout their breeding season in Connecticut
158	Eastern Ontario Grasshopper Sparrow	Tracking movement and migration patterns of Grasshopper Sparrows in southern Ontario
161	Migration connectivity of the Rusty Blackbird	Description not available
162	Western MA Tree Swallows	Description not available

Appendix G

Detection probability of BOEM automated radio telemetry stations

We strategically installed our BOEM-funded tower array with the objective to maximize the number of detections of our focal species in the Study Area. Due to the tradeoffs involved in siting a limited number of towers, we set up a high-density array near tagging sites at nesting locations, and for coverage of known post-breeding dispersal and staging areas for Common Terns, Roseate Terns, and Piping Plovers that are adjacent to BOEM Lease and Planning Areas throughout the Study Area. The array in 2014 consisted of 11 telemetry towers distributed from Cape Cod, MA to eastern Long Island, NY. The array was expanded in 2015 to include a total of 16 telemetry towers from Cape Cod to western Long Island. In 2016, we added 14 tracking towers at priority sites in New Jersey, Delaware, and Virginia. This expanded array remained in operation through 2017.

To aid in this effort, we developed coverage maps to identify areas of low-to-high detection probability within our study region. First, we depicted the horizontal radiation pattern of a single antenna (Fig. G-1), to illustrate the relationship between transmitter altitude and detection range of automated radio telemetry towers. There are two relationships to note here: 1) signal strength is inversely related to horizontal range r, i.e. a bird flying closer to an antenna at a given radial angle (ψ) will have a relatively stronger signal and 2) as long as the flight altitude is less than the horizontal range (i.e., $z < r$), signal strength and altitude are positively related (i.e., the higher a bird, the stronger the received signal strength). This means that high flying birds can be detected at greater distances from receivers than low flying birds, due to both the increased signal strength propagation, as well as the farther detection horizon (given the curvature of the earth).

Second, we estimated the detection probability from a single receiver as a function of radial angle using data from calibration surveys (conducted by flying a test tag from a kite that was towed behind a boat running a GPS unit). The detection rate per antenna within a 40 second total scan time (the duty cycle of the 9-element Lotek Yagi arrays) was calculated by averaging the calibration data within each 40 second time window and calculating the range and bearing to each of the two receiving towers. Figure G-2 depicts this within-cycle detection rate as a function of bearing to the receiver (solid line) and the angle of transmitter to receiver (dot-dashed line). Across the calibration surveys, the overall detection rate was approximately $p = 0.5$ (and highest along the main beam axis), and varied less strongly with the angle of transmitter to receiver (which our location model does not account for).

Third, we calculated the detection probability of a single tower based on the radiation pattern and overall detection probability, as estimated from the kite validation. Fourth, we calculated each tower's probability of detecting a tagged target, given the target's altitude and signal strength value of corresponding detection (unitless, range 1 to 255). We used data from the calibration surveys to determine an overall detection rate $p = 0.5$ (given target height = 30 m), where p = the proportion of test-tag locations that were detected by the towers. Across the calibration surveys, the overall detection rate was highest along the main beam axis, i.e., bearing close to zero degrees, and varied marginally with the angle of transmitter to receiver. Next, we calculated the probability of detection by all antennas on a single tower. This probability varied depending on the location of the target within the radiation pattern, because side lobes from one antenna overlapped with the main beam and side lobes from other antennas. The probability of detection at any point in the radiation pattern = P, where $P = 1 – (1-p)n$, and n = the number of overlapping beams at that location (i.e. 6 beams for a six-antenna tower).

Lastly, we mapped the overlapping detection probabilities of the BOEM tower array by year, given the target's altitude (20 m and 200 m, Figs. G-2 to G-5). We assumed the same detection rate, $p = 0.5$, across all heights. Towers from the global Motus network that detected our tagged birds provide extended coverage, which is not depicted here, due to variability in tower detections set up using different configurations. At higher flight altitudes, tower coverage overlaps due to increased detection range; in these cases, we display the maximum detection probability. Such overlapping ranges indicate where one target is likely to be detected simultaneously by multiple towers. Simultaneous detections provide more accurate estimates of altitude and spatial coordinates than what can be estimated from single detections. This information can help to provide guidelines for further research, based on the average flight height and distribution of focal species. Future studies should aim to maximize the number of overlapping tower ranges, to improve the altitude and location accuracy of their target estimates, given greater potential for simultaneous detections.

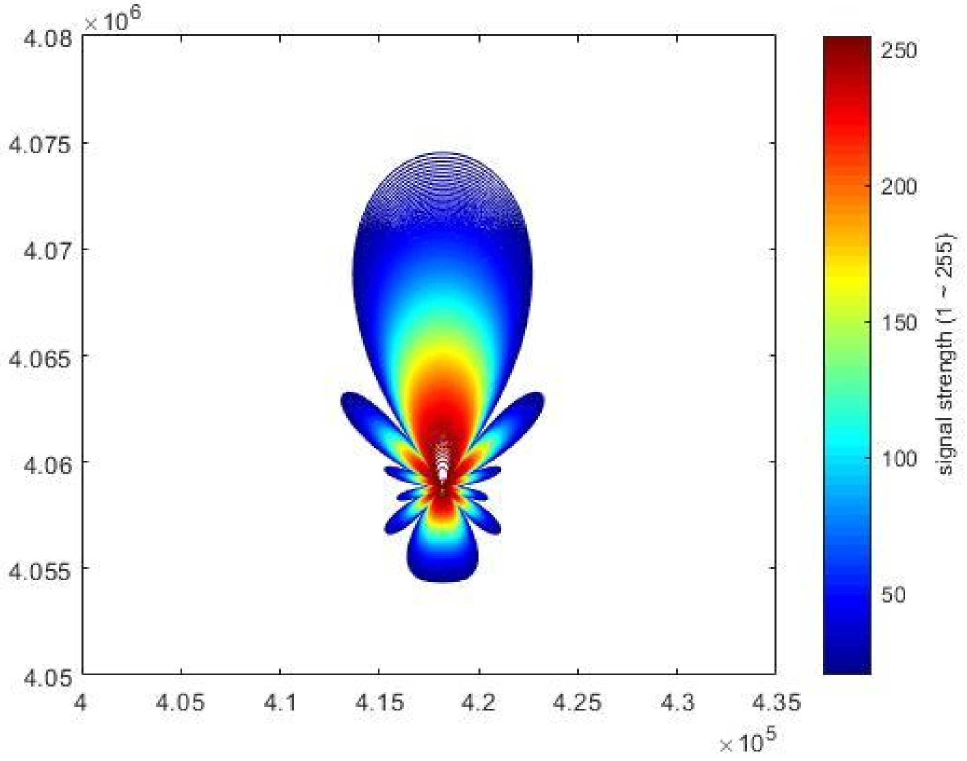

Figure G-1. Two-dimensional radiation pattern of 9-element Yagi antenna.
Example main beam (pointed upwards) and side lobes (e.g., from backscatter) associated with a tower antenna, given a target's range of signal strengths (1-255, scale bar), height (100 m), and map resolution (100 m). Each line represents a signal strength, where the outermost value = 1 and the innermost value = 255. The heat map scaling indicates a higher density of signal strengths closer to the tower, where a bird is most likely to be detected at high signal strength values. The x- and y-axes are in meters, such that this antenna has a range of approximately 40 km. Note that each signal strength has an equal probability of occurrence.

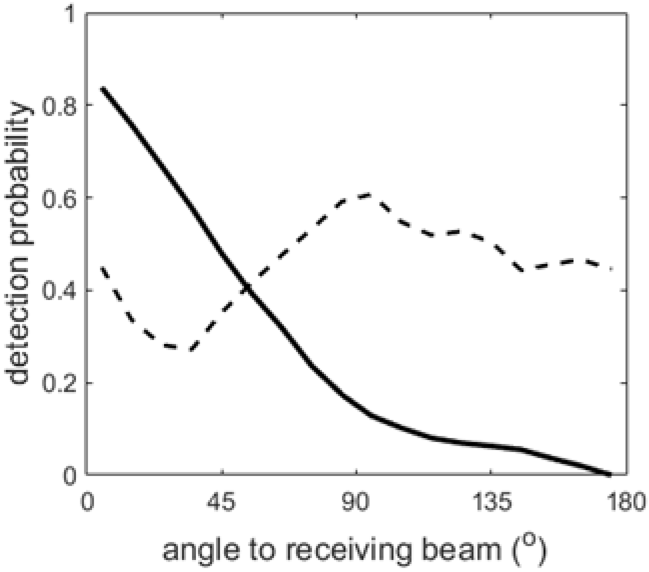

Figure G-2. Detection probability of kite in relation to receiver location and transmitter alignment
Detection probability was calculated as proportion of received signals within each 40 second duty cycle, based on (solid line) the kite's GPS location and the angles of kite to the main axis of the receiver antenna and (dot-dashed line) the angle of the transmitter antenna to the main receiver axis. Across the calibration surveys, the overall detection rate was approximately 0.5, highest for bearings along the main axis of receiving antennas (77% of detection events occurred from directions within 35° of the main axis), but varied less strongly with the angle of transmitter to receiver.

A.

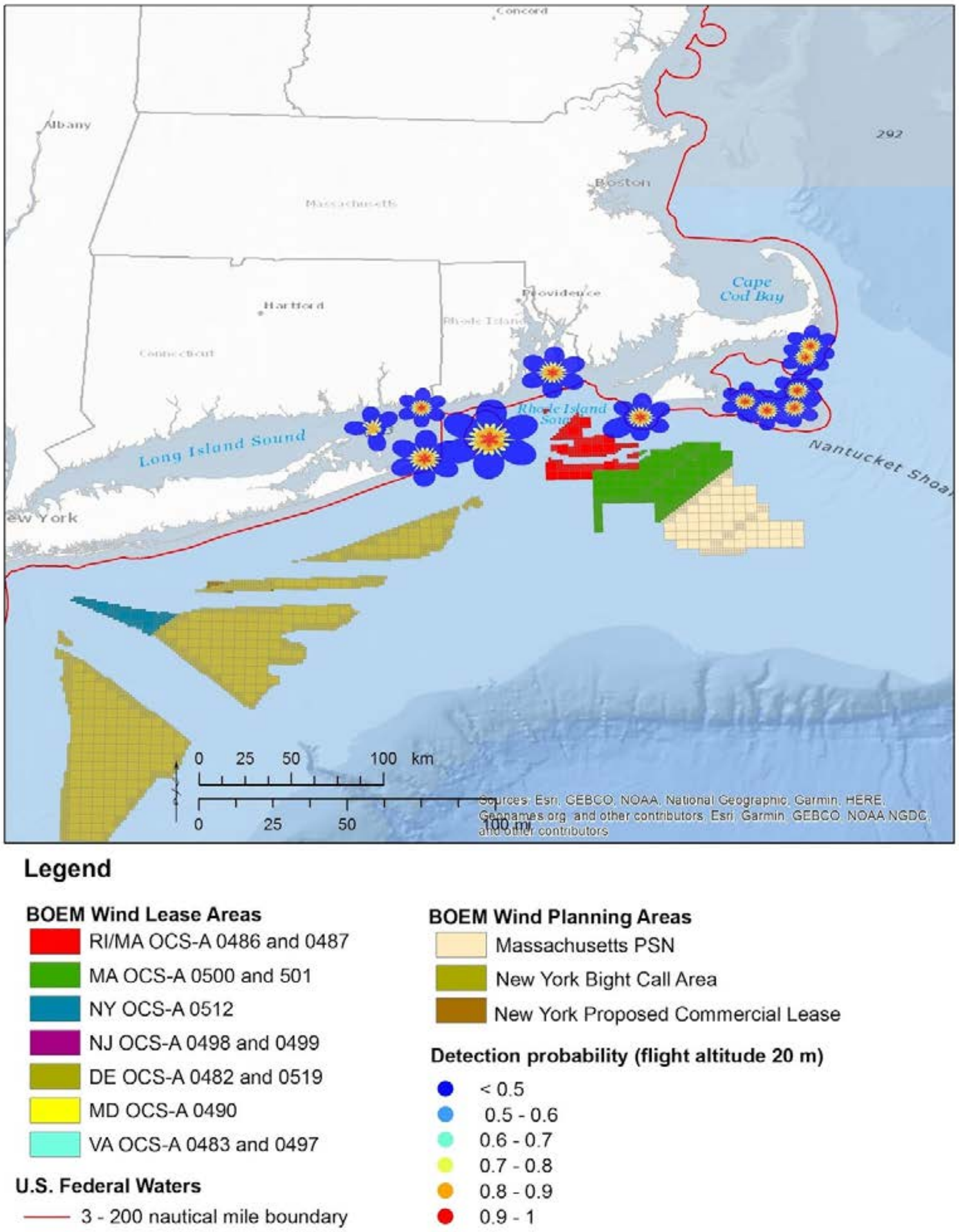
Concord
Albany
292
Boston
Massachusetts
Cape Cod Bay
Providence
Hartford
Rhode Island
Connecticut
Rhode Island Sound
Long Island Sound
Nantucket Shoal
New York
0 25 50 100 km
0 25 50 100 mi
Sources: Esri, GEBCO, NOAA, National Geographic, Garmin, HERE, Geonames.org, and other contributors, Esri, Garmin, GEBCO, NOAA NGDC, and other contributors
Legend
BOEM Wind Lease Areas
🟥 RI/MA OCS-A 0486 and 0487
🟩 MA OCS-A 0500 and 501
NY OCS-A 0512
NJ OCS-A 0498 and 0499
DE OCS-A 0482 and 0519
MD OCS-A 0490
VA OCS-A 0483 and 0497
U.S. Federal Waters
3 - 200 nautical mile boundary
BOEM Wind Planning Areas
Massachusetts PSN
New York Bight Call Area
New York Proposed Commercial Lease
Detection probability (flight altitude 20 m)
● < 0.5
● 0.5 - 0.6
● 0.6 - 0.7
● 0.7 - 0.8
● 0.8 - 0.9
● 0.9 - 1

B.

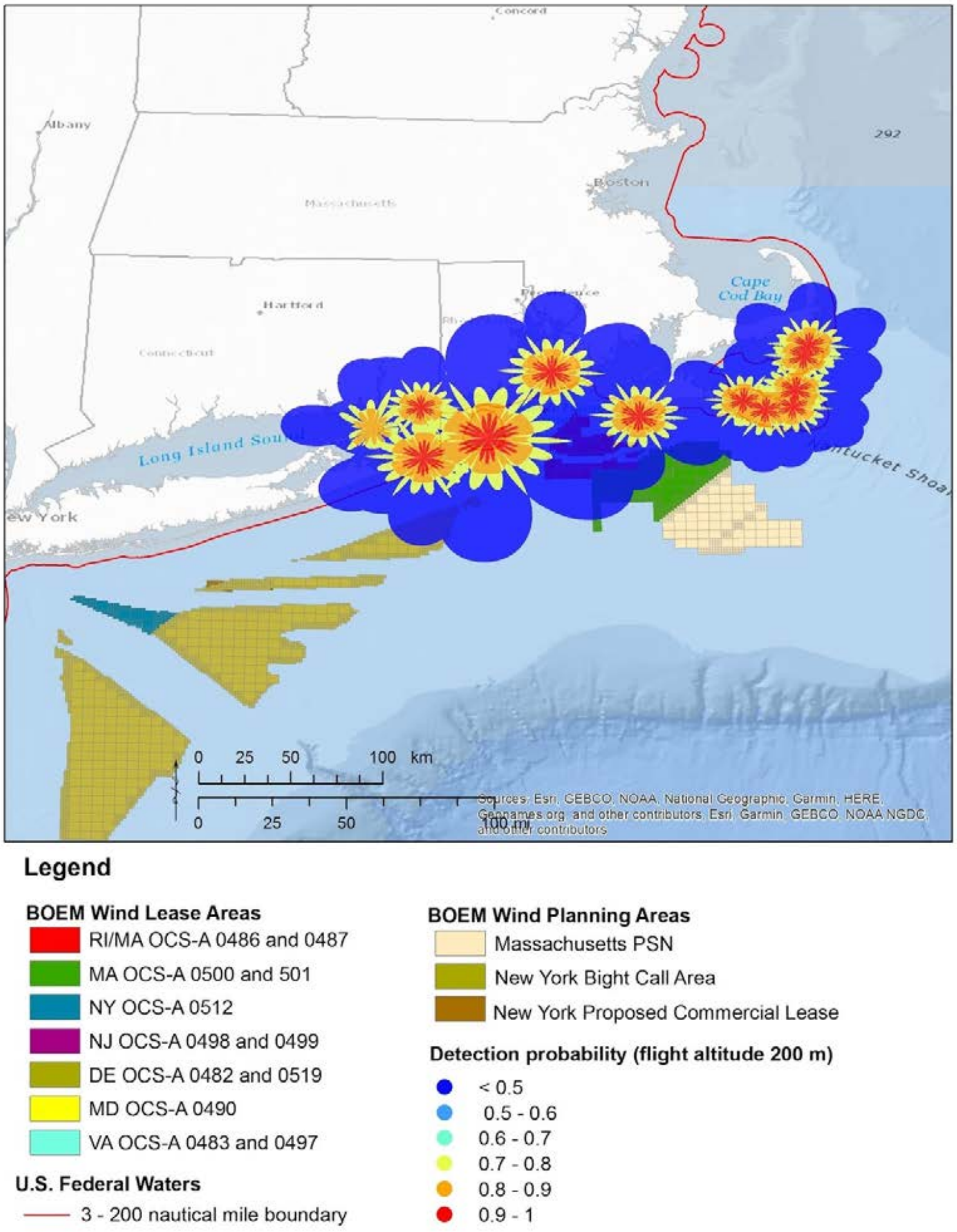

Figure G-3. Coverage map from 2014 BOEM-funded tracking towers showing the probability of detecting a bird flying at (A) 20 m, and (B) 200 m

Coverage assumes signal strength value = 5. Higher signal strengths would be likely to show a similar probability distribution, but with contracted coverage consistent with Fig. G-1. Overlapping tower ranges indicate the capacity for simultaneous detections to provide more accurate estimates of the target's altitude and spatial coordinates than what can be estimated from the single detections

A.

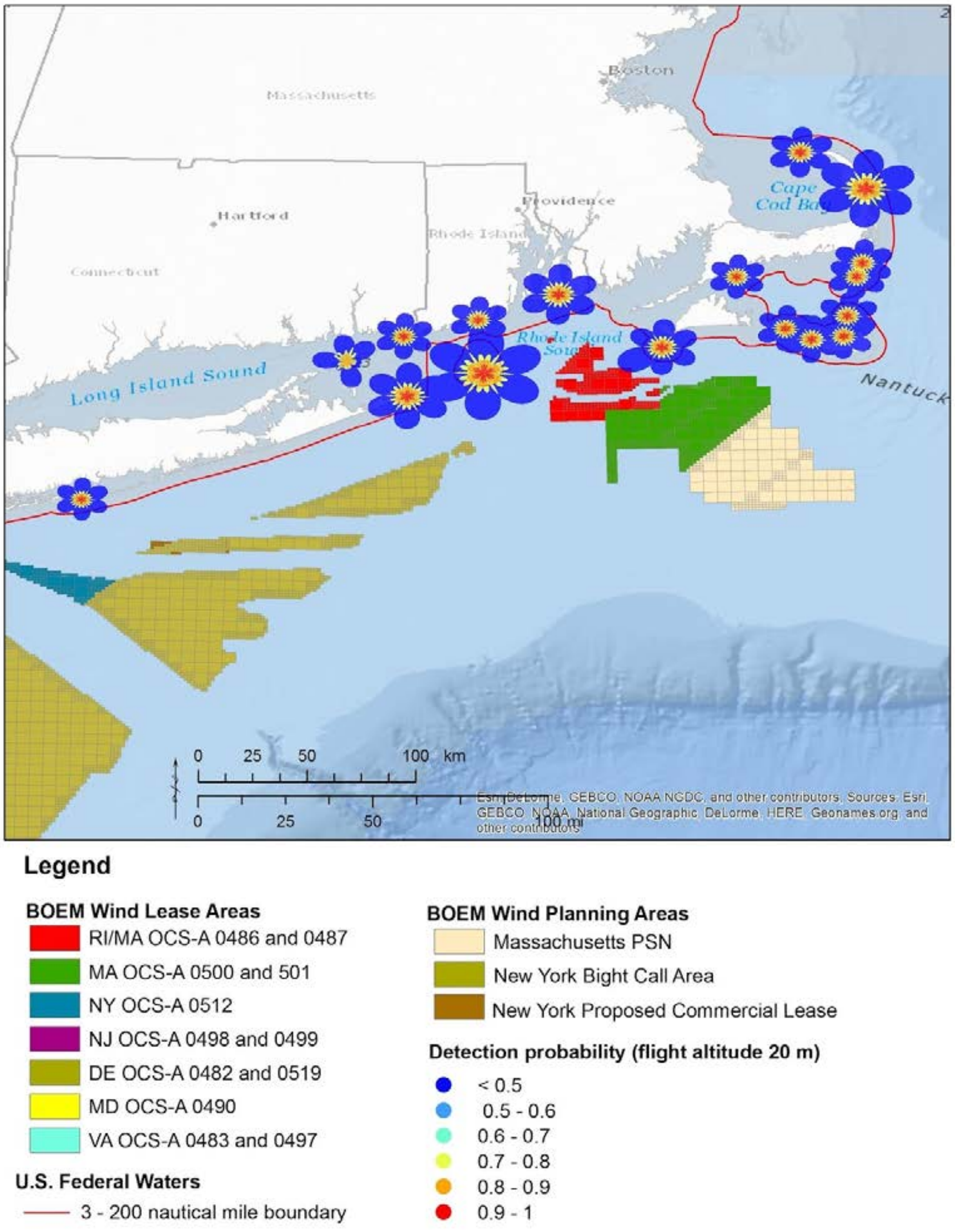
Boston
Massachusetts
Hartford
Providence
Rhode Island
Connecticut
Cape Cod Bay
Long Island Sound
Rhode Island Sound
Nantuck
0 25 50 100 km
0 25 50 100 mi
Esri, DeLorme, GEBCO, NOAA NGDC, and other contributors, Sources: Esri, GEBCO, NOAA, National Geographic, DeLorme, HERE, Geonames.org, and other contributors
Legend
BOEM Wind Lease Areas
RI/MA OCS-A 0486 and 0487
MA OCS-A 0500 and 501
NY OCS-A 0512
NJ OCS-A 0498 and 0499
DE OCS-A 0482 and 0519
MD OCS-A 0490
VA OCS-A 0483 and 0497
U.S. Federal Waters
3 - 200 nautical mile boundary
BOEM Wind Planning Areas
Massachusetts PSN
New York Bight Call Area
New York Proposed Commercial Lease
Detection probability (flight altitude 20 m)
< 0.5
0.5 - 0.6
0.6 - 0.7
0.7 - 0.8
0.8 - 0.9
0.9 - 1

B.

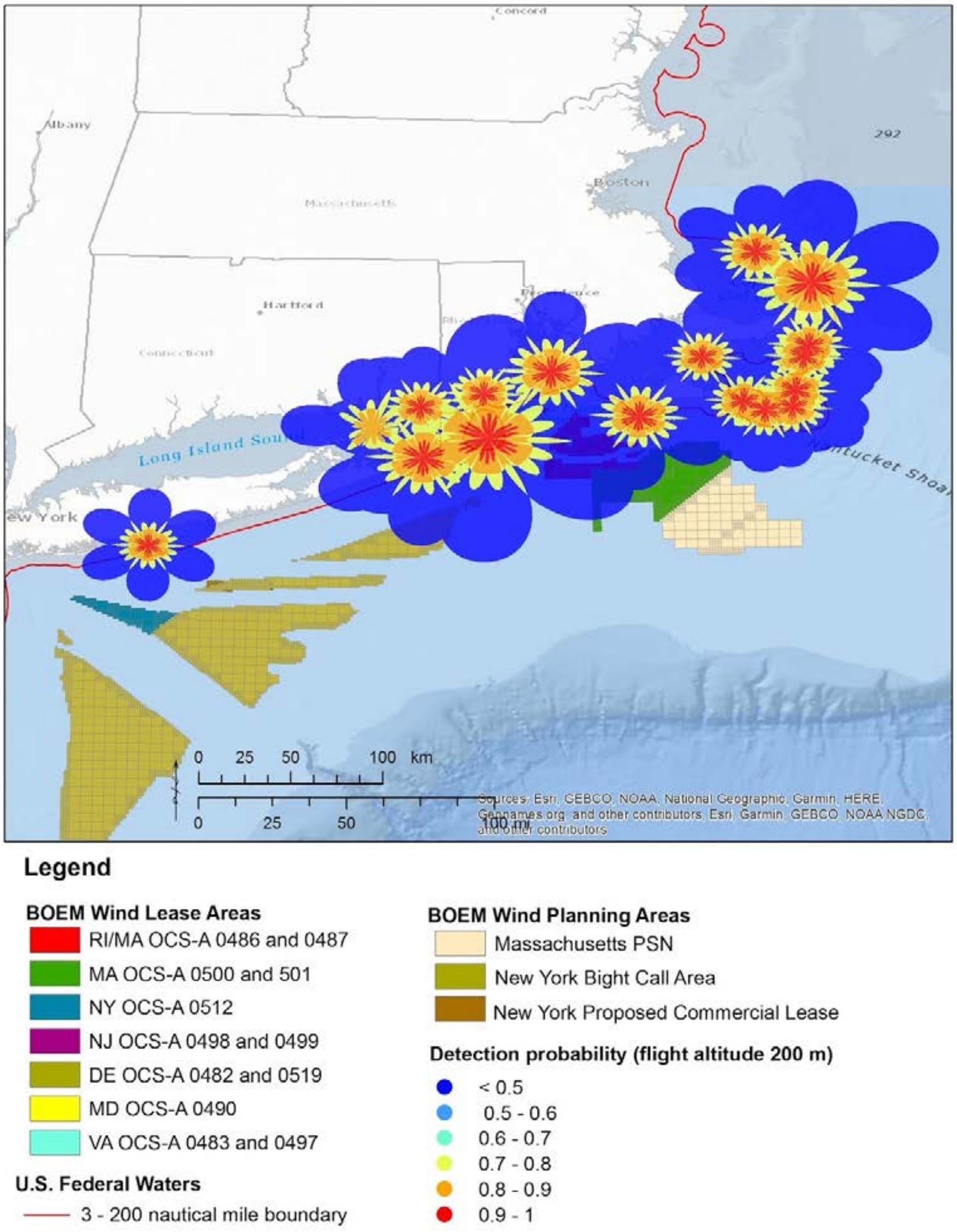

Figure G-4. Coverage map from 2015 BOEM-funded tracking towers showing the probability of detecting a bird flying at (A) 20 m, and (B) 200 m.
Coverage assumes signal strength value = 5. Higher signal strengths would be likely to show a similar probability distribution, but with contracted coverage consistent with Fig. G-1. Overlapping tower ranges indicate the capacity for simultaneous detections to provide more accurate estimates of the target's altitude and spatial coordinates than what can be estimated from the single detections.

A.

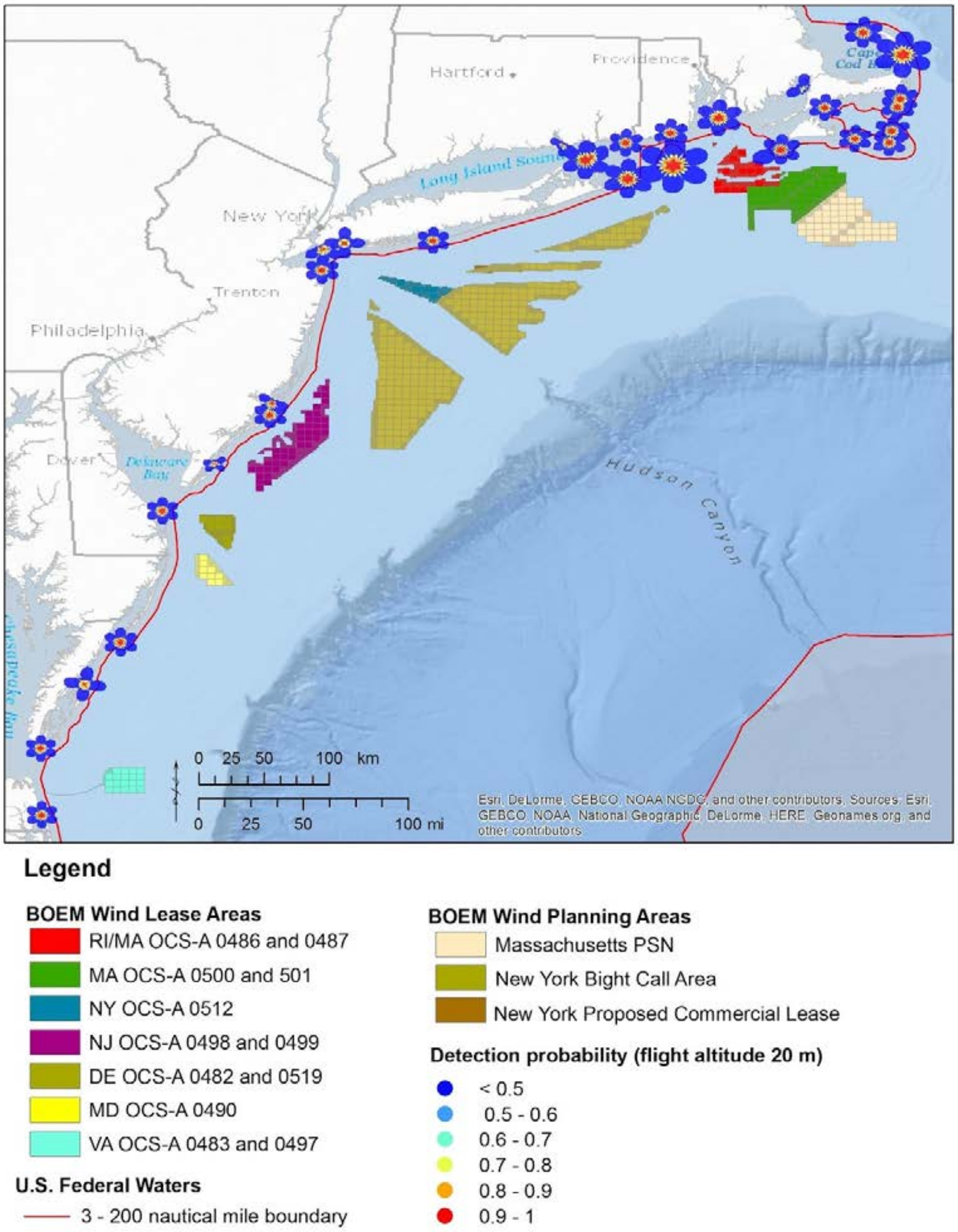

Esri, DeLorme, GEBCO, NOAA NGDC, and other contributors, Sources: Esri, GEBCO, NOAA, National Geographic, DeLorme, HERE, Geonames.org, and other contributors

B.

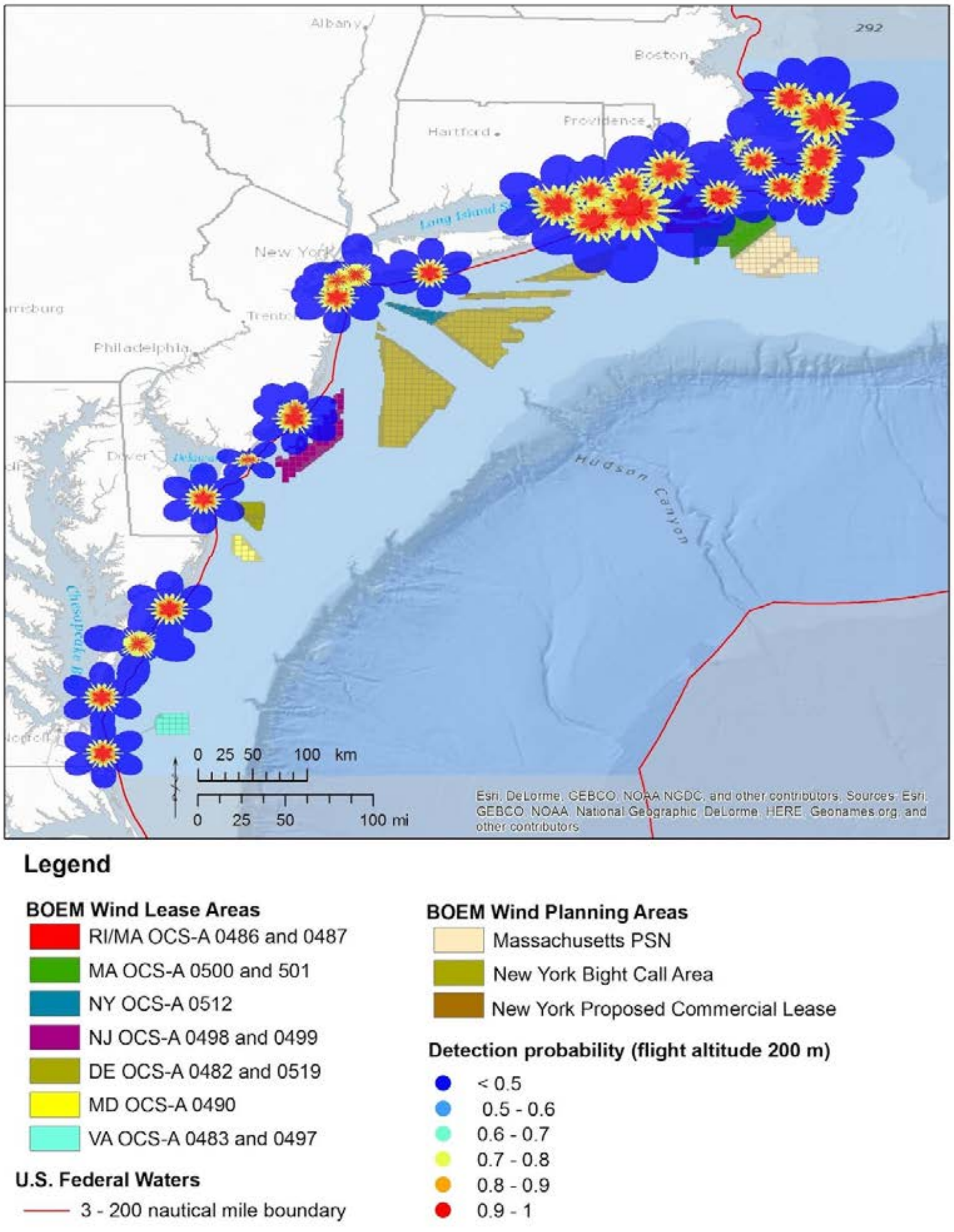

Esri, DeLorme, GEBCO, NOAA NGDC, and other contributors, Sources: Esri, GEBCO, NOAA, National Geographic, DeLorme, HERE, Geonames.org, and other contributors

Figure G-5. Coverage map from 2016-2017 BOEM-funded towers showing the probability of detecting a bird flying at (A) 20 m, and (B) 200 m.
Coverage assumes signal strength value = 5. Higher signal strengths would be likely to show a similar probability distribution, but with contracted coverage consistent with Fig. G-1. Overlapping tower ranges indicate the capacity for simultaneous detections to provide more accurate estimates of the target’s altitude and spatial coordinates than what can be estimated from the single detections

Appendix H

Summary of geospatially referenced detection data from all Common Terns, Roseate Terns, and Piping Plovers in this study submitted to BOEM as a supplemental material to this report

As supplementary material to this report, we have provided movement model output and associated meteorological covariate data on a 1-minute time step for all birds in this study by year and species (Appendix H – [species]_location_estimates_and_weather_data_[year]. In addition, we provide all processed data from the BOEM array and broader Motus Wildlife Tracking System for all tagged birds in this study (Appendix H – [species]_motus_detection_data_[year]_boem_study.csv).

Field descriptions of each file appear below:

File name: Appendix_H-Location_Estimates_and_Weather_Data_[spp]_[year].csv

Fields:

bird_id: unique identifier of each tagged bird, where prj = Motus project number and id = id of transmitter

ts_gmt: time stamp of estimated location, in Greenwich Mean Time (GMT)

x: mean x-coordinate of location estimate in UTM Zone 18N (units in m)

y: mean y-coordinate of location estimate in UTM Zone 18N (units in m)

z: mean altitude estimate (units in m)

stdx: standard deviation of x-coordinate of location estimate in UTM Zone 18N (units in m)

stdy: standard deviation of y-coordinate of location estimate in UTM Zone 18N (units in m)

lqz: lower quartile of z (units in m)

uqz: upper quartile of z (units in m)

wind_sp: wind at a pressure level of 1000 mb (about 100 m above sea level), quantified as wind speed (m/s), Zonal (Eastward) and Meridional (Northward) wind components (m/s)

wind_dirn: the direction wind blows toward, measured in degrees clockwise from geographic North

air_temp: air temperature (units in Kelvins, surface level)

precipn: precipitation accumulation kg/m^2, surface level)

visibility: visibility (units in m, surface level)

pressure: barometric pressure (units in Pa, surface level)

windsupport: the tailwind component (units in m/s) in a bird's flight direction (where negative values are headwinds), which can be considered as supportive under the assumption that birds fully compensate for drift, i.e. that flight directions represent intended (goal) directions.

windcross: crosswind component (units in m/s) relative to a bird's flight direction, i.e. under the presumption of full compensation for crosswind, i.e. that flight directions represent intended (goal) directions. Positive values are to the left (clockwise) relative to the flight direction.

groundsp: magnitude of ground speed (units in m/s) airsp: magnitude of a bird’s airspeed vector (units in m/s), i.e. excluding any wind effect. The airspeed vector is derived by vector subtraction of the wind vector (at 1000 mb) from the bird’s ground speed vector.

File name: Appendix_H-Motus_Detection_Data_[spp]_[year].csv

Fields:

id: nanotag ID number

spp: species (cote = Common Tern, rost = Roseate Tern, pipl = Piping Plover)

depLoc: geographic location of tag deployment

depLat: Latitude of tag deployment (decimal degrees)

depLon: Longitude of tag deployment (decimal degrees)

depDate: Date of tag deployment

age: age of bird. AHY = After Hatch Year

sex: sex of bird. M = male, F = female, U = unknown (not determined)

band: US Geological Survey (USGS) issued band number

aux: code and color of uniquely coded auxiliary marker(s)

tagRet = 1 (tag retention unknown), 0 (known tag drop)

ts_gmt: time stamp of detection, in GMT

site: name of automated radio telemetry station that recorded detection

siteant: combination of automated radio telemetry station name and receiving antenna number

sig: signal strength of detection

lat: latitude of automated radio telemetry station (in decimal degrees)

lon: longitude of automated radio telemetry station (in decimal degrees)

tsOrig: original format of timestamp (in seconds, origin = 1970-01-01 00:00.00 GMT)

Appendix I

Summary of northbound migration data from Piping Plovers tagged during spring of 2017 in the Bahamas

Pamela H. Loring[1], Daniel H. Catlin[2], Daniel Gibson[2], Kelsi L. Hunt[2], Scott Johnson[3], Matthew Jeffery[4]

[1] U.S. Fish and Wildlife Service, Division of Migratory Birds, Hadley, MA, USA
[2] Virginia Tech, Department of Fish and Wildlife Conservation, Blacksburg, VA, USA
[3] Bahamas National Trust, Nassau, The Bahamas
[4] National Audubon Society, International Alliances Program, Washington DC, USA

The Bahamas is an important non-breeding area for Piping Plovers and may support over one third of the Atlantic coast population (Gratto-Trevor et al. 2016). During spring migration, Piping Plovers arrive at Atlantic coast nesting areas from March through early May, but there is little information on the specific routes that Piping Plovers take from their wintering grounds to the breeding areas (Elliott-Smith and Haig 2004). This Appendix summarizes results of a pilot study on the spring migratory routes of Piping Plovers that were tagged at wintering areas in the Bahamas prior to their northbound migration.

Tag deployment and movement summaries

The tagging sites for this study were located in the northwestern Bahamas on North Andros (Young Sound and Kamalame Cay) and the Joulter Cays. From March 1 to 9, 2017, study partners captured and nano-tagged a total of 10 AHY Piping Plovers (sex unknown) and tracked migratory movements using the array of BOEM funded tracking towers along the U.S. Atlantic coast and the broader Motus network.

In total, six plovers were detected by the tracking towers, and the remaining four were not detected. Plovers were detected up to 53 days following tag attachment (Table I-1). Detection data were sparse for most individuals, but provided some evidence of nocturnal migratory flights for Piping Plovers during spring migration. Two individuals (IDs 10 and 8), tagged in Young Sound on March 2, were detected flying by a Motus tracking station on Bulls Island, SC during the night (20:00 to 23:00 hrs EST) on March 17, and 30th, respectively. ID 10 was subsequently detected on a station at Chincoteague NWR, VA from April 8 to 14. The single Piping Plover tagged at Kamalame Cay on March 5 was detected by the Kamalame Cay tracking station through March 21. It was subsequently detected flying past the south antenna of the station on Montauk Point, NY during the early morning (04:00 hrs EST) on April 3. Although the time difference between its last detection at Kamalame Cay and first detection by the Montauk Point station was too long (16 days) to infer direct flight across the Atlantic OCS, the bird appeared to enter detection range of the Montauk tower from offshore waters south of Long Island prior to sunrise, suggesting a nocturnal transit through the New York Bight. Piping Plover ID 13, tagged in the Joulter Cays, was detected flying by towers around midnight along the coast of New Jersey at North Brigantine Natural Area on March 27 (23:36 to 23:57 hrs EST) and Sandy Hook on March 29 (00:06 to 00:07 hrs EST).

Two Piping Plovers tagged in the Bahamas were tracked for longer portions of their northbound migration (Fig. I-1). ID 17, tagged in the Joulter Cays, was detected flying by a Motus station in coastal Georgia on April 21, close to midnight (23:53 to 23:56 hrs EST). This individual was subsequently detected on the evening of April 28, flying past a Motus station on Cape Romain NWR in SC (21:24 to 21:34 hrs) and was tracked at an estimated flight speed of 24 m/s (assisted by a tail-wind blowing to the northeast at 9 m/s) to a station on Back Bay NWR in southern Virginia (02:49 to 03:06 hrs EST on April 29). It then continued north across Federal waters off the coast of Virginia to Assateague National Seashore. When crossing Federal waters, mean wind speed was 13 m/s (sd 2 m/s) and mean wind direction was 48 degrees (sd 6 deg), providing strong wind support (mean 9.2 m/s, sd 2.5). Mean visibility was low (180 m, sd 320 m) and mean precipitation accumulation was minimal 0.01 kg/m^2 (sd 0.02 kg/m^2). On the evening of May 1 (from 19:03 to 19:38 hrs EST), it was detected in flight by the station at Sandy Hook, NJ and tracked across Federal waters of New York Bight to the station at Fire Island National Seashore on Long Island, NY. Wind conditions were favorable while in Federal waters of New York Bight: mean wind speed was 8.9 m/s (sd 0.7 m/s) and mean wind direction was 6 degrees (sd 4 degrees), providing strong wind support (8.3 m/s, sd 0.5). During this flight, mean visibility was low (5,857 m, sd 2,331 m) and mean precipitation accumulation was 0.11 kg/m^2 (sd 0.16 kg/m^2).

ID 7 was tagged in Young Sound on March 1 and detected by the station at Kamalame Cay during the evening of March 23. It departed from Kamalame Cay on March 24 at 20:05 hrs EST and was detected flying by the Motus station on Cape Romain NWR in SC on March 25 (22:38 to 22:40 hrs EST).

Euclidian flight speed from the Bahamas to SC was 10 m/s, indicating a direct transit across the AOCS spanning over 900 km. During this transit across Federal waters, mean wind direction was to the northwest (310 degrees, sd 12 degrees) at a mean speed of 8.9 m/s (sd 1.9 m/s), providing high wind support (mean 6.6, sd 0.9). Visibility was high (19,995 m) and there was no precipitation (mean < 0.001 kg/m^2). This individual was subsequently detected on a northbound flight on April 3, past Cedar Island, NC (16:14 to 16:16 hrs EST), Pea Island, NC (17:42 to 17:50 hrs EST), and North Brigantine, NJ (21:49 to 22:28 hrs EST). The model estimated track spanned nearly 600 km at an estimated speed of 20 m/s, and intersected Federal waters off the coasts of NC to southern NJ, with exposure to WEAs in NC and VA (Fig. I-1, inset) from 18:00 to 19:00 hrs EST. During exposure to Federal waters and WEAs, mean wind speed was 12.8 m/s (sd 1.2 m/s), blowing towards the north-northwest (mean direction 344 degrees, sd 1.4 degrees), providing strong wind support (mean 11.7, sd 1.2). Mean visibility was 18,496 m (sd 1,749 m) and there was little precipitation (mean 0.013 kg/m^2, sd 0.011 kg/m^2). During exposure to WEAs, the mean estimated altitude (454 m) was above the RSZ.

Table J-1. Tag deployment and detection summaries of Piping Plovers tagged in the Bahamas during March 2017.

Tag ID	Band ID	Deploy Location	Deploy Latitude	Deploy Longitude	Deploy Date	Last Detection	Days Detected
5	PF(0V)	Young Sound	24.6629	-77.751	3/1/2017	NA	0
6	PF(3H)	Young Sound	24.6629	-77.751	3/1/2017	NA	0
7	PF(5E)	Young Sound	24.6629	-77.751	3/1/2017	4/3/2017	33
8	PF(2E)	Young Sound	24.6629	-77.751	3/2/2017	3/30/2017	28
9	PF(5X)	Young Sound	24.6629	-77.751	3/2/2017	NA	0
10	PF(6T)	Young Sound	24.6624	-77.751	3/2/2017	4/14/2017	43
12	PF(74)	Kamalame Cay	24.8509	-77.901	3/5/2017	4/3/2017	29
13	PF(2U)	Joulter Cays	25.3158	-78.139	3/8/2017	3/29/2017	21
17	PF(34)	Joulter Cays	25.3158	-78.139	3/9/2017	5/1/2017	53
67	PF(3K)	Joulter Cays	25.3158	-78.139	3/9/2017	NA	0

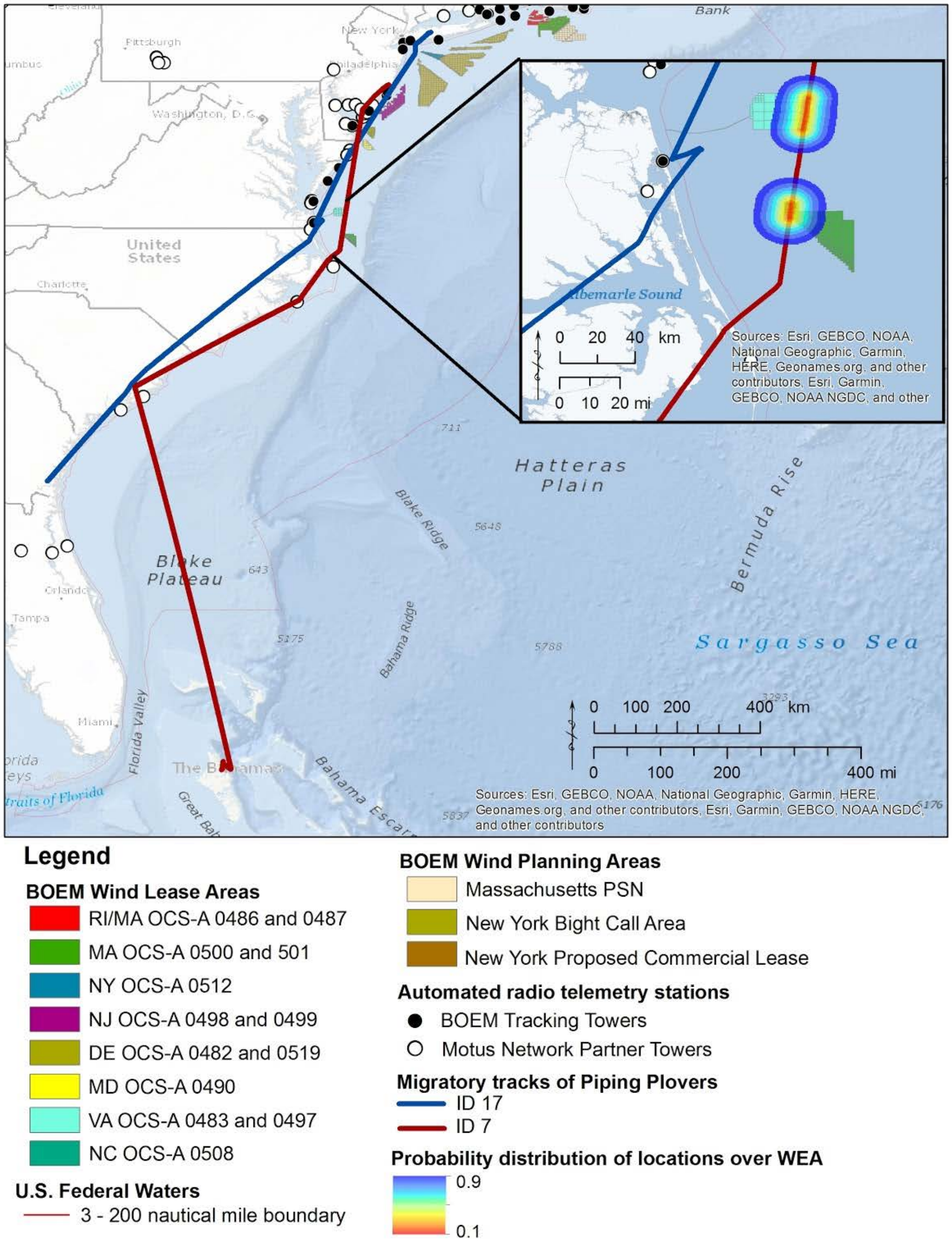

Figure J-1. Estimated northbound flight paths of Piping Plovers ID 7 (red) and ID 17 (blue) tagged in the Bahamas in March 2017.
Probability bands (inset) show spatial error around locations during estimated exposure of ID 7 to BOEM Lease Areas NC OCS-A 0508 and VA OCS-A 0483 on April 3, 2017.

Discussion

Detections of spring tagged Piping Plovers were highly variable. Only 60% of the Piping Plovers tagged in the Bahamas were detected by stations on the US Atlantic coast, and only 20% tracked over a significant portion of their route. The lack of detections could be due to a limited number of towers running in spring of 2017 along the US Atlantic coast, as many tracking towers are only active or maintained from early summer through fall migration (for a map of deployed towers by date, see https://motus.org/data/receiversMap?lang=en). In this study, we were not able to monitor tag retention of Piping Plovers. However, we suspect that the rates of tag loss were higher for birds tagged in spring because most were in heavy body molt within the intrascapular region at the time of tag attachment.

Despite variable detection probability, these data provide new insights on the movements of individual Piping Plovers within the US Atlantic OCS during spring migration. All of the birds tracked by the array were detected making nocturnal movements, providing strong evidence that Piping Plover migration occurs at night. This finding supports results from our expanded study of Piping Plover movements during fall, as well as from previous work assessing the migratory ecology shorebirds in the Canadian Maritimes detected by surveillance radar (Richardson 1979).

Movements also were highly associated with wind condition, as birds selected winds blowing in their direction of travel: northwest heading from Bahamas to the US Atlantic coast, and north-northeast while traveling along coast. We also documented flights of Piping Plovers across Federal waters of the mid-Atlantic and New York Bight, rather than a longer route following the coast, providing further evidence to support the "short-cut" hypothesis of Burger et al (2011). These data provided some indication of Piping Plovers flying offshore in low visibility conditions (<200 m). Shorebirds may be subjected to more inclement weather during spring migration versus fall (O'Reilly and Wingfield 1995), and this may result in exposure to WEAs under higher-risk conditions for collision. In the present study, we documented exposure of one tagged Piping Plover to two WEAs off the coast of North Carolina and Virginia. This exposure occurred just prior to sunrise, during high visibility, little precipitation, and with strong wind support. However, due to the relatively sparse amount of information collected during the pilot study, a more focused study examining the exposure of Piping Plovers to WEAs during spring migration is recommended to more fully assess risk to this species from wind energy development in the US Atlantic OCS.

Acknowledgements

This study was funded in part by the U.S. Department of the Interior, Bureau of Ocean Energy Management through Interagency Agreement M13PG00012 with the U.S. Department of the Interior, Fish and Wildlife Service. We thank Bahamas National Trust, Kamalame Cay Resort, Virginia Tech Shorebird Program, the U.S. Army Corps of Engineers, and cooperators on the Motus Wildlife Tracking Network for logistical support.

References

Burger J, Gordon C, Niles L, Newman J, Forcey G, Vlietstra L. 2011. Risk evaluation for Federally listed (Roseate Tern, Piping Plover) or candidate (Red Knot) bird species in offshore waters: A first step for managing the potential impacts of wind facility development on the Atlantic Outer Continental Shelf. Renewable Energy 36:338-351.

Elliott-Smith E, Haig SM. 2004. Piping Plover (*Charadrius melodus*), The Birds of North America Online (A. Poole, Ed.). [accessed 2017 August 20]; https://doi.org/10.2173/bna.2

Gratto-Trevor C, Amirault-Langlais D, Catlin D, Cuthbert F, Fraser J, Maddock S, Roche E, Shaffer F. 2012. Connectivity in piping plovers: Do breeding populations have distinct winter distributions? The Journal of Wildlife Management 76:348–355.

Gratto-Trevor C, Haig SM, Miller MP, Mullins TD, Maddock S, Roche E, Moore P. 2016. Breeding sites and winter site fidelity of piping plovers wintering in The Bahamas, a previously unknown major wintering area. Journal of Field Ornithology 87(1):29-41.

O'Reilly KM, Wingfield JC. 1995. Spring and Autumn Migration in Arctic Shorebirds: Same Distance, Different Strategies, Integrative and Comparative Biology 35(3):222-233.

Richardson WJ. 1979. Southeastward shorebird migration over Nova Scotia and New Brunswick in autumn: a radar study. Canadian Journal of Zoology 57(1):107-124.

Appendix J

Common Tern Satellite Telemetry Pilot Study

Pamela H. Loring[1], Linda J. Welch[2], Sara Williams[2], Kenneth D. Meyer[3]

1. U.S. Fish and Wildlife Service, Division of Migratory Birds, Hadley, MA, USA
2. U.S. Fish and Wildlife Service, Maine Coastal Island National Wildlife Refuge, Milbridge, ME, USA
3. Avian Research and Conservation Institute, Gainesville, FL, USA

INTRODUCTION

The recent miniaturization of satellite transmitters now makes it possible to track high-resolution movements of small-bodied birds worldwide. In 2017, we conducted a pilot study using 1.9-g solar-powered satellite transmitters to track annual-cycle movements of Common Terns tagged during the incubation period at their nesting colony on Petit Manan Island in the Gulf of Maine. This study represents the first attempt to track local to hemispheric movements of Common Terns using satellite telemetry. Our aim was to field-test the use of satellite transmitters on Common Terns to address the following objectives:

1) Evaluate the safety and efficacy of using a back-pack harness to attach transmitters to Common Terns for full-annual cycle deployment.
2) Estimate movements and utilization distributions of Common Terns throughout the annual cycle.
3) Estimate the exposure of Common Terns to Federal Waters and to each BOEM Lease Area and BOEM Planning Area in the Atlantic OCS Study Area during breeding, post-breeding, and migratory phases of the annual cycle.
4) Quantify meteorological conditions (e.g., wind speed, wind direction, barometric pressure, temperature, visibility, precipitation), temporal variation (time of day, date), and demographic variation (sex, reproductive success) associated with exposure of Common Terns within Federal waters and WEAs within the Atlantic OCS Study Area.

METHODS

Tag deployment and monitoring

On June 14, 2017 we used walk-in traps to capture adult Common Terns at their nest sites during the mid-incubation period. All birds were captured at nest sites that were clearly visible from the field station, so that detailed observations of tagged birds could be conducted. Terns that were not previously banded were marked with an incoloy U.S. Geological Survey (USGS) band on the tarsometatarsus. Morphometric measurements collected from each bird included wing chord (± 1 mm) and mass (± 0.1 g). From each bird, we collected three to five contour feathers for molecular-based determination of gender (Avian Biotech, Gainesville, FL).

Following banding, we attached a 1.9-g solar-powered Platform Terminal Transmitter (PTT) satellite transmitter (Microwave Telemetry, Columbia, MD) using a back-pack harness made 6 mm-wide Teflon thread (Bali Ribbon Co., Bali, Pennsylvania). The combined weight of the transmitter and attachment materials was ≤2% of the body weight of tagged individuals. The average weight of tagged birds was 126-g at the time of capture and before transmitter attachment (males 129-g, females 122-g). The total weight of PTT tags and harness was approximately 2.5-g. Total handling time, from capture to release, ranged from 25 to 45 min per individual. For each tagged nest, we selected the closest neighboring nest with a similar clutch size to serve as a control nest for monitoring tag effects using a paired design. At each control nest, one adult was captured, measured, banded, and held for up to 45 minutes, but not marked with a satellite transmitter.

Field staff conducted daily nest observations (weather permitting) from the initial tagging date through the fledge date of chicks. Observations were conducted visually and with GoPro cameras placed near the nests of tagged and control terns to collect additional behavioral data and information on feeding rates and types of prey delivered. In addition, field staff collected productivity data (number of chicks fledged per nest) at each tagged and control nest.

The transmitters were monitored by satellites on the Argos system and operated continuously to the extent the battery charge allowed, which varied with available daylight. When messages from the transmitters were received by satellites, the Argos system estimated locations of transmitters using the Doppler effect on transmission frequency (Argos 2016). The Argos system assigned each location one of the following Location Class (LC) categories corresponding to its respective estimated error radius: LC3 = <250 m; LC2 = 250 to 500 m; LC1 = 500 to 1500 m, LC0 = >1500 m (Argos 2016). All satellite telemetry data were managed online using Movebank (Kranstauber et al. 2011). We retained LC3, LC2, LC1, LC0 locations for analysis. The estimated error radius of each location was provided by Movebank as one standard deviation of the estimated location error (in m) and assumed to be isotropic. Because the tags were solar powered, they were capable of operating for over two years. Only a limited number of these 1.9-g transmitters have been deployed since development in 2017, therefore lifespan of our tag deployments was uncertain. To control for possible abnormal behavior associated with transmitter or harness effects, we conservatively removed data collected during the first month of tagging from subsequent analyses of movement patterns and exposure to Federal waters.

Data Analysis

For analysis of exposure to Federal waters and WEAs, we divided the annual cycle into phases: 1) pre-fledging period; 2) post-breeding and staging; 3) fall (south-bound) migration; 4) wintering; and 5) spring (north-bound) migration. We used the Move package in R (Kranstauber et al. 2018) to calculate individual and composite dynamic Brownian-bridge movement model (DBMM) surfaces for each phase in the annual cycle. From the composite DBMM surfaces, we calculated 0.50 isopleths to represent core-use areas and 0.95 isopleths to represent utilization distributions. For computational efficiency, we used different spatial resolution of the DBBMM surfaces for different phases of the annual cycle depending on the spatial extent of movements. For the pre-fledgling period, when movements were localized around the nesting colony, we used a resolution of 250 m. For post-breeding dispersal and migration we used a resolution of 1 km, and for the wintering data that ranged throughout South America we used a resolution of 2 km.

To estimate individual movement tracks, we spatiotemporally interpolated the irregular location estimates into one-minute time steps using a Brownian Bridge model (Horne et al. 2007). Uncertainty of one-minute horizontal location estimates was quantified as the root-mean square of estimated variance in location from detections and due to time gaps between detections (via a horizontal flight speed of 10 m/s for terns; see Horne et al. 2007). We assessed occurrence in WEAs and Federal waters of the Atlantic OCS using the mean and standard deviations in locations estimates (X and Y, in UTM coordinates) of the tracks interpolated to a one-minute time step.

To examine movements relative to meteorological covariates, we obtained satellite-derived North American Regional Reanalysis environmental data in 3-hr time steps and approximately 32-km spatial resolution (National Oceanic and Atmospheric Administration 2017). The specific meteorological covariates that we included were: wind at a pressure level of 1000 mb (about 100 m above sea level), quantified as wind speed (m/s), Zonal (Eastward) and Meridional (northward) wind components (m/s), and wind direction (the direction wind blows toward, measured clockwise from geographic north); and additionally four other weather covariates at surface level values: barometric pressure (Pascal [Pa]), precipitation accumulation (kg/m^2), air temperature (Celsius [C]) and visibility (m).

These data were interpolated from their native Lambert conic grid to each location along the predicted trajectory (stored in the model in NAD83 UTM 18N coordinates), using a cubic spline based on the nearest 8 spatial locations, and linearly interpolated in time (MATLAB routines lambert1 and latln2val, respectively). We also estimated wind support (i.e., tailwind) and crosswind components for each individual at each 1-minute time step, based on equations described in Kemp et al. (2012).

We considered locations as exposed to Federal waters or WEAs when the mean estimated coordinates intersected a WEA and/or Federal water polygon, and calculated summary statistics for each temporal and meteorological variable by phase in annual cycle (for exposure to Federal waters) and by event (for exposure to WEAs). For circular variables (time of day, in hours Eastern Standard Time [EST] and wind direction, in degrees relative to true north) we calculated the mean based on the circular distribution (R package 'Circular', Agostinelli and Lund 2017). To examine exposure to Federal waters and WEAs relative to daylight, we used the R package 'maptools' (Bivand and Lewin-Koh 2016) to calculate local sunrise and sunset times for each minute of exposure to Federal Waters or WEAs. Exposure that occurred between the time of local sunrise and the time of local sunset were considered to have occurred during daytime hours. Conversely, exposure that occurred between the time of local sunset and the time of local sunrise were considered to have occurred during nighttime hours. For each remaining variable (wind speed, wind support, crosswind, barometric pressure, precipitation accumulation, temperature, visibility) we report summary statistics (mean, SD, range) associated with exposure to Federal waters and WEAs, respectively.

RESULTS

Location Data and movement summaries

DNA analysis of feather samples from tagged birds indicated we tagged two females and three male Common Terns in 2017. Common Terns were tracked for an average of 272 days (SD 178 days; range 102 to 501 days; Table J-1). We retained for analysis all locations of accuracy class LC3, LC2, LC1, and LC0, that occurred during the late fledging period in 2017 (Jul 11) through spring migration 2018 (or date of final transmission for tags that failed earlier). This resulted in a total of 6,174 locations, with 7% of class LC3, 12% of class LC2, 36% of class LC1, 45% of class LC0 (Table J-2). Average estimated error of locations by Location Class was: LC3 192 m (SD 32 m; range 121 - 250 m); LC2 371 m (SD 72 m; range 250 -500 m); LC1 972 m (SD 285 m; range 501-1,500 m); and LC0 4,578 m (SD 5,713 m; range 1,501 - 98,864 m). Average length of time between locations was 3.85 hours (SD 3.77 hours; range 21 seconds - 68.78 hours).

Data collection during the late pre-fledging period began on July 11 (18 to 21 days following chick hatch) and ended on the fledge date of each nest (Jul 20-22). Four of five satellite-tagged Common Terns successfully fledged at least one chick (mean productivity 1.0 chicks per pair). The remaining male (ID 169741) lost its nest on Jun 27. During the pre-fledging period, tracks of individual terns ranged up to 50 km of the nesting colony (Fig. J-1). The composite core-use area was centered within 20 km of the colony and utilization distribution extended up to 75 km from the colony (Fig. J-2).

The post-breeding period ranged from chick fledge (or following nest loss for ID 169741) to the onset of fall migration. During the post-breeding period, all five Common Terns traveled from the Gulf of Maine to staging areas in southeastern Massachusetts between August 1 and September 12 (Fig. J-3). Females departed from the Gulf of Maine in early August, and males made their final departure later, in mid-September (Table J-1). One male (ID 169745) ranged more widely during the staging period, departing from the Gulf of Maine on August 31 and passing through Nantucket, MA heading southwest across the mid-Atlantic Bight. On September 2, he turned west towards the coast of Virginia and flew northwards, parallel to the coast, along southern Long Island and into Buzzards Bay to stage for another 8 days within southeastern Massachusetts. All five birds staged in Massachusetts prior to initiating fall migration. One male (ID 169742) last transmitted from southeastern Massachusetts on Sept 26.

Composite core-use areas during post-breeding were located in the northern Gulf of Maine along the border of the U.S. and Canada, within Machias Bay and Passamaquoddy Bay (Fig. J-4). Composite core-use areas in southeastern Massachusetts were located within Cape Cod, Nantucket, and Buzzards Bay.

The two females initiated fall migration from Massachusetts staging areas on Aug 8 and 16 and arrived in South America on Aug 14 and 22 (Fig. J-5). The two remaining males initiated migration on Sep 13 and 16, and both arrived in South America on Sept 23. All four terns departed on a southern trajectory across the Atlantic OCS, approximately 150 km to over 850 km offshore, across the West Indies, arriving in Venezuela (Fig. J-6). One male (ID 169741) stopped transmitting upon arrival to Venezuela, but returned to nest site on Petit Manan Island during the 2018 breeding period. Field crews retrapped this individual at its nest site on Jul 3, 2018, removed the inactive transmitter, and reported that the body condition appeared normal and weight was 110 g. The remaining male transmitted data through the wintering period until 26 Feb 2018. The two females transmitted complete data through the wintering period and spring migration 2018. The composite wintering range extended from Venezuela to Argentina, with core-use areas off the coast of French Guiana and Marajo Bay, Brazil (Fig. J-7). The two females initiated spring migration from South America on May 2 and 7, staged on Cape Cod, MA for 2 days and 3.5 days, and arrived back to Petit Manan Island in the Gulf of Maine on May 9 and 15, respectively (Figs. J-8 and J-9). One female (ID 169743) is still actively transmitting as of December 2018.

Table J-1. Timing of annual cycle events of satellite tagged Common Terns (n=5 individuals) from the nesting colony on Petit Manan Island in the Gulf of Maine.

Tag ID	Sex	Tag Date	Hatch Date	Fledge Date	Depart ME	Depart MA	Arrive South America	Depart South America	Arrive South America	Offline
169741	M	6/14/17	6/21/17	*(6/27/17)	8/19/17	9/16/17	9/23/17	NA	NA	9/23/17
169742	M	6/14/17	6/22/17	7/21/17	9/12/17	NA	NA	NA	NA	9/26/17
169743	F	6/14/17	6/20/17	7/20/17	8/1/17	8/8/17	8/14/17	5/7/18	5/15/18	active
169744	F	6/14/17	6/23/17	7/22/17	8/3/17	8/16/17	8/22/17	5/2/18	5/9/18	7/19/18
169745	M	6/14/17	6/23/17	7/21/17	8/31/17	9/13/17	9/23/17	NA	NA	2/26/18

* fail date

Table J-2. Frequency of locations by accuracy class of satellite tagged Common Terns (n=5 individuals) from the nesting colony on Petit Manan Island in the Gulf of Maine from tag deployment through spring migration, 2018.

Tag ID	L3	L2	L1	L0	Total
169741	26	54	178	198	456
169742	73	94	187	258	612
169743	94	196	600	726	1,616
169744	147	221	749	850	1,967
169745	94	160	510	759	1,523
Total	434	725	2,224	2,791	6,174

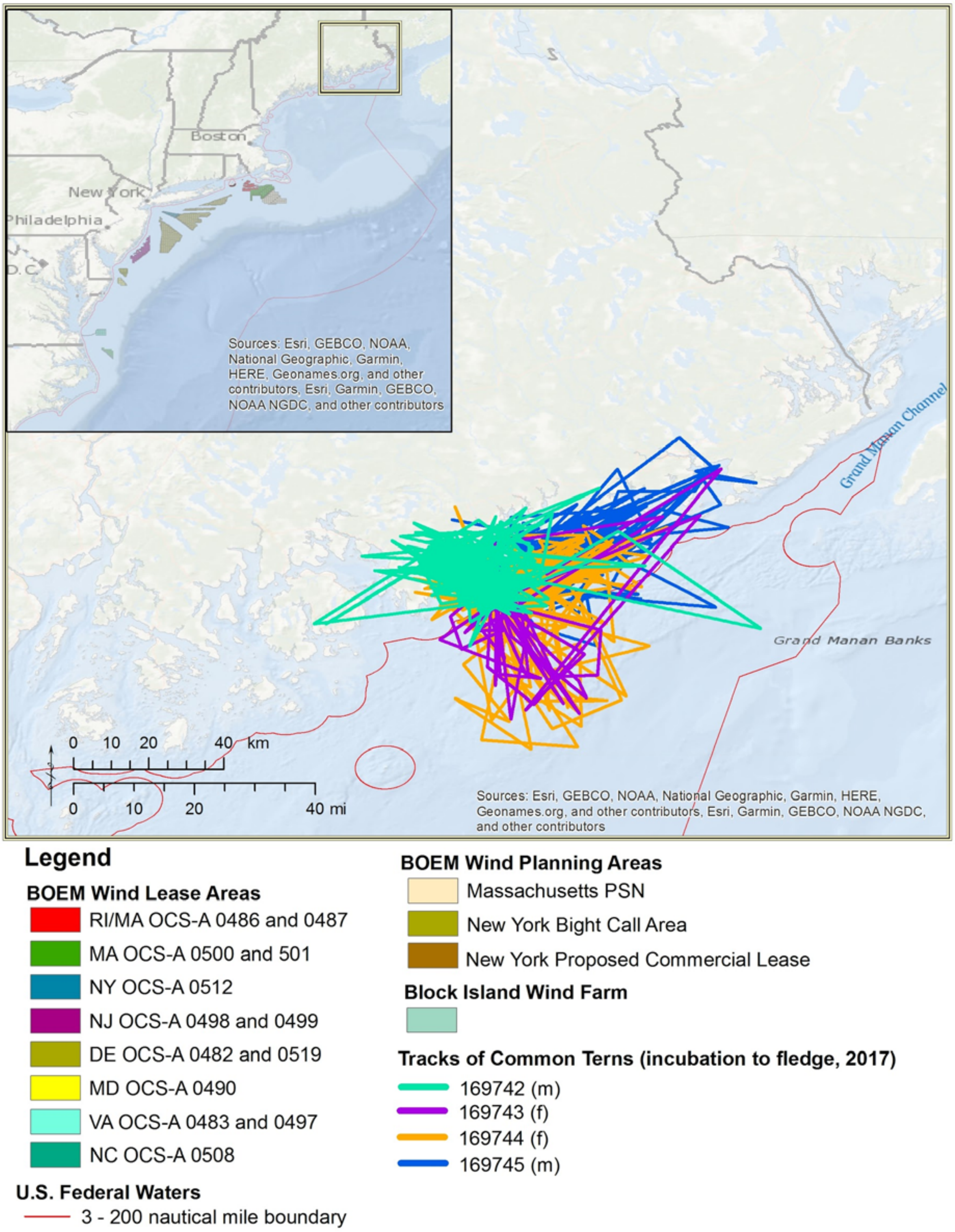

Sources: Esri, GEBCO, NOAA, National Geographic, Garmin, HERE, Geonames.org, and other contributors, Esri, Garmin, GEBCO, NOAA NGDC, and other contributors

Sources: Esri, GEBCO, NOAA, National Geographic, Garmin, HERE, Geonames.org, and other contributors, Esri, Garmin, GEBCO, NOAA NGDC, and other contributors

Figure J-1. Model-estimated tracks of Common Terns (n=4) during the late pre-fledging period, 11 July - 17 August 2017.

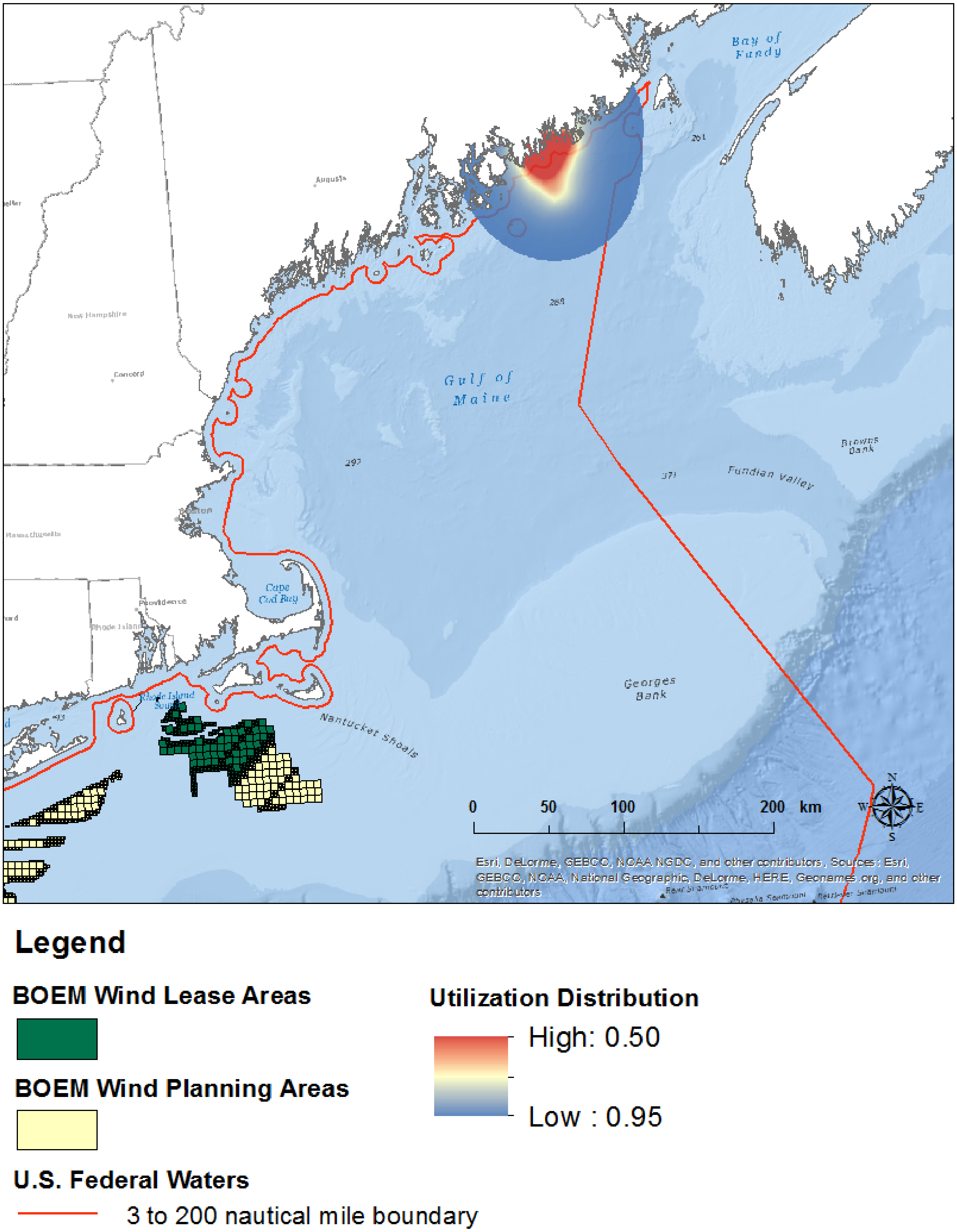

Esri, DeLorme, GEBCO, NOAA NGDC, and other contributors, Sources: Esri, GEBCO, NOAA, National Geographic, DeLorme, HERE, Geonames.org, and other contributors

Figure J-2. Composite utilization distribution of Common Terns (n=4) during the late pre-fledging period, 11 July - Aug 22, 2017

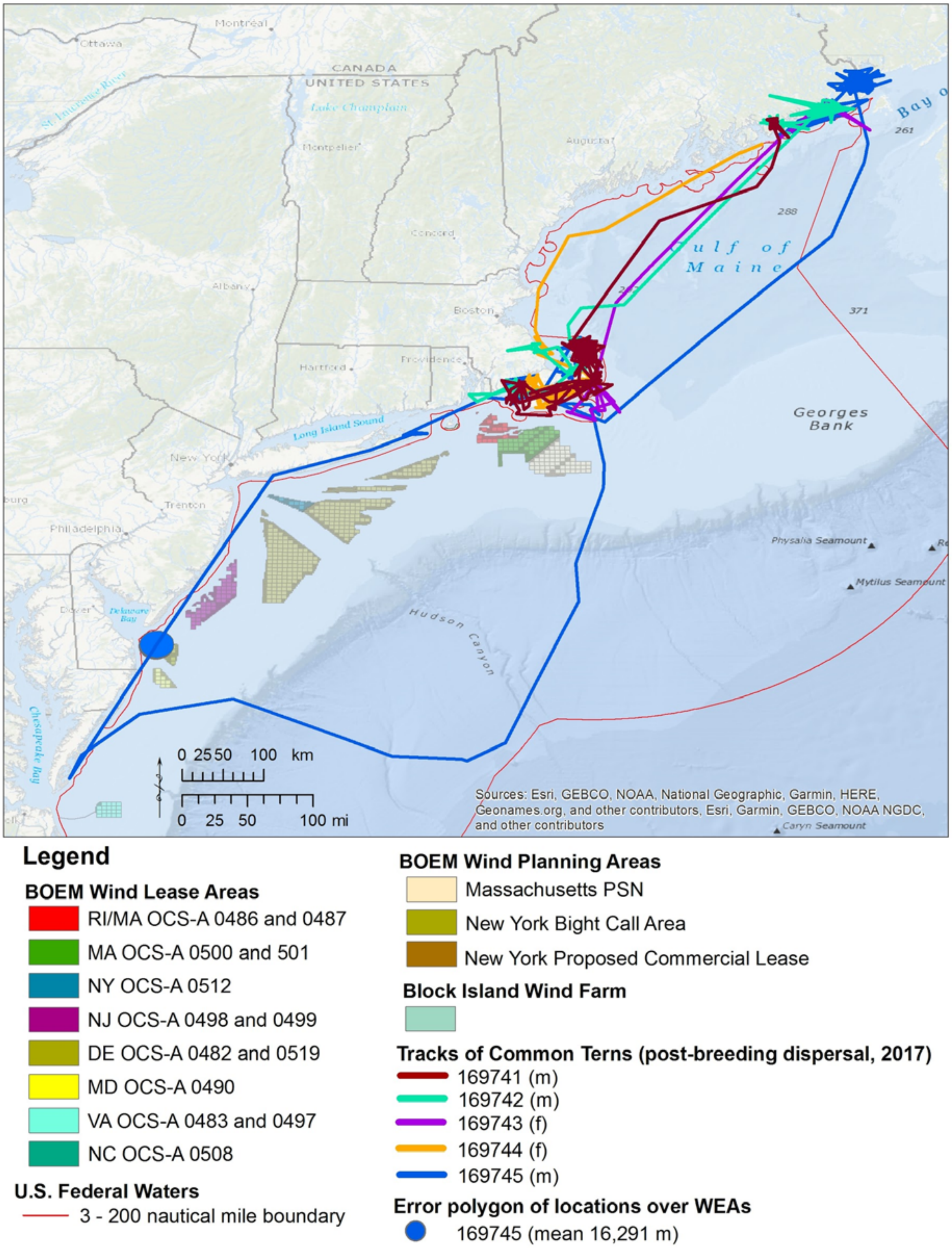

Figure J-3. Model-estimated tracks of Common Terns (n=5) during the post-breeding dispersal period, 29 July - 26 Sep 2017.

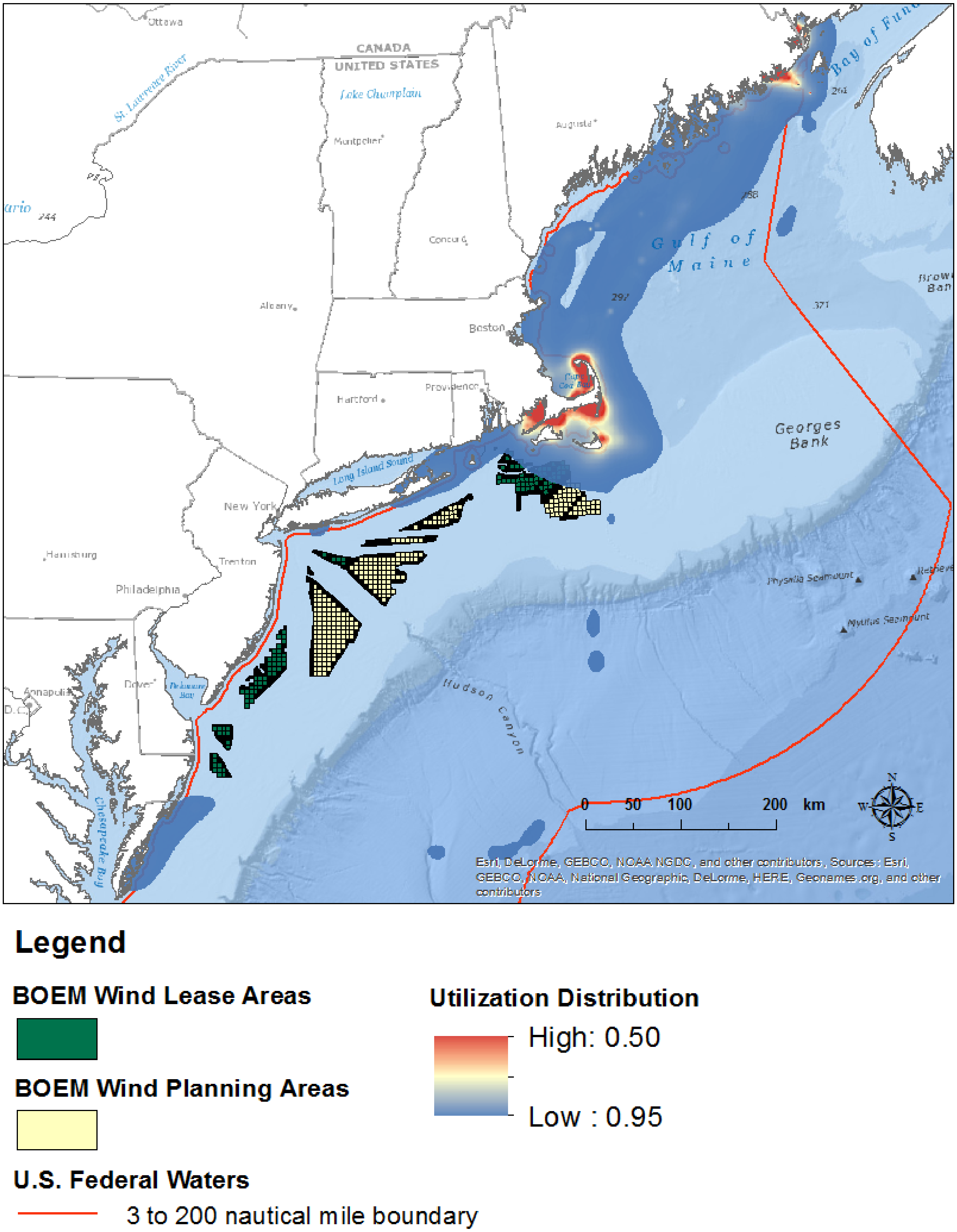

Esri, DeLorme, GEBCO, NOAA NGDC, and other contributors, Sources: Esri, GEBCO, NOAA, National Geographic, DeLorme, HERE, Geonames.org, and other contributors

Figure J-4. Composite utilization distribution of Common Terns (n=5) during the post-breeding dispersal period, 29 July - 26 Sep 2017.

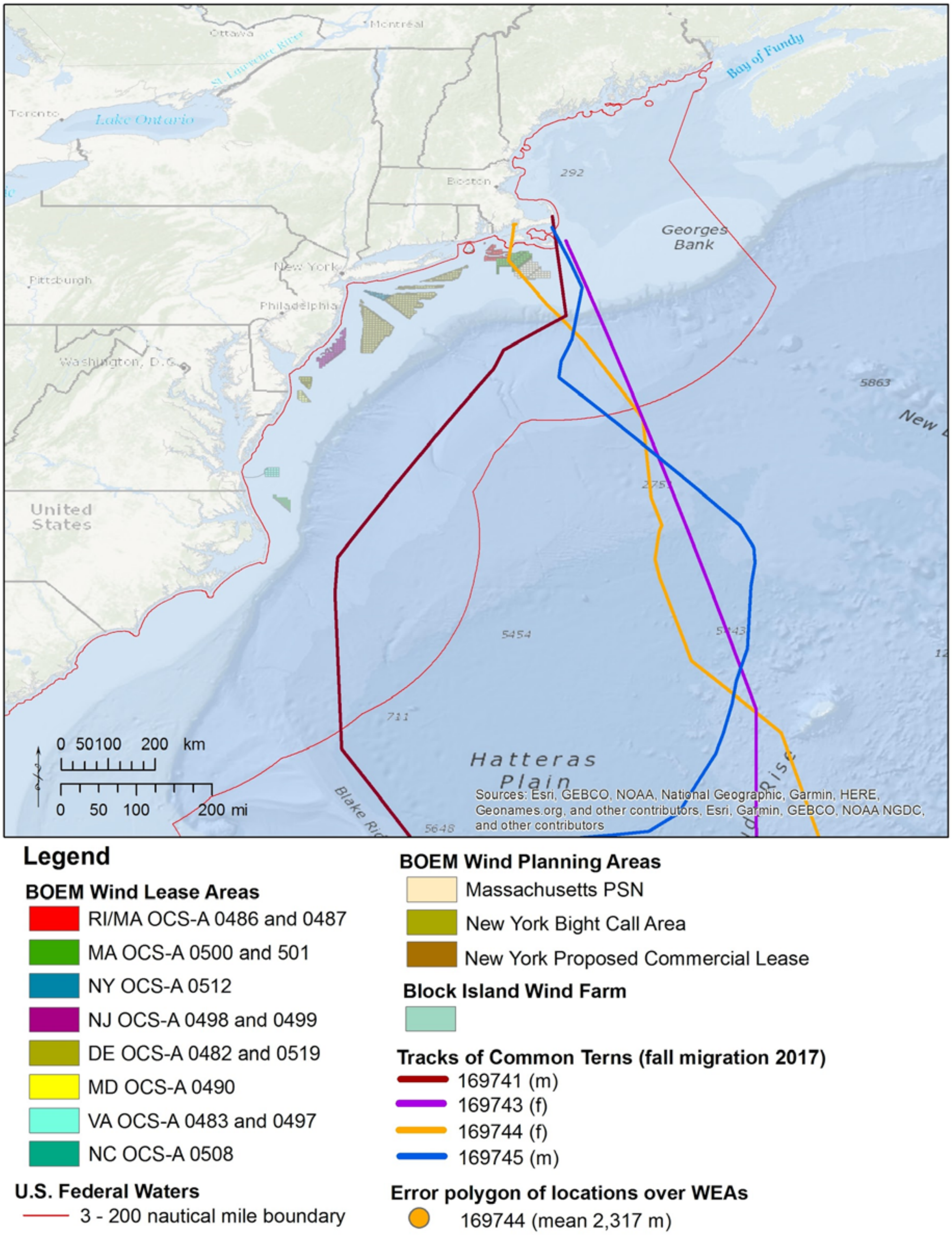

Sources: Esri, GEBCO, NOAA, National Geographic, Garmin, HERE, Geonames.org, and other contributors, Esri, Garmin, GEBCO, NOAA NGDC, and other contributors

Figure J-5. Model-estimated tracks of Common Terns (n=4) during fall migration, 6 August - 24 September 2017.

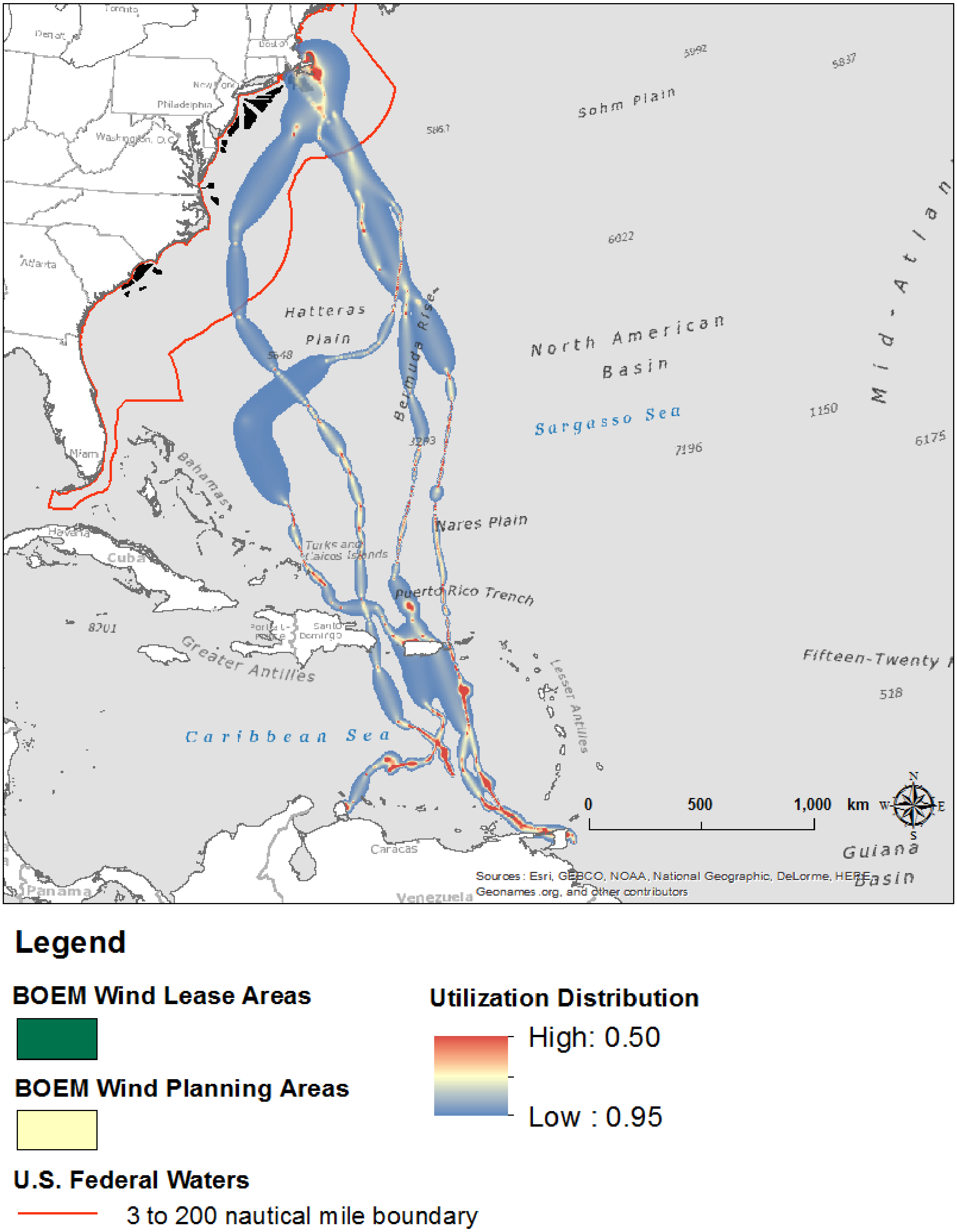

Figure J-6. Composite utilization distribution of Common Terns (n=4) during fall migration, 6 August - 24 September 2017.

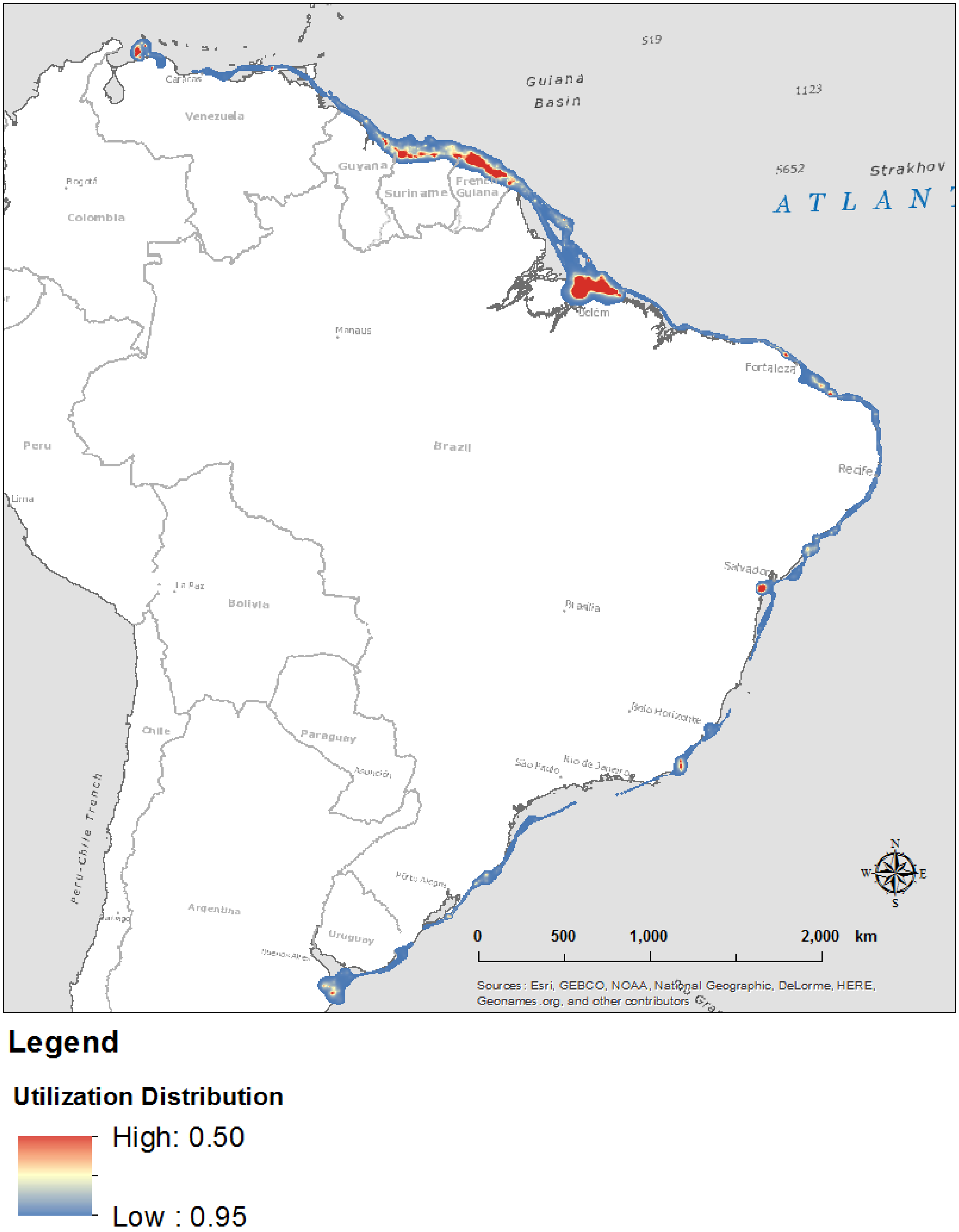

Figure J-7. Composite utilization distribution of Common Terns (n=3) during the non-breeding period, 14 August 2017 - 5 May 2018.

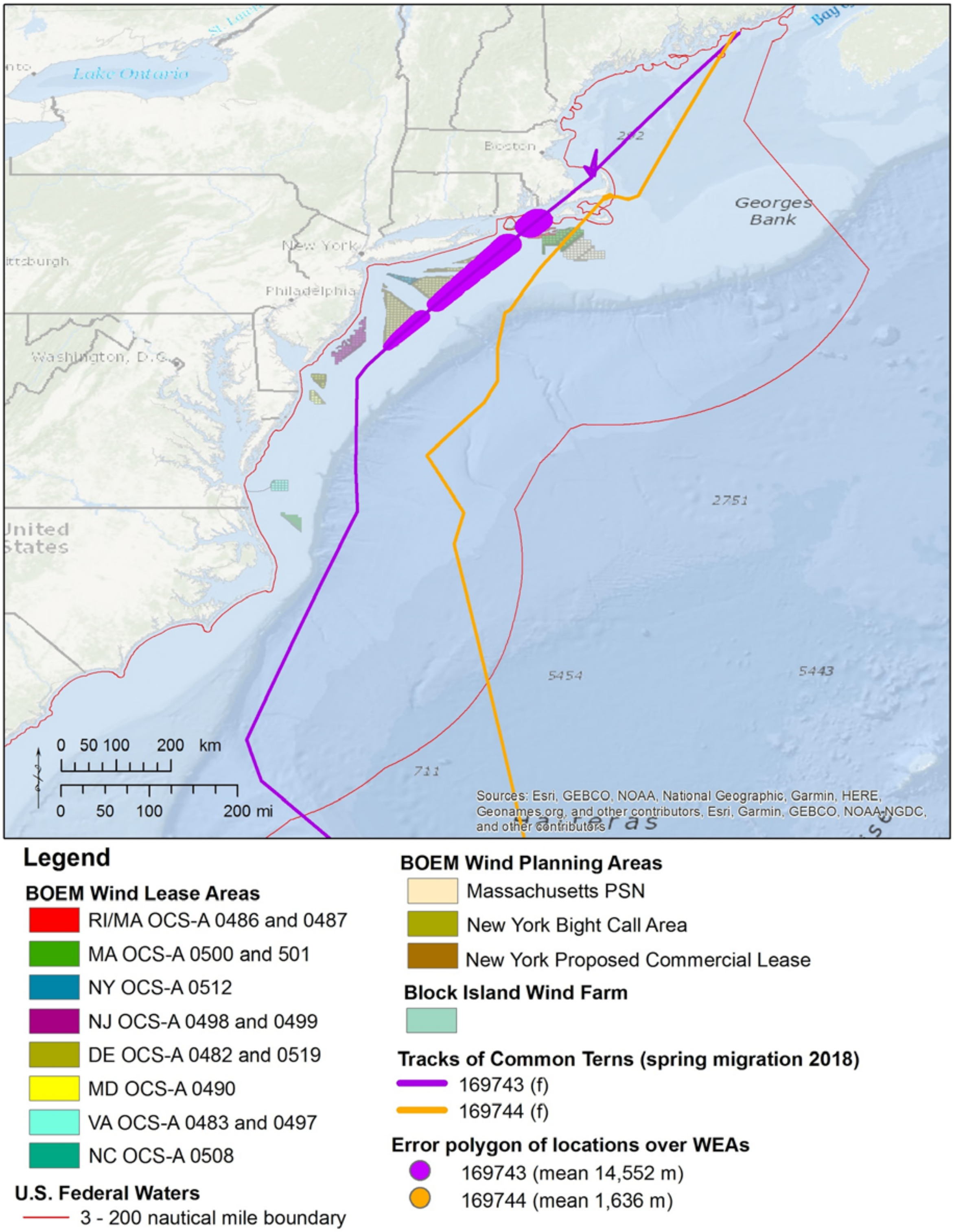

Figure J-8. Model-estimated tracks of Common Terns (n=2) during spring migration, 23 April 2018 - 18 May 2018.

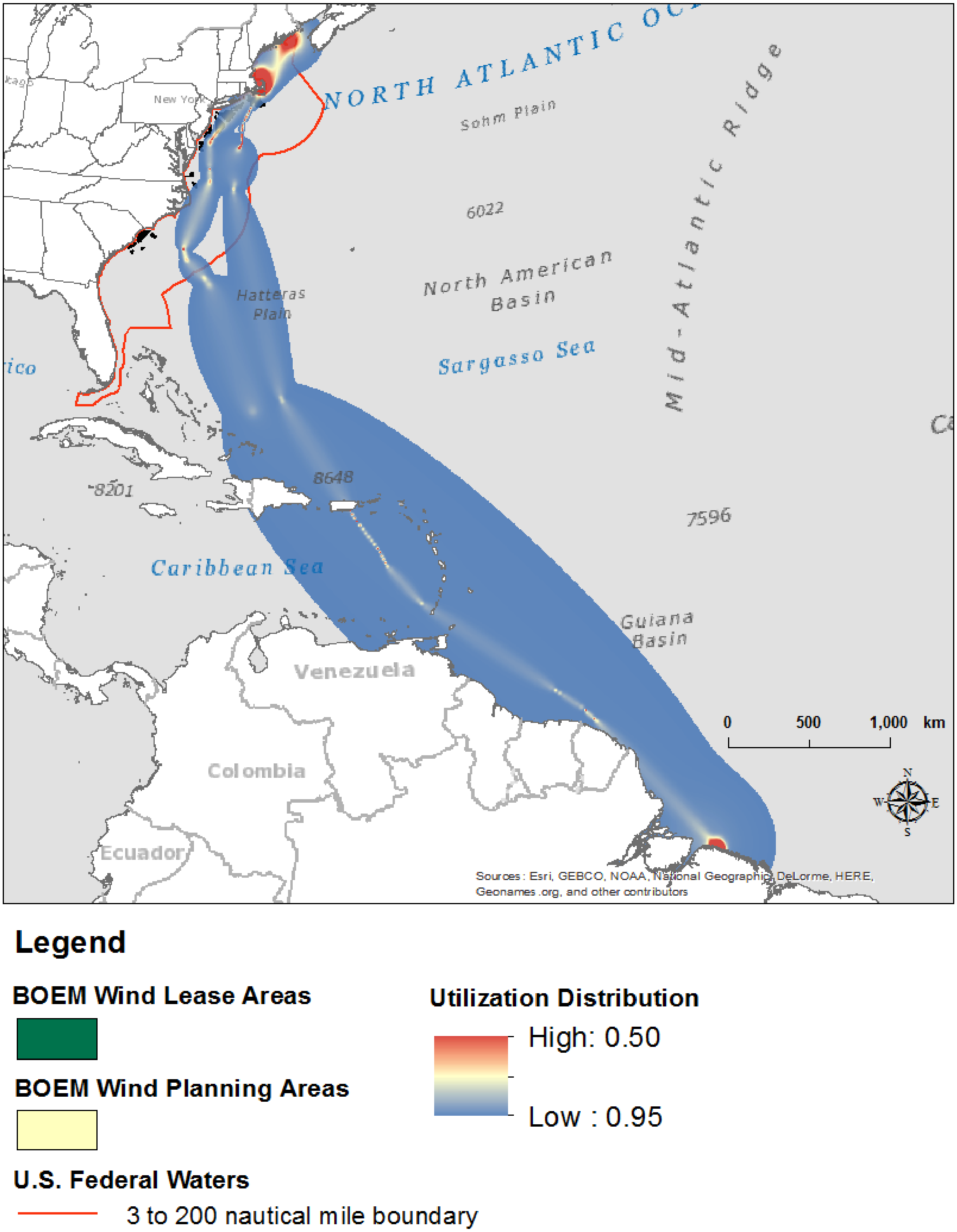

Figure J-9. Composite utilization distribution of Common Terns (n=2) during spring migration, 23 April 2018 - 18 May 2018.

Exposure to Federal waters

Common Terns were exposed to Federal waters (>5.5 km offshore) of the Atlantic OCS throughout the annual cycle, except during the non-breeding period (mid-September to May) when they were in South America (Fig. J-9). Exposure to Federal waters occurred throughout all hours of the day and night (Fig. J-11) and varied by stage in the annual cycle. During the pre-fledging period, exposure to Federal waters was generally lower at night (24% of exposure at night; Table J-3) versus during the post-breeding dispersal period (43% of exposure at night; Table J-4), fall migration (58% of exposure at night; Table J-6) and spring migration (45% of exposure at night; Table J-7). Mean exposure time to Federal waters was lower during fall migration (Table J-6) versus spring migration (Table J-7), which intersected a larger portion of the Atlantic OCS (Fig. J-8). Across all stages, exposure to Federal waters was generally associated with moderate wind speeds (mean 5 to 8 m/s) and high visibility (mean >15 km). Mean precipitation accumulation during exposure to Federal waters ranged from 0.014 kg/m^2 (during the pre-fledging period) to 0.640 kg/m^2 during fall migration. The tracks of the two tagged males intersected the tracks of multiple hurricanes during fall migration, with estimated maximum wind speeds of 18.71 m/s and estimated maximum precipitation accumulation of 3.73 kg/m^2 .(Table J-6). All tagged terns were exposed to Federal waters during low visibility conditions (<2.5 km) throughout the annual cycle (Tables J-4 to J-7).

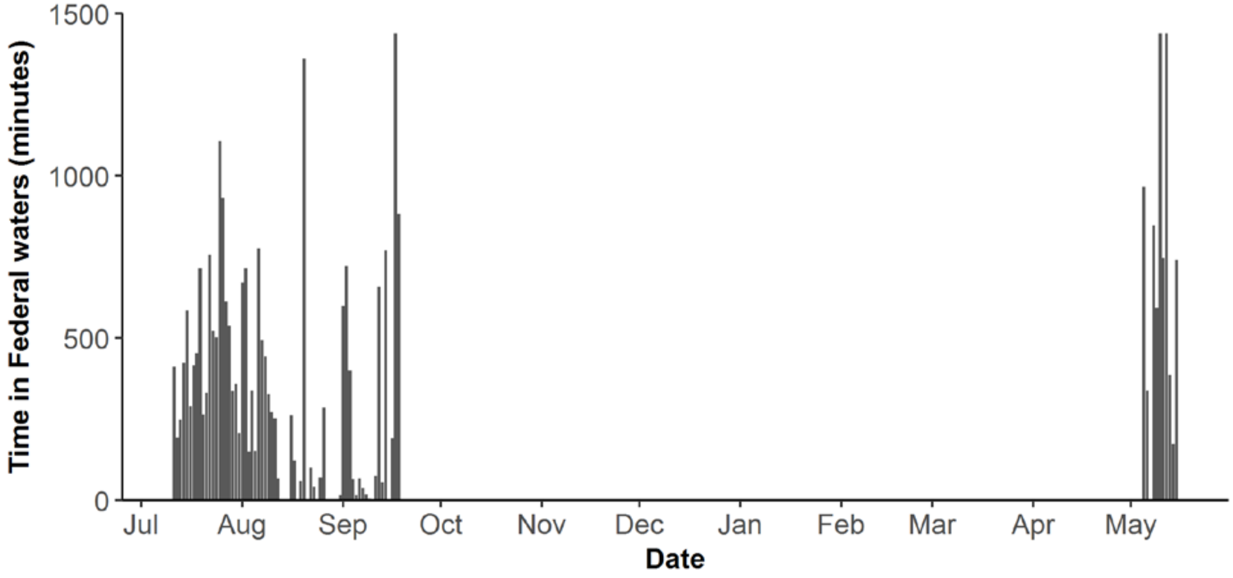

Figure J-10. Mean number of minutes spent in Federal waters by calendar date of satellite tagged Common Terns from pre-fledging (mid-Jul 2017; n=5 individuals) through spring migration (mid-May 2018; n=2 individuals).

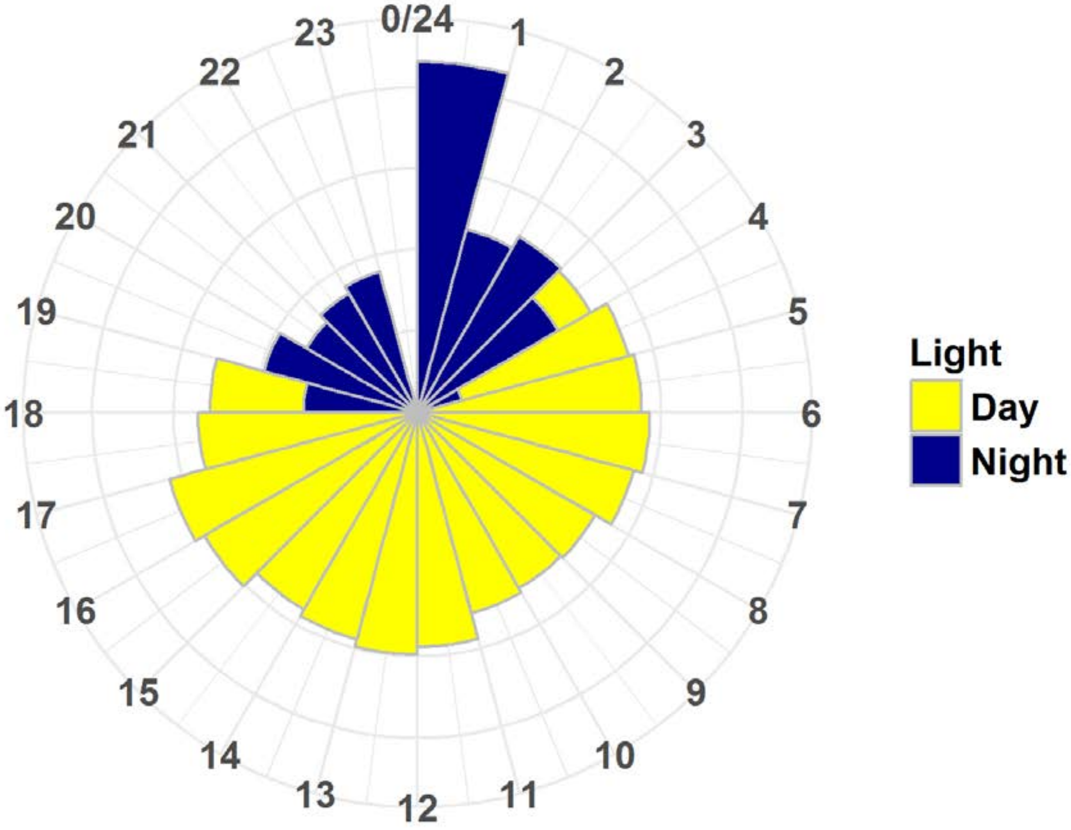

Figure J-11. Diel variation (hrs, in EST) of time spent in Federal waters of satellite tagged Common Terns (n=5) from post-breeding dispersal and fall migration (2017) through spring migration (2018), categorized by daylight using timing of local sunrise and sunset.

Table J-3. Summary statistics of mean meteorological conditions and time spent in Federal waters by satellite tagged Common Terns (n=4 individuals and n=34,995 minutes in Federal waters) during the pre-fledging period in 2017.

	mean	sd	min	max
Wind speed (m/s)	5.03	2.62	0.12	13.71
Wind support (m/s)	-0.48	4.09	-11.74	10.59
Visibility (m)	15,681	6,192	0.00	20,779
Precipitation (kg/m^2)	0.014	0.060	0.00	0.78
Air temperature (C)	18.40	2.45	12.98	24.77
Pressure (Pa)	101,504	459	100,506	102,374
Time spent during daylight (minutes)	5,287	4319	624	10,631
Time spent at night (minutes)	1,711	1,851	247	4,831

Table J-4. Summary statistics of meteorological conditions and time spent in Federal waters by satellite tagged Common Terns (n=5 individuals and n=12,130 minutes in Federal waters) during the post-breeding dispersal period in 2017.

	mean	sd	min	max
Wind speed (m/s)	6.22	2.2	1.67	11.19
Wind support (m/s)	0.34	4.20	-9.07	9.74
Visibility (m)	18,095	4,370	0.00	20,748
Precipitation (kg/m^2)	0.049	0.230	0.00	2.74
Air temperature (C)	19.96	2.38	13.17	25.36
Pressure (Pa)	101,649	377	100,339	102,409
Time spent during daylight (minutes)	1,386	1149	249	3,273
Time spent at night (minutes)	1,040	561	419	1,580

Table J-6. Summary statistics of meteorological conditions and time spent in Federal waters by satellite tagged Common Terns (n=4 individuals and n=4,822 minutes in Federal waters) during fall migration in 2017.

	mean	sd	min	max
Wind speed (m/s)	7.91	4.86	1.29	18.74
Wind support (m/s)	1.56	7.34	-9.58	18.45
Visibility (m)	15,801	6,193	0.00	21,393
Precipitation (kg/m^2)	0.640	0.951	0.00	3.732
Air temperature (C)	23.51	1.64	20.73	26.78
Pressure (Pa)	101,577	449	100,406	102,209
Time spent during daylight (minutes)	507	434	150	1,109
Time spent at night (minutes)	698	520	151	1,406

Table J-7. Summary statistics of meteorological conditions and time spent in Federal waters by satellite tagged Common Terns (n=2 individuals and n=8,266 minutes in Federal waters) during spring migration in 2017.

	mean	sd	min	max
Wind speed (m/s)	6.50	3.50	0.59	15.23
Wind support (m/s)	1.92	6.19	-9.99	14.65
Visibility (m)	16,916	5,532	61.34	20,231
Precipitation (kg/m^2)	0.022	0.096	0	1.23
Air temperature (C)	13.97	3.41	8.58	21.02
Pressure (Pa)	101,887	448	100,766	102,604
Time spent during daylight (minutes)	2,271	573	1,865	2,676
Time spent at night (minutes)	1,863	1,155	1,046	2,279

Exposure to Wind Energy Areas

Seven WEA exposure events occurred during the study period (Table J-8 and Fig. J-12). Three WEA exposure events occurred during daylight hours and four events occurred at night (Fig. J-13). During post-breeding dispersal (2017), male ID 169745 flew across WEA OCS-A 0500 in Rhode Island Sound on September 3 at night (Fig. J-3). During fall migration (2017), female ID 169744 flew across OCS-A 0500, OCS-A 0501, and Massachusetts PSN during the afternoon of August 16 while departing to the south across the Atlantic OCS from staging areas in southeastern Massachusetts (Fig. J-5). Both females tracked during spring migration (2018) were exposed to WEAs on their northbound flights across the Atlantic OCS at night (Fig. J-8). ID 169744 flew across OCS-A 0501 at night on May 6, and ID 169743 flew across the New York Bight Call Area and OCS-A 0486 in Rhode Island Sound at night on May 11. Overall, terns spent an average of 69 minutes (SD 119 minutes, range 5 to 338 minutes) crossing individual WEAs (n=7 events). Average speed across WEAs was 12.77 m/s (SD 4.80 m/s; range 7.88 to 17.94 m/s). Average error of location estimates that intersected WEAs was 8,388 m (8,337 m; range 1,636 to 20,809 m).

Estimated WEA exposure occurred during meteorological conditions favorable to offshore flight (Table J-13). All WEA events occurred under conditions with wind blowing in the direction of travel (Fig. J-14), at mean speed of 6.18 m/s (Fig. J-15), providing positive wind-support (Fig. J-16). Flights across WEAs were generally associated with conditions providing high visibility (mean 16,665 m; Fig. J-17), little to no precipitation (mean 0.06 kg/m^2; Fig. J-18), mild air temperatures (mean 20.00 degrees C; Fig. J-19), and high atmospheric pressure (mean 101,427 Pa, Fig. J-20).

Table J-8. Timing, duration (minutes), estimated mean ground speed (m/s), and estimated mean location error (m) of WEA exposure events (n=7) of satellite tagged Common Terns from post-breeding dispersal and fall migration (2017) through spring migration (2018).

Date	Period	Bird ID	WEA	Minutes	Speed	Error
2017-08-16	Fall migration	169744	OCS-A 0500	33	10.75	2,291
2017-08-16	Fall migration	169744	OCS-A 0501	14	17.94	1,980
2017-08-16	Fall migration	169744	Massachusetts PSN	26	17.94	1,692
2017-09-03	Post-breeding	169745	OCS-A 0482	5	7.89	16,291
2018-05-06	Spring migration	169744	OCS-A 0501	39	17.44	1,636
2018-05-11	Spring migration	169743	OCS-A 0486	29	8.55	20,809
2018-05-11	Spring migration	169743	New York Bight Call Area	338	8.59	14,015

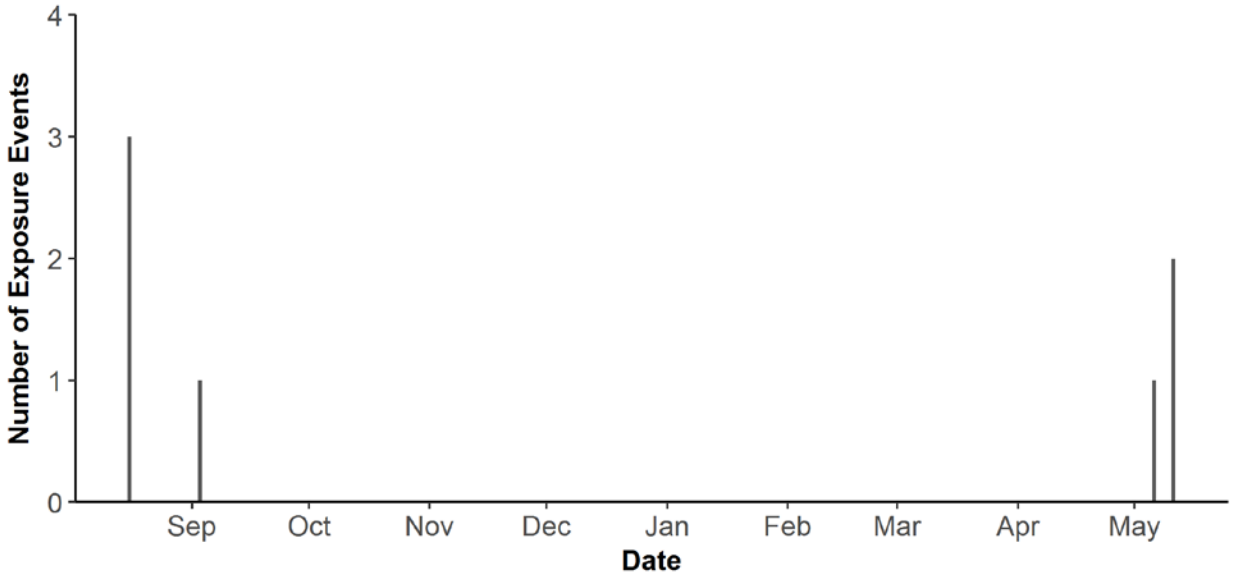

Figure J-12. Frequency distribution in calendar date of WEA exposure events (n=7) of satellite tagged Common Terns from post-breeding dispersal and fall migration (2017) through spring migration (2018).

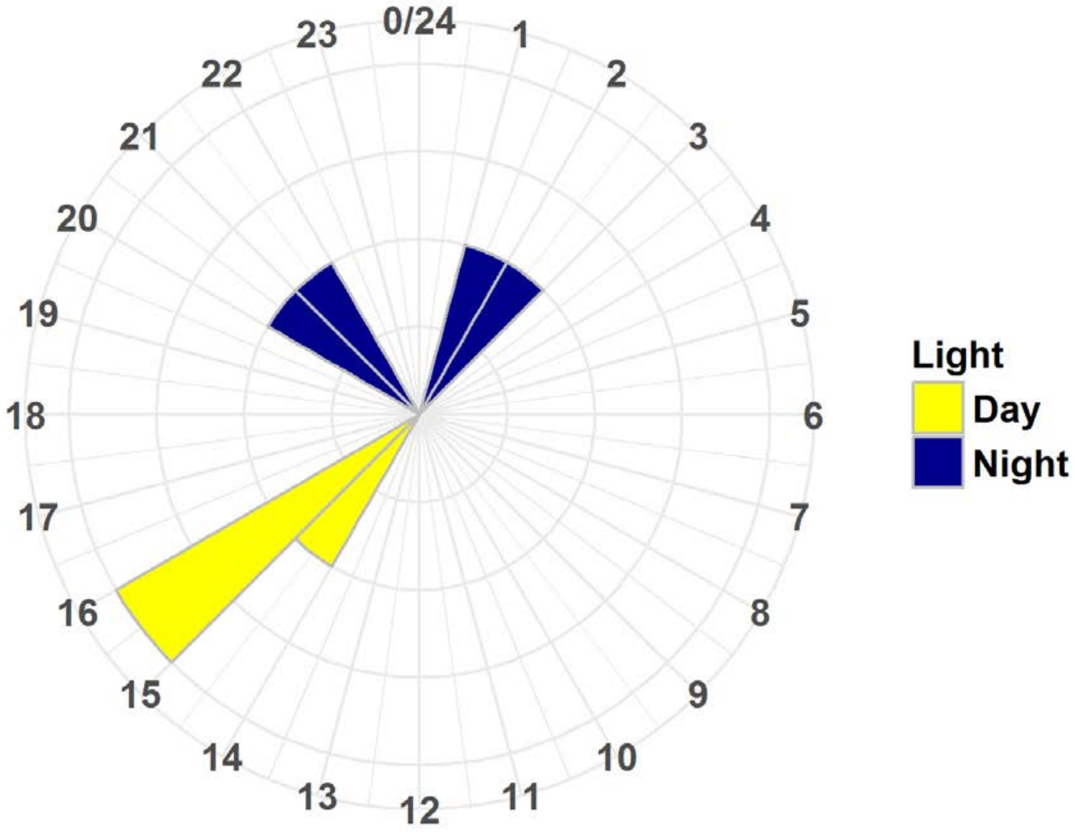

Figure J-13. Diel variation (hrs, in EST) in timing of WEA exposure events (n=7) of satellite tagged Common Terns from post-breeding dispersal and fall migration (2017) through spring migration (2018), categorized by daylight using timing of local sunrise and sunset.

Table J-13. Summary statistics of meteorological conditions during WEA exposure events (n=7) of satellite tagged Common Terns from post-breeding dispersal and fall migration (2017) through spring migration (2018).

	mean	sd	min	max
Wind speed (m/s)	6.18	4.50	2.59	13.07
Wind support (m/s)	5.50	4.06	2.37	12.57
Visibility (m)	16,665	6,171	4,517	20,258
Precipitation (kg/m^2)	0.06	0.12	0.00	0.34
Air temperature (C)	20.00	5.34	12.90	25.36
Pressure (Pa)	101427	314	100969	101937

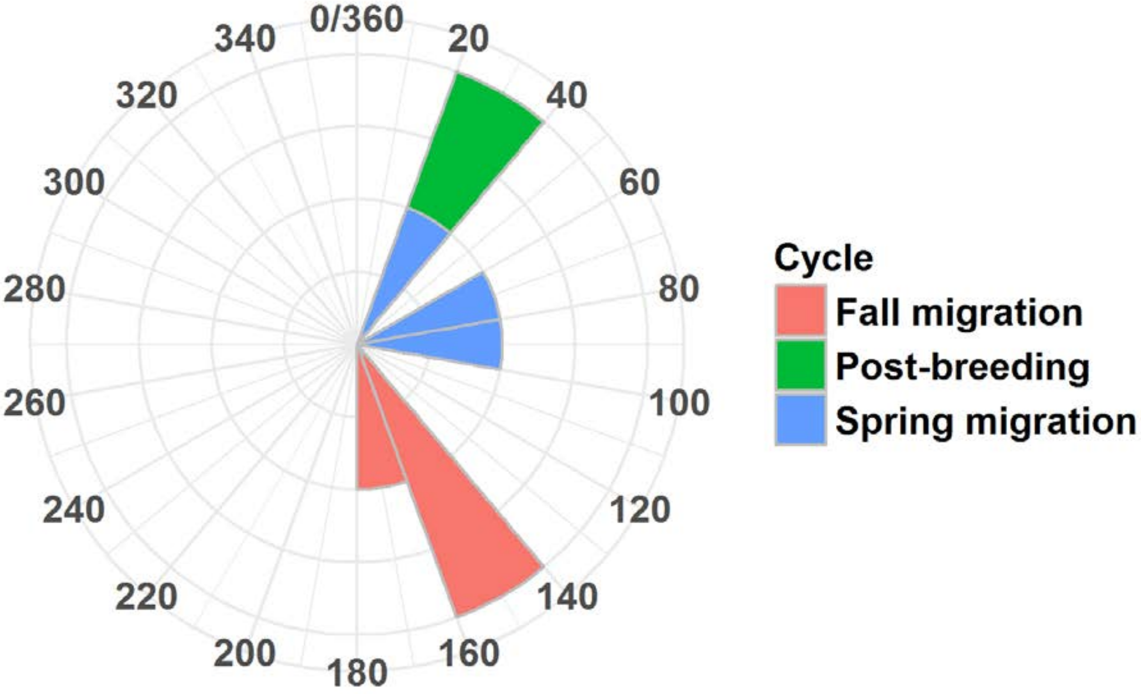

Figure J-14. Circular histogram of wind direction (degrees clockwise from N) during WEA exposure events (n=7) of satellite tagged Common Terns from post-breeding dispersal and fall migration (2017) through spring migration (2018).

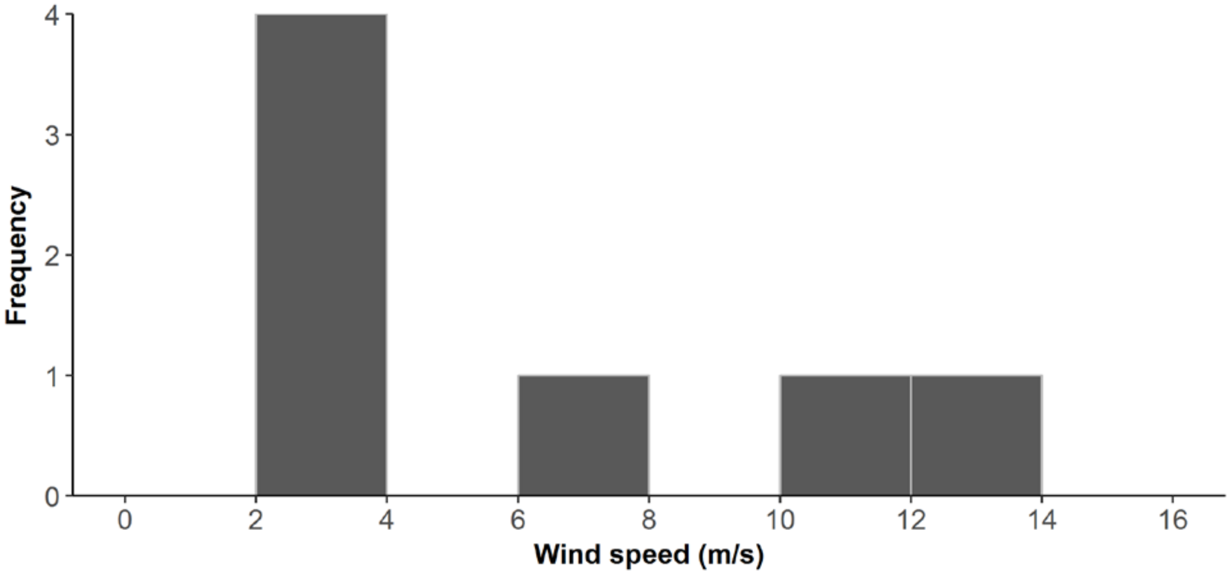

Figure J-15. Frequency distribution of wind speed (m/s) during WEA exposure events (n=7) of satellite tagged Common Terns from post-breeding dispersal and fall migration (2017) through spring migration (2018).

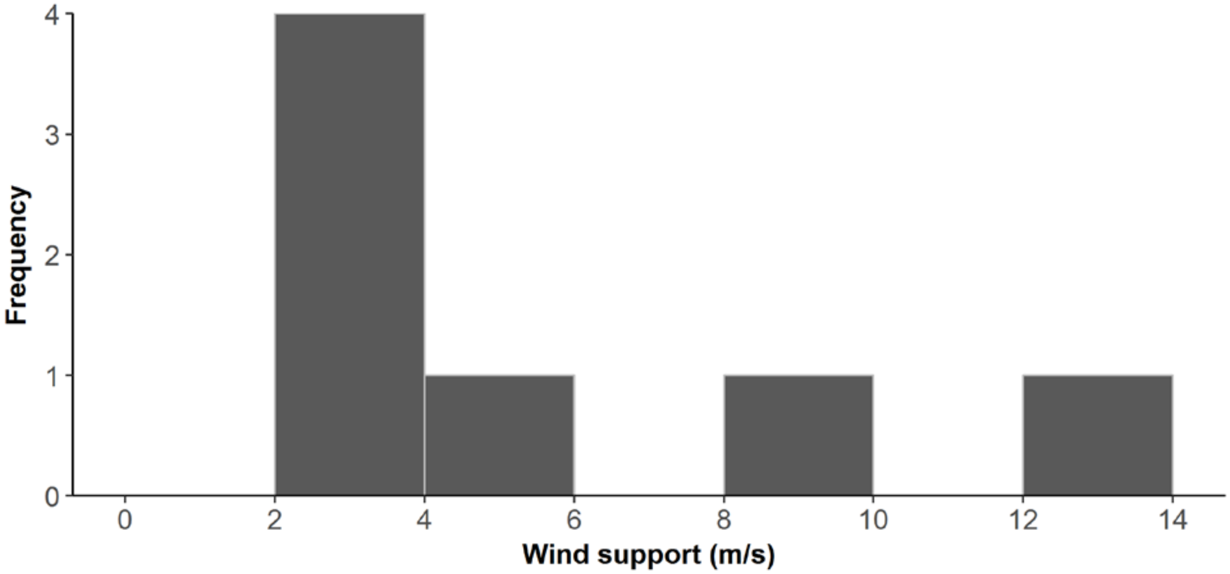

Figure J-16. Frequency distribution of wind support (m/s) during WEA exposure events (n=7) of satellite tagged Common Terns from post-breeding dispersal and fall migration (2017) through spring migration (2018).

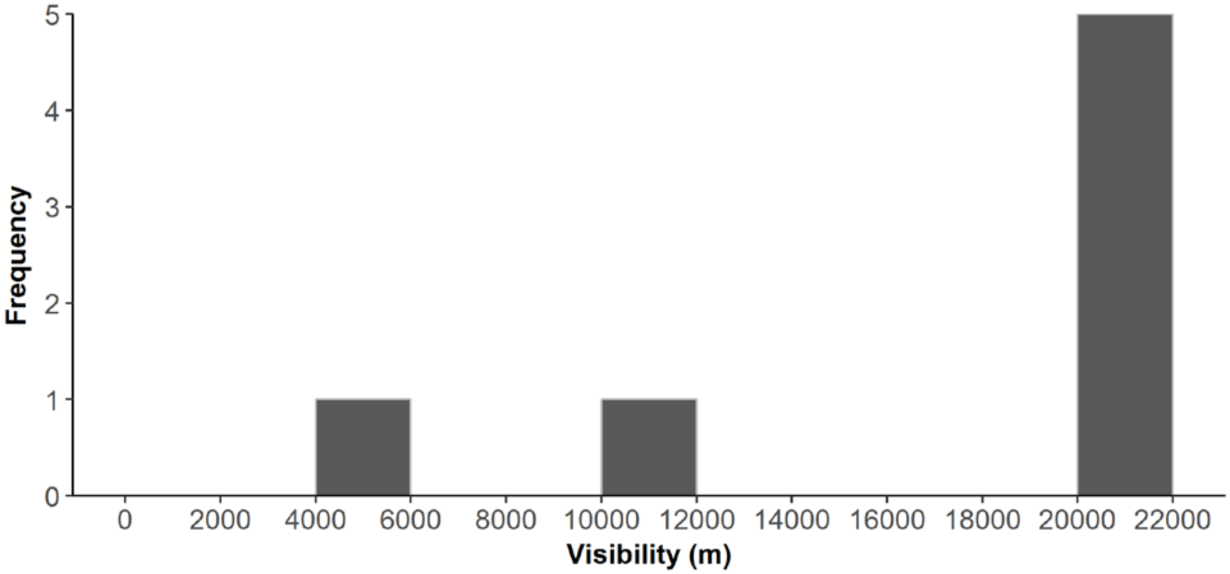

Figure J-17. Frequency distribution of visibility (m) during WEA exposure events (n=7) of satellite tagged Common Terns from post-breeding dispersal and fall migration (2017) through spring migration (2018).

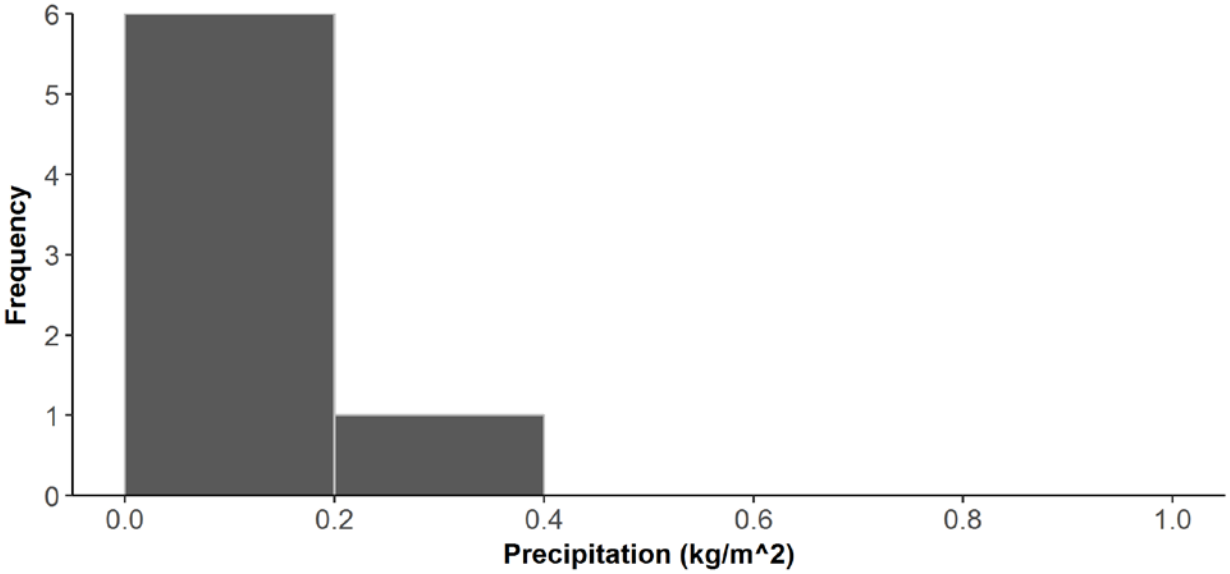

Figure J-18. Frequency distribution of precipitation accumulation (kg/m^2) during WEA exposure events (n=7) of satellite tagged Common Terns from post-breeding dispersal and fall migration (2017) through spring migration (2018).

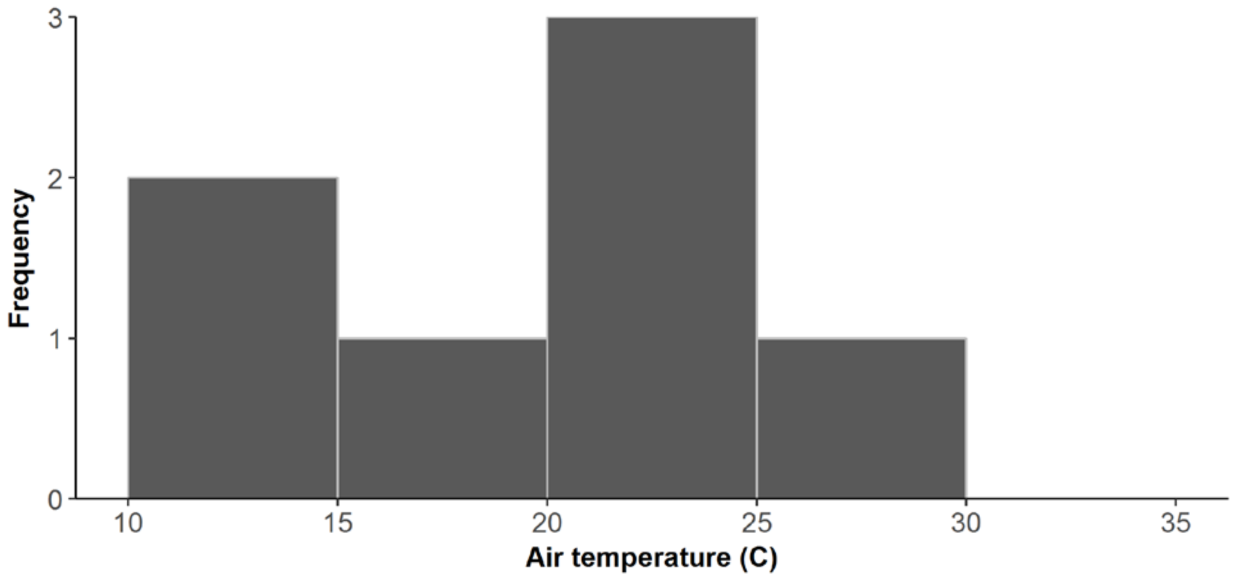

Figure J-19. Frequency distribution of air temperature (C) during WEA exposure events (n=7) of satellite tagged Common Terns from post-breeding dispersal and fall migration (2017) through spring migration (2018).

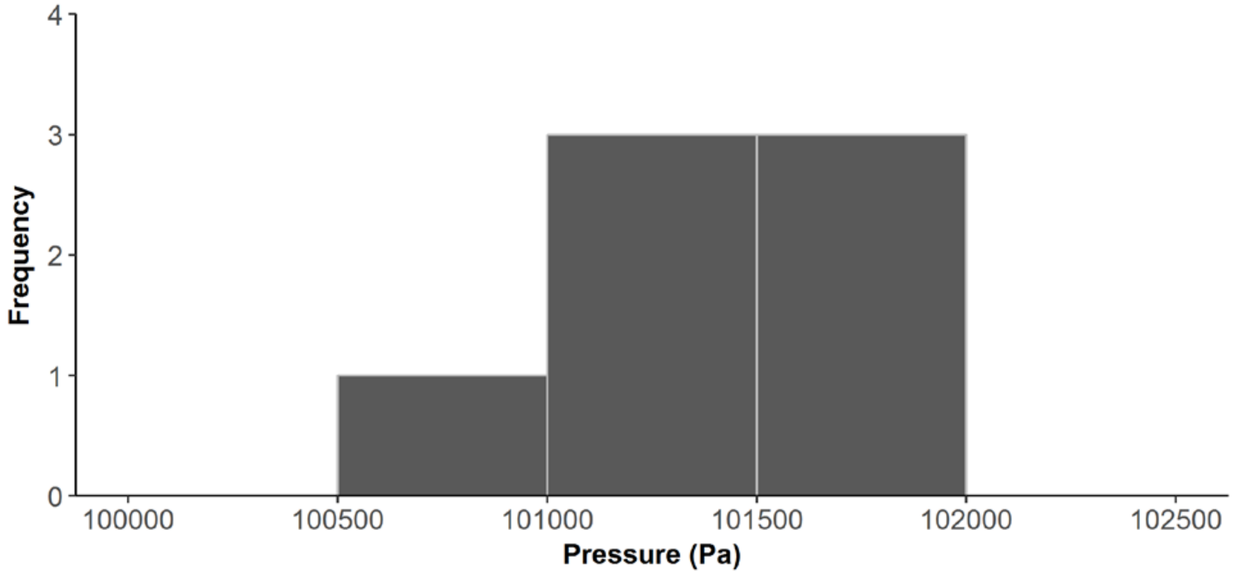

Figure J-20. Frequency distribution of barometric pressure (Pa) during WEA exposure events (n=7) of satellite tagged Common Terns from post-breeding dispersal and fall migration (2017) through spring migration (2018).

DISCUSSION

Despite a small sample size, results from this pilot study provided new information on the safety and effectiveness of satellite transmitters to track movements of Common Terns offshore. Through monitoring of tagged birds at their nest sites, we found no indication of behavioral or physical adverse effects of the transmitters or backpack harness attachment. Four of five tagged terns successfully fledged at least one chick, and productivity of tagged nests did not differ from non-tagged control nests. However, a pilot study conducted in 2018 indicated that the same back-pack style harness was not suitable for use on Roseate Terns due to mortality associated with bill entanglement in the harness material across the breast (Paton et al., in prep). Therefore, we recommend that additional pilot studies using harnesses on terns test a leg-loop design that avoids the breast and wings, and are easier for birds to shed relative to backpack style harnesses used in the present study (Thaxter et al. 2015).

In the present study, each of the five tagged terns transmitted location data through at least a portion of annual cycle, and two individuals collected data throughout entire annual cycle. These data provided novel information on the movements and utilization distributions of terns at different stages throughout the annual cycle, including precise estimates of the amount of time spent in Federal waters and WEAs. During the pre-fledging period, tagged terns commuted to foraging areas located up to 50 km away from the nesting colony. Movement tracks modeled from the satellite telemetry data provided more detailed information on foraging locations and distances of foraging flights during the pre-fledging period than has been previously published on Common Terns by studies using other methods. For example, a meta-analysis of studies using VHF tracking methods or boat-based surveys, Thaxter et al. (2012) estimated a maximum foraging range of 30 km for Common Terns.

During the post-breeding period, all five tagged terns dispersed to staging areas in southeastern Massachusetts. Previous VHF tracking studies and band resighting surveys have shown that the Cape Cod and Islands (Martha's Vineyard and Nantucket) region of southeastern Massachusetts is an important staging area for Common and Roseate Terns from breeding colonies throughout the western North Atlantic (Althouse et al. 2016; Loring et al. 2017; Trull et al. 1999). The present study collected new information about detailed movements of satellite-tagged terns among specific staging sites in southeastern Massachusetts. The study also documented a long-distance movement during the staging period that intersected several hundred kilometers of Federal waters in the mid-Atlantic Bight, including a WEA off the coast of Delaware. These results indicate that terns may range widely during the post-breeding period, and exposure to WEAs located hundreds of kilometers away from major staging areas is possible. A larger sample size of satellite-tagged individuals is needed to determine the frequency of long-distance movements and exposure of staging Common Terns to Federal waters and WEAs throughout the Atlantic OCS.

Each of the four tagged Common Terns tracked during fall migration departed on a southern trajectory from staging areas in southeastern Massachusetts over the Atlantic OCS. Three terns departed east of WEAs off the coast of Massachusetts, and the remaining tern intersected multiple WEAs south of Martha's Vineyard and Nantucket. In a previous study using geolocators, Nisbet et al. (2011a) collected the first data on offshore migratory routes of Common Terns departing from staging areas in Massachusetts, but the error of location estimates from geolocators was too large (50 km to >300 km) to assess exposure to specific WEAs. In both the present study and in the previous study using geolocators, females departed on fall migration prior to males (Nisbet et al. 2011b).

Common Terns tracked during spring migration intersected with a more extensive portion of the Atlantic OCS relative to fall migration, where the majority of the migratory tracks occurred offshore of the U.S. Exclusive Economic Zone. The more inshore routes of Common Terns in spring resulted in increased exposure to WEAs off the coast of New York, Rhode Island, and Massachusetts. Using predictive modeling of the distributions of Common Terns from survey data, Winship et al. (2018) also predicted higher exposure of Common Terns to Federal waters and WEAs of the Atlantic OCS during spring relative to fall migration.

In the present study, pairing satellite derived tracks with satellite-derived environmental covariates yielded new information on the weather conditions of offshore movement events. Long-distance staging and migratory movements were strongly associated with supportive tailwind conditions. Offshore movements generally occurred during periods of high visibility and low precipitation, consistent with results from the nanotag study on movements during breeding and post-breeding dispersal (Sections 3.1.4 and 3.1.5). However, exposure to Federal waters during low visibility conditions occurred infrequently throughout the annual cycle. In addition, an active hurricane season during September 2017 resulted in the migratory routes of males intersecting with multiple storm systems during their southbound flights across the Atlantic OCS. Inclement weather conditions such as high wind, precipitation, and limited visibility may increase risk of collision with offshore wind turbines (Hüppop et al. 2006), therefore this type of information on offshore movements relative to weather conditions is an important component of risk assessments.

Results of this pilot study have demonstrated that satellite telemetry offers several advantages over nanotag technology for addressing information gaps on bird movements and offshore wind energy. Unlike nanotag technology, which is limited by geographic range of tracking towers (generally <20 km for terns), satellite tracking technology is global in scale. Applying movement models to interpret tracks between satellite-derived locations yields unbiased estimates on the amount of time spent in Federal waters and WEAs of the Atlantic OCS. The satellite data in this pilot study provided the first robust estimates of cumulative exposure of terns to multiple WEAs in the Atlantic OCS throughout the annual cycle, particularly during offshore migration events that are out of range of the nanotag network. More broadly, the full-annual-cycle data collected by satellite transmitters has potential to address critical information gaps during migration and on the wintering grounds, when most mortality is thought to occur (Nisbet et al. 2017).

Although miniaturized satellite transmitters represent a major technological advancement for remotely tracking small-bodied species, the Argos-system transmitters used in the present study are not currently capable of estimating altitude. Altitude estimates are critical for assessments of exposure to the Rotor Swept Zone of offshore wind turbines (Fox et al. 2006). Coarse estimates of flight altitude from nano-tagged Common and Roseate Terns during the breeding and post-breeding dispersal period were primarily below the RSZ (Section 3.1.5.3). Migrating terns tracked with radar were recorded at much higher altitudes (1,000 to 3,000 m, Alerstam 1985), although there is a lack of information on the migratory altitudes of terns in the Atlantic OCS. Recent advancements in tracking technology include light-weight (1-g) archival GPS transmitters that estimate altitude within an estimated error range of 20 m (M. Vandentillaart, pers. comm.). We suggest that future studies continue to pilot new tracking technology to support assessments of offshore bird movements using the best available science.

ACKNOWLEDGEMENTS

This study was funded in part by the U.S. Department of the Interior, Bureau of Ocean Energy Management through Interagency Agreement M13PG00012 with the U.S. Department of the Interior, Fish and Wildlife Service. We thank the staff of Maine Coastal Islands National Wildlife Refuge for logistical support. We thank Dr. Paul Howey (Microwave Telemetry) for providing transmitters for this study and for technical support. We thank Hua Bai (University of Massachusetts, Amherst) for assistance with data analysis.

REFERENCES

Agostinelli C, Lund U. 2017. R package 'Circular': Circular Statistics (version 0.4-93); [accessed 2017 July 1]. https://cran.r-project.org/web/packages/circular/.

Alerstam T. 1985. Strategies of migratory flight, illustrated by Arctic and Common Terns, *Sterna paradisaea* and *Sterna hirundo*. Contributions in Marine Science Supplement 27:580-603

Althouse MA, Cohen JB, Spendelow JA, Karpanty SM, Davis KL, Parsons KC, Luttazi CF. 2016. Quantifying the effects of research band resighting activities on staging terns in comparison to other disturbances. Waterbirds 39: 415-419.

Argos. 2016. User's Manual. Toulouse, CLS/Service Argos. [accessed 2018 Jul 15]. http://www.argos-system.org/manual/

Bivand R, Lewin-Koh N. 2016. R package 'Maptools' (version 0.9-2); [accessed 2017 July 1]. https://cran.r-project.org/web/packages/maptools/.

BOEM. 2018. Renewable Energy GIS Data (version 25 Jul 2018); [accessed 2018 August 20]. https://www.boem.gov/Renewable-Energy-GIS-Data/.

Burger J, Gordon C, Niles L, Newman J, Forcey G, Vlietstra L. 2011. Risk evaluation for Federally listed (Roseate Tern, Piping Plover) or candidate (Red Knot) bird species in offshore waters: A first step for managing the potential impacts of wind facility development on the Atlantic Outer Continental Shelf. Renewable Energy 36:338–351.

Fox AD, Desholm M, Kahlert J, Christensen TK, Petersen IBK. 2006. Information needs to support environmental impact assessment of the effects of European marine offshore wind farms on birds. Ibis 148:129-144.

Horne JS, Garton EO, Krone SM, Lewis JS. 2007. Analyzing animal movements using Brownian bridges. Ecology 88:2354-2363

Hüppop O, Dierschke J, Exo KM, Fredrich E, Hill R. 2006. Bird Migration Studies and Potential Collision Risk with Offshore Wind Turbines. Ibis 148:90-109

Kemp MU, Shamoun-Baranes J, van Loon EE, McLaren JD, Dokter AM, Bouten W. 2012. Quantifying flow-assistance and implications for movement research. J Theor Biol 308:56-67

Kranstauber B, Cameron A, Weinzerl R, Fountain T, Tilak S, Wikelski M, Kays R. 2011. The Movebank data model for animal tracking. Environmental Modelling & Software 26(6):834-835.

Kranstauber B, Smolla M, Scharf AK. 2018. move: Visualizing and Analyzing Animal Track Data. R package version 3.1.0. [accessed 2018 September 1]. https://CRAN.R-project.org/package=move

Loring PH, Ronconi R, Welch L, Taylor P, Mallory M. 2017. Post-breeding dispersal and staging of Common and Arctic Terns throughout the western North Atlantic. Avian Conservation and Ecology, 12(2).

National Oceanic and Atmospheric Administration. 2017. National Centers for Environmental Prediction North American Regional Reanalysis; [accessed 2017 May 20]. http://www.esrl.noaa.gov/psd/data/gridded/data.narr.html.

Nisbet ICT, Mostello CS, Veit RR, Fox JW, Afanasyev V. 2011a. Migrations and winter quarters of five Common Terns tracked using geolocators. Waterbirds 34:32-39.

Nisbet ICT, Szczys P, Mostello CS, Fox JW. 2011b. Female Common Terns Sterna hirundo start autumn migration earlier than males. Seabird 24:103-106.

Thaxter, CB, Lascelles B, Sugar K, Cook ASCP, Roos S, Bolton M, Langston RHW, Burton NHK. 2012. Seabird foraging ranges as a preliminary tool for identifying candidate Marine Protected Areas. Biological Conservation 145:53-61.

Thaxter CB, Ross-Smith VH, Clark JA, Clark NA, Conway GJ, Marsh M, Leat EHK, Burton NHK. 2015. A trial of three harness attachment systems methods and their suitability for long-term use on Lesser Black-backed Gulls and Great Skuas. Ringing and Migration 29:65-76.

Winship A, Kinlan B, White T, Leirness J, Christensen J. 2018. Modeling At-Sea Density of Marine Birds to Support Atlantic Marine Renewable Energy Planning: Final Report. U.S. Department of the Interior, Bureau of Ocean Energy Management, Office of Renewable Energy Programs, Sterling, VA. OCS Study BOEM 2018-010. x+67 pp

Appendix K

Summary of Exposure of Common and Roseate Terns at the Block Island Wind Farm

This Appendix summarizes results from an exposure analysis of Common and Roseate Terns to the Block Island Wind Farm, a 30-MW offshore wind energy facility located in state waters of Rhode Island (Fig. K-1). The Block Island Wind Farm is the first offshore wind facility in US waters and has five 6-MW turbines that have a RSZ of 29 to 189 m ASL. The turbines were constructed during 2016, and have been in operation since December 2016. We analyzed tracking data from Common and Roseate terns to assess temporal, demographic, meteorological variation in exposure to Block Island Wind Farm prior to construction (2015), during construction (2016), and during year one of operation (2017).

This analysis includes data from Common Terns (n=91) and Roseate Terns (n=90) tagged from 2015 to 2017 at the nesting colony on Great Gull Island in eastern Long Island Sound, NY, located approximately 50 km from Block Island. For analysis of exposure to the Block Island Wind Farm, we used the boundary of the Renewable Energy Zone (~34 km^2) in state waters of Rhode Island (Northeast Regional Ocean Council 2017). Methods for assessing occurrence within the Block Island Wind Farm are described in section 2.10 and 2.11 of the main report. We implemented methods described in section 2.12 of the main report to predict exposure to the Block Island Wind Farm relative to temporal, demographic, and meteorological covariates using a regression-based method, boosted GAMs (R package 'mboost' using function 'gamboost'; Buhlmann and Hothorn 2007). To assess the significance of the predicted covariate responses, we performed bootstrap analysis (using function confint with 100 model fits) to produce 95% confidence intervals for each covariate response. We also report summary statistics of temporal and meteorological variables associated with exposure events, calculated using methods described in section 2.12 of the main report.

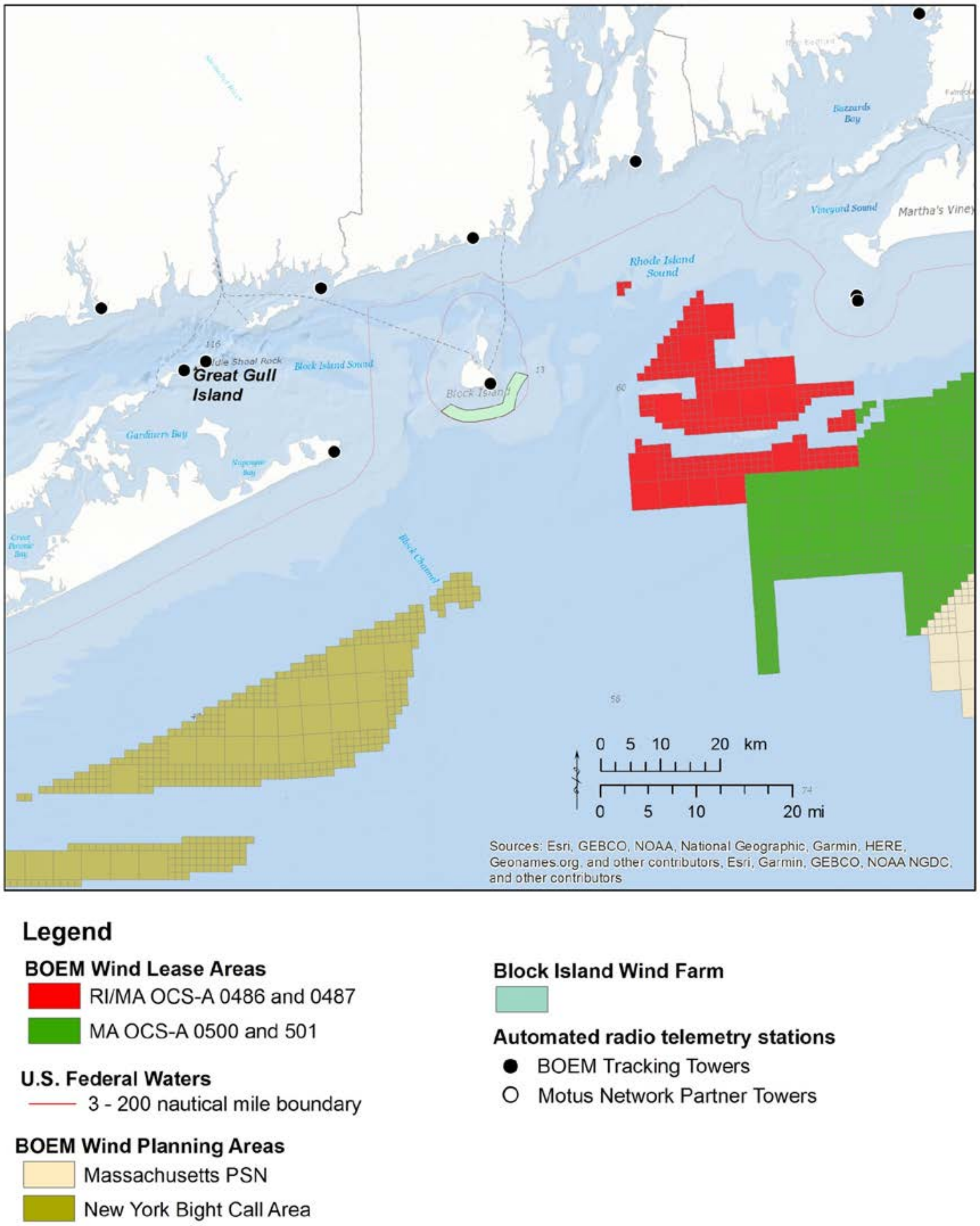

Figure K-1. Map showing location of Block Island Wind Farm and Great Gull Island
Federal waters of the U.S Atlantic are delineated by the red boundary (3 to 200 nautical miles). Within this boundary, the Block Island Wind Farm and all current (July 2018) BOEM Wind Energy Areas and Planning Areas shown as polygons. Points show locations automated radio telemetry stations active from from 2015 to 2017.

Summary of exposure by species

Of the 89 Common Terns from Great Gull Island detected by the telemetry array from 2015 to 2017, 49% (n=44) had estimated exposure to the Block Island Wind Farm (Table K-1). Of the 90 Roseate Terns from Great Gull Island detected by the telemetry array from 2015 to 2017, 23% (n=21) had estimated exposure to Block Island Wind Farm (Table K-2). Mean number of exposure events per bird and year ranged from 2.34 events (sd 1.66; range 1 to 8 events) for Common Terns and 1.77 events (sd 1.00, range 1 to 5 events) for Roseate Terns. Exposure was higher among females versus males for both Common Terns (55% females of n=40) and Roseate Terns (71% females of n=21).

Mean spatial error of individual location estimates with exposure to the Block Island Wind Farm among Common Terns was 8,622 m (sd 8,083 m; range 298 to 29,094 m) and among Roseate Terns was 5,612 m (sd 5,183 m; range 312 m to 19,301 m). Using individual location estimates with exposure to the Block Island Wind, we calculated species-specific composite utilization distributions of Farm for Common Terns (Fig. K-2) and Roseate Terns (Fig. K-3). These utilization distributions were centered on the Block Island Renewable Energy Zone and are included to show the overall spatial resolution of the exposure analysis.

Table K-1. Tag deployment and detection summaries of adult Common Terns tagged on Great Gull Island, 2015-2017

	2015	2016	2017	Total
Number of individuals tagged	31	30	30	**91**
Number of individuals detected	31	30	28	**89**
Number with estimated exposure to BIWF	17	20	7	**44**

Table K-2. Tag deployment and detection summaries of adult Roseate Terns tagged on Great Gull Island, 2015-2017

	2015	2016	2017	Total
Number of individuals tagged	30	30	30	**90**
Number of individuals detected	30	30	30	**90**
Number with estimated exposure to BIWF	11	9	1	**21**

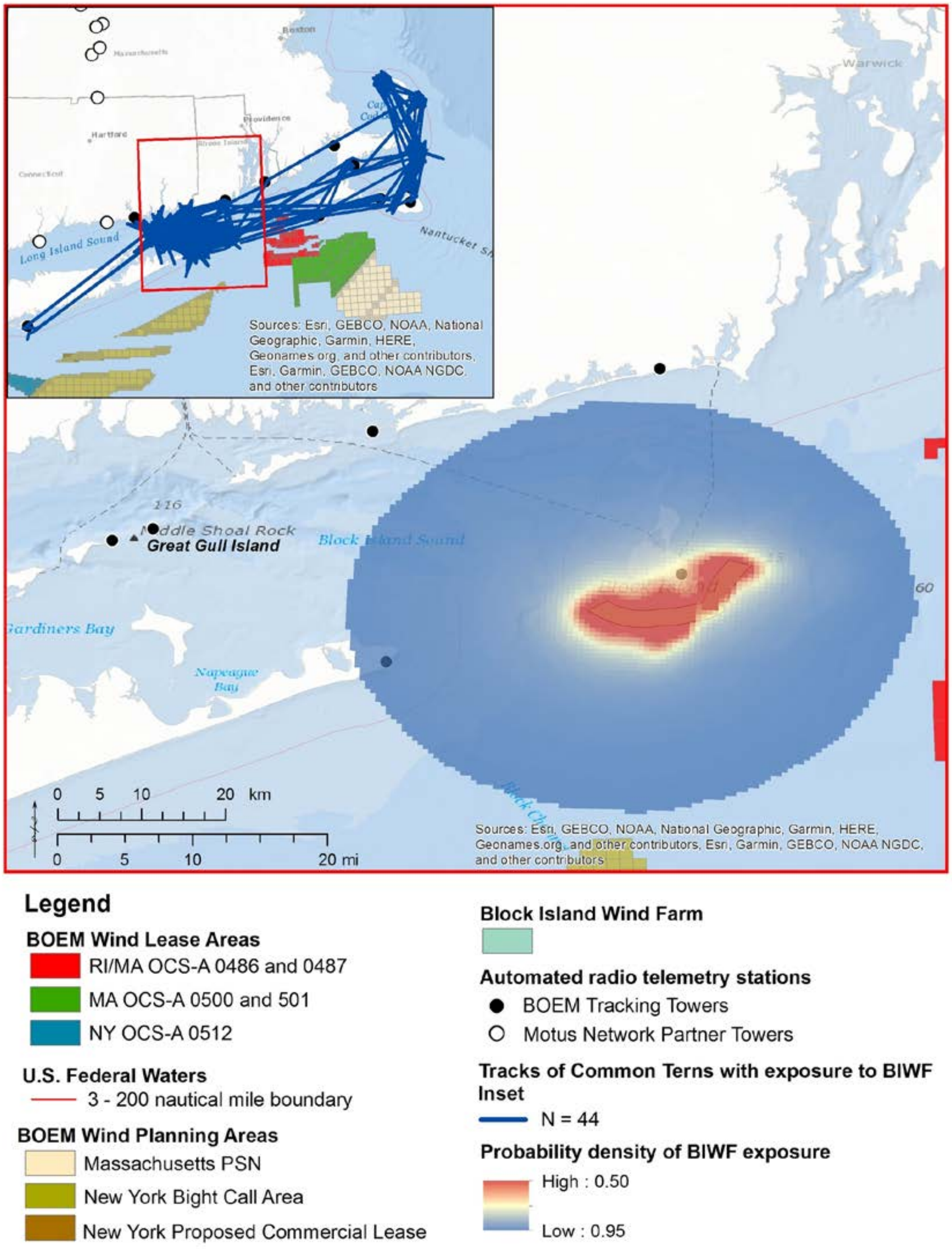

Figure K-2. Movement tracks (inset) and composite probability density of locations with estimated exposure to the Block Island Wind Farm among Common Terns (n=44) tagged on Great Gull Island in 2015 to 2017 (pooled).

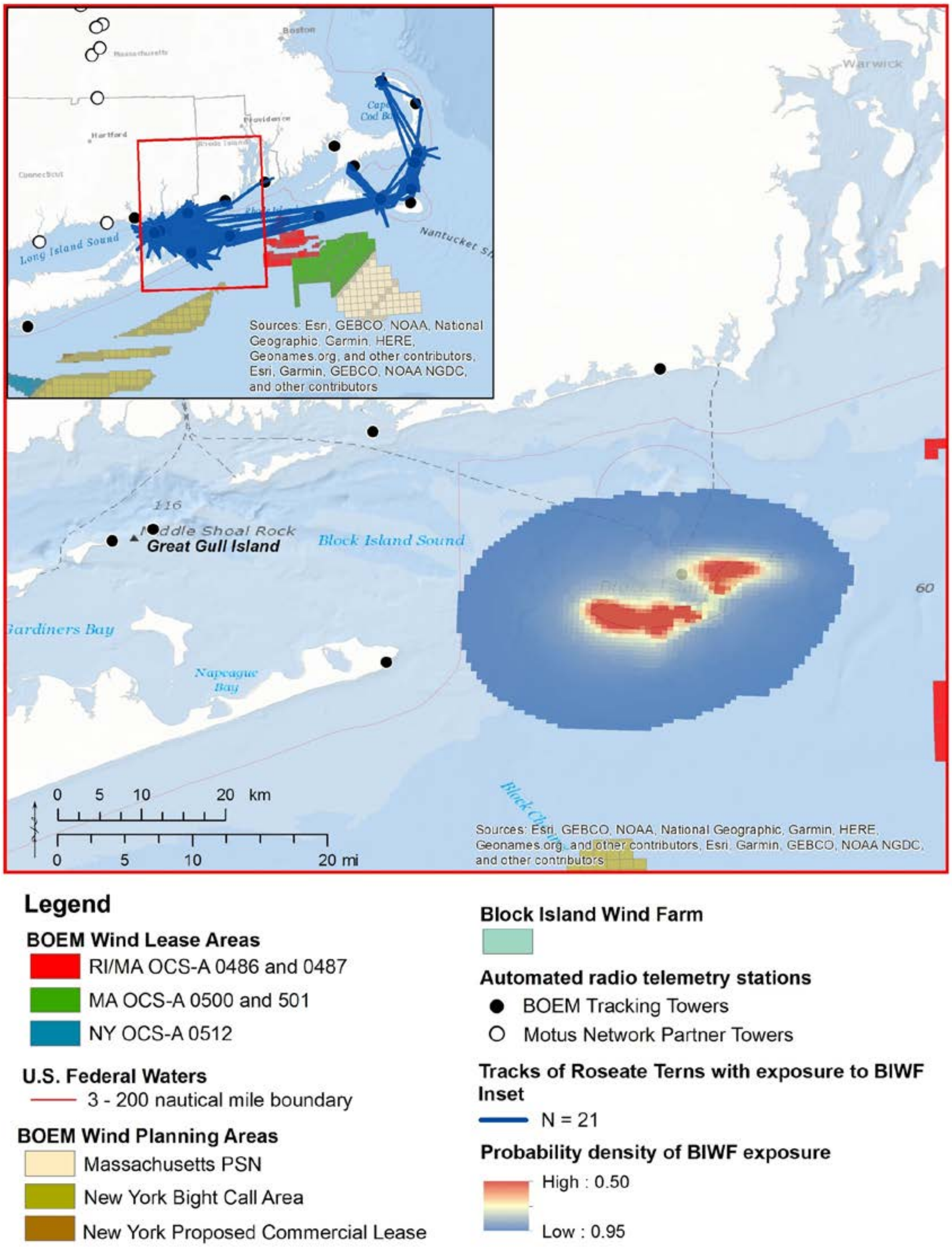

Sources: Esri, GEBCO, NOAA, National Geographic, Garmin, HERE, Geonames.org, and other contributors, Esri, Garmin, GEBCO, NOAA NGDC, and other contributors

Sources: Esri, GEBCO, NOAA, National Geographic, Garmin, HERE, Geonames.org, and other contributors, Esri, Garmin, GEBCO, NOAA NGDC, and other contributors

Figure K-3. Movement tracks (inset) and composite probability density of locations with estimated exposure to the Block Island Wind Farm among Roseate Terns (n=21) tagged on Great Gull Island in 2015 to 2017 (pooled).

Summary of temporal and atmospheric variation

Estimated exposure of Common and Roseate Terns to the Block Island Wind Farm occurred from June 22 through August 30, with peak exposure in early July (Fig. K-4). Among Common Terns, estimated exposure to the Block Island Wind Farm primarily occurred during the day (76%, n=84) versus night (24%, n=26), with peak exposure during morning hours (Fig. K-5). Estimated exposure of Roseate Terns also peaked during morning hours (Fig. K-6), and was higher during day (86%, n=32) versus night (14%, n=5). Among both species, mean day of year of daytime exposure events was Jul 12, whereas the mean day of year of night exposure was Jul 24-25 (Table K-3).

Among both species, estimated exposure to the Block Island Wind Farm predominantly occurred during east or southwest winds (Fig. K-7), with a mean speed of 5.35 m/s (Fig. K-8). Wind support values were approximately normally distributed and centered near zero (mean -0.14 m/s, Fig. K-9). In general, estimated exposure to the Block Island Wind Farm occurred during favorable weather conditions, with high visibility (mean 17,454 m; Fig. K-10), little to no precipitation (mean 0.03 kg/m^2; Fig. K-11), mild air temperatures (mean 21.92 degrees C; Fig. K-12), and high atmospheric pressure (mean 101,441 Pa, Fig. K-13). However, there was some evidence of estimated exposure during inclement weather, including low visibility (< 500 m), rain (0.85 kg/m^2), and high winds (13.42 m/s; Table K-4).

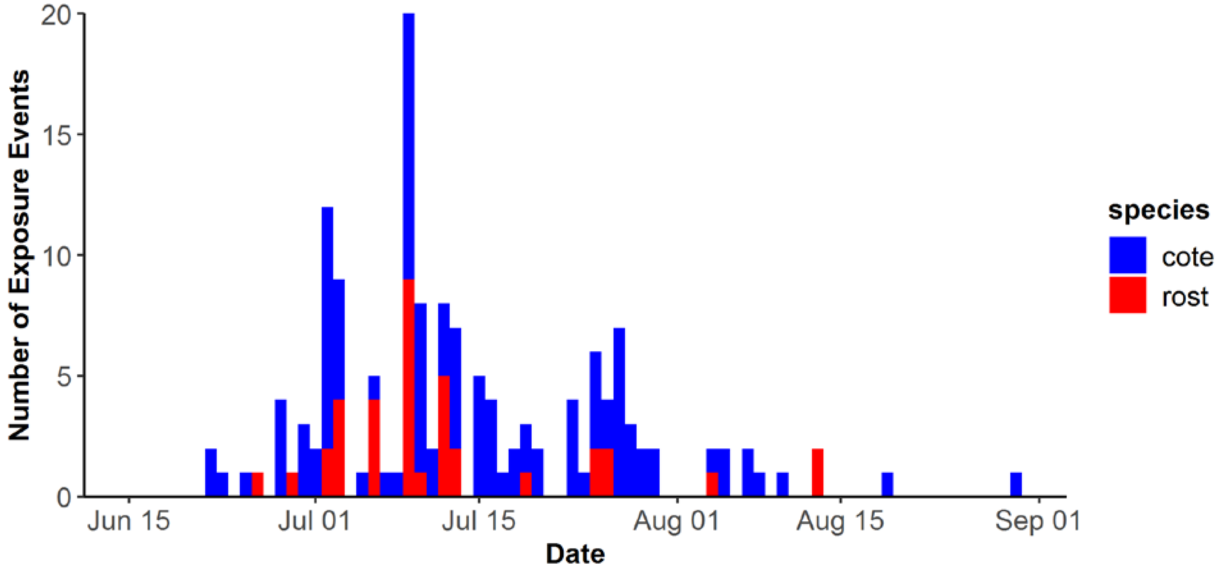

Figure K-4. Frequency distribution in calendar date of estimated exposure events at the Block Island Wind Farm (n=147) of Common Terns (blue) and Roseate Terns (red) tagged on Great Gull Island, NY from 2015 to 2017 (pooled).

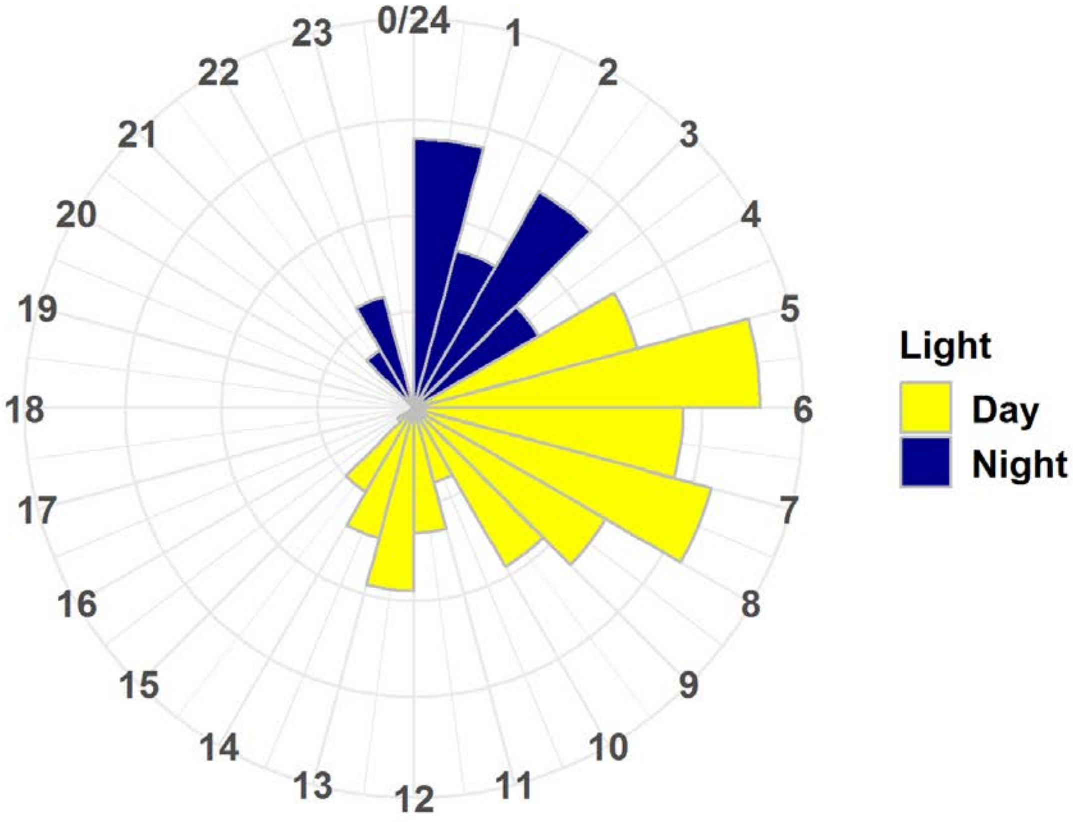

Figure K-5. Diel variation (hrs, in EST) in timing of estimated exposure events at the Block Island Wind Farm (n=110) of Common Terns tagged on Great Gull Island, NY, categorized by daylight using timing of local sunrise and sunset.

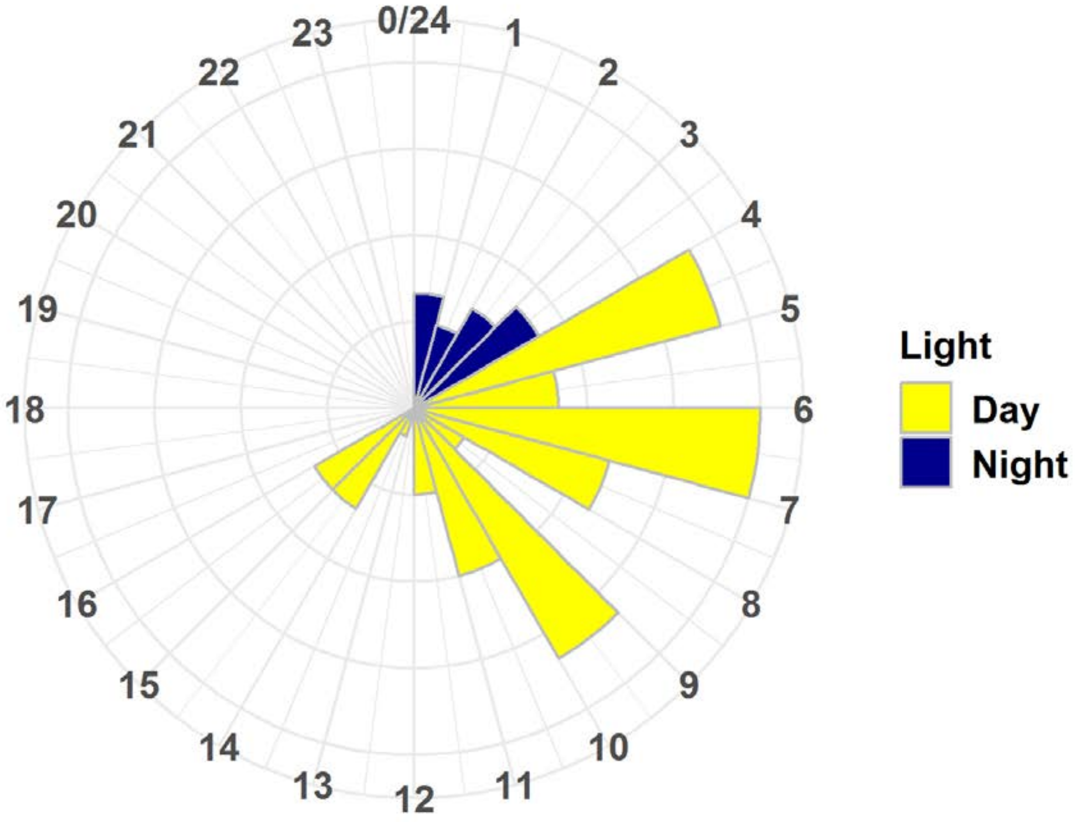

Figure K-6. Diel variation (hrs, in EST) in timing of estimated exposure events at the Block Island Wind Farm (n=37) of Roseate Terns tagged on Great Gull Island, NY, categorized by daylight using timing of local sunrise and sunset.

Table K-3. Summary statistics of day of year of estimated exposure events at the Block Island Wind Farm by day versus night, among Common Terns (n=110) and Roseate Terns (n=37) tagged on Great Gull Island, NY from 2015 to 2017.

	Mean	Min	Max
Common Terns			
Day	07-12	06-24	08-12
Night	07-24	06-24	08-21
Roseate Terns			
Day	07-12	06-28	08-15
Night	07-25	07-14	08-06

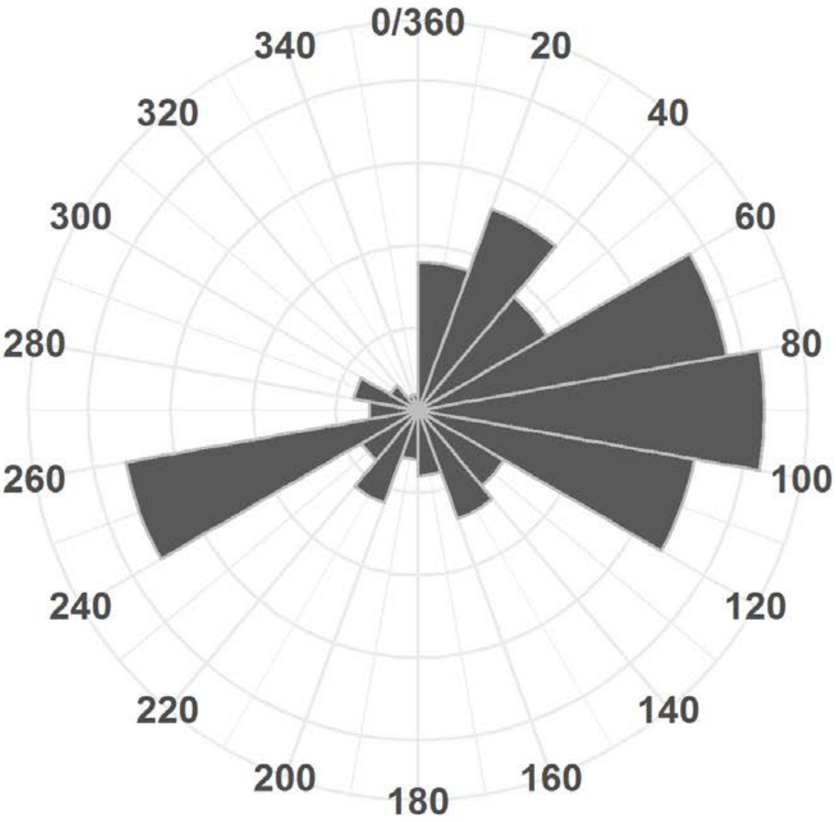

Figure K-7. Circular histogram of wind direction (degrees clockwise from N) during estimated exposure events at the Block Island Wind Farm (n=147) of Common Terns and Roseate Terns tagged on Great Gull Island, NY from 2015 to 2017 (pooled).

Table K-4. Summary statistics of meteorological conditions during estimated exposure events at the Block Island Wind Farm (n=147) of Common Terns and Roseate Terns tagged on Great Gull Island, NY from 2015 to 2017 (pooled).

	mean	sd	min	max
Wind speed	5.35	2.22	0.70	13.42
Wind support (m/s)	-0.14	3.03	-10.48	11.65
Visibility (m)	17,454	4,553	256	20,199
Precipitation (kg/m^2)	0.03	0.13	0.00	0.85
Air temperature (C)	21.92	2.03	16.04	27.22
Pressure (Pa)	101,441	402	100,225	102,407

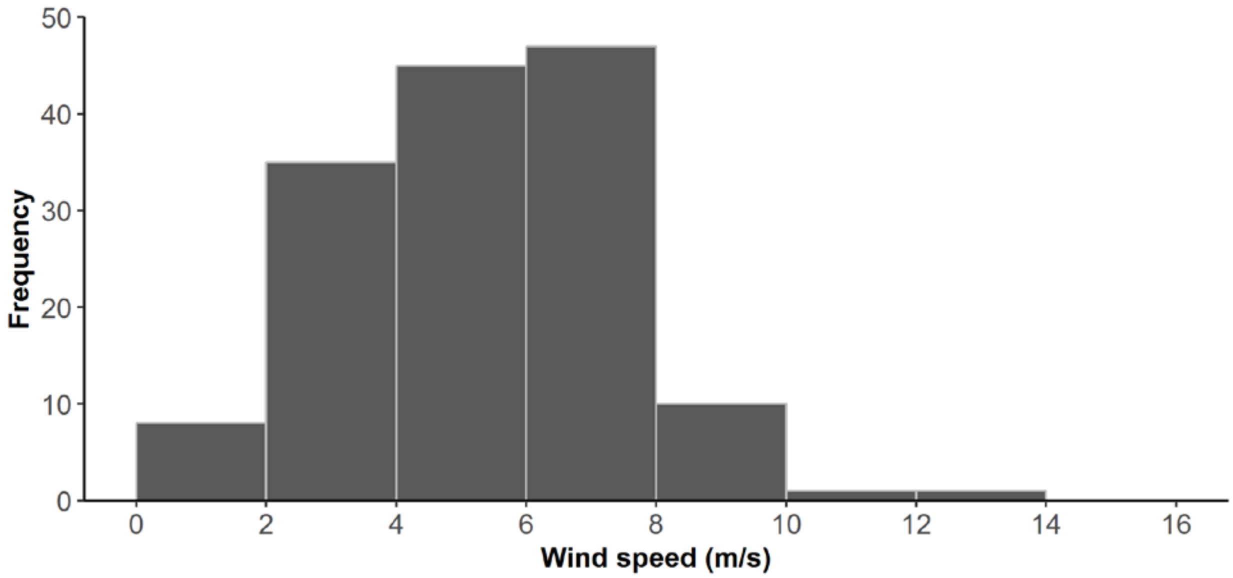

Figure K-8. Frequency distribution of wind speed (m/s) during estimated exposure events at the Block Island Wind Farm (n=147) of Common Terns and Roseate Terns tagged on Great Gull Island, NY from 2015 to 2017 (pooled).

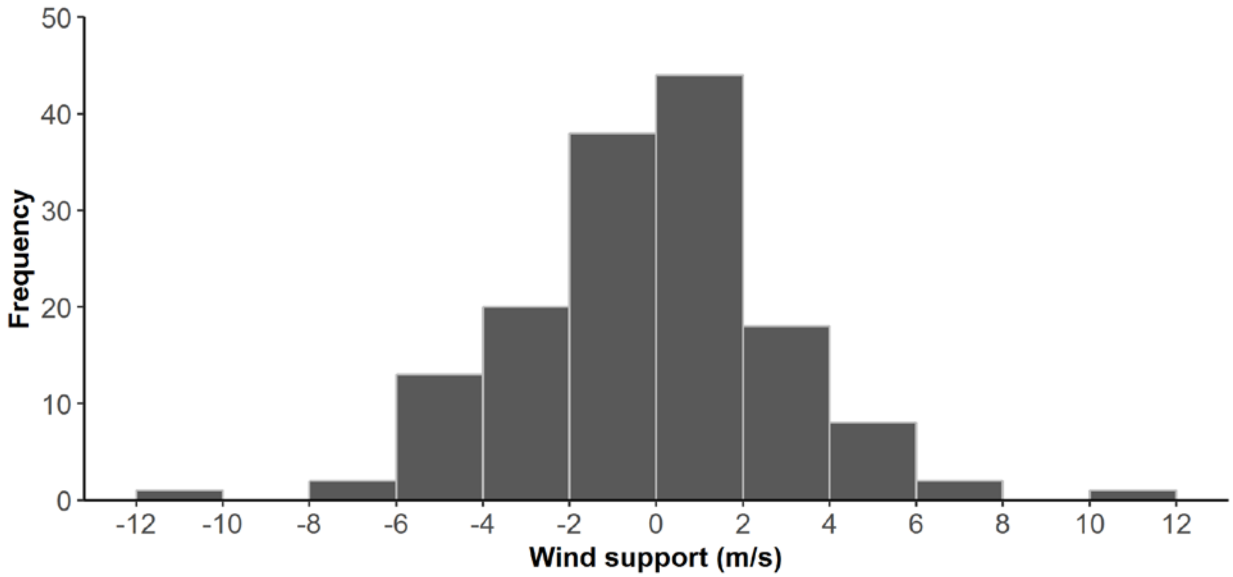

Figure K-9. Frequency distribution of wind support (m/s) during estimated exposure events at the Block Island Wind Farm (n=147) of Common Terns and Roseate Terns tagged on Great Gull Island, NY from 2015 to 2017 (pooled).

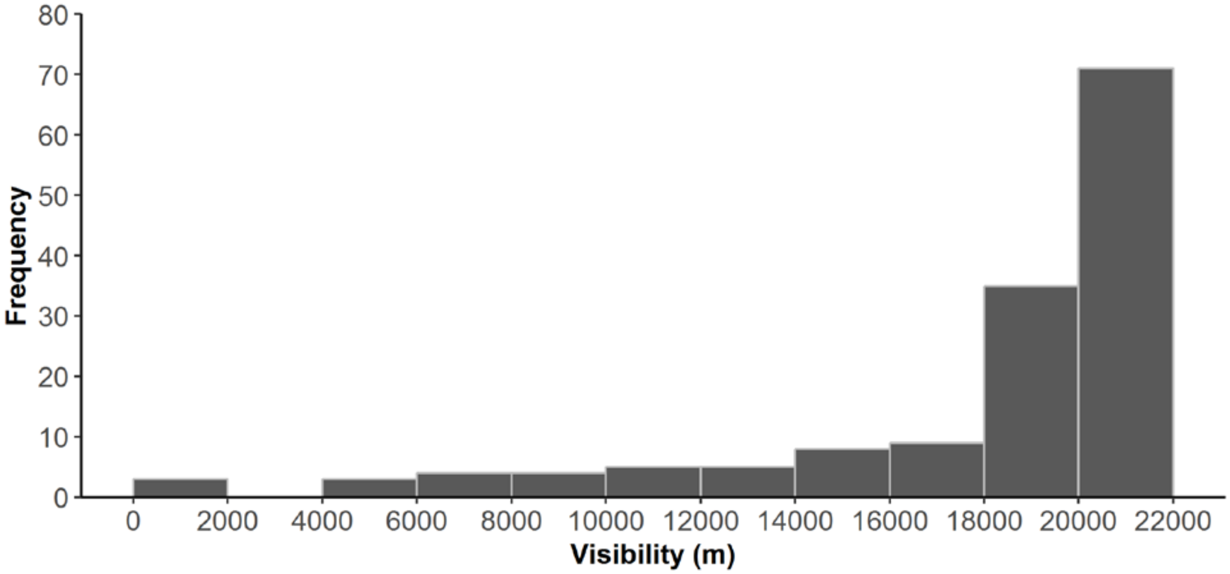

Figure K-10. Frequency distribution of visibility (m) during estimated exposure events at the Block Island Wind Farm (n=147) of Common Terns and Roseate Terns tagged on Great Gull Island, NY from 2015 to 2017 (pooled).

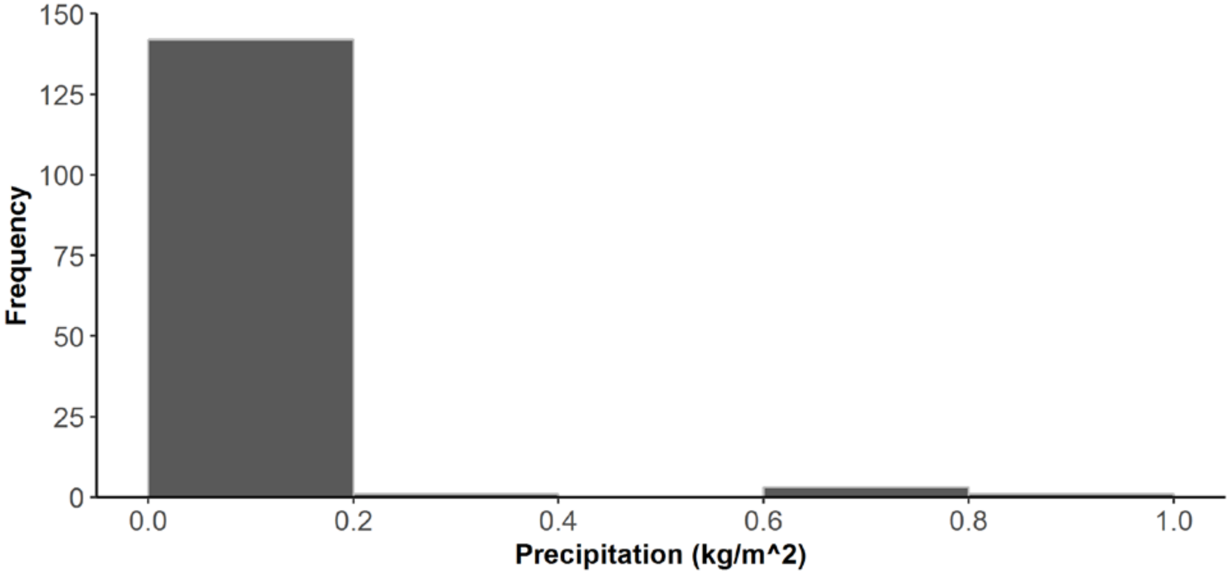

Figure K-11. Frequency distribution of precipitation accumulation (kg/m^2) during estimated exposure events at the Block Island Wind Farm (n=147) of Common Terns and Roseate Terns tagged on Great Gull Island, NY from 2015 to 2017 (pooled).

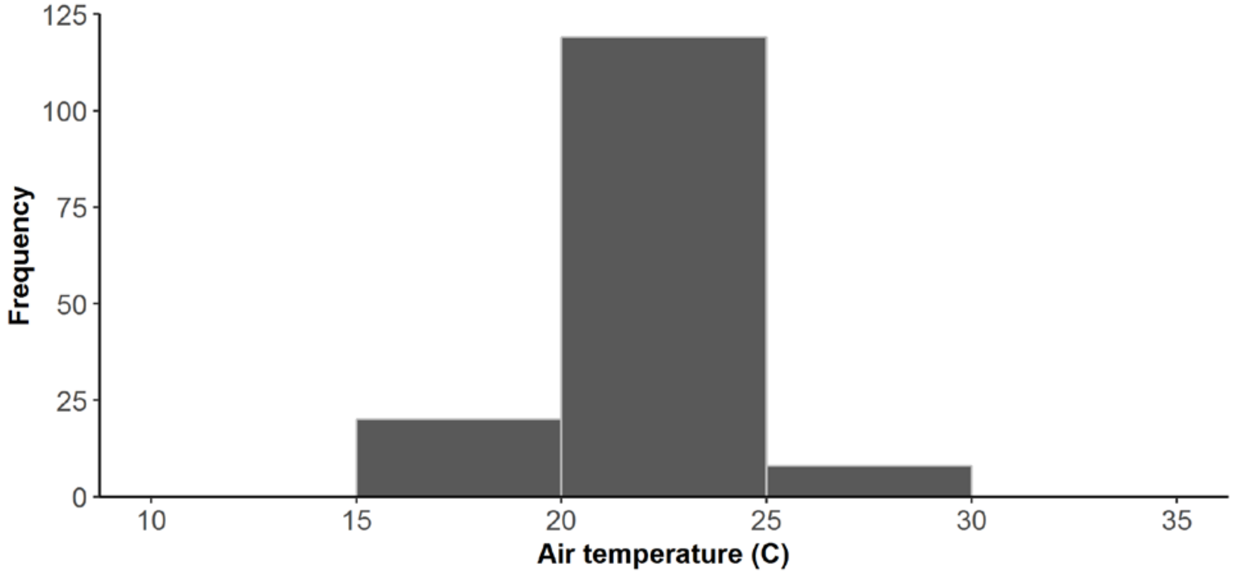

Figure K-12. Frequency distribution of air temperature (C) during estimated exposure events at the Block Island Wind Farm (n=147) of Common Terns and Roseate Terns tagged on Great Gull Island, NY from 2015 to 2017 (pooled).

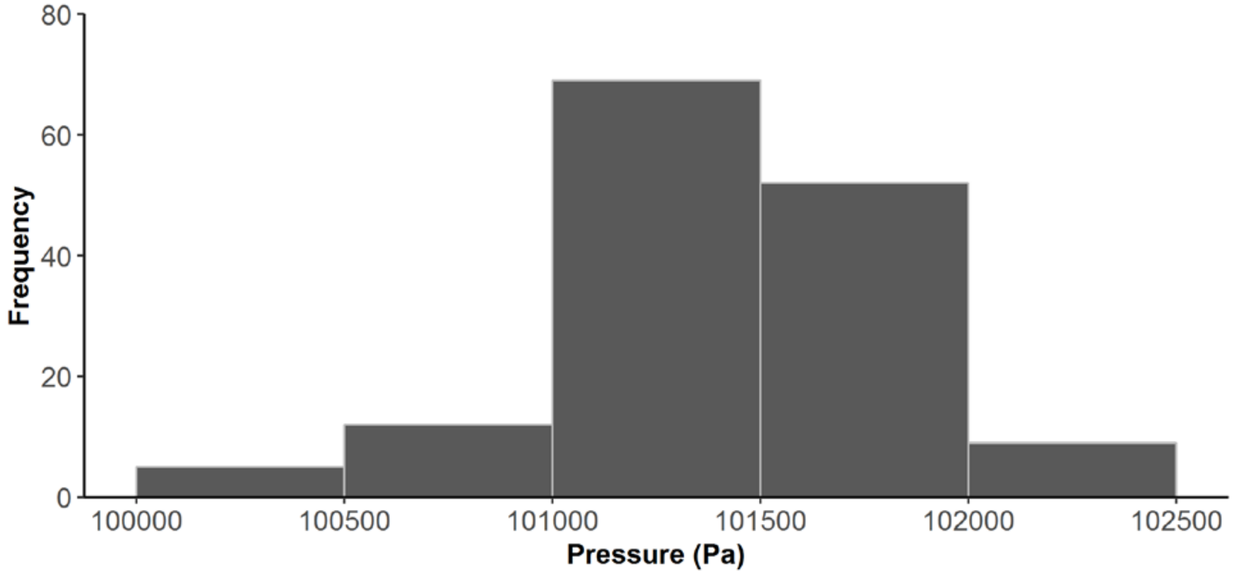

Figure K-13. Frequency distribution of barometric pressure (Pa) during estimated exposure events at the Block Island Wind Farm (n=147) of Common Terns and Roseate Terns tagged on Great Gull Island, NY from 2015 to 2017 (pooled).

Integrated covariate analysis

The boosted GAM model revealed that hour (EST) of the day was the strongest predictor of exposure to the Block Island Wind Farm among Common and Roseate Terns (Table K-5). Estimated probability of exposure was highest during the morning hours (03:00 to 09:00 hrs EST), with a peak near sunrise (05:30 hrs EST; Fig. K-14). By day of year, predicted exposure to Block Island Wind Farm peaked during the fledging period in mid-July and decreased during the post-breeding period through mid-September (Fig. K-15). Predicted responses to the meteorological variables indicated that exposure to the Block Island Wind Farm peaked during moderate wind speeds (7 and 12 m/s; Fig. K-16), and were weakly associated with wind direction (Fig. K-17), increasing atmospheric pressure (Fig. K-18), and air temperatures between 20 and 25 degrees C (Fig. K-19). The model predicted slightly higher exposure in 2015 and 2016 relative to 2017 (Fig. K-20), and slightly higher exposure of Common Terns relative to Roseate Terns (Fig. K-21).

Table K-5. Description and selection frequencies of covariates in binomial Boosted GAM analysis of estimated exposure of Common and Roseate Terns from the Great Gull Island colony to the Block Island Wind Farm, 2015 to 2017.

Covariate (units)	Fitting function	Selection Frequency
Hour (EST)	cyclical p-spline	0.22
Date (Julian)	p-spline	0.16
Wind speed (m/s)	p-spline	0.15
Bird ID	Random intercept	0.12
Wind direction (° true N)	cyclical p-spline	0.10
Pressure (Pa)	p-spline	0.07
Year	categorical (2015, 2016, 2017)	0.07
Species	categorical (COTE, ROST)	0.06
Air temperature (°C)	p-spline	0.05
Precipitation (kg/m^2)	p-spline	0.00
Visibility (m)	p-spline	0.00
Wind support	p-spline	0.00
Sex	categorical (M, F, unknown)	0.00
Date * Sex	categorical	0.00

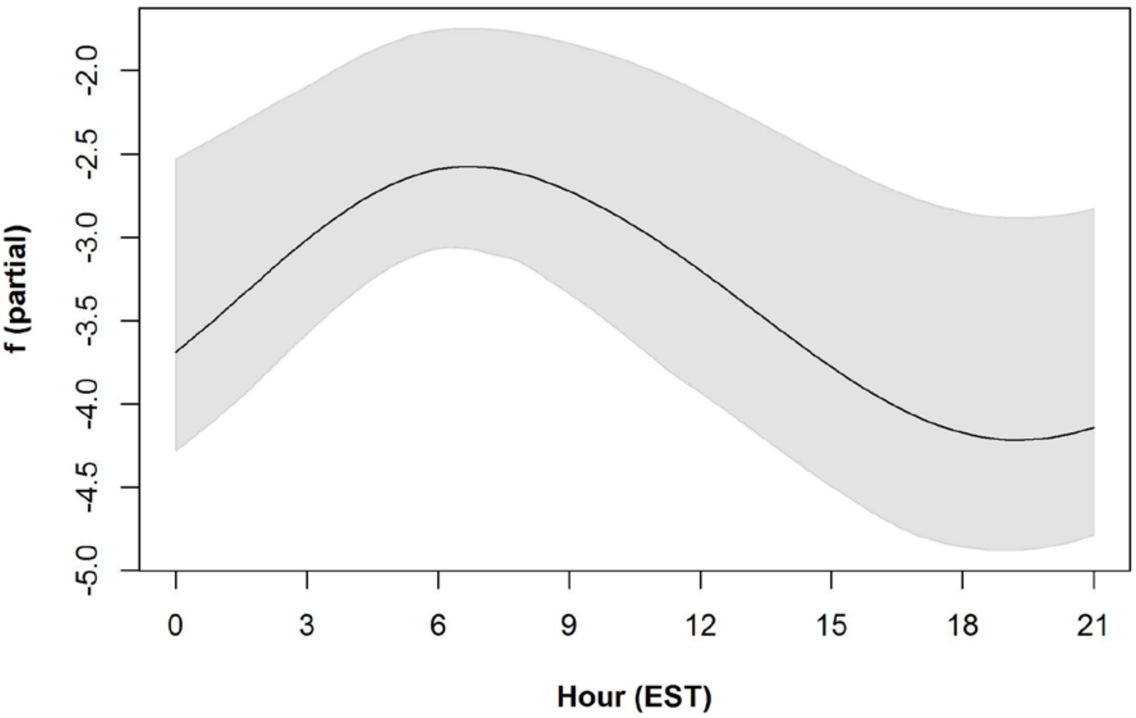

Figure K-14. Boosted GAM prediction for the partial contribution of the hour of day (EST) covariate (x-axis) to the likelihood (log-transformed odds ratio) of estimated exposure to the Block Island Wind Farm among Common and Roseate Terns (y-axis) in 2015, 2016, and 2017 (pooled). The gray-shaded area represents the 95% confidence interval for the response based on 100 bootstrapped models.

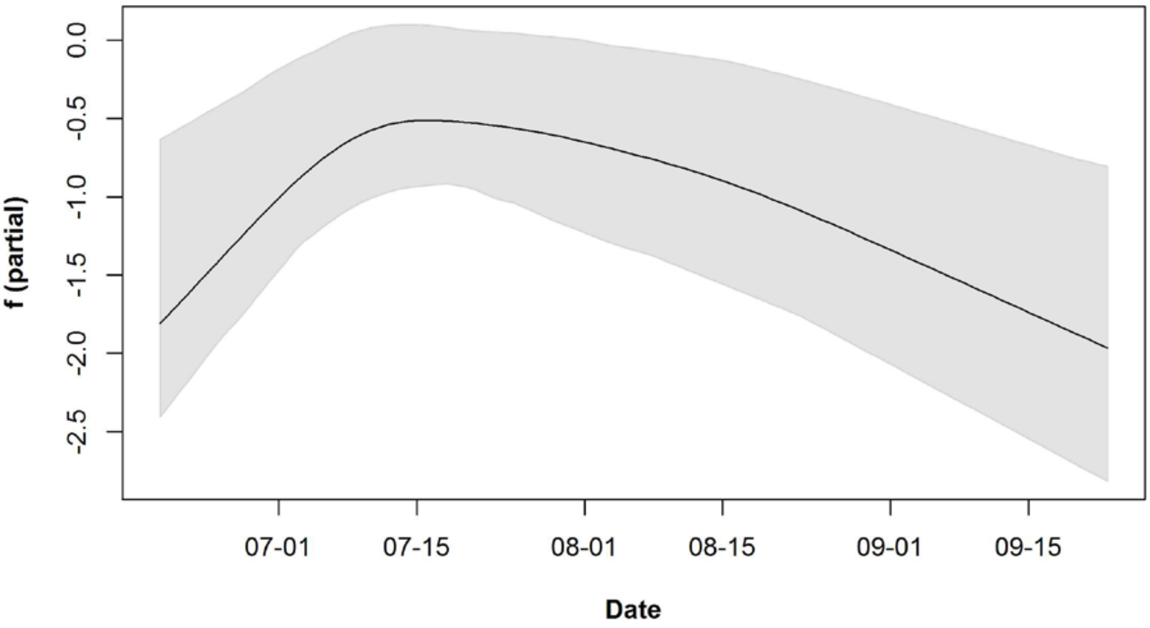

Figure K-15. Boosted GAM prediction for the partial contribution of the date of year covariate (x-axis) to the likelihood (log-transformed odds ratio) of estimated exposure to the Block Island Wind Farm among Common and Roseate Terns (y-axis) in 2015, 2016, and 2017 (pooled).
The gray-shaded area represents the 95% confidence interval for the response based on 100 bootstrapped models.

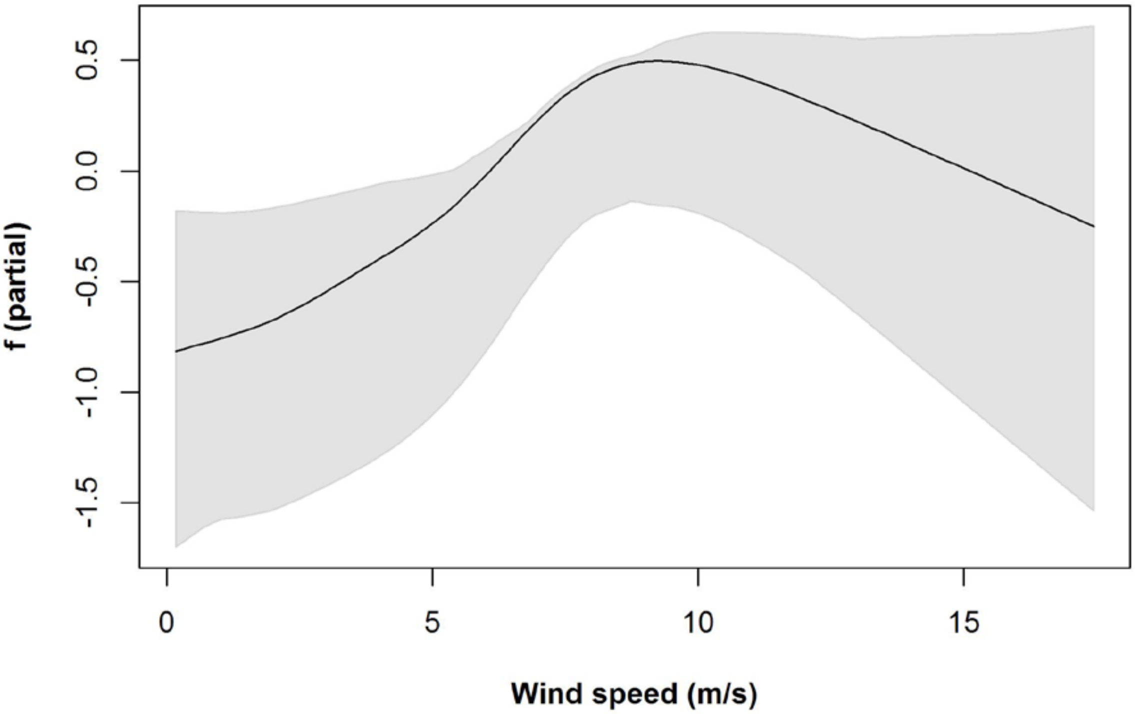

Figure K-16. Boosted GAM prediction for the partial contribution of the wind speed covariate (x-axis) to the likelihood (log-transformed odds ratio) of estimated exposure to the Block Island Wind Farm among Common and Roseate Terns (y-axis) in 2015, 2016, and 2017 (pooled).
The gray-shaded area represents the 95% confidence interval for the response based on 100 bootstrapped models.

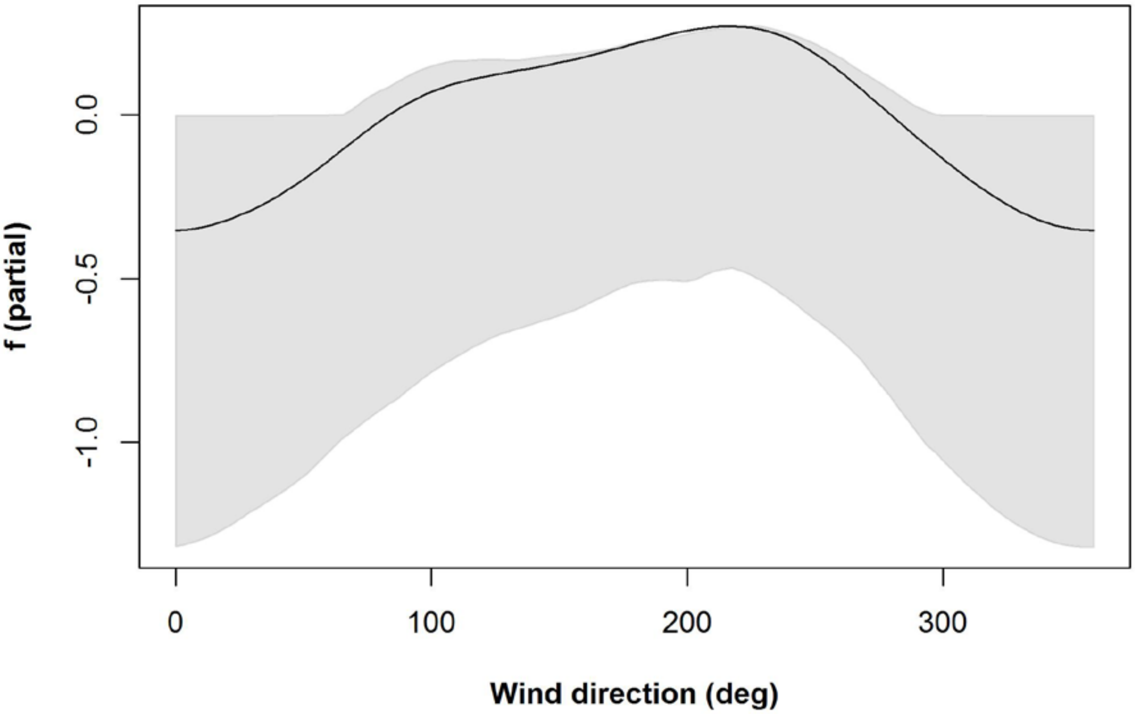

Figure K-17. Boosted GAM prediction for the partial contribution of the wind direction covariate (x-axis) to the likelihood (log-transformed odds ratio) of estimated exposure to the Block Island Wind Farm among Common and Roseate Terns (y-axis) in 2015, 2016, and 2017 (pooled).
The gray-shaded area represents the 95% confidence interval for the response based on 100 bootstrapped models.

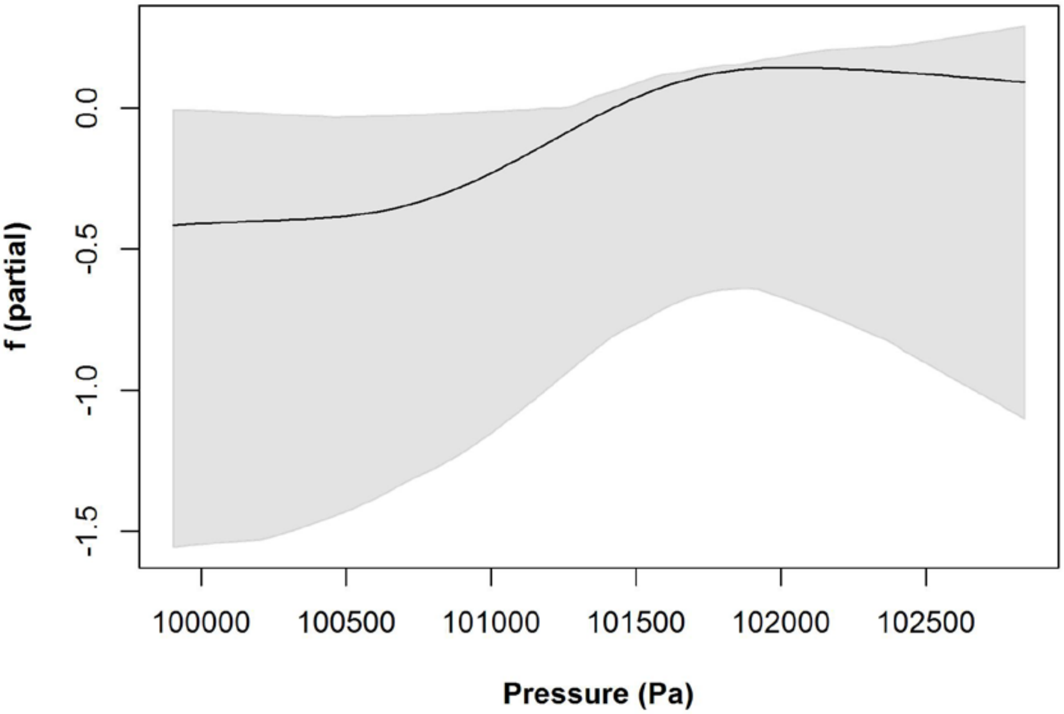

Figure K-18. Boosted GAM prediction for the partial contribution of the meterological pressure covariate (x-axis) to the likelihood (log-transformed odds ratio) of estimated exposure to the Block Island Wind Farm among Common and Roseate Terns (y-axis) in 2015, 2016, and 2017 (pooled). The gray-shaded area represents the 95% confidence interval for the response based on 100 bootstrapped models.

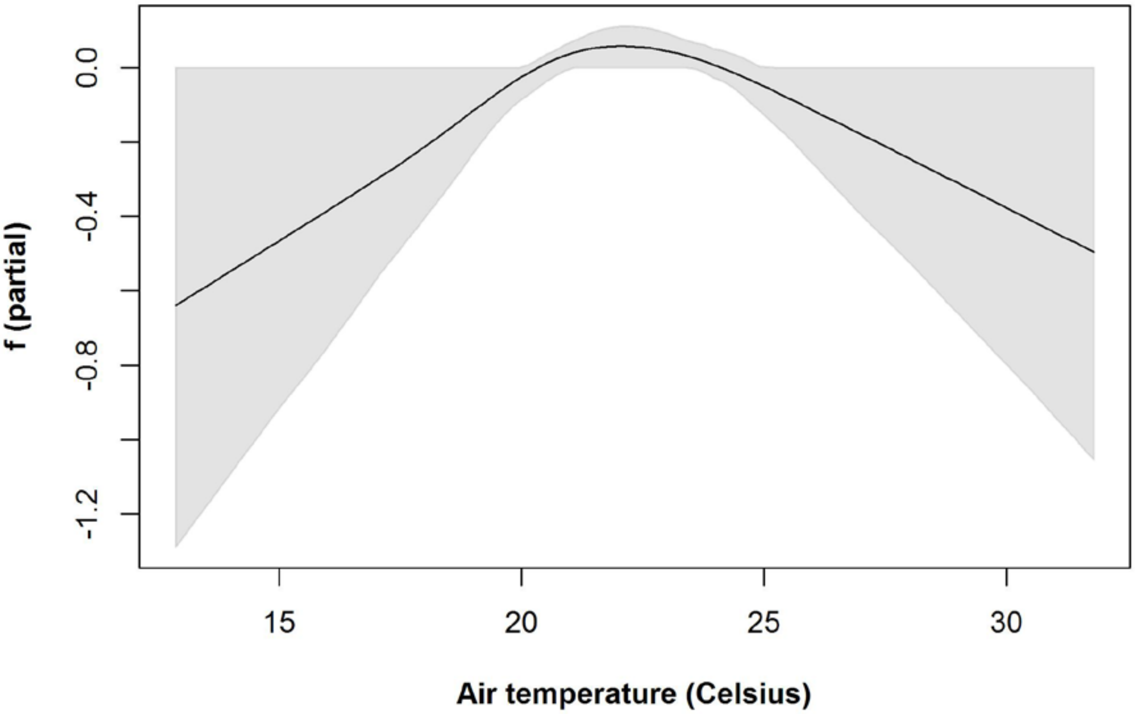

Figure K-19. Boosted GAM prediction for the partial contribution of the air temperature covariate (x-axis) to the likelihood (log-transformed odds ratio) of estimated exposure to the Block Island Wind Farm among Common and Roseate Terns (y-axis) in 2015, 2016, and 2017 (pooled). The gray-shaded area represents the 95% confidence interval for the response based on 100 bootstrapped models.

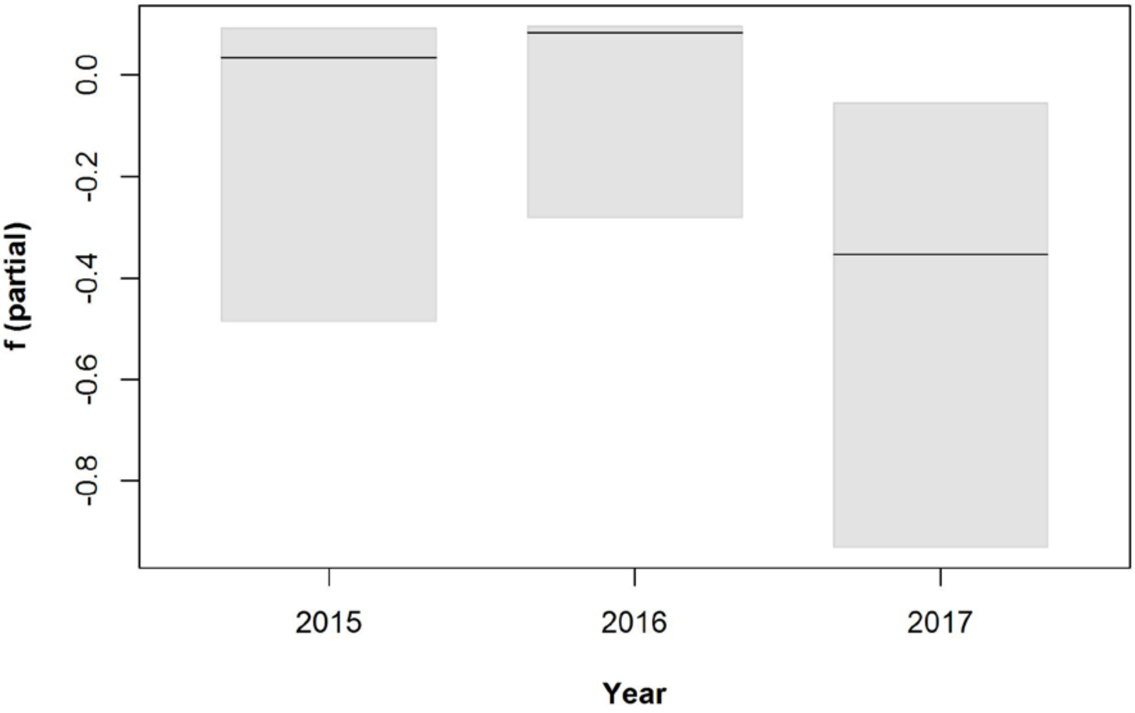

Figure K-20. Boosted GAM prediction for the partial contribution of the year covariate (x-axis) to the likelihood (log-transformed odds ratio) of estimated exposure to the Block Island Wind Farm among Common and Roseate Terns (y-axis) in 2015, 2016, and 2017.
The gray-shaded area represents the 95% confidence interval for the response based on 100 bootstrapped models.

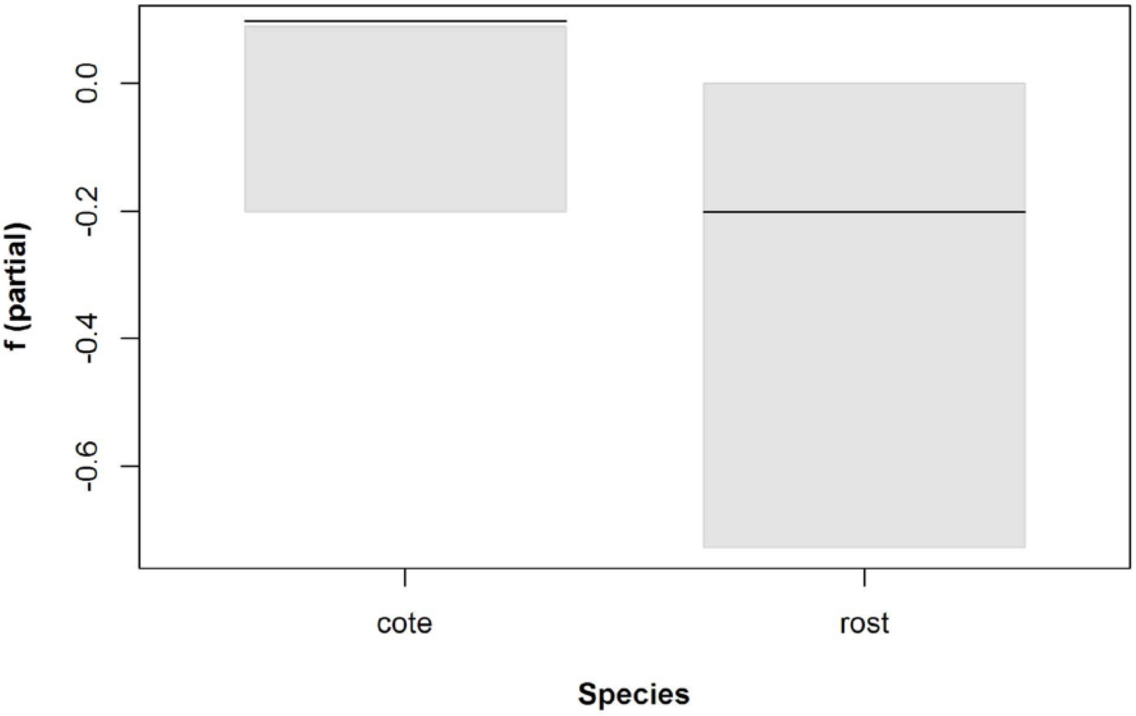

Figure K-21. Boosted GAM prediction for the partial contribution of the species covariate (x-axis) to the likelihood (log-transformed odds ratio) of estimated exposure to the Block Island Wind Farm between Common and Roseate Terns (y-axis) in 2015, 2016, and 2017 (pooled). The gray-shaded area represents the 95% confidence interval for the response based on 100 bootstrapped models.

Altitude distribution during exposure to Block Island Wind Farm

During exposure to the Block Island Wind Farm, estimated flight altitudes of Common and Roseate terns were similar and predominantly occurred below the RSZ (29 to 189 m). Overall mean estimated altitudes were 16 m among Common Terns (5-95 % range 11-25 m; Fig. K-22) and 15 m among Roseate Terns (5-95 % range 11-23 m; Fig. K-23). Based on predicted (mean model) altitudes, exposure to RSZ was 0.6% among Common Terns and 0.0% among Roseate Terns. However, estimates of exposure to the RSZ should be interpreted in the context of the model range (uncertainty) in plausible altitudes, which generally exceeded the range in estimated altitudes.

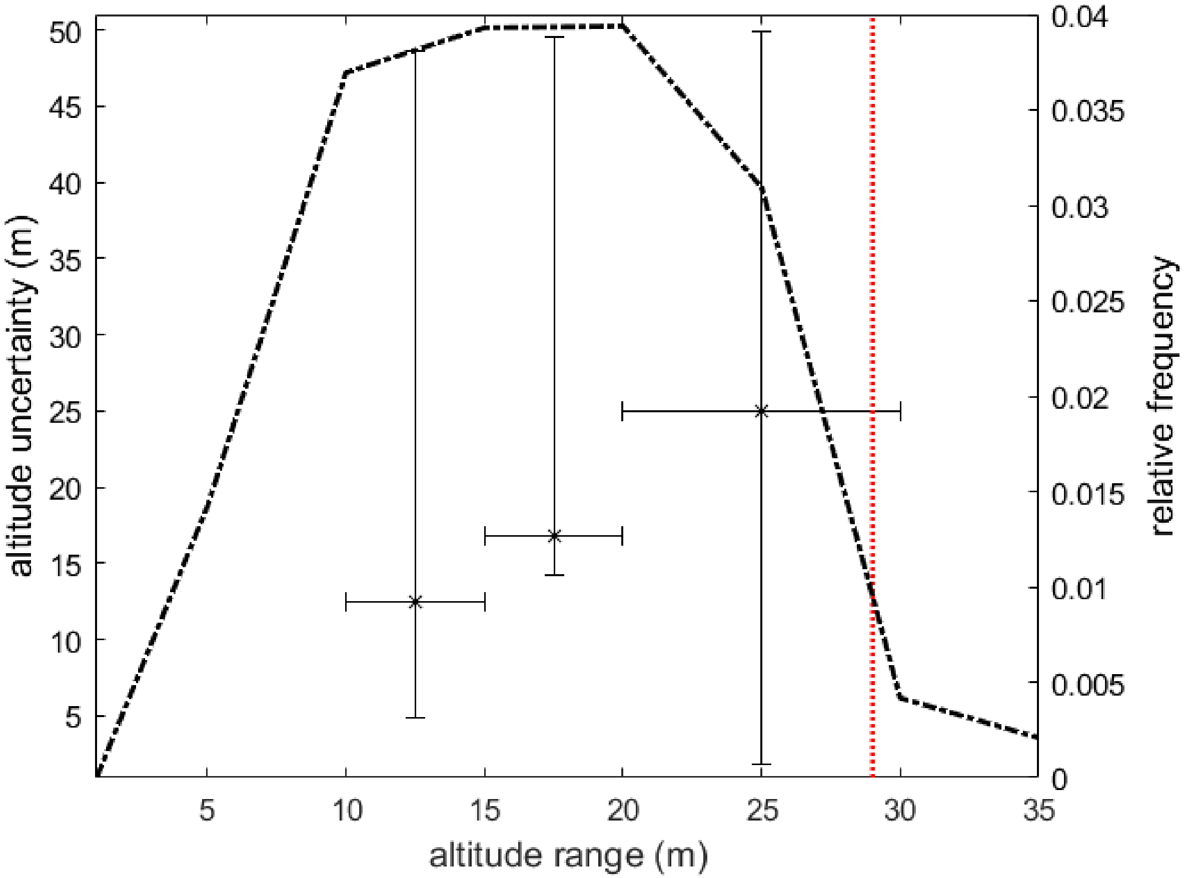

Figure K-22. Uncertainty in (left y-axis) and relative frequency of (right y-axis) predicted flight altitudes of Common Terns during exposure to Wind Energy Areas in Block Island.

The horizontal crosses represent ranges within altitudinal bins and vertical crosses represent model uncertainty when flight altitudes fell within those bins (uncertainty was quantified by upper and lower bounds in predicted mean altitude). The black dot-dashed line represents the frequency distribution of altitudes among all 10-minute intervals during estimated exposure to the Block Island Wind Farm. The red dot-dashed line delineates the lower bound of the altitude range of the RSZ (29 to 189 m asl).

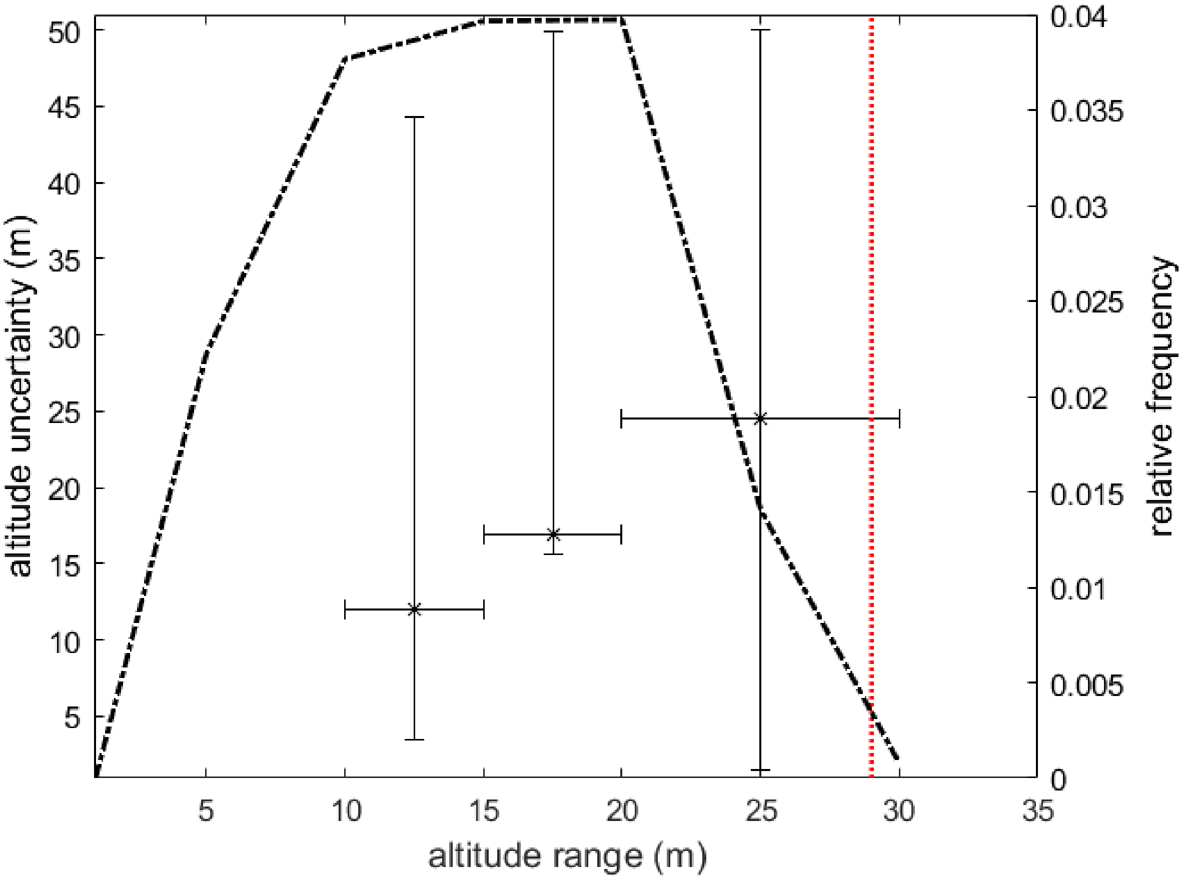

Figure K-23. Uncertainty in (left y-axis) and relative frequency of (right y-axis) predicted flight altitudes of Roseate Terns during exposure to Wind Energy Areas in Block Island.
The horizontal crosses represent ranges within altitudinal bins and vertical crosses represent model uncertainty when flight altitudes fell within those bins (uncertainty was quantified by upper and lower bounds in predicted mean altitude). The black dot-dashed line represents the frequency distribution of altitudes among all 10-minute intervals during estimated exposure to the Block Island Wind Farm. The red dot-dashed line delineates the lower bound of the altitude range of the RSZ (29 to 189 m asl).

Discussion

Among both species, exposure to the Block Island Wind Farm occurred within days following tagging (chick hatch) in late June, peaked during the pre-fledging period in early July (within 10-20 days following tagging), and continued through the post-breeding dispersal period during late July and August. Overall, exposure was highest during morning hours, coinciding with timing of peak foraging activity of terns reported by previous studies (Burger and Gochfeld 1991; Galbraith et al. 1999).

During the breeding period of Common and Roseate Terns, both members of a pair alternate between attending unfledged chicks at the nest site, commuting to foraging areas, and delivering prey items to chicks (Nisbet et al. 2014, Nisbet et al. 2017). As chicks age, parents spend an increasing time away from the nest (Nisbet et al. 2014, Nisbet et al. 2017). A study conducted in Massachusetts estimated that chick attendance by Common Terns during morning hours decreased to <5% when chicks were 15 days old

(Oswald et al. 2005); this timing corresponds to the peak timing of exposure of Common and Roseate Terns to the Block Island Wind Farm.

Exposure to the Block Island Wind Farm was higher for Common Terns versus Roseate Terns, which may be due in part to differences in their foraging ecology. Previous studies have shown that Roseate Terns primarily foraged for sandlance (*Ammodytes* spp.) in shallow, warmer waters near shoals, inlets, and rip currents close to shore (Safina 1990; Safina et al. 1990; Heinemann 1992; Rock et al. 2007). In contrast, Common Terns fed on a broader array of fish species in deeper, colder waters, often for forage fish driven to the surface by bluefish (*Pomoatomus saltatrix*; Safina 1990; Safina et al. 1990). The Block Island Wind Farm is located approximately 50 km away from the nesting colony on Great Gull Island, beyond than the maximum foraging range of 20 to 30 km reported by previous studies of Common and Roseate Terns in the western North Atlantic (Duffy 1986, Heinemann 1992; Nisbet et al. 2014; Nisbet et al. 2017). This is not unexpected as only recently has technology become available to accurately assess true foraging capabilities of smaller marine birds such as Common and Roseate terns.

Exposure of Common and Roseate Terns to the Block Island Wind Farm predominantly occurred during fair weather conditions, with high visibility, little to no precipitation, mild temperatures, and high atmospheric pressure. Fair weather and daylight provide favorable conditions for birds to detect and avoid obstructions in flight, reducing risk of collision (Fox et al. 2006). However, there was some evidence of exposure of terns to the Block Island Wind Farm at night and during inclement weather conditions (low visibility, precipitation, high winds) that could increase risk of collision (Exo et al. 2003; Drewitt and Langston 2006; Hüppop et al. 2006). Across both species, exposure at night peaked during late July. Common and Roseate Tern chicks fledge within 22 to 30 days following hatch and disperse away from the colony site with adults during July and early August (Nisbet et al. 2014; Nisbet et al. 2017). Late-season exposure to the Block Island Wind Farm at night may have been associated with nocturnal dispersal movements during the post-breeding period (Loring et al. 2017).

Continued, strategic monitoring of tern activity at the Block Island Wind Farm is important for assessments of potential effects, particularly for Roseate Terns that are listed as Endangered under the ESA. The Boosted GAM analysis revealed that hour of the day and day of year were the strongest predictors of Common and Roseate tern activity at the Block Island Wind Farm, with peak occurrence during the early morning (03:00 to 09:00 hrs EST) in mid-July. This information could be used to target future monitoring efforts during timing of peak tern activity. The Block Island Wind Farm Construction and Operations Plan (COP) includes radar monitoring of nocturnal bird flight and collisions during late summer and fall migration periods at select wind turbines (Deepwater Wind 2012). The COP also includes periodic boat-based surveys to monitor displacement of migrating and foraging birds (Deepwater Wind 2012). Radar monitoring and boat-based surveys conducted during periods of peak tern activity (i.e. morning hours in mid-July) could provide useful information on fine-scale occurrence, densities, behaviors, and collision risk of Common and Roseate terns within the Block Island Wind Farm.

The Boosted GAM analysis also indicated some variation in exposure of terns to the Block Island Wind Farm among years, with higher occurrence during 2015 (pre-construction) and 2016 (construction) versus 2017 (operation). A review of 20 post-construction studies in Europe classified Common Terns and Arctic Terns (*Sterna paradisaea*) as showing no recognizable effects of avoidance or attraction to offshore wind energy facilities (Dierschke et al. 2016). Inter-annual variability in the spatial distribution of terns may be associated with environmental variability, such as shifting prey (Safina and Burger 1989, Hall et al. 2000). Tracking studies using nanotags and automated radio telemetry arrays to assess tern movements around the Block Island Wind Farm are continuing during 2018 and 2019, and will provide additional information on occurrence of terns at the Block Island Wind Farm during the operational phase.

While nanotags facilitate continuous monitoring of the exposure of tagged terns to the Block Island Wind Farm at coarse spatial scales, additional information is needed on fine-scale movements and altitudes to more fully assess collision risk (Burger et al. 2011). Coarse estimates of flight altitudes from nanotag data indicate that Common and Roseate Terns were predominately below the RSZ during exposure to the Block Island Wind Farm. However, altitude estimates were subject to large amounts of uncertainty (>50 m), resulting in error bars that overlapped a portion of the RSZ. Additional studies focused on collecting fine-scale data on the movements and flight altitudes of terns are recommended to improve assessments of exposure to the RSZ. Additional, fine-scale data could be conducted through boat-based surveys using a rangefinder to estimate flight height (Harwood et al. 2018), through observer-calibrated radar monitoring (Fijn et al. 2015), or through deployment of newly-available light-weight (≥ 1-g) archival GPS transmitters (Gustin et al. 2018).

References

Bühlmann P, Hothorn T. 2007. Boosting Algorithms: Regularization, Prediction and Model Fitting. Statist. Sci. 22(4):477-505.

Burger J, Gordon C, Niles L, Newman J, Forcey G, Vlietstra L. 2011. Risk evaluation for Federally listed (Roseate Tern, Piping Plover) or candidate (Red Knot) bird species in offshore waters: A first step for managing the potential impacts of wind facility development on the Atlantic Outer Continental Shelf. Renewable Energy 36:338–351.

Deepwater Wind. 2012. Block Island Wind Farm and Block Island Transmission System Environmental Report / Construction and Operations Plan; [accessed 2018 Dec 3]. http://dwwind.com/wp-content/uploads/2014/08/Environmental-Report-Exec-Summary.pdf

Dierschke V, Furness RW, Garthe S. 2016. Seabirds and offshore wind farms in European waters: Avoidance and attraction. Biological Conservation 202:59-68.

Duffy DC. 1986. Foraging at patches: interactions between Common and Roseate Terns. Ornis Scandinavica 17:47-52.

Exo KM, Huppop O, Garthe S. 2003. Birds and offshore wind farms: a hot topic in marine ecology. Wader Study Group Bulletin 100:50-53.

Fijn RC, Krijgsveld KL, Poot MJ, Dirksen, S. 2015. Bird movements at rotor heights measured continuously with vertical radar at a Dutch offshore wind farm. Ibis 157:558-566.

Fox AD, Desholm M, Kahlert J, Christensen TK, Petersen IBK. 2006. Information needs to support environmental impact assessment of the effects of European marine offshore wind farms on birds. Ibis 148:129-144.

Gustin M, Giglio G, Pellegrino SC, Frassanito A, Ferrarini A. 2018. Nocturnal flights lead to collision risk with power lines and wind farms in Lesser Kestrels: a preliminary assessment through GPS tracking. Comput Ecol Softw. 8:15-22.

Hall CS, Kress SW, Griffin CR. 2000. Composition, spatial and temporal variation of Common and Arctic Tern chick diets in the Gulf of Maine. Waterbirds 23:430-439.

Harwood AJ, Perrow MR, Berridge RJ. 2018. Use of an optical rangefinder to assess the reliability of seabird flight heights from boat-based surveyors: implications for collision risk at offshore wind farms. J. Field Ornithol. 89:372-383.

Heinemann D. 1992. Foraging Ecology of Roseate Terns on Bird Island, Buzzards Bay, Massachusetts. Unpublished Report to U.S. Fish and Wildlife Service, Newton Corner, MA.

Loring PH, Ronconi R, Welch L, Taylor P, Mallory M. 2017b. Post-breeding dispersal and staging of Common and Arctic Terns throughout the western North Atlantic. Avian Conservation and Ecology, 12(2).

Nisbet ICT, Arnold JM, Oswald SA, Pyle P, Patten MA. 2017. Common Tern (*Sterna hirundo*) The Birds of North America (P. G. Rodewald, Ed.). Ithaca: Cornell Lab of Ornithology; Retrieved from the Birds of North America Online: https://doi.org/10.2173/bna.comter.03

Northeast Regional Ocean Council. 2017. Northeast Ocean Data Portal; [accessed 2017 May 20]. https://www.northeastoceandata.org/data-explorer/.

Oswald SA, Arnold JM, Hatch JJ, Nisbet ICT. 2005. Effect of intraspecific interactions on seasonal decline in productivity of Common Terns *Sterna hirundo*. Bird Study no. 52:70-79.

Rock JC, Leonard ML, Boyne A. 2007. Foraging habitat and chick diets of Roseate Tern, *Sterna dougallii*, Breeding on Country Island, Nova Scotia. Avian Conservation and Ecology 2:4

Safina C, Burger J. 1989. Inter-annual variation in prey availability for Common Terns at different stages in their reproductive cycle. Colonial Waterbirds 12:37-42.

Safina, C. 1990. Foraging habitat partitioning in Roseate and Common Terns. Auk 107:351-358.

Safina C, Wagner RH, Witting DA, Smith KJ. 1990. Prey delivered to Roseate and Common Tern chicks; Composition and temporal variability. Journal of Field Ornithology 61:331-338.

Taylor IR. 1983. Effect of wind on the foraging behaviour of Common and Sandwich Terns. Ornis Scand. 14:90-96.